Founder-Editor-in-Chief : **Prof.Dr. İskender AKKURT**

dergipark.org.tr/en/pub/ijcesen

Indexing/Abstracting Databases

Table of Contents

Personalized Intraoperative Radiotherapy Balloon Applicator Design and Production With 3D Printer

Öykü YÜZER[1]*, Betül ÖZER[2], S. Enes ÖZDEL[3], Osman GÜNAY[4]

[1]Yıldız Technical University, Faculty of Electrical & Electronics, Biomedical Engineering Department, İstanbul-Turkey
* **Corresponding Author**: **Email:** oyku.yuzer0@gmail.com - **ORCID:** 0009-0001-0387-864X

[2]Yıldız Technical University, Faculty of Electrical & Electronics, Biomedical Engineering Department, İstanbul-Turkey
Email: ozerbetul78@gmail.com - **ORCID:** 0009-0007-2299-0091

[3]Yıldız Technical University, Faculty of Electrical & Electronics, Biomedical Engineering Department, İstanbul-Turkey
Email: salihenesozdel@gmail.com - **ORCID:** 0009-0004-0951-8102

[4]Yıldız Technical University, Faculty of Electrical & Electronics, Biomedical Engineering Department, İstanbul-Turkey
Email: ogunay@yildiz.edu.tr - **ORCID:** 0000-0003-0760-554X

Abstract:

Radiation is the energy released from matter. Radiation is divided into two according to its source: natural and artificial radiation. Artificial radiation is used in treatment methods in medicine. One of these treatment methods is brachytherapy. Brachytherapy treatment is applied by placing small radioactive sources inside the body and sending beams directly to the cancerous cell. The main thing to consider in brachytherapy treatment is the selection of the applicator. The applicator is the device that enters the patient's body cavity. In this study, based on the applicators currently used in the medical field, a patient-specific, biocompatible, sterilized, and reusable applicator will be created from PLA material by using a 3D printer. The applicator to be designed will consist of 2 parts: the intrauterine tube and the spherical tip. The spherical tips, which vary according to the size of the tumor, will be pressed to integrate with the tube part of the applicator. Thus, a patient-specific design will be realized by using the spherical tip suitable for the patient's tumor region. As a result of the project, since the applicator will have spherical tips of different sizes, it completely covers the intrabody cavity of the patient. Thus, the movement of the applicator is limited, and dose distribution is prevented. The treatment process of the patient is improved. Another result is that the prototype applicator printed with PLA filament is produced at a very low cost. Thus, access to the applicator becomes easier and its use in the medical field increases.

1. Introduction

1.1 Radiation

Today, radiation is a concept that we frequently encounter in our environment. Radiation is the energy released from matter. Physically, it is the propagation of various types of energy in waves [1]. According to energy and frequency level, radiation is divided into two main categories: ionizing and non-ionizing. Ionizing radiation creates ions in the material it hits, and energy is transferred by electron detachment from this ion [2]. It is also referred to as nuclear radiation. The type of radiation used in the medical field is ionizing radiation. They have high frequency, low wavelength, and damage tissues due to their high energy. They have the energy to break down the DNA inside the cell as a result of uncontrolled exposure. Due to the damage to DNA, it causes many diseases in the body, including cancer [3]. Non-ionizing radiation is ultraviolet rays, visible light and infrared rays, microwaves, and radio frequency that do not ionize the environment [4]. In this type of radiation with low frequency and high wavelength, ionization does not occur. In contrast to ionizing radiation, non-ionizing radiation does not have the energy to detach electrons from molecules. Therefore, it is not directly harmful to the human body. However, continuous exposure to high doses of non-ionizing radiation can damage the tissue due to the heat emitted.

There are many sources of radiation energy. The sun, radioactive materials, medical devices, and X-rays are some of these sources. These sources can be analyzed into two categories: natural and artificial. Natural radiation is the radiation that exists in nature without human contribution. The main headings of natural radiation can be grouped as cosmic, terrestrial, and internal radiation [5]. The radiation we are exposed to from the sun, stars, Earth, rock, soil, water, and air, and the types of radiation naturally found in the human body (Potassium-40/ Carbon-14 isotopes) are examined under this heading.

Artificial radiation sources can also be divided into two as medical sources and industrial products. Since there is no continuous exposure like natural sources, exposure may vary depending on the person's daily lifestyle. Medical sources are the area of use of ionizing radiation. It is the type of radiation exposure due to medical diagnosis and treatment areas such as radiography, radiotherapy, and nuclear medicine [5]. In radiography and imaging methods, low doses of radiation are used for diagnostic purposes without harming the cells and the patient. However, since apoptosis occurs in radiotherapy, high doses of radiation are targeted.

While radiation can be extremely harmful to the human body, it can also be beneficial. For example, while it can cause cancer as a harmful effect, at the same time, cancer can be cured with radiation used in the appropriate dose and area. For this reason, to use the effects of radiation correctly, an appropriate and controlled dose should be selected, and the duration of exposure should be adjusted correctly. Measurement units are used internationally to adjust this dose correctly and to obtain reliable results in studies.

The number of decays of radioactive nuclei per unit of time is known as activity and its unit is Becquerel (Bq) [6].

The amount of radiation energy stored as energy due to ionization in the environment is the absorbed dose. The unit of this dose is Gray (Gy) [7].

Stochastic and deterministic effects may occur if radiation is not used at the appropriate dose and duration. These effects are extracellular effects. Deterministic effects are the effects when radiation damages a tissue or organ, and the body reacts. There is a certain threshold value and if a dose smaller than this threshold value is received, the effect is zero. However, if radiation is received above this threshold, damage occurs in the body. The damage increases depending on this dose. The most common effects are infertility, sudden death, and cataracts. For example, cataracts can occur with 5 Gy or more radiation to the eye [7]. Stochastic effects are those observed without any threshold value. They occur as the effects of low doses of radiation. Their effects are not sudden like deterministic effects but are observed later. Here the damage/ threshold connection is linear. The more exposure to radiation, the greater the damage/ disease that will develop [7].

1.2 Use of Radiation in Healthcare

Radiation is used in various fields of health such as diagnostic imaging and radiation therapy. It is important to use radiation safely and appropriately to minimize health risks. There are various radiation devices used for different purposes in healthcare. Some of the radiation devices used in healthcare include X-rays, CT, PET, MRI, and radiotherapy. X-rays provide imaging of the internal structures of the body using ionizing radiation with X-rays. Computed tomography (CT) provides detailed imaging of the body using ionizing radiation and is used to diagnose internal injuries and diseases by combining X-ray images taken from different angles [8]. Positron Emission Tomography (PET) provides metabolic and functional imaging using a radioactive tracer injected intravenously. Magnetic Resonance Imaging (MRI) uses magnets to emit magnetic fields and radio waves to create images of the body. Radiotherapy uses high-energy radiation to target and destroy cancer cells. There are different radiation therapy machines. These include beam radiation therapy, brachytherapy, and proton therapy.

These devices play an important role in the diagnosis and treatment of diseases. With the right radiation used in the health field, early diagnosis of diseases, non-invasive treatments and a more comfortable treatment process for the patient can be realized. Radiation doses should be monitored and minimized to reduce harmful effects due to the radioactive effects of the devices.

1.3 Radiation and Radiotherapy in Cancer

Cancer is a disease caused by the uncontrolled and irregular growth and division of cells in the body [9]. During this uncontrolled growth process, the cells cause great damage by damaging the healthy tissues around them.

The most common types of cancer are breast cancer, cervical cancer, colon cancer, and prostate cancer. Risk factors include genetic factors, age, and environmental factors.

Early diagnosis makes cancer treatment more effective. However, the treatment process may vary depending on the stage and type of cancer. There are different treatment methods such as chemotherapy, surgery, and radiotherapy. Almost 50% of cancer patients receive radiotherapy [10].

Radiotherapy is one of the most common treatment methods [7]. While its main purpose is to destroy cancer cells using high-energy radiation beams, it can also be used to shrink cancerous tissue and relieve symptoms. These beams are directed directly at the cancerous cells, causing damage to the structure of the cancerous cell, and slowing/ stopping the cancer. The duration and dose of treatment is determined depending on the patient and the course of the disease.

The radiotherapy method may also change according to the course of the disease. The most used radiotherapy methods can be explained as follows. In EBRT (External Beam Radiation Therapy), high-energy beams are used for cancerous cells. The machine with the radiation source rotates around the patient, focusing the beams on the cancerous cells. IGRT (Image Guided Radiation Therapy) uses imaging techniques to directly target the cancerous area. The most common imaging techniques in this method are CT and MRI. Since the area is directly targeted, radiation can be directed more accurately. Tomotherapy treatment is one of the most common IGRT methods. Dosimetric planning is provided with 3D imaging. Another method is intraoperative radiotherapy.

1.4 What is Intraoperative Radiotherapy?
The word brachytherapy is a combination of the Greek words $brachy + therapy$, which means short distance + treatment [11]. In this method, the radioactive material is placed in direct contact with the cancerous cell and inside the cancerous tissue, exposing the tissue to radiation. It is applied after the removal of cancerous tissue during surgery [12]. Cancerous tissue cannot be completely removed from healthy tissue when surgically intervened. As explained in the previous section, the effectiveness of the treatment is quite high in this method since IORT directly contacts the cells intensively. For the same reason, the damage caused by IORT to healthy tissue is also minimal [12].

The radiation sources used in this method are high-energy x-rays, electrons, and gamma rays. Since breast, pancreatic, uterine, head, and neck cancers are more prone to spread, IORT is highly utilized for these cancers [13].

Unlike conventional radiotherapy, IORT delivers a higher dose of radiation to cancerous tissue while at the same time protecting healthy cells more [14]. This reduces the duration of the patient's treatment [15]. Due to the protection of healthy cells, side effects can be observed less frequently.

It is applied with a device placed in the tissue after surgery. Electron radiation has a limited range and thus causes less damage to surrounding tissues.

Gamma rays are applied to the tissue with a special device. It provides a more homogeneous radiation distribution compared to other radiation methods.

As a result, the choice of method for IORT should be carefully and meticulously selected in light of the patient's condition, the course of the disease, and the doctor's attention [16]. IORT, which offers highly effective treatment in a short time, is costly due to the devices, heads, and other external factors used. In addition, the fact that the applicators used to directly contact the tissue and destroy the cancerous area are compatible with the patient will increase the effect of the treatment. Thanks to the applicators we have discussed and designed in this study, we aim to increase the preference and effectiveness of the treatment result by reducing the cost and increasing the patient compatibility of the applicators.

2. Material and Methods

In order to print the prototype applicator, which we expect to be used in the brachytherapy method, using an FDM type 3D printer, a product design was made in 3D space with the Autodesk Fusion 360 program. In the product design, the Axxent electronic applicator, which is used in the literature for breast cancer treatment, was used as a template for the drawing, inspired by the studies in the literature. The product designed is made up of two main parts, the applicator tube, and the spherical tip.

The spherical tips, which vary according to the size of the tumor, were 3D printed to integrate with the tube part of the applicator. Spherical tips, which provide patient-specific applicator design and differ in size from each other, were developed in accordance with the patient's tumor region. The tube part of the applicator, unlike balloon applicators, contains only a port suitable for radiation entry. Produced in accordance with the use of Ir-192 high dose rate (HDR) radiation source and/ or electronic x-ray source, the applicator transmits the radioactive material from the radiation port to the spherical tip. The two-piece prototype applicator was turned into an object by on a printing on 3D printer, using PLA polymer material which is a commercially available inexpensive, biocompatible, and high-resolution filament.

3. Results and Discussions

Devices for creating three-dimensional objects from digital designs are called 3D printers. 3D printing can be defined as the process of creating objects by adding the material used layer by layer. Therefore, production in 3D printers is an additive process. It is

formed by the combination of layer sections at the specified resolution [17].

Designs for 3D prints can be easily edited and reprinted, allowing test-based optimization. Additionally, 3D-printed devices do not require a cleanroom fabrication environment. Consumables for 3D printing are usually just resin and solvent to remove support materials, so costs can be low [18].

Various types of 3D printers are available on the market, including Fused Deposition Modelling (FDM), Stereolithography (SLA), Digital Light Processing (DLP), and Selective Laser Sintering (SLS). FDM 3D printers, which operate by heating and extruding a plastic filament to form an object, are the most popular and affordable type of 3D printers. To form an object with FDM, the filament is melted and extruded through a hot tip nozzle moving in the x, y and z axes, and the molten filament is deposited layer by layer. In other words, the basic concept of the FDM manufacturing process is simply to melt the raw material and shape it to create new shapes. The material is fed through a nozzle placed on a roller, pulled by a drive wheel, and then temperature controlled.
It is a filament that is put on the head and heated until it becomes semi-liquid [19]. FDM 3D printers are frequently used in prototyping, manufacturing, and product design work. In addition, FDM printers can print with various materials such as PLA, and PETG, which are easily available in the market. These features also make them useful.

FDM 3D printers, which create objects by depositing melted filaments layer by layer, create objects using various filaments. The filaments used are mainly PLA (Polylactic Acid), PETG (Polyethylene Terephthalate Glycol), Nylon, TPU (Thermoplastic Polyurethane), ABS (Acrylonitrile Butadiene Styrene).

Although FDM-type 3D printers are compatible with working with many filaments, PLA is the most preferred filament due to its usefulness and cheapness. PLA filament is a widely used material for 3D printers. PLA is a naturally sourced, biodegradable, and environmentally friendly material and is often produced from natural raw materials such as corn starch. Polylactic Acid (PLA) is the most used thermoplastic and natural fibers can be used as a filler [20]. Biocomposite filaments consist of a biodegradable composite matrix and biofillers. Additives can make fibers or particles. Therefore, PLA is a popular thermoplastic material used in fusion deposition modeling (FDM) with a wide variety of medical uses [21].

PLA filaments are a type of thermoplastic material that melts when heat is applied and can be reshaped. PLA is suitable for high-precision printers and can be used to produce very precise parts. Made from renewable resources with a low melting point, biodegradable, biocompatible, low bending coefficient PLA filament allows users to create safe, good dimensional stability prototypes.

A good material for bioengineering is PLA. It has a wide range of medicinal applications, including orthopedic and dental purposes as well as tissue engineering and regenerative medicine. The advantages of this material have helped engineers and scientists [22].
It has minimal to no documented carcinogenic impact, and is easily manufactured, recyclable, biodegradable, and biocompatible [23]. Also permitted by the FDA for direct contact with biological fluids is PLA.

A method to exterminate all microbial life forms, such as viruses and bacteria, is referred to as sterilization [24]. Especially in the medical field, sterilization of these microbial life forms is of great importance as they are undesirable substances. Recently, with PLA being a frequently used material in medicine, studies have also been conducted on its sterilization and sterility in surgical use. Among these studies, hydrogen peroxide sterilization is the most suitable method for 3D-printed PLA materials. The sterilization with hydrogen peroxide prevents the deformation of 3D-printed PLA materials during autoclave sterilization [25]. With sterilization with hydrogen peroxide, the designed applicator can be used intraoperatively many times.

Depending on the molecular weight and degree of crystallinity of the polymer, PLA's mechanical characteristics can change [26]. With different PLA isomers and functional groups, these values alter. Table 1 lists the PLA's mechanical and physical characteristics. varied isomers and functional groups have varied values for these parameters.

Table 1. Physical and Mechanical Properties of PLA [27]

Properties	PLA
Polymer Density	1.21-1.25 g/cm^3
Tensile Strength	21.0-60.0 Mpa
Tensile Modulus	0.35-3.50 Gpa
Ultimate Strain	2.5-6%
Specific Tensile Strength	16.8-48.0 Nm/g
Specific Tensile Modulus	0.28-2.80 KNm/g
Melting Temperature	150-162 ºC

The most important factor to consider when choosing a polymer to utilize as a biomaterial is whether its mechanical characteristics and rate of degradation are appropriate for the application.

Physical features are also crucial for a medical device; therefore, the designer must take into account the product's dimensions, size, and weight specifications. For instance, the design should safeguard the product against weights, pressures, and impacts while yet being light enough for the surgeon to handle precisely [28].
Tensile strength, tensile elongation, tensile modulus, impact resistance (all for toughness), and flexural modulus are significant mechanical qualities.

Applications for PLA include tissue engineering, medication delivery systems, orthopedic and fixation devices, and wound care and stents. In one work, a polymer based on lactic acid was used to create an implantable decomposable inflated balloon [29]. By separating the prostate rectum with balloons during radiation treatment for cancer, or to cure severe rotator cuff injuries, it has been employed as a sub-acromial separator [30].

Various software programs are used for designing and prototyping 3D models. Software developed for Computer-Aided Design (CAD) allows users to create 3D models, simulate their designs, and prototyping by providing various features. Today, actively used, and popular software: Autodesk Fusion 360, SolidWorks, SketchUp, and Blender can be listed as.

Autodesk Fusion 360 is a design and manufacturing software. This software is designed for the design, simulation, manufacturing, and learning of products and offers a variety of design tools, simulation features, manufacturing features, and learning tools. Autodesk Fusion 360, a cloud-based CAD/CAM (Computer Aided Design/ Computer Aided Manufacturing) software, offers a host of features for designing and prototyping 3D models, including parametric modeling, sculpting, and direct modeling, as well as tools to simulate the performance and behavior of designed parts. allows users to test their designs before producing them. Thus, it is widely used in various industries including engineering, product design, and manufacturing. The fact that Fusion 360 is a cloud-based software prevents data storage in local memory, while project files can be accessed from anywhere with an internet connection. Another advantage is that it allows users to collaborate on projects in real-time.

In additive manufacturing, the slope of a downward-facing surface (protrusion) of the object is above a critical value relative to the base plate for the object to be self-supporting. If a part contains regions with projection angles below this critical value in the intended construction direction, it will not be self-supporting and cannot be printed as it is [31]. Therefore, the critical angle must be determined, and the design must be made accordingly. However, changing an optimized geometry can degrade the object's performance or even render it inapplicable. For this reason, it is a more preferred method to support the object with traditional supports and remove it from the object when the printing process is completed.

Thanks to the "overhang optimization" or "self-supporting structures" methods, balloon-shaped object output can be obtained without using support structures. In addition, these methods aim to reduce material waste and post-processing efforts. "Mesh Structures" and "Gradual Overhangs" are some of the techniques used for these methods. There is a special design on the basis of these methods. The use of supports can be minimized by using gradual angles and curves in the design.

In our study, the FDM type 3D printer PLA material is deposited layer by layer and the object comes out of the printer. This causes the resulting object to have a rough structure. In our study, sanding and polishing processes were carried out respectively to make the object smooth. Thanks to these methods, which are frequently used in the production of medical devices with 3D printers, the use of support can be minimized, and the created device can be smoothed.
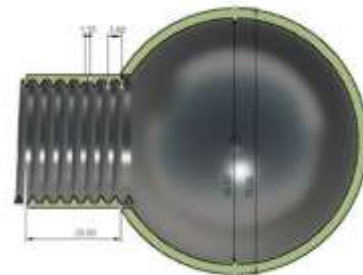
Figure 1. Spherical Tip Sketch
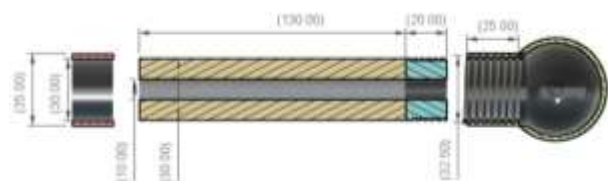
Figure 2. Whole Applicator Sketch

Figure 3. Whole Applicator 3D View with Two Different Spherical Tips

Figure 4. Three Different Spherical Tips with the Radius Parameter

Figure 5. Three Different Spherical Tips

In the Figure 1, the spherical tip sketch made in Autodesk Fusion 360 is shown with the parameters. Figure 2 shows the whole applicator design with the applicator tube, and the spherical tip.

The general view of the applicator is shown in Figure 3. The tube and spheric type are shown in this figure with their external appearance.

Figure 4 shows the cross-section of the spherical tips. This figure shows the parameters and the cross-section of the tips with different diameters.

The whole view of the cross-sectional images given in Figure 4 can be observed in Figure 5. In this figure, the whole appearance of the tips with different radii is shown.

The design of the applicator to be used in the intraoperative treatment has been completed and its external appearance and drawings are given in the figures. Accordingly, applicators, which are drawn and printed according to different diameters, are expected to be effective for treatment in cases that vary according to different tumor sizes and the size of the patient's internal cavity. In addition, the applicator, which basically consists of two parts (tube and cylindrical tip), offers a simple solution for the use of paramedics and improves the treatment

process based on the separate-clean-connect-use principle.

4. Conclusions

Traditional application methods and applicators used in brachytherapy treatment were examined in the literature. As a result of the literature review, the development process of the currently used applicators was examined and some deficiencies were revealed. The unique value of this study is the development of balloon applicators suitable for cervical cancer treatment using 3D printing and the creation of a sterilized and reusable applicator. The applicator to be created consists of two parts: a tube and a spherical tip. The spherical tips, which vary according to the size of the tumor, will be pressed to be integrated with the tube part of the applicator. Thus, a patient-specific design will be realized by using a spherical tip suitable for the patient's tumor area. The intrauterine tube will limit the movement of the biocompatible applicator to be produced, closing the gap in the tumor area, and facilitating access to the area to be exposed to radiation. This study will be one of the pioneering studies in the field and will be a reference for future studies. When compared with similar studies to be conducted in the coming years, this study will reveal the importance of applicators created with 3D printers for use in brachytherapy treatment in cervical cancer treatment.

Author Statements:

References

[1] Weisstein, E. W. (n.d.). Eric Weisstein's World of Physics. Eric Weisstein's World of Physics. https://scienceworld.wolfram.com/physics/

[2] Extremely Low-Frequency Fields. (2007). World Health Organization.

[3] Shah, D. J., Sachs, R. K., & Wilson, D. J. (2012). Radiation-Induced Cancer: A Modern View. *The British Journal of Radiology.* 85:1020. https://doi.org/10.1259/bjr/25026140

[4] Ng, K.H. (2003). Non-Ionizing Radiations – Sources, Biological Effects, Emissions, and Exposures.

[5] Hacıosmanoğlu, T. (2017). Natural and Artificial Radiation Sources and Personal Dose Additives. *Nuclear Medicine Seminars*, 3(3); 166–171. https://doi.org/10.4274/nts.2017.017

[6] Latarjet, R., & Jagger, J. (1995). Rads and Grays: Becquerels and Curies. *Radiation Research,* 141(1); 105. https://doi.org/10.2307/3579098

[7] Yeyin, N. (2015). Biological Effects of Radiation. *Nuclear Medicine Seminars,* 1(3); 139–143. https://doi.org/10.4274/nts.002

[8] Pearce, M. S., Salotti, J. A., Little, M. P., McHugh, K., Lee, C., Kim, K. P. & et al. (2012). Radiation Exposure From CT Scans in Childhood and Subsequent Risk of Leukaemia and Brain Tumours: A Retrospective Cohort Study. *The Lancet,* 380(9840); 499–505. https://doi.org/10.1016/s0140-6736(12)60815-0

[9] Kastan, M. B., & Bartek, J. (2004). Cell-Cycle Checkpoints and Cancer. *Nature,* 432(7015); 316–323. https://doi.org/10.1038/nature03097

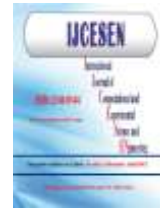[10] Delaney, G., Jacob, S., Featherstone, C., & Barton, M. (2005). The Role of Radiotherapy in Cancer Treatment. *Cancer,* 104(6); 1129–1137. https://doi.org/10.1002/cncr.21324

[11] Mayer, C., Gasalberti, D. P., & Kumar, A. (2023). Brachytherapy. In StatPearls. StatPearls Publishing.

[12] Paunesku, T., & Woloschak, G. E. (2017). Future Directions of Intraoperative Radiation Therapy: A Brief Review. *Frontiers in Oncology,* 7. https://doi.org/10.3389/fonc.2017.00300

[13] Abe, M., & Takahashi, M. (1981). Intraoperative Radiotherapy: The Japanese Experience. *International Journal of Radiation Oncology*Biology*Physics*, 7(7); 863–868. https://doi.org/10.1016/0360-3016(81)90001-8

[14] Kyrgias, G., Hajiioannou, J., Tolia, M., Kouloulias, V., Lachanas, V., Skoulakis, C., et al. (2016). Intraoperative Radiation Therapy (IORT) in Head and Neck Cancer. *Medicine,* 95(50). https://doi.org/10.1097/md.0000000000005035

[15] Harris, E. E., & Small, W. (2017). Intraoperative Radiotherapy for Breast Cancer. *Frontiers in Oncology*, 7. https://doi.org/10.3389/fonc.2017.00317

[16] Akboru, M. H., Dincer, S. T., & Gursel, O. K. (2014). Intraoperative Radiotherapy. *The Medical Journal of Okmeydani Training and Research Hospital,* 29(Supplement 1); 25–34. https://doi.org/10.5222/otd.supp1.2013.025

[17] Şahin, K., & Turan, B. O. (2018). Comparative Analysis of 3D Printer Technologies. *Stratejik ve Sosyal Araştırmalar Dergisi,* 2(2); 97–116. https://doi.org/10.30692/sisad.441648

[18] Nielsen, A. V., Beauchamp, M. J., Nordin, G. P., & Woolley, A. T. (2020). 3D Printed Microfluidics. Annual review of analytical chemistry (Palo Alto, Calif.), 13(1); 45–65. https://doi.org/10.1146/annurev-anchem-091619-102649

[19] Kristiawan, R. B., Imaduddin, F., Ariawan, D., Ubaidillah, & Arifin, Z. (2021). A Review on the Fused Deposition Modeling (FDM) 3D Printing: Filament Processing, Materials, and Printing Parameters. *Open Engineering,* 11(1); 639–649. https://doi.org/10.1515/eng-2021-0063

[20] Pakkanen, J., Manfredi, D., Minetola, P., & Iuliano, L. (2017). About the Use of Recycled or Biodegradable Filaments for Sustainability of 3D Printing. *Sustainable Design and Manufacturing* 2017; 776–785. https://doi.org/10.1007/978-3-319-57078-5_73

[21] Joseph Arockiam, A., Karthikeyan Subramanian, Padmanabhan, R. G., Rajeshkumar Selvaraj, Dilip Kumar Bagal, & Rajesh, S. (2022). A Review on PLA with Different Fillers Used as a Filament in 3D Printing. *Materials Today: Proceedings,* 50;2057–2064. https://doi.org/10.1016/j.matpr.2021.09.413

[22] Jamshidian, M., Tehrany, E. A., Imran, M., Jacquot, M., & Desobry, S. (2010). Poly-Lactic Acid: Production, Applications, Nanocomposites, and Release Studies. *Comprehensive Reviews in Food Science and Food Safety*, 9(5); 552–571. https://doi.org/10.1111/j.1541-4337.2010.00126.x

[23] Farah, S., Anderson, D. G., & Langer, R. (2016). Physical and Mechanical Properties of PLA, and Their Functions in Widespread Applications — A Comprehensive Review. *Advanced Drug Delivery Reviews,* 107; 367–392. https://doi.org/10.1016/j.addr.2016.06.012

[24] Crow S. (1993). Sterilization processes. Meeting the demands of today's health care technology. *The Nursing Clinics of North America,* 28(3); 687–695.

[25] Oth, O., Dauchot, C., Orellana, M., & Glineur, R. (2019). How to sterilize 3D-printed objects for surgical use? An evaluation of the volumetric deformation of 3D-printed GENIOPLASTY Guide in PLA and PETG after sterilization by low-temperature hydrogen peroxide gas plasma. *The Open Dentistry Journal*, 13(1); 410–417. https://doi.org/10.2174/1874210601913010410

[26] Perego, G., Cella, G. D., & Bastioli, C. (1996). Effect of Molecular Weight and Crystallinity on Poly(lactic acid) Mechanical Properties. *Journal of Applied Polymer Science,* 59(1); 37–43. https://doi.org/10.1002/(sici)1097-4628(19960103)59:1<37::aid-app6>3.0.co;2-n

[27] Van de Velde, K., & Kiekens, P. (2002). Biopolymers: Overview of Several Properties and Consequences on Their Applications. *Polymer Testing,* 21(4); 433–442. https://doi.org/10.1016/s0142-9418(01)00107-6

[28] McKeen, L. W. (2014). Plastics Used in Medical Devices. *Handbook of Polymer Applications in Medicine and Medical Devices*, 21–53. https://doi.org/10.1016/b978-0-323-22805-3.00003-7

[29] Levy, Y., Paz, A., Yosef, R. B., Corn, B. W., Vaisman, B., Shuhat, S., et al. (2009). Biodegradable Inflatable Balloon for Reducing Radiation Adverse Effects in Prostate Cancer. *Journal of Biomedical Materials Research Part B: Applied Biomaterials,* 91B(2), 855–867. https://doi.org/10.1002/jbm.b.31467

[30] Melchert, C., Gez, E., Bohlen, G., Scarzello, G., Koziol, I., Anscher, M., et al. (2013). Interstitial Biodegradable Balloon for Reduced Rectal Dose During Prostate Radiotherapy: Results of a Virtual Planning Investigation Based on the Pre- and Post-Implant Imaging Data of an International Multicenter Study. *Radiotherapy and Oncology*, 106(2); 210–214. https://doi.org/10.1016/j.radonc.2013.01.007

[31] Langelaar, M. (2016). Topology optimization of 3D self-supporting structures for additive manufacturing. *Additive manufacturing,* 12; 60-70.

IoT Band: A Wearable Sensor System to Track Vital Data and Location of Missing or Earthquake Victims

Esma Nur SOYSAL[1], Havin GURKAN[2], Emrehan YAVSAN[3]*

[1]Necmettin Erbakan University, Engineering Faculty, Mechatronics Department, 42140, Konya-Turkey
Email: esmanursoysal@hotmail.com - **ORCID:** 0009-0005-6209-7041

[2]Necmettin Erbakan University, Engineering Faculty, Mechatronics Department, 42140, Konya-Turkey
Email: nivahgrk34@gmail.com - **ORCID:** 0009-0007-9120-4146

[3]Tekirdag Namik Kemal University, Department of Electronics and Automation, 59030, Tekirdag-Turkey
***Corresponding Author** : **Email:** eyavsan@nku.edu.tr - **ORCID:** 0000-0001-9521-4500

Abstract:

Natural disasters, especially earthquakes, have caused and still cause serious loss of life in our country. Since many of our cities are located on fault lines, earthquake or collapse risks threaten our lives. In this study, a wearable sensor and tracking system has been developed to prevent or minimize the loss of life after a possible earthquake. The presented system consists of a wristband prototype designed to instantly monitor the vital data and location of victims trapped under the rubble. The wristband prototype includes a GPS module, a temperature sensor and a pulse oximeter. While the vital data of the victim is monitored by the temperature sensor and pulse oximeter, the location information of the victim is received via GPS. The data read from these sensors via a controller is transferred to a display screen through a wireless communication module. A computer and a mobile application were developed as the display screen. A Wi-Fi module was preferred for wireless communication. As an alternative to the Wi-Fi module, a GSM module was added to the wristband prototype. Thus, the order and time of rescue interventions for people trapped under the rubble can be determined. The presented work can be used not only for collapse and earthquake victims but also for Alzheimer's patients or people with poor mental development thanks to the GSM module. In this case, the patient's vital data and location will be transmitted to the user's relatives.

1. Introduction

Natural disasters are a threat to our lives today as well as in the future. Especially earthquakes have taken and continue to take a high number of lives today. If precautions specifically for earthquakes are not increased, these casualties may increase [1]. If the earthquake is considered in 3 stages, precautions should be increased for all 3 stages of a possible earthquake. These stages are 1) before the earthquake, 2) during the earthquake and 3) after the earthquake.

In case of natural disasters, the expeditious identification of individuals who have survived within structures that have collapsed is of the utmost significance. The prevailing approach for searching is reliant upon the accounts of survivors, to ascertain the conceivable existence of casualties beneath the debris. To reduce mortality after a natural disaster, it is important to monitor vital data of a person trapped under rubble [2, 3].

Zhang et al. [4] proposed a system consisting of a CO_2 sensor, a thermal camera and a microphone to detect people trapped under rubble. However, CO_2 detection in open air is difficult. Also, thermal cameras alone are not very reliable in detecting people behind various obstacles such as piles of metal. Instead of these sensors, the vital data of people under the rubble can be tracked with alternative sensors. These sensors are mostly found in health monitoring systems. Demirtas et al. [5] developed a patient monitoring system that enables instant recording of data from biomedical sensors such as ECG, heart rate, temperature, movement, etc. Baig and Gholamhosseini [6] provide an overview of smart health monitoring systems in their

Figure 1. *Workflow schematic of the system*

research. They discuss the design and modeling of smart health monitoring systems and provide an overview of the different types of sensors used in these systems. Pantelopoulos and Bourbakis [7] conducted a survey on wearable sensor-based systems for health monitoring and prognosis. They provide an overview of the different types of wearable sensors used in health monitoring systems and discuss the challenges associated with these systems. Anikwe et. al. [8], synthesized research efforts on mobile and wearable sensors for health monitoring. They categorized health monitoring systems as dual sensor-based studies that utilized two sensor modules for various health monitoring researches. Kaur et. al. [9], explored wearable sensors for heart rate, pulse rate, ECG, blood pressure, and body temperature for health monitoring purposes. They also discussed personalized medicine and cancer biomarkers in the case of different diseases. Lou et. al [10], discussed wearable health monitoring systems have emerged as the subsequent epoch of personal portable devices for telemedicine implementation. These devices operate on the principle of supervising various types of biological signals exuded by human beings, including but not limited to saliva, urine, respiration, and cutaneous perspiration. Although for different purposes, most of the sensors preferred in health monitoring systems in the literature can be used to detect and rescue earthquake victims under the rubble.

In this study, a wearable sensor and tracking system has been prototyped to prevent or minimize possible loss of life after an earthquake. The sensors on the system consist of a GPS module, an IR temperature sensor and a pulse oximeter. The data read from these sensors through a controller is transferred to a tracking or a monitoring screen via a wireless communication protocol. A mobile application interface was developed as a tracking screen. Sensor data can also be monitored from a web interface created in addition to the mobile application.

2. Material and Methods

The working diagram of the proposed system is given in Fig. 1. The prototyping process was carried out based on this scheme. In the first stage, the sensors in the system were read separately in different scenarios. Thus, sensor data was verified.
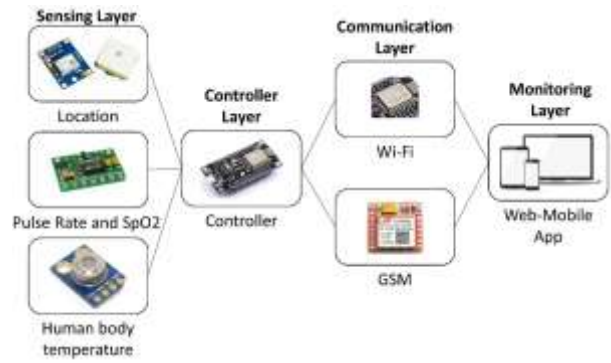
The system is divided into sensing, control, communication and display layers. The prototyping progressed through these layers.

2.1 Sensing Layer

In the first step of the prototyping process, the sensor components in the system were read through a controller. ESP8266NodeMCU was preferred as the controller [11]. Fig. 2 shows the data received from GPS, MAX30102 pulse oximeter [12] and MLX90614 [13] temperature sensor respectively.

(a) GPS

(b) Hearth Rate (Beat Per Minute) and percentage of oxygen in blood (SpO2)

```
Room Temp = 26.07
Object temp = 36.41
Room Temp = 26.11
Object temp = 36.37
Room Temp = 26.15
Object temp = 36.55
Room Temp = 26.17
Object temp = 36.93
Room Temp = 26.21
Object temp = 36.17
```

(c) Temperature (°C)

Figure 2. *Sensors data for the validation. (a) GPS data, MAX30102 pulse oximeter data on LCD, and (c) MLX90614 temperature sensor data*

2.2 Wireless Data Transfer and Web Interface

Wi-Fi [14] was preferred to transfer the data of the sensors in Fig. 2. For this, instead of using an external module, the internal Wi-Fi module on the NodeMCU development board was used.

```
🔗  https://espdeneme-1b396-default-rtdb.firebaseio.com

⚠  Your security rules are defined as public, so anyone can steal, moo

https://espdeneme-1b396-default-rtdb.firebaseio.com/
    ── BPM: 70
 ▼  ── GPS
        ── latitude: 37.93544
        ── longitude: 32.49866
    ── SpO2: 94
    ── body temperature: 36.770011902
```

Figure 3. *Monitoring sensor data from Firebase database*

The sensor data was sent synchronously via Wi-Fi to the interface created in the real-time database (firebase) [1, 15]. This interface is shown in Fig. 3. In Fig. 3, synchronously read heartbeat, GPS, SpO2 and, body temperature data can be monitored from the firebase interface.

2.3 Mobile Application

A mobile application has been realized in order to monitor the data on the web interface from mobile devices other than PCs. The mobile application was developed in App Inventor environment [16]. The data in firebase is sent to this application in real time. The application was tested on a smart mobile device with Android operating system. The mobile application and its pages are depicted in Fig. 4.
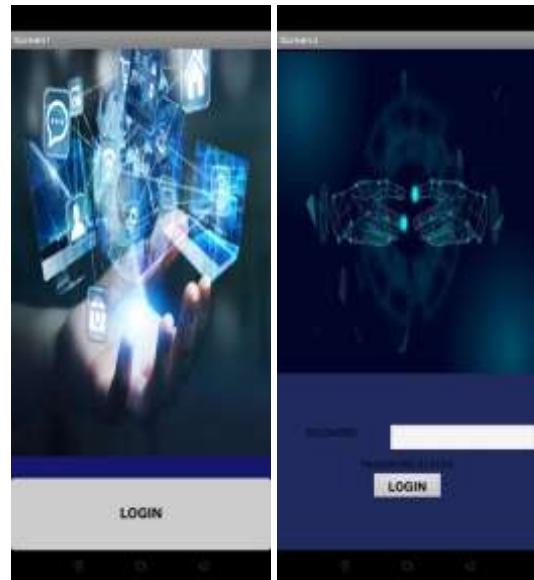
(a)
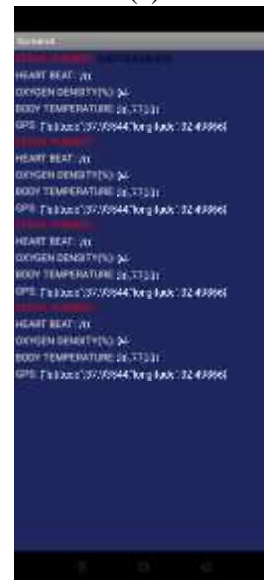
(b)

Figure 4. *The mobile application pages (a) login page and (b) multi-user data*

2.4 Prototyping

The first prototype was established by integrating the presented system components on a platform that can be wearable on the wrist. This prototype is provided in Fig. 5. The proposed design is available for further development and the efforts to improve this design are ongoing. Apart from the controller and GPS module, a GSM module is integrated on the top side of the first prototype in Fig. 5. Through this module, when there is a disconnection in the Wi-Fi, an SMS notification can be sent over the GSM line. Besides, the Wi-Fi connection can be observed by the user wearing the wristband

(a)

(b)

(c)

Figure 5. *The first prototype. (a) top, (b) bottom and (c) wrist-worn view of the prototype.*

by means of the LED on the same side. In the event of a possible wreck, this person can press the button next to the led when he/she sees that there is no internet connection and can share his/her instant vital data with smart mobile devices registered. Fig. 6 demonstrates the data sent by the wristband wearer over a GSM line to a pre-registered phone number. The prototype was tested indoor in a home environment. Sensor data was sent to the web interface and the mobile application from different rooms of the house. As a result of this transmission, ±2 m accurate GPS data was obtained. GPS data was verified via Google Maps. Other sensor data was transmitted synchronously without any delay. The measurements were repeated many times and similar measurements were obtained.
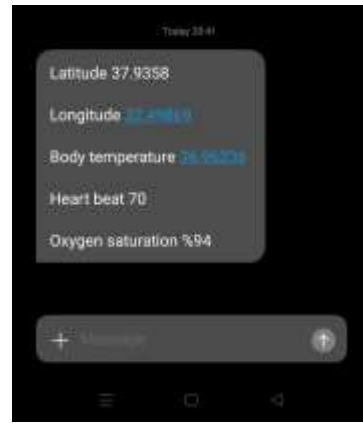
Figure 6. *SMS with vital data of the wristband wearer*

3. Results and Discussions

In the literature, the number of studies in which the sensors on the proposed prototype are combined is scarce. Furthermore, in the literature and in the commercial product market, only bluetooth or Wi-Fi connection can be provided from the related devices. In this study, as an alternative to Wi-Fi connectivity, the ability to send SMS through GSM is addressed. Most of the studies in the literature have been developed for monitoring diseases such as Covid-19 [12, 17] or blood pressure [18, 19]. In this study, a wristband prototype is proposed to prevent or reduce the loss of life after an earthquake. However, the prototype can also be used to tracking Alzheimer's patients or people with poor mental development. Thus, these people can be prevented from getting lost.

4. Conclusions

In this study, a wristband prototype with a GPS, an IR temperature sensor and a pulse oximeter module is proposed to prevent the loss of life of individuals trapped under the rubble after an earthquake. The proposed prototype is garage-made and tested in a closed indoor environment. The synchronized data provided by the prototype was monitored from a real-time database. A mobile application was developed to facilitate the tracking of this data. The database on the web and the mobile application were accessible from an external source, e.g. by a rescue team. A GSM module was embedded as a backup to the web connection. The prototype is able to instantly measure the user's location, body temperature and pulse rate. The measured values can be shared with external users via a web interface, a mobile application and an SMS when there is no web connection.

Hence, people under the rubble can be intervened as soon as possible and loss of life can be reduced.
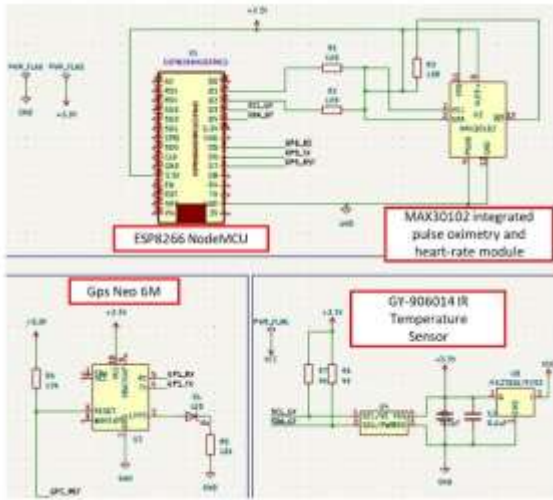
(a)
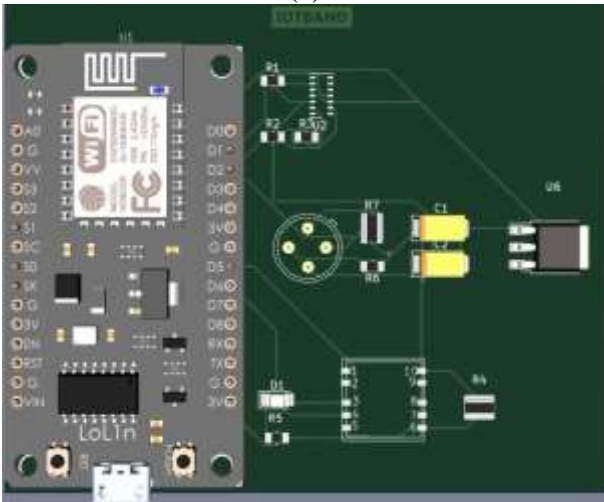
(b)

Figure 7. *Electronic circuit designs. (a) schematic and (b) PCB drawing of the electronic circuit design to develop the prototype*

As future studies, electronic circuit designs are ongoing to improve the mechanics of the prototype. Within the scope of these studies, one of the circuit designs realized through the open source KiCad [20] program is given in Fig. 7. In addition, work is being carried out to improve the web interface and to add features such as logging sensor data and graphical display to this interface.

Author Statements:

- **Ethical approval:** The conducted research is not related to either human or animal use.

- **Conflict of interest:** The authors declare that they have no known competing financial interests or personal relationships that could have appeared to influence the work reported in this paper

- **Acknowledgement:** The authors declare that they have nobody or no-company to acknowledge.

- **Author contributions:** The authors declare that they have equal right on this paper.

- **Funding information:** The authors declare that there is no funding to be acknowledged.

- **Data availability statement:** The data that support the findings of this study are available on request from the corresponding author. The data are not publicly available due to privacy or ethical restrictions.

References

[1] Maulidi, R., Kristanto, B. K., & Listio, Y. D. (2020). Earthquake Information Push Notification System in Android Application Using Google Firebase. IJISCS *International Journal of Information System and Computer Science*, 4(2), 98-112.

[2] https://spinoff.nasa.gov/Spinoff2018/ps_1.html. Access Date: 1 April 2023.

[3] Akansel, V. H., & Özkula, G. The 30 October 2020, Mw 6.6 Sisam (Samos) Earthquake: Interpretation of Strong Ground Motions and Post-Earthquake Condition of Nearby Structures. *European Journal of Engineering and Applied Sciences*, 4(2), 66-89.

[4] Zhang, D., Sessa, S., Kasai, R., Cosentino, S., Giacomo, C., Mochida, Y., & Takanishi, A. (2018). Evaluation of a sensor system for detecting humans trapped under rubble: A pilot study. *Sensors,* 18(3), 852.

[5] Demirtaş, M., Tulum, G., Sağbaş, M., & Ayten, U. Multi platform online patient monitoring system. *Sakarya University Journal of Science,* 22(1), 1-7.

[6] M.M. Baig and H. Gholamhosseini, "Smart Health Monitoring Systems: An Overview of Design and Modeling," *Journal of Medical Systems.*

[7] A. Pantelopoulos, N.G. Bourbakis, "Survey on Wearable Sensor-Based Systems for Health Monitoring and Prognosis," *IEEE Transactions on Systems Man and Cyberbetics-Part* C: Applications and Review.

[8] Anikwe, C. V., Nweke, H. F., Ikegwu, A. C., Egwuonwu, C. A., Onu, F. U., Alo, U. R., & Teh, Y. W. (2022). Mobile and wearable

sensors for data-driven health monitoring system: State-of-the-art and future prospect. *Expert Systems with Applications*, 117362.

[9] Kaur, B., Kumar, S., & Kaushik, B. K. (2023). Novel wearable optical sensors for vital health monitoring systems—A review. *Biosensors,* 13(2), 181.

[10] Lou, Z., Wang, L., Jiang, K., Wei, Z., & Shen, G. (2020). Reviews of wearable healthcare systems: Materials, devices and system integration. *Materials Science and Engineering: R: Reports,* 140, 100523.

[11] Aziz, D. A. (2018). Webserver based smart monitoring system using ESP8266 node MCU module. *International Journal of Scientific & Engineering Research*, 9(6), 801-808.

[12] Turanli, M., Ilhan, I., & Yavsan, E. (2022) Pulse Oximeter Based System Prototype to Monitor Vital Signs of COVID-19 Patients in Quarantine. *3rd International Conference on Engineering and Applied Natural Sciences (ICEANS'22),* pp. 1273-1276. July 20-23, 2022, Konya, Turkey.

[13] Jin, G., Zhang, X., Fan, W., Liu, Y., & He, P. (2015). Design of non-contact infra-red thermometer based on the sensor of MLX90614. *The Open Automation and Control Systems Journal*, 7(1).

[14] Kurniawan, A. (2019). Internet of Things Projects with ESP32: Build exciting and powerful IoT projects using the all-new Espressif ESP32. *Packt Publishing* Ltd.

[15] Oo, Z., Lai, T., Ko, S., & Moe, A. (2019). IoT based Weather Monitoring System Using Firebase Real Time Database with Mobile Application. *In International Symposium on Environmental-Life Science and Nanoscales Technology.*

[16] Patton, E. W., Tissenbaum, M., & Harunani, F. (2019). MIT app inventor: Objectives, design, and development. *Computational thinking education,* 31-49.

[17] Al Bassam, N., Hussain, S. A., Al Qaraghuli, A., Khan, J., Sumesh, E. P., & Lavanya, V. (2021). IoT based wearable device to monitor the signs of quarantined remote patients of COVID-19. Informatics in medicine unlocked, 24, 100588.

[18] Ilhan, I., Yıldız, İ., & Kayrak, M. (2016). Development of a wireless blood pressure measuring device with smart mobile device. *Computer methods and programs in biomedicine*, 125, 94-102.

[19] Ilhan, I. (2018). Smart blood pressure holter. *Computer Methods and Programs in Biomedicine*, 156, 1-12.

20] Kanagachidambaresan, G. R. (2021). Introduction to KiCad Design for Breakout and Circuit Designs. In Role of Single Board Computers (SBCs) in rapid IoT Prototyping (pp. 165-175). Cham: Springer International Publishing.
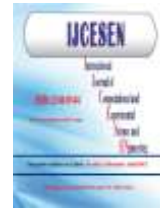
Emission and Lubrication Performance of Hazelnut Oil as A Lubricant

Arzu KEVEN[1*], Cengiz ONER[2]

[1] *Dep. of Vehicle and Transp. Technol., Golcuk Voc. High School, Kocaeli University, Kocaeli, Turkey.*
* **Corresponding Author** : **Email:** arzu.keven@kocaeli.edu.tr - **ORCID:** 0000-0003-0040-9167

[2]*Dep. of Mechanical Engineering, Bingol University, Bingol, Turkey.*
Email: coner@bingol.edu.tr - **ORCID:** 0000-0002-3278-2831

Abstract:

The aim of this study is to search the tribological and emission performances of hazelnut oil as a lubricant in one cylinder two-stroke gasoline engine and simulation-testing machine. The tribological and emission performances of mineral oil and hazelnut oil as lubricant were compared. In the experiments, simulation-testing machine and one cylinder two-stroke gasoline engine were used to determine the tribological performance of these two lubricants. The wears on the surfaces of cylinder were analyzed to examine the lubricant performances. In addition to lubrication performance, exhaust emissions of the lubricants were also measured. To observe the effects of different kinds of cylinder surface materials, TiN, CrN and gray cast iron coated cylinder surfaces were used in simulation testing machine. The wear as well as the soot formation on the cylinder surfaces increased when hazelnut oil was used as the engine lubricant. However, hazelnut oil exhibited good lubrication properties in simulation testing machine. When hazelnut oil was used, CO and HC emissions increased while CO_2 emission decreased.

1. Introduction

Turkey is an important hazelnut producer country in the world. This makes it a popular choice as alternative fuel and lubricant. The rise in energy demand and the finite reserves have made the renewable alternative energy sources, the high efficiency of energy conversions, the minimal harmful effects to the environment and the recovery of previously unused energies very important [1, 2, 3, 4]. As can be seen in literature, investigations of harmless, alternative, low emissions fuels to use in energy producing equipment are the real problem must be solved [5, 6, 7]. The moving parts of a two-stroke engine are lubricated either by adding lubricant into the fuel of by pumping oil from a separate tank. Two-stroke internal combustion engines produce more contaminations and emission than the four-stroke ones, because of oil burning in the combustion chamber [8]. Since the ineffective lubrication caused from different lubricant system, the wear occurred in a two-stroke engine is more than that of a four-stroke one [9]. The wear and friction mechanism of a fuel engine is very important and essential topic to study on. The new methods have been improved to reduce friction and wear in

the surface of the cylinder and the piston ring of the internal combustion engines therefore various lubricating oil were produced. There is an increasing interest about using of vegetable oil which can be played a very important role to substitute the petroleum lubricant, as it possesses lots of advantages over base lubricant like environmentally friendly, renewability, less toxicity, biodegradability and so on [10]. Some authors suggest the importance of the use of vegetable oils for the engine wear because of the mineral oil derived from petroleum oil is toxic and non-biodegradable [11]. Masjuki *et al* [12] used mineral oil-based lubricants and palm oil in a two-stroke single cylinder gasoline engine. In exhaust emission tests, the engine was operated at different loads while constant load was used in wear tests. The results of the experiment showed that the palm oil-based lubrication oil has a better performance in wears, and the mineral oil-based lubricating oil showed better performance about the friction. Also, showed that the palm oil-based lubricant is better effective in reducing of CO and HC emission levels. By using a universal wear and friction test machine to simulate a two-stroke internal combustion engine bench wear test is done. Igartua *et al* [8] investigated alternative eco-friendly

lubes for clean two-stroke internal combustion engines. By selection of optimal synthetic esters base oil high performance lubricant with ethanol-containing fuels was improved. From this lubricant, very good wear resistance obtained, also ashless and low carbon soot deposit formation were happened. Jayadas *et al* [10] investigated tribological performance of coconut oil as lubricant. They evaluated the tribological properties of coconut oil by using a four-ball tester and a test equipment to test the wear of a two-stroke engine. The antiwear/extreme pressure additive influence on the tribological performance of coconut oil was investigated. The AW/EP addition improved the lubricity of coconut oil and decreased the wear on the surface considerably. İşler *et al* [13] investigated different oils for 10w40 motorcycle engine with four strokes. Mineral, bio mineral, synthetic, biosynthetic based oils were prepared and the lubricant properties are showed in their study. The best lubricity values for engine oils were obtained for biosynthetic lubricants at ambient temperatures. In this paper, it was concluded that 5% addition of canola methyl ester to the motor oil would give a lot of advantages to national renewable resources then importing crude oil. Tung and Gao [14] simulated the tribological characteristics using a modified friction machine with high frequency reciprocating. In a fixture holder reciprocating against the cylinder liner segment a section of piston ring installed. The ring coatings with thermal-sprayed CrN and physical vapor deposited diamond-like-carbon. The test results showed that compared to CrN coated piston ring, Diamond-like-carbon (DLC) coating decreased the wear of the cylinder surface but piston ring did not change. The micro-hardness and corrosion resistance of CrN coated cylinder is higher compared with gray cast iron cylinder, moreover the friction coefficient of CrN coated cylinder is smaller than that of gray cast iron cylinder [15, 16, 17]. In this study, to determine the tribological and emission performances of mineral oil and hazelnut oil by using in one cylinder two-stroke gasoline engine and in a simulation-testing machine as lubricant were aimed. Moreover, analyzing the wears on the TiN, CrN and gray cast iron coated cylinder surfaces and the soot formation on the cylinder surfaces were aimed.

2. Material and Methods

In the experiments, one cylinder two-stroke air cooled gasoline engine and simulation testing machine were used to determine the tribological performance of hazelnut oil. The two-stroke gasoline engine is an engine with displacement of 98.2 cc, maximum power of 3.5 hp and fuel/oil ratio of 20/1.

The gasoline engine was loaded by pumping water from the water reservoir. In the two-stroke gasoline engine, lubrication was occurred by using mixture of oil and gasoline. The mixture of oil and gasoline burnt in combustion chamber. The gasoline engine is tested for 100 hours by using mineral oil and hazelnut oil as lubricant. After the experiments, the surfaces of cylinder were examined by using scanning electron microscopy to investigate the wear. In this study, the simulation testing machine was designed to obtain the wear mechanism similar to two-stroke gasoline engine. The simulation testing machine is shown in Fig.1.

Figure 1. *Simulation testing machine.*

In the simulation testing machine, the pressure applied by the piston ring to cylinder surface was 3.436 MPa. This testing machine was operated at constant load of 10 N and constant speed of 147 rpm. The gray cast iron, TiN and CrN coated cylinder samples were used as cylinder sample in testing machine. The cylinder samples were coated with 2 μm thickness using PVD (physical vapor deposition) technique. Stroke length of the cylinder sample is 120 mm. The simulation testing machine was run 40 hours for each cylinder material including gray cast iron, TiN and CrN coatings. To simulate the engine operating conditions, the temperatures of the lubricants and surface materials were increased to 200 °C by using a heater. The contact area between piston rings and cylinder surface was lubricated by pumping hazelnut oil and mineral oil. After the experiments in the testing machine completed, the wear losses in the cylinder samples were measured by using a sensitive balance.

3. Results and Discussions

3.1. Experimental studies in the two-stroke gasoline engine

Two-stroke gasoline engine was operated with mineral oil and hazelnut oil as lubricant at constant

speed of 2800 rpm and constant load for wear tests. Fuel-oil ratio of engine was 20:1. After the experiments for both oils, the cylinder surfaces were examined. When mineral oil and hazelnut oil were used as lubricant, the situations of cylinders from two-stroke engine are given in Fig. 2 and Fig. 3, respectively. When hazelnut oil was used, wear and soot amount on the cylinder surface increased compared to mineral oil as seen in the Fig. 2 and Fig. 3. If the cylinder surfaces are examined carefully, cracks on these surfaces will clearly be seen in the Fig. 2 and Fig. 3. The wear and soot on the cylinder surfaces may be an indicator of abnormal combustion caused from hazelnut oil.

Figure 2. *The surface of cylinder when mineral oil when was used as lubricant.*

The cetane number of hazelnut oil was measured as 52. The higher cetane number (the lower octane number) of hazelnut oil may cause autoignition of fuel-air mixture. In a gasoline engine, autoignition causes abnormal combustion. In addition to cetane number, the carbon number of hazelnut oil was determined. The carbon number measured of hazelnut oil was 56. This carbon content of hazelnut oil may be caused soot formation. Properties of hazelnut oil and mineral oil were given Table 1. In the experiments, scanning electron microscopy (SEM) was used to understand the tribological performance of hazelnut oil and mineral oil.

Table 1. *Properties of hazelnut oil and mineral oil*

Property	Hazelnut oil	Mineral oil
Viscosity (cst) at 40 ºC	35	40
Viscosity (cst) at 100ºC	6.5	7.1
Carbon number	56	35

Figure 3. *The surface of cylinder hazelnut oil was used as lubricant.*

SEM analyses of the cylinder parts obtained the middle of the stroke when mineral oil and hazelnut oil were used as lubricant, are given in Fig. 4 and Fig. 5, respectively. These SEM analyses showed that wear on the surface of cylinder increased when hazelnut oil was used as lubricant as can be seen in Fig. 5. In addition to wear, Fig. 5 showed that hazelnut oil caused surface cracks on cylinder walls. SEM analyses of the surfaces obtained from near TDC (top dead center) of the cylinder when mineral oil and hazelnut oil were used, are given in Fig. 6 and Fig. 7, respectively. When SEM photomicrographs were compared, it was seen that wear of surface in TDC was more than that of surface in middle of stroke as can be seen in Fig. 6 and Fig. 7. From Fig. 7, it is understood that hazelnut oil caused more wear on cylinder surface than mineral oil as can be seen clearly. The wear and cracks on the surface of cylinder may be caused from worse lubrication properties of hazelnut oil compared to mineral oil. One of the most important factors which are effective lubricity performance of a lubricant is its sulfur content [16]. Sulfur content of lubricants and gasoline is given in Table 2. From Table 2, hazelnut oil has less sulfur content than mineral oil as can be seen. In this case, lubricant property of hazelnut oil was decreased. In Table 3, surface roughness values of the cylinder are presented. Table 3 showed that the surface roughness increased when hazelnut oil was used as lubricant. In addition, there was more surface roughness in TDC.

Table 2. *Sulfur content of lubricants and fuel*

Lubricants and fuel	Sulfur content (ppm)
Mineral oil	>990 ppm
Gasoline	9,1 ppm
Hazelnut oil	4,3 ppm

Table 3. *The surface roughness of the cylinder when mineral oil and hazelnut oil were used as lubricant.*

Cylinder surface	In used mineral oil surface roughness (Ra)	In used hazelnut oil surface roughness (Ra)
TDC	0,51 μm	0,67 μm
Mid-stroke	0,45 μm	0,50 μm
BDC	**0,41 μm**	**0,43 μm**

Figure 6. *SEM analyses of TDC (top dead center) of cylinder when mineral oil was used as lubricant.*

Figure 4. *SEM analyses of the middle part of the cylinder when mineral oil was used as lubricant.*
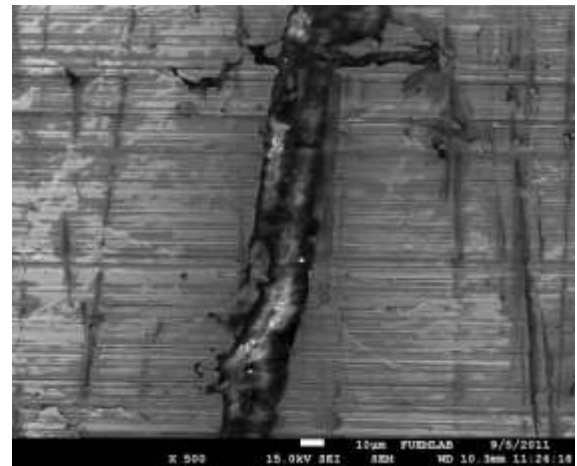
Figure 7. *SEM analyses of TDC (top dead center) of cylinder when hazelnut oil was used as lubricant.*

Figure 5. *SEM analyses of the middle part of cylinder when hazelnut oil was used as lubricant.*

3.2. Experimental studies in the simulation testing machine

Simulation testing machine was designed to simulate wear mechanism in internal combustion engine.

This testing machine was operated at regular interval (10 h). TiN and CrN coating in cylinder samples were used for reducing wear. At first, testing machine was operated by using gray cast iron cylinder sample. Then, testing machine was operated by using cylinder samples coated with CrN and TiN, respectively. The contact area between piston rings and cylinder surface was lubricated by pumping hazelnut oil and mineral oil. After the experiments, tested cylinder samples were cleaned using acetone and dried. These cylinder samples were weighted by using a sensitive balance to determine the wear loss. The weight losses of cylinder samples are given in Fig. 8 and Fig. 9 as can be seen. These figures showed that weight loss of cast iron cylinder sample was more than those of samples coated with CrN and TiN. In addition, the weight loss of cylinder sample coated with TiN was slightly more than that of sample coated with CrN. The properties of CrN and TiN are given in Table 4 as can be seen. From Table 4, friction coefficient of TiN was more than CrN as its seen clearly.

Table 4. Properties of CrN and TiN

Chemical composition	CrN	TiN
Coating range (μm)	2	2
Hardness, kg/mm^2	2200±400	2900±200
Friction coefficient	0,5	0,66
Surface roughness, Ra	0,2	0,2
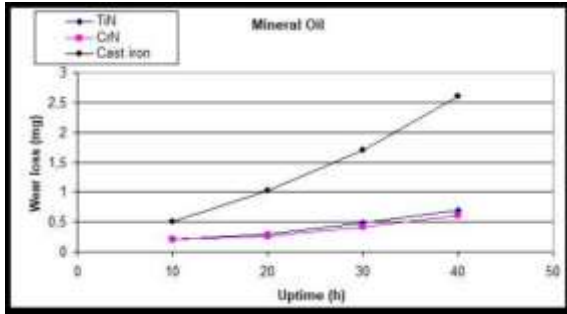
Figure 8. *Weight loss of cylinder samples when mineral oil was used.*

The more surface friction coefficient, the more wear. The wear resistance of cylinder samples coated CrN and TiN was more than that of cast iron cylinder sample. When Fig. 8 and Fig. 9 were compared with each other it was seen that hazelnut oil exhibited wear loss similar to mineral oil. The experimental results exhibited that hazelnut oil was not a good lubricant in two-stroke gasoline engine, but hazelnut oil was as a good lubricant as mineral oil in simulation testing machine. From table 1, viscosity change with temperature of hazelnut oil is similar to mineral oil as can be seen. Due to this viscosity property of hazelnut oil, it may be occurred as good a lubricant film as mineral oil between the piston ring and cylinder sample.
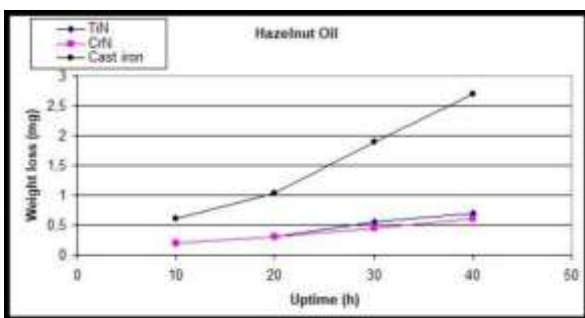
Figure 9. *Weight loss of cylinder samples when hazelnut oil was used.*

3.3. Exhaust emissions

In two-stroke gasoline engine, exhaust emission values were measured at constant speed of 2800 rpm. CO and CO_2 emissions are given in Fig. 10 and Fig. 11, respectively. It is known that CO emissions are formed because of incomplete combustion and dissociation of CO_2. When using hazelnut oil, CO emission increased while CO_2 emission decreased as can be seen clearly in Fig. 10 and Fig. 11. In addition to CO and CO_2, as can be seen in Fig. 12, hazelnut oil caused more HC formation than mineral oil. CO and HC emissions are the indicators of incomplete combustion. This incomplete combustion may be caused from knock resulting from low octane number of hazelnut oil compared to mineral oil.
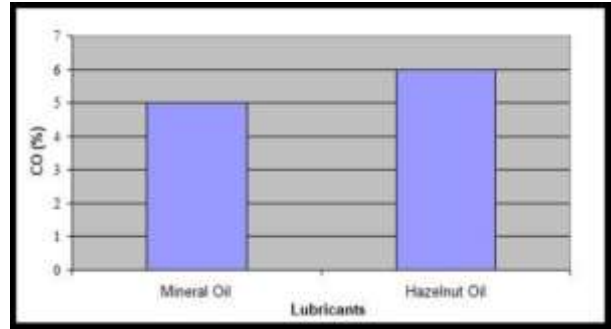
Figure 10. *CO emissions measured at 2800 rpm.*
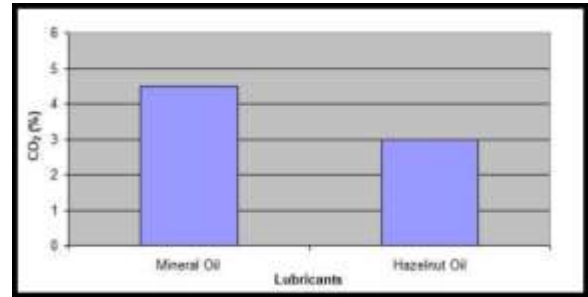
Figure 11. *CO_2 emissions measured at 2800 rpm.*
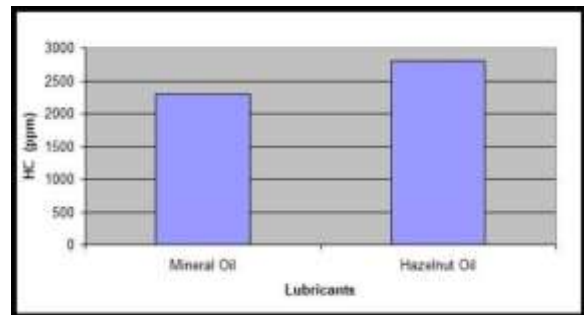
Figure 12. *HC emissions measured at 2800 rpm.*

4. Conclusions

In one cylinder-two-stroke gasoline engine, the analysis of SEM and surface roughness value exhibited that hazelnut oil caused more wear than mineral oil. The sulfur content, which one of most important parameters in terms of lubricity, of a mineral oil was much higher than that of hazelnut oil. As the result of low sulfur content, the lubricity performance of hazelnut oil was worse than that of mineral oil. In addition to wear, soot amount increased and cracks occurred in the surface of cylinder when hazelnut oil was used as lubricant The exhaust emission performance of hazelnut oil is not

as good as mineral oil. When using hazelnut oil, CO and HC emission increased while CO_2 emission decreased. Mineral oil caused more good combustion within cylinder than hazelnut oil. The most sulfur content was found in mineral oil. This case exhibited that lubricant property of mineral oil was better than hazelnut oil. The experimental results demonstrated that are not useful hazelnut oil as lubricant in two-stroke gasoline engine. In the simulation testing machine, the best tribological properties were found in CrN coating. The weight loss of the TiN sample was slightly more than that of CrN sample. Hazelnut oil occurred as nearly good a lubricant film as mineral oil between two metal surfaces in testing machine. This study showed that hazelnut oil was not a good lubricant in two-stroke gasoline engine due to increasing wear and cracks on the cylinder surfaces while it was as a good lubricant in simulation testing machine.

Author Statements:

- **Ethical approval:** The conducted research is not related to either human or animal use.
- **Conflict of interest:** The authors declare that they have no known competing financial interests or personal relationships that could have appeared to influence the work reported in this paper
- **Acknowledgement:** The authors declare that they have nobody or no-company to acknowledge.
- **Author contributions:** The authors declare that they have equal right on this paper.
- **Funding information:** The authors declare that there is no funding to be acknowledged.
- **Data availability statement:** The data that support the findings of this study are available on request from the corresponding author. The data are not publicly available due to privacy or ethical restrictions.

References

[1]Keven A., Karaali R. (2015). Investigation of an Alternative Fuel for Diesel Engines. *Acta Physica Polonica A*, 128(2B);282 – 286. DOI: 10.12693/APhysPolA.128.B-282

[2]Şanlı, H., Alptekin, E., Çanakç, M. (2022). Using low viscosity micro-emulsification fuels composed of waste frying oil-diesel fuel-higher bio-alcohols in a turbocharged-CRDI diesel engine, *Fuel,* 308;1-13.

[3]Karaali, R. (2016). Thermodynamic Analysis of a Cascade Refrigeration System. *Acta Phys. Pol. A* 130(1);101-106. DOI:10.12693/APhysPolA.130.101

[4]Alptekin, E., Şanlı, H., Çanakç, M. (2019). Combustion and performance evaluation of a common rail DI diesel engine fueled with ethyl and methyl esters, *Applied Thermal Engineering*, 149; 180-191. https://doi.org/10.1016/j.applthermaleng.2018.12.042

[5]Karaali, R. (2010). *Thermoeconomic optimization of cogeneration power plants* (Doctoral dissertation, PhD Thesis. Kocaeli Univ).

[6]Şanlı, H. (2018). An experimental investigation on the usage of waste frying oil-diesel fuel blends with low viscosity in a Common Rail DI-diesel engine. *Fuel,* 222;434-443. DOI: 10.1016/j.fuel.2018.02.19

[7]Karaali R., Öztürk İ.T. (2017). Performance Analyses of Gas Turbine Cogeneration Plants. *ISI Bilimi ve Teknigi Dergisi-Journal of Thermal Science and Technology*. 37(1);25 – 33.

[8]Igartua, A., Nevshupa, R., Fernandes, X., Conte M., Zabala, R., Bernaola, J., Zabala, P., Kuther, R., Rausch, J. (2011). Alternative eco-friendly lubes for clean two-stroke engines. *Tribology International*. 44;727-736.

[9]Tan, Y.M., Ripin, Z.M. (2010). Frictional behavior of piston rings of small utility two stroke engine under secondary motion of piston. *Tribology International*. 42;561-568. DOI: 10.1016/j.triboint.2010.12.009

[10]Jayadas, N.H., Nair, K.P., Ajithkumar, G. (2007). Tribological evaluation of coconut oil as an enviroment-friendly lubricant. *Tribology International*. 40;350-354. https://doi.org/10.1016/j.triboint.2005.09.021

[11]Wander, P.R., Altafini, C.R., Colombo, A.L., Perera, S.C. (2011). Durability studies of mono-cylinder compression ignition engines operating with diesel, soy and caster oil methyl esters. *Energy*. 36;3917-3923. https://doi.org/10.1016/j.energy.2010.10.037

[12]Masjuki, H.H., Maleque, M.A., Kubo, A., Nonaka ,T. (1999). Palm oil and mineral oil based lubricants—their tribological and emission performance. *Tribology International*. 32;305–314. https://doi.org/10.1016/S0301-679X(99)00052-3

[13]Işler, A., Yakaboylu, O., Alyakut, T., Karaosmanoğlu F. (2012). Bioalternatives for four stroke motorcycle engine oils. *Industrial lubrication and tribology*. 64;54-59.

[14]Tung, S.C., Gao, H. (2003). Tribological characteristics and surface interaction between piston ring coatings and a blend of energy-conserving oils and ethanol fuels. *Wear*. 255;1276-1285. https://doi.org/10.1016/S0043-1648(03)00240-0

[15]Hazar, H. (2004). The experimental investigation of wear behavior or a diesel engine with cylinder having ceramic coated surface. *PhD Thesis, Firat University Graduate School of Natural and Applied Sciences,* Elazig.

[16]Owen, K., Coley, T. (1995). *Automotive Fuel Reference Book.* Second Edition, SAE.

[17]Shahabuddin M., Masjuki, H.H., Kalam, M.A. (2013). Experimental investigation into tribological characteristics of bio-lubricant formulated from Jatropha oil. *Procedia Engineering*. 56; 597-606. https://doi.org/10.1016/j.proeng.2013.03.165

Optimizing Infill Parameters for Improved Mechanical Performance and Cost Savings in Additive Manufacturing

Volkan ARIKAN*

Osmaniye Korkut Ata University, Department of Mechanical Engineering, 80000, Osmaniye, Turkey
* **Corresponding Author**: **Email:** volkanarikan@osmaniye.edu.tr - **ORCID:** 0000-0002-6102-6584

Abstract:

In this study, compression tests were performed on the samples produced with PLA filament with different infill parameters and infill densities by additive manufacturing method and their mechanical performances & static energy absorption capabilities were evaluated. According to the results obtained, it was determined that the samples with triangular and tri-hexagonal infill parameters performed better and it has been shown that time, material and energy can be saved without losing materials mechanical performance.

1. Introduction

3D printing, also known as additive manufacturing, is a process of creating a physical object from a digital model by building it up layer by layer. The first patent for a 3D printing process was filed in 1986, but the technology has been in development for much longer than that. One of the earliest 3D printing techniques, known as stereolithography, was developed in the 1980s by Chuck Hull [1]. This process involved using a laser to cure layers of photopolymer resin, creating a solid object from a pool of liquid. Other early 3D printing techniques included selective laser sintering, which used a laser to fuse particles of plastic, metal, or ceramic powder into a solid object, and fused deposition modeling, which extruded layers of melted plastic to build up an object.

Over the years, 3D printing technology has continued to evolve and improve. Today, there are many different types of 3D printers available, ranging from small desktop models to industrial-scale machines. They can use a variety of materials, including plastics, metals, ceramics, and even living cells, to create a wide range of objects [2]. 3D printing has become increasingly popular in recent years and has a variety of applications, including

prototyping, manufacturing, and even creating custom prosthetics and other medical devices.

Traditional manufacturing methods involve the removal of material to shape a part or product, while additive manufacturing methods involve the addition of material to build a part or product layer by layer. This fundamental difference leads to several other differences between the two approaches: complexity of shape, material options, lead time, cost, waste, accuracy and design freedom. There are both positive and negative aspects to each of these methods. Some of the positives include the ability to create complex and customized objects, the potential for mass customization and on-demand production, and the ability to use a wide range of materials. However, there are also some negative aspects to consider, such as the high cost of some 3D printing systems and the relatively slow speed of the printing process. Additionally, 3D printed objects may not have the same level of strength and durability as objects made using traditional manufacturing methods. There are several different methods used in additive manufacturing, also known as 3D printing. Some of the most common methods include: Stereolithography (SLA), Selective laser sintering (SLS), Fused deposition modeling (FDM),

Digital light processing (DLP), Powder bed fusion (PBF), Material jetting, Sheet lamination [3-6]
Additive manufacturing can use a wide range of materials, including plastics, metals, ceramics, and composite materials [7]. Some common materials used in additive manufacturing given in Table 1. It's worth noting that the material choices for additive manufacturing are constantly expanding, and new materials are being developed and introduced all the time.

There are several factors that can influence the mechanical properties of samples produced with additive manufacturing technology. Some of the most important factors include: material, process parameters, microstructure, part geometry, post-processing [8,9]. Overall, the mechanical properties of objects produced using additive manufacturing technology can be influenced by a combination of these and other factors. It is important to carefully consider these factors in order to optimize the mechanical performance of the finished object. There are studies on this subject in the literature and different materials and different production parameters have been evaluated.
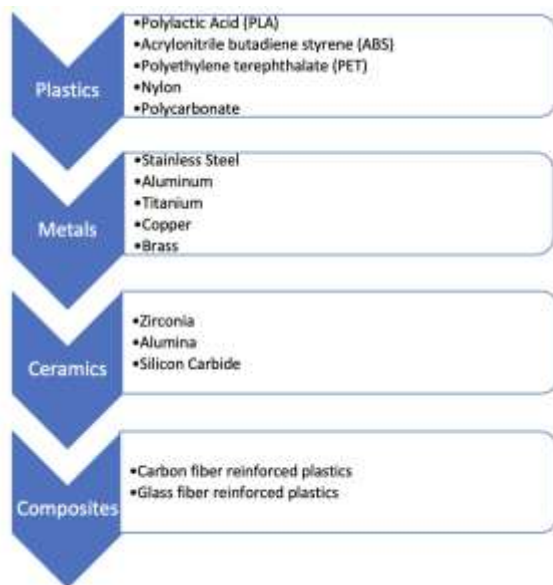
Figure 1. *Materials used in additive manufacturing*

Vicente et al. [10] determined infill patterns and infill density as parameters and applied tensile tests to the samples produced from ABS filament. As a result of their tests, they stated that the samples with 100% fill rate reached the highest strength values. Motoparti et al. [11] investigated how printing parameters such as build direction and raster angle

affect compression modulus and yield strength. In their studies, they applied compression tests to the samples produced from ABS material. They reported that the build direction and raster angle are important parameters that affect the yield strength of the samples. Abbas et al. [12] applied compression tests to PLA samples produced with different infill densities in their study. According to their results, they showed that increasing the infill density increased the compressive strength. Chacon et al. applied three-point bending tests to PLA samples produced with different variations of build orientation, layer thickness and feed rate. They reported that ductility decreased as the layer thickness and feed rate increased [13]. Lebedev et al. [14] compared the mechanical properties of the samples produced by hot press and 3D printing methods. They found that the samples produced by the hot press method showed better mechanical performance. Panes et al. [15] , in their study comparing PLA and ABS materials, produced samples with different layer thicknesses and different fill rates. They stated that the infill density is a very important factor. Nadernezhad et al. [16] performed mechanical and thermal tests on the samples they produced using different variations of parameters such as layer thickness, infill density, infill pattern. They reported that the residual thermal stresses increase as the layer thickness increases, and decreasing the infill density decreases the material strength. Ezeh and Susmal [17] investigated the effect of build direction on fatigue strength in their study. Tanveer et al. [18] investigated the effect of infill density on the tensile and impact strength of the material. They showed that the impact strength changes proportionally with the infill density. Yao et al. [19] subjected the samples produced at different angles and with different layer thicknesses to tensile tests. According to the results they obtained, they showed that the tensile strength of the samples with small printing angles decreased. Samykano et al. [20] produced different values of layer thickness, raster angle and infill density in their study. Tensile and hardness tests were applied to the samples they produced. They reported that the optimum density ratio to be selected for the ABS sample is 80%. Aloyaydi et al. [21] applied low velocity impact tests to the samples they produced using different infill patterns. They reported that samples with a

triangular pattern showed the best performance in absorbing energy. Gunasekaran et al. [22] applied tensile, impact, bending and hardness tests to PLA samples produced at different infill densities. They reported that the increase in infill density increased the mechanical performance of the material. Rajpurohit and Dave [23] produced samples using PLA material with different raster angles, raster widths and layer thicknesses. They compared the impact performance of the samples they produced and emphasized that the raster angle is an important parameter affecting the impact strength. Yadav et al. [24] applied compression tests to the samples they produced with different infill patterns. They reported that the infill pattern with Hilbert curve design gave the best results. Farazin and Mohammadimehr [25] investigated the effects of infill density, infill pattern and layer thickness on tensile and compression strengths. They reported that the material showed a more brittle character at high densities. Mishra et al. [26] performed impact tests on the samples they produced with different infill patterns and densities, and reported that they reached the best absorbed energy value at 85% density. In their study, Patil [27] et al. compared the surface roughness of the materials they produced under variables such as different infill patterns, densities, velocity and layer thickness. They showed that the infill density had the most significant effect on the GRG (Gray Relational Grade). Samykano [28] compared the tensile and hardness strengths of the materials produced at different infill densities and reported the optimum printing parameters.

We can say there are several ways to increase the strength of a part produced by additive manufacturing against compression force; using a high-strength material, increasing the layer thickness, using a honeycomb or lattice structure, using support structures, using post-processing techniques, optimizing the design, material, process parameters, microstructure, part geometry. Overall, the mechanical properties of objects produced using additive manufacturing technology can be influenced by a combination of these and other factors. It is important to carefully consider these factors in order to optimize the mechanical performance of the finished object. In this study, sandwich samples were produced by the additive manufacturing method. Fused deposition modeling

(FDM) method was chosen as the production method. Production was carried out with different infill densities and infill parameters, and then the static energy absorption amounts were measured by performing compression tests. Thus, the effects of production parameters on the static energy absorption ability were investigated.

2. Material and Method

In this study, fused deposition modeling was used as the production method. Fused Deposition Modeling (FDM) is a type of 3D printing technology that creates a physical object by laying down and fusing successive layers of material, typically thermoplastic filament (such as ABS or PLA), layer by layer. The material is melted and extruded through a heated nozzle onto a build platform, where it solidifies and forms the desired shape. The process is controlled by computer-aided design (CAD) software. FDM is a low-cost and accessible 3D printing technology, widely used for prototyping and producing small batch production runs.

The printing processes of the samples were made with Ender-3 S1 printer. The Ender-3 S1 is a 3D printer made by Creality. It is a more compact and lightweight version of previous model, designed for use in smaller spaces. It has a build volume of 220 x 220 x 250 mm and a print resolution of up to 100 microns. The printer is powered by a 32-bit motherboard and uses a filament sensor to automatically pause printing when the filament runs out or breaks. It is capable of printing with a variety of materials, including PLA, PETG, TPU, ABS and more. It features a removable, flexible magnetic build plate for easy removal of printed objects and an upgraded extruder to improve print quality.

In this study all samples were produced using Polylactic Acid (PLA) filament. PLA is a biodegradable and environmentally friendly 3D printing material made from renewable resources such as corn starch or sugarcane. It is one of the most popular 3D printing materials due to its easy printability, low warping, and low odor. PLA is a strong and stiff material with good layer adhesion, making it suitable for a wide range of applications. It is commonly used for prototyping and model making. One of the main advantages of PLA is that it does not require a heated bed, making it easier to print with and more suitable for use on basic 3D printers. However, it has a lower melting temperature compared to other materials like ABS,

which means it may deform or warp when exposed to high temperatures. It is also more brittle than other materials. Overall, PLA is a good choice for 3D printing and for projects that do not require high levels heat resistance. In Table 1, the infill parameters used in the printing process and the general printing parameters are given. The masses of all samples were measured and given in Table 2. It was observed that the masses of the samples with the same infill density were close to each other. The samples were produced as three pieces for each combination and this study has total 60 samples of 15 different combinations (Fig. 2), which consists 5 different infill patterns and 3 different densities. The compression tests (Fig. 3) were carried out on a 200kN capacity universal testing machine and force-displacement data collected. The test speed was chosen as 4 mm/min, with a total test time of 1-3 minutes.

3. Results and Discussion

Force and displacement data were obtained from compression tests and force-displacement graphs were created. There are three points to note in these charts. These are the maximum force reached until the crush starts, the average force at which the crush occurs, and the crush stroke. As can be seen in figure 4, it is seen that the compressive strength of the samples increases as the infill density increases for all infill pattern types.

Table 1. *Infill and printing parameters.*

Infill Parameters	Infill Pattern	Line (Li)	Cubic (Cu)	Octet (Oc)	Triangles (Ta)	Trihexagon (Th)
	Infill Density (%)	*10*	*10*	*10*	*10*	*10*
		15	*15*	*15*	*15*	*15*
		20	*20*	*20*	*20*	*20*
Printing Parameters	*Layer Height*	*Top Thickness*	*Bottom Thickness*	*Infill Density*	*Bed Temperature*	*Print Speed*
	0.2 mm	*1 mm*	*1 mm*	*0,1*	*60*	*50mm/s*

Table 2. *Sample masses.*

Infill Density (%)	Cu			Li			Oc			Ta			Th		
	10	15	20	10	15	20	10	15	20	10	15	20	10	15	20
Mass (g)	20,16	24,22	28,65	20,1	24,38	28,55	20,17	24,17	28,5	20,15	24,63	28,74	20,15	24,28	28,75
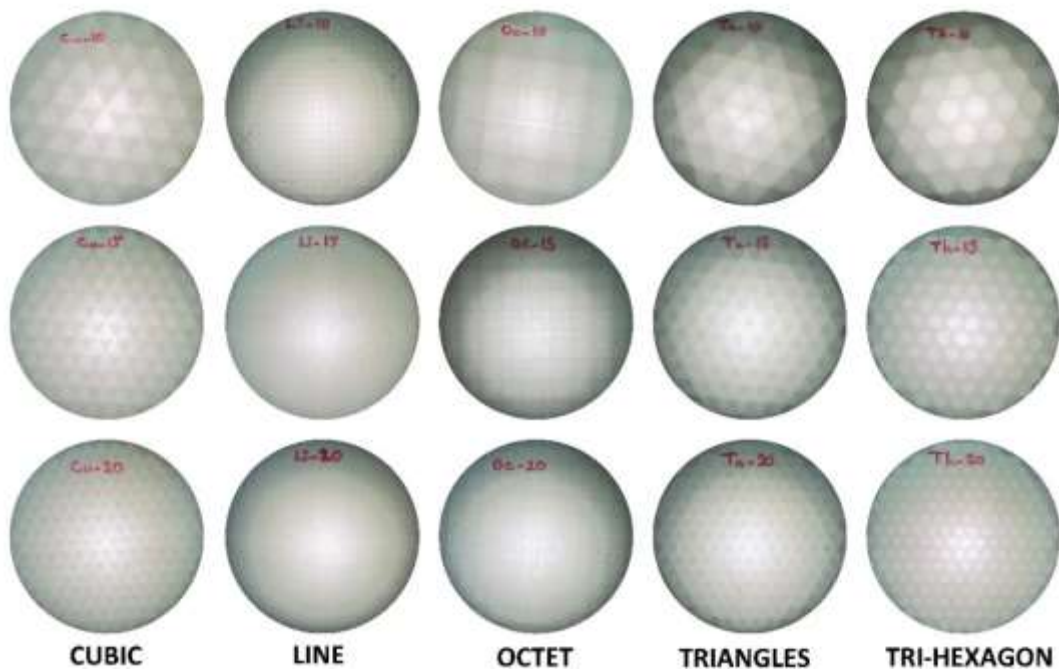
Figure 2. *Sample types*

Figure 3. *Compression test*
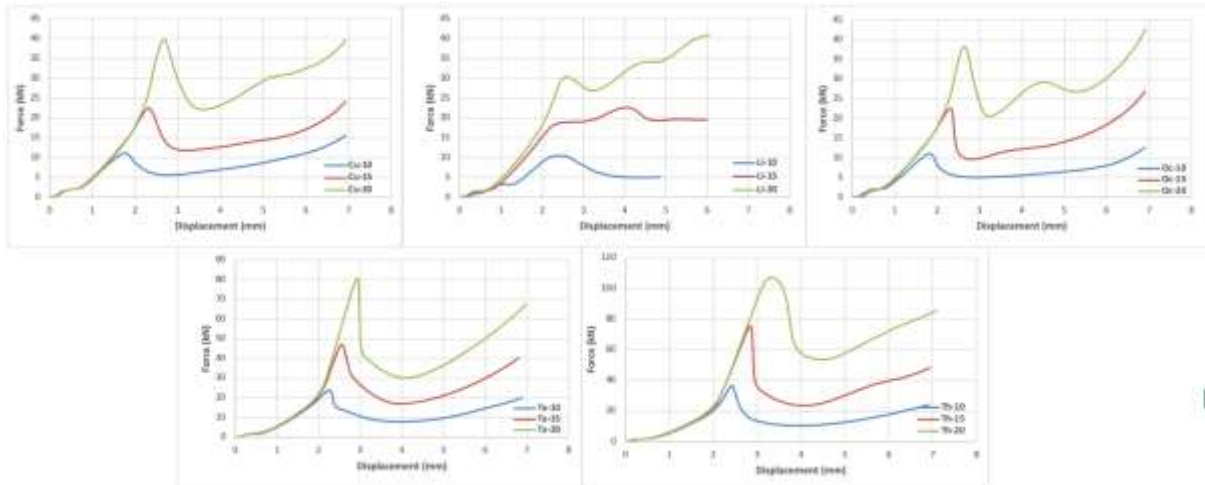
Figure 4. *Force-Displacement curves of the tested samples with respect to infill densities.*
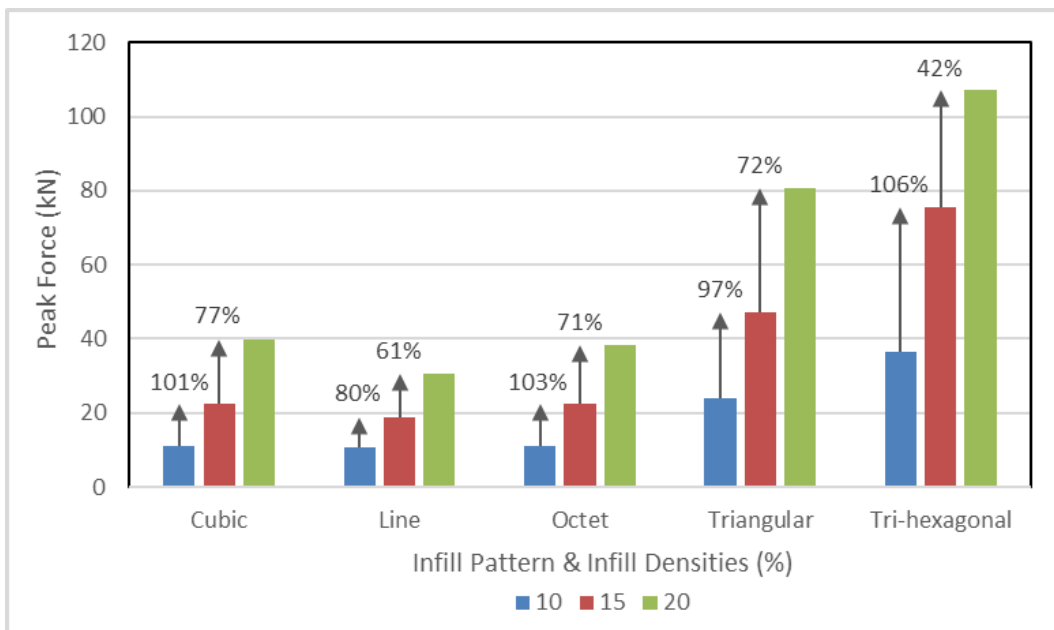
Figure 5. *Peak force values of samples with respect to infill pattern and densities.*

When the slope of the curves until the first damage is evaluated, it is seen that the increase in the infill density does not show a change in the stiffness of the structures. Since the increase in the infill density increases the cross-sectional area, the maximum force values are improved. Therefore, an increase in the inner density, that is, filling it with a denser infill pattern, did not contribute to the stiffness of the material. Again, as seen in Figure 4, as the density increases, the crush stroke value decreases and densification begin earlier. In this state, the early initiation of In figure 5, the peak force values reached by the samples with different infill patterns and densities are given. It has been previously stated that the strength increases with the increase of infill density. In this graph, we can see more clearly at what rate this increase occurs in samples with different infill patterns. It is seen that the samples with the highest percentage increase in the peak force value due to the increase in infill density are the samples with cubic, octet and triangular infill patterns respectively. If the graphics are evaluated in terms of Infill patterns, it is seen that the lowest strength values are in the samples with line (Li) pattern, and the highest strength is in the samples with tri-hexagonal (Th) and triangle (Ta) pattern types. In Figure 6, force displacement curves of samples filled with different patterns with 20%

densification provides an increase in the amount of static energy absorbed by the material. When the graph of the samples with Line (Li) infill pattern is examined, it is seen that they reach lower maximum force values, but considering the force values at which crushing occurs, it is seen that these are the samples where the average crushing force is closest to the peak force value. Based on these data, it can be said that the crush resistance is higher and that can make sample with line infill pattern safer at the time of damage.

infill density are shown. From this graph, it can be said that the stiffnesses of the samples with Cubic, Line and Octet infill patterns are close to each other, while the stiffness of the samples with Triangle and Tri-hexagonal patterns is higher. When the samples with the line pattern with the lowest compressive strength were examined, Li20 (Line pattern, %20 infill density) sample which has the highest infill density reached a maximum value of 30.45 kN. On the other hand, Th10 sample, which is the lowest density sample produced with tri-hexagonal pattern, reached up to 36 kN load. In this context, it seems, it's possible to work at lower infill density rates by applying tri-hexagon pattern instead of producing at 20% infill density with line pattern. Thus, production time will be shortened, raw materials will be saved and costs will be reduced.
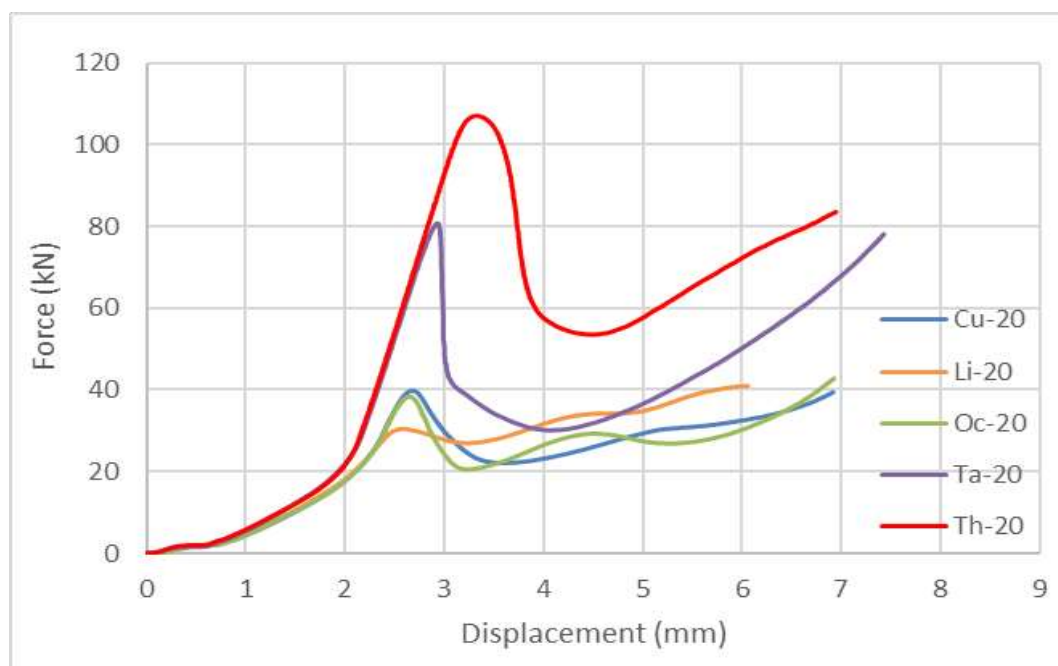
Figure 6. *Force-displacement curves of samples produced at 20% infill density with different infill patterns.*

4. Conclusion

In this study, the compression performance of samples with different infill parameters and infill densities was investigated. The following conclusions can be drawn from the mechanical characterization carried out through experimental analysis;

- As the infill density increases, the compressive strength of the material increases.
- The increase in density did not make a significant difference in the stiffness of the material.
- The change of the infill pattern increased the stiffness of the structure. The samples produced with Triangular and tri-hexagonal patterns had more rigid structures.
- Despite the same percentage increase in density, the samples showing the best increase in material strength were cubic, octet and triangular samples, respectively. From this point of view, it can be said that these samples are more sensitive to the increase in density.
- The most successful samples in terms of static energy absorbing ability were triangular and tri-hexagonal samples.
- It was observed that the crushing force and peak force were closer to each other in the samples with line pattern. This showed that the structure would operate in a safer range in case of sudden damage.
- According to the data obtained, it is possible to produce structures with lower densities and higher strength by using triangular and tri-hexagonal infill patterns. In this way, it will provide significant savings in terms of material, time and energy.

Author Statements:

- **Ethical approval:** The conducted research is not related to either human or animal use.
- **Conflict of interest:** The authors declare that they have no known competing financial interests or personal relationships that could have appeared to influence the work reported in this paper
- **Acknowledgement:** The authors declare that they have nobody or no-company to acknowledge.
- **Author contributions:** The authors declare that they have equal right on this paper.

- **Funding information:** The authors declare that there is no funding to be acknowledged.
- **Data availability statement:** The data that support the findings of this study are available on request from the corresponding author. The data are not publicly available due to privacy or ethical restrictions.

5. References

[1] S.K. Selvamani, W.K. Ngui, K. Rajan, M. Samykano, Reji Kumar R, Avinash M. Badadhe, (2022). Investigation of bending and compression properties on PLA-brass composite using FDM, *Physics and Chemistry of the Earth* 128

[2] Rajan, K., Samykano, M., Kadirgama, K., Harun, W.S.W., Rahman, M.M., 2022. Fused deposition modeling: process, materials, parameters, properties, and applications. *Int. J. Adv. Manuf. Technol.* 120 (3–4); 1531–1570.

[3] T.D. Ngo, A. Kashani, G. Imbalzano, K.T.Q. Nguyen, D. Hui. (2018) Additive manufacturing (3D printing): a review of materials, methods, applications and challenges, *Compos. Part B Eng.* 143;172–196.

[4] O. Abdulhameed, A. Al-Ahmari, W. Ameen, S.H. Mian. (2019). Additive manufacturing: challenges, trends, and applications. *Adv. Mech. Eng.* 11 (2).

[5] K.V. Wong, A. Hernandez, (2012). A review of additive manufacturing, *ISRN Mech. Eng.* 1–10

[6] M. O. Oteyaka, F. H. Çakir, M. A. Sofuoglu. (2022). Effect of infill pattern and ratio on the flexural and vibration damping characteristics of FDM printed PLA samples, *Materials Today Communications* 33.

[7] Kumaresan, R., Samykano, M., Kadirgama, K., Ramasamy, D., Keng, N.W., Pandey, A.K., (2021). 3D printing technology for thermal application: a brief review. *J. Adv. Res. Fluid Mech. Therm. Sci.* 83 (2); 84–97.

[8] Braconnier, D.J., Jensen, R.E., Peterson, A.M., (2020). Processing parameter correlations in material extrusion additive manufacturing. *Addit. Manuf.* 31 https://doi.org/ 10.1016/j.addma.2019.100924.

[9] Md. Qamar Tanveer, Gautam Mishra, Siddharth Mishra, Rohan Sharma (2022). Effect of infill pattern and infill density on mechanical behaviour of FDM 3D printed Parts- a current review, *Materials Today: Proceedings* 62;100-108.

[10] M. Fernandez-Vicente, W. Calle, S. Ferrandiz, A. Conejero. (2016). Effect of Infill Parameters on Tensile Mechanical Behavior in Desktop 3D Printing, 3D Print, *Addit. Manuf.* 3 (3): 183–192.

[11] K.P. Motaparti, G. Taylor, M.C. Leu, K. Chandrashekhara, J. Castle, M. Matlack, (2016).

Effects of build parameters on compression properties for ULTEM 9085 parts by fused deposition modeling, Solid Free. *Fabr. 2016 Proc. 27th Annu. Int. Solid Free. Fabr. Symp. - An Addit. Manuf. Conf. SF*F. 964–977.

[12] D. Abbas, D. Mohammad Othman, H. Basil Ali, C. Author (2017). Effect of infill Parameter on compression property in FDM Process, *Int. J. Eng. Res. And Application* Www.Ijera.Com. 7; 16–19. 10.9790/9622-0710021619.

[13] J.M. Chacón, M.A. Caminero, E. García-Plaza, P.J. Núñez, (2017). Additive manufacturing of PLA structures using fused deposition modelling: Effect of process parameters on mechanical properties and their optimal selection, *Mater. Des.* 124; 143–157.

[14] S.M. Lebedev, O.S. Gefle, E.T. Amitov, D.V. Zhuravlev, D.Y. Berchuk, E.A. Mikutskiy. (2018). Mechanical properties of PLA-based composites for fused deposition modeling technology, *Int. J. Adv. Manuf. Technol*. 97 (1-4): 511–518.

[15] A. Rodríguez-Panes, J. Claver, A. Camacho. (2018). The Influence of Manufacturing Parameters on the Mechanical Behaviour of PLA and ABS Pieces Manufactured by FDM: *A Comparative Analysis, Materials (Basel)*. 11 :1333.

[16] A. Nadernezhad, S. Unal, N. Khani, B. Koc. (2019). Material extrusion-based additive manufacturing of structurally controlled poly(lactic acid)/carbon nanotube nanocomposites, *Int. J. Adv. Manuf. Technol.* 102 (5-8): 2119–2132.

[17] O.H. Ezeh, L. Susmel. (2019). Fatigue strength of additively manufactured polylactide (PLA): effect of raster angle and non-zero mean stresses, *Int. J. Fatigue.* 126 :319–326.

[18] M.Q. Tanveer, A. Haleem, M. Suhaib. (2019). Effect of variable infill density on mechanical behaviour of 3-D printed PLA sample: an experimental investigation, *SN Appl. Sci.* 1: 1701.

[19] T. Yao, Z. Deng, K. Zhang, S. Li. (2019). A method to predict the ultimate tensile strength of 3D printing polylactic acid (PLA) materials with different printing orientations*, Compos. Part B Eng.* 163:393–402.

[20] M. Samykano, S.K. Selvamani, K. Kadirgama, W.K. Ngui, G. Kanagaraj, K. Sudhakar. (2019). Mechanical property of FDM printed ABS: influence of printing parameters, *Int. J. Adv. Manuf. Technol.* 102 (9-12): 2779–2796.

[21] B. Aloyaydi, S. Sivasankaran, A. Mustafa. (2020). Investigation of infill-patterns on mechanical response of 3D printed poly-lactic-acid, *Polym. Test.* 87.

[22] K.N. Gunasekaran, V. Aravinth, C.B. Muthu Kumaran, K. Madhankumar, S. Pradeep Kumar. (2021). Investigation of mechanical properties of PLA printed materials under varying infill density, *Mater. Today Proc.* 45: 1849–1856.

[23] S.R. Rajpurohit, H.K. Dave. (2021). Impact strength of 3D printed PLA using open source FFF-based 3D printer, *Prog. Addit. Manuf.* 6 (1): 119–131.

[24] P. Yadav, A. Sahai, R.S. Sharma. (2021). Strength and Surface Characteristics of FDM Based 3D Printed PLA Parts for Multiple Infill Design Patterns, *J. Inst. Eng. Ser. C.* 102 (1): 197–207.

[25] A. Farazin, M. Mohammadimehr. (2021). Effect of different parameters on the tensile properties of printed Polylactic acid samples by FDM: experimental design tested with MDs simulation, *Int. J. Adv. Manuf. Technol.*

[26] P.K. Mishra, P. Senthil, S. Adarsh, M.S. Anoop. (2021). An investigation to study the combined effect of different infill pattern and infill density on the impact strength of 3D printed polylactic acid parts, *Compos. Commun.* 24.

[27] P. Patil, D. Singh, S.J. Raykar, J. Bhamu. (2021). Multi-objective optimisation of process parameters of Fused Deposition Modeling (FDM) for printing Polylactic Acid (PLA) polymer components, *Mater. Today Proc.* 45: 4880–4885.

[28] M. Samykano. (2021). Mechanical Property and Prediction Model for FDM-3D Printed Polylactic Acid (PLA), *Arab. J. Sci. Eng.* 46 (8): 7875–7892.

Research Article
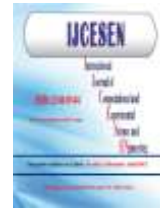
Analysis of Factors Affecting Common Use of Generative Artificial Intelligence-Based Tools by Machine Learning Methods

Yasin KIRELLİ*

Kütahya Dumlupınar University, Faculty of Applied Sciences, Management Information Systems, Kütahya-Türkiye
* **Corresponding Author**: **Email:** yasin.kirelli@dpu.edu.tr **ORCID:** 0000-0002-3605-8621

Abstract:

Artificial Intelligence is a sub-branch of artificial intelligence used to produce new data or content. These methods can create recent examples in different categorical fields such as natural language processing, image processing, music, and video creation by using models from learning clusters with artificial intelligence (AI) tools in this field. AI tools that can solve real-world problems are also created using different methods apart from generative AI methods. With generative-based artificial intelligence tools, it can facilitate people's work in jobs that require creativity. However, they can offer the opportunity to build advanced models that learn from data with other artificial intelligence methods. In the study, the public dataset has been used. This dataset includes trending artificial intelligence tools, AI methods, and user scores. In this study the working area and user trend of the ai tools in the dataset and the effect of generative AI methods on the development of the tool are discussed. Random Forest and Naive Bayes algorithms from classification methods have been used to measure the impact and estimation. Several AI tools help solve real-life problems. Identifying what type of category is needed for AI tools and method selection are interlinked, and the research provides an overview of this connection.

1. Introduction

Artificial intelligence (AI) is the ability to create applications or tools with computer programs that aim to think like humans, similar to human intelligence. The field of AI was studied in 1956 by a computer scientist at Dartmouth College. They have been based on the identifiability assumption of intelligence and aimed to make the simulation a machine. Thus, it seeks to enable people to solve problems specific to humans and learn from data [1–4]. The primary purpose is to solve the issues that people can learn or solve with their cognitive intelligence with the help of machines or applications. These problems can be in different categories, such as language comprehension, music creation, image recognition, and decision support systems. The human ability in these categories is to be able to meet similar. The primary purpose of artificial intelligence tools is to create advanced systems with cognitive intelligence in many fields,

such as health, education, entertainment, image, video, and the military. Artificial intelligence systems, which can interpret human input with applications such as chatbots and convert it from text to text or from text to picture with natural language processing techniques, serve effectively in many areas today. It has become a personal assistant tool that can help in different areas, such as customer service, search engines, and code generators [5]. As data-based learning systems depend on statistical data, artificial intelligence tools have developed rapidly. Two main reasons have been influential in these tools' widespread use and development. The first of these is the general use of data storage systems and data sets, and the other reason is the increasing computing power of computers. With the deep learning sub-artificial intelligence field, powerful personal assistants such as Siri and Alexa were introduced in 2010. Today, ChatGPT has reached widespread use as an advanced personal

assistant and a language processing tool offered by OpenAI [1].

The deep learning technique is a structure created by combining forms of artificial intelligence with machine learning models [6–8]. Unlike neural networks, which use only one-layer, deep learning structures use multiple layers. Thus, a better estimation model can be made. Deep learning is defined as a multi-layered neural network structure. This neural network transfers information to the last layer in a non-linear form between layers, which is possible with activation functions. In the convolutional form, activation functions take place as parameters between layers in the transfer of information and are used to disrupt linearity. Thus, the deep learning structure will achieve better learning ability. Minimizing the loss value by forward and backward propagation is the main goal [1,9].

The Generative Adversarial Networks (GAN) architecture method is among the artificial intelligence methods that attract great attention today. It is a deep learning method frequently preferred in natural language processing, image, and video processing with artificial intelligence tools created with this method. Creating powerful personal assistant applications such as healthcare or ChatGPT, such as the production of new drugs, is a promising method [10–13]. Responsible use of artificial intelligence is among the discussion topics that come with it. Presenting the text and images produced by AI as an 'original work' is also a research topic [14].

In the study, the artificial intelligence tools dataset in the publicly available Kaggle database is discussed. Today, widely used artificial intelligence tools are listed in this dataset. Extra details, such as usage areas and development methods, are given. It has been tried to analyze the effect of generative artificial intelligence methods or other artificial intelligence methods on the widespread use of the tools in the study, depending on the subject area targeted by an artificial intelligence tool. Random forest, support vector machine, and logistic regression from machine learning techniques have been used for estimation. Evaluation metrics and

analysis are also has been discussed in the following sections.

2. Material and Methods

In this chapter, GAN, which is the most preferred method for the development of ai tools, is explained. The following sections give an exploratory analysis of the data set used. In the last section, the evaluation of the model is given.

2.1. Generative Adversarial Networks Architecture

According to the Generative Adversarial Networks architecture, it is a deep learning method in the convolutional artificial neural network structure. Goodfellow et al. proposed this in 2014 [15,16]. It has been frequently used and preferred as a deep learning method. This method uses real data as input and learns the sample distribution. This produces outputs similar to real data [17]. It is an effective method to create tools such as ChatGPT by giving outcomes above human capabilities [18]. This method, preferred in data creation, is also essential for data imbalance problems. With the development of deep neural network architectures, variants of the GAN architecture have also emerged. It has been proposed as a preferred variant for unsupervised learning (DCGAN), for increased stability (WGAN), and poor sample quality problems (WGAN-GP) [19]. As seen in Figure 1, there is a producer (G) and a separator (D) object. The GAN method is presented in Equation 1. According to the formula, the goal is for Pda to converge to Pg with a gradient.
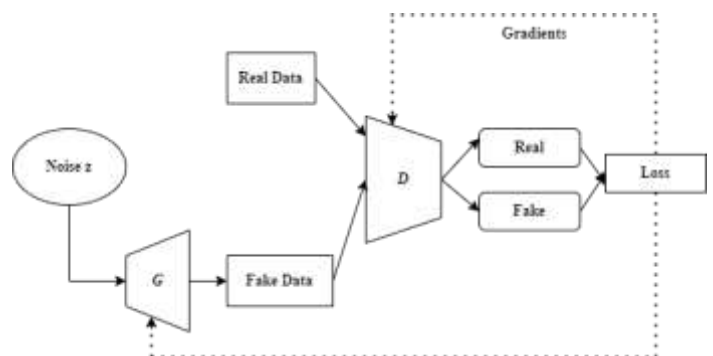
Figure 1. *GAN Architecture*

According to the formula, G Generator, D stands for the discriminator. Pz distribution of the random noise; Pda represents the real sample distribution. D(x) is the discriminant probability value, and G(z) is the sample output.

$$L(G, D) = \min_{G} \max_{D} E_{x \sim P_{da}}[log D(x)] \quad (1)$$
$$+ E_{z \sim P_z} [log(1 - D(G(z)))]$$

According to Equation 1, when Pda = Pg, it is assumed that the generated data distribution is equal to the actual data distribution [19].

2.2. Exploratory Data Analysis (EDA)

The dataset contains publicly available AI tools and information from the Kaggle database. This dataset is currently widely used and is a resource for discovering new tools [20]. The dataset includes the target subject area, user scores and ai methods information of these tools. The data set consists of 1012 rows and sample 5 records are shown in Figure 2.

***Figure 2.** Data set sample records*

According to the records in the data set and Figure 3., the most AI tools are in 110 Copywriting, 91 Generative Art and 84 Chat subject areas. According to the results, considering the use of artificial intelligence tools by individual users, personal assistants that assist in writing texts are widely used. It is seen that multimedia solutions are the next most used area. Figure 4 shows the most preferred ai tool categories and the applied methods according to user comments. According to the graph, GAN architecture has been mostly preferred as a method in developing AI tools. In Figure 5, if the AI tools are sorted according to user preferences, it is seen that "LeiaPix," "GPT-3," and "Codeium" have the most votes. All three tools have been developed using the artificial intelligence method. In addition, these tools are in the "LeiaPix" image improvement category, "GPT-3" copywriting, and "Codeium" generative code category, respectively. If it is

considered a personal assistant tool, it attracts attention from users. Figure 6 shows each ai tool in the dataset and a word cloud according to the description field and word frequencies in the dataset. It can be seen that the emphasis is placed on 'generative artificial intelligence' and 'personal assistant' in the word cloud.

2.3 Implementation and Evaluation of the Model

The dataset's 'ai tool development technique' has been chosen as the estimation or dependent variable.

***Figure 3.** Category and usage rates*

***Figure 4.** Category and AI Methods for Top 100 AI Tools*

	precision	recall	f1-score
GAN	0.79	0.79	0.79
Other Methods	0.73	0.73	0.73
Accuracy			0.76
Macro Avg	0.76	0.76	0.76
Weighted Avg	0.76	0.76	0.76

The accuracy scores of the evaluation and criteria are presented in Table 1, Table 2, and Table 3. According to the models created, it is seen that the highest accuracy rate in the analysis has been obtained with the Random Forest model at 96%. It is seen that the next closest and with the highest metric ratio is Logistic Regression. While creating the models, hyperparameter tuning has been performed in order to select the most suitable model parameters for the data set. Thus, it can be suitable for the data set, and the estimation rate is increased.

3. Conclusion

Generative artificial intelligence is presented to produce a response, unlike other techniques. It can create outputs similar to human intelligence beyond just generating answers but also go beyond that. AI tools such as ChatGPT are among the popular tools preferred by users in this study as an example of generative intelligence that includes different methods rather than just producing natural language processing output. Due to the increased machine capacities and data processing speeds today, they have become personal assistants in daily life thanks to successful AI tools. According to the study, since artificial intelligence tools created using the generative artificial intelligence technique are preferred as personal assistant services for individual users, using these tools has become more widespread with the users' upvotes. The primary purpose is to use the information provided by generative artificial intelligence tools for ethical and goodwill purposes by their users. Therefore, ethical principles and bias in the effective widespread use of artificial intelligence are another discussion topic. For this reason, it is a different need to confirm the accuracy of the information produced by generative artificial intelligence tools.

Author Statements:

- **Ethical approval:** The conducted research is not related to either human or animal use.

Figure 5. *Trends of AI tools by user ratings*

Figure 6. *AI Tools description field word frequencies*

The dependent variable 'ai tool development technique' consists of two categorical values: 'GAN' or 'Other Methods.' The independent variables are the upvotes of the users and the categorical area addressed by the artificial intelligence tool. While creating the prediction model, Python programming version 3.10 and the Sklearn library have been used. Logistic Regression, Random Forest, and Support Vector Machine machine learning techniques have been used for the prediction model, respectively.

Table 1. *Support Vector Machine Model Evaluation Metrics*

	precision	recall	f1-score
GAN	0.68	0.93	0.79
Other Methods	0.83	0.45	0.59
Accuracy			0.72
Macro Avg	0.76	0.69	0.69
Weighted Avg	0.75	0.72	0.70

Table 2. *Random Forest Model Evaluation Metrics*

	precision	recall	f1-score
GAN	0.97	0.95	0.96
Other Methods	0.95	0.97	0.96
Accuracy			0.96
Macro Avg	0.96	0.96	0.96
Weighted Avg	0.96	0.96	0.96

Table 3. *Logistic Regression Model Evaluation Metrics*

- **Conflict of interest:** The authors declare that they have no known competing financial interests or personal relationships that could have appeared to influence the work reported in this paper
- **Acknowledgement:** The authors declare that they have nobody or no-company to acknowledge.
- **Author contributions:** The authors declare that they have equal right on this paper.
- **Funding information:** The authors declare that there is no funding to be acknowledged.
- **Data availability statement:** The data that support the findings of this study are available on request from the corresponding author. The data are not publicly available due to privacy or ethical restrictions.

References

[1] A. Holzinger, K. Keiblinger, P. Holub, K. Zatloukal, and H. Müller, (2023). AI for life: Trends in artificial intelligence for biotechnology," *N Biotechnol,* 74;16–24 doi: 10.1016/j.nbt.2023.02.001.

[2] N. Eslamirad, F. De Luca, K. Sakari Lylykangas, and S. Ben Yahia, (2023). Data generative machine learning model for the assessment of outdoor thermal and wind comfort in a northern urban environment, *Frontiers of Architectural Research,* doi: 10.1016/j.foar.2022.12.001.

[3] V. Couteaux et al., (2023). Synthetic MR image generation of macrotrabecular-massive hepatocellular carcinoma using generative adversarial networks, *Diagn Interv Imaging,* doi: 10.1016/j.diii.2023.01.003.

[4] H. Woldesellasse and S. Tesfamariam, (2022). Data Augmentation Using conditional Generative Adversarial Network (cGAN): Application for Prediction of Corrosion Pit Depth and Testing Using Neural Network, *Journal of Pipeline Science and Engineering,* p. 100091 doi: 10.1016/j.jpse.2022.100091.

[5] S. O'Connor and ChatGPT, (2023). Open artificial intelligence platforms in nursing education: Tools for academic progress or abuse?, *Nurse Education in Practice,* vol. 66. Elsevier Ltd, doi: 10.1016/j.nepr.2022.103537.

[6] T. Ching et al., (2018). Opportunities and obstacles for deep learning in biology and medicine," *J R Soc Interface,* 15;141 doi: 10.1098/RSIF.2017.0387.

[7] D. Dana et al., (2018). Deep Learning in Drug Discovery and Medicine; Scratching the Surface, *Molecules,* 23;9 doi: 10.3390/molecules23092384.

[8] E. Lin, P. H. Kuo, Y. L. Liu, Y. W. Y. Yu, A. C. Yang, and S. J. Tsai, (2018). A Deep Learning Approach for Predicting Antidepressant Response in Major Depression Using Clinical and Genetic Biomarkers. *Front Psychiatry,* 9 doi: 10.3389/FPSYT.2018.00290.

[9] Y. Chauvin and D. E. Rumelhart, Backpropagation : theory, architectures, and applications. Lawrence Erlbaum Associates, 1995. Accessed: Mar. 13, 2023. [Online]. Available: https://www.routledge.com/Backpropagation-Theory-Architectures-and-Applications/Chauvin-Rumelhart/p/book/9780805812596

[10] H. Zhao, H. Li, S. Maurer-Stroh, and L. Cheng, (2018). Synthesizing retinal and neuronal images with generative adversarial nets. *Med Image Anal,* 49;14–26, doi: 10.1016/j.media.2018.07.001.

[11] B. Hu, Y. Tang, E. I.-C. Chang, Y. Fan, M. Lai, and Y. Xu, (2017). Unsupervised Learning for Cell-level Visual Representation in Histopathology Images with Generative Adversarial Networks. doi: 10.1109/JBHI.2018.2852639.

[12] M. Mardani et al., (2019). Deep Generative Adversarial Neural Networks for Compressive Sensing MRI. *IEEE Trans Med Imaging,* 38(1);167–179, doi: 10.1109/TMI.2018.2858752.

[13] E. Lin, S. Mukherjee, and S. Kannan, (2020). A deep adversarial variational autoencoder model for dimensionality reduction in single-cell RNA sequencing analysis. *BMC Bioinformatics,* 21(1);64, doi: 10.1186/s12859-020-3401-5.

[14] D. O. Eke, (2023). ChatGPT and the rise of generative AI: Threat to academic integrity?. *Journal of Responsible Technology,* 13;100060, doi: 10.1016/j.jrt.2023.100060.

[15] C. Kruchko, Q. T. Ostrom, H. Gittleman, and J. S. Barnholtz-Sloan, (2018). The CBTRUS story: providing accurate population-based statistics on brain and other central nervous system tumors for everyone. *Neuro Oncol,* 20(3);295–298, doi: 10.1093/neuonc/noy006.

[16] I. J. Goodfellow et al., "Generative Adversarial Networks," Jun. 2014.

[17] R. Ranjbarzadeh, A. Caputo, E. B. Tirkolaee, S. Jafarzadeh Ghoushchi, and M. Bendechache, (2023). Brain tumor segmentation of MRI images: A comprehensive review on the application of artificial intelligence tools," *Computers in Biology and Medicine,* 152 doi: 10.1016/j.compbiomed.2022.106405.

[18] W. M. Lim, A. Gunasekara, J. L. Pallant, J. I. Pallant, and E. Pechenkina, (2023). Generative AI and the future of education: Ragnarök or reformation? A paradoxical perspective from management educators. The *International Journal of Management Education,* 21(2);100790, doi: 10.1016/j.ijme.2023.100790.

[19] S. Liu, H. Jiang, Z. Wu, Y. Liu, and K. Zhu, (2022). Machine fault diagnosis with small sample based on variational information constrained generative adversarial network. *Advanced Engineering Informatics,* 54 doi: 10.1016/j.aei.2022.101762.

[20] Cutting-Edge AI Tools: An Up-to-Date Dataset Kaggle"https://www.kaggle.com/datasets/yasirabdaali/740-ai-tools-for-everyone (accessed Mar. 13, 2023).

Research Article

Radiation Attitudes in Associate Degree Students

Nurdan KARPUZ*

Amasya University, Sabuncuoğlu Şerefeddin Vocational School of Health Services, Department of Medical Services and Techniques, Amasya, Turkey
* **Corresponding Author** : **Email:** nurdankarpuz@amasya.edu.tr - **ORCID:** 0000-0003-4911-8846

Abstract:

The radiation that has existed throughout human history is always present in our environment, in our bodies and in space. Radiation has been used in almost every aspect of medicine, science and industry since it was discovered. Technologies that use radiation make people's lives easier, and people's lives are saved through early detection and treatment of diseases, especially in medical applications. With rapidly evolving technology, medical staff are exposed to more radiation doses due to increased radiation use in medicine. Since life without radiation is unlikely, there needs to be a sufficient level of information about radiation to protect against the harmful effects of radiation. In universities, which constitute an important part of education and training, the better the radiation knowledge of the students in the field of health, which will shape the future, the better the transfer of radiation knowledge level to future generations and at the same time to the people they serve since these students will be the health personnel of the future. Health personnel should be able to protect themselves from the harmful effects of radiation, take the necessary precautions during diagnosis and treatment, and increase their level of knowledge in this regard. In this study, it was aimed to evaluate the level of awareness of health services vocational school students, who will be health personnel in the future, towards the concept of radiation and radiation protection.

1. Introduction

Physics is a fundamental science that helps us understand the fundamental structures of nature and discover the laws underlying the events that take place in the universe. Physics studies phenomena at all levels, from the quantum level to cosmic dimensions, and aims to explain natural phenomena with mathematical expressions. Physics enables the understanding of complex concepts such as radiation and the discovery of many phenomena that form the basis of our daily life as well as our technological and scientific progress. "Radiation," an important concept in physics, refers to different forms of energy. In general terms, radiation is the process of emitting and transmitting energy in waves or particles. One of the most remarkable aspects of radiation is radioactive radiation, which radioactive materials emit naturally and artificially. Although the ritual of exposure to radiation has continued since the beginning of the universe, mankind discovered radiation in the last years of the nineteenth century. After its discovery, it began to be used in various fields [1]. Since its discovery,

radiation has been employed in a variety of disciplines, including energy generation in power plants, radiological applications in medicine, fundamental scientific research, and industry [2]. After the discovery of X-rays in 1895, ionising radiations have been widely used in many fields from medicine to industry [3]. Radiological applications in medicine have a large share of the areas of use of radiation. In the medical field, radiation is a vital tool in diagnosis and treatment processes. Radiation therapy is a form of cancer treatment that uses radiation to destroy malignant cells [4]. Imaging methods such as X-ray, magnetic resonance imaging (MRI) and computed tomography (CT) are of great help to healthcare personnel in the diagnosis and detection of diseases. Thanks to these methods, it is possible to diagnose diseases early and manage treatment processes more effectively.

Two important types of radiation used in medicine are X and gamma rays. These ionising radiations carry high enough energy to interact inside cells and break down DNA. Thanks to these properties, they are effectively used in the radiotherapy method

used in cancer treatment. Ionising radiation from medical applications has the largest share among the artificial radiations to which society is exposed [5]. The most affected by artificial radiation used for medical purposes are the patients exposed to the procedure and the health personnel working in these units [6]. In addition, 95 per cent of radiation exposure is due to diagnostic X-rays [7]. Computed tomography (CT), X-ray and mammography are among the most commonly used diagnostic X-ray devices, especially in Turkey. [8]. It is of vital importance to ensure the radiation safety of those working with all these radiation emitting sources and devices. Occupational doses received by those working with ionising radiation should be continuously monitored and these doses should be minimised [9].

Such targeted and effective use of radiation in medicine aims to minimise damage to healthy tissue while increasing treatment success. In addition, these vital uses of radiation in medicine are of great importance for the progress of humanity and the improvement of the quality of life. However, strict controls, training and guidelines must be followed for the effective and safe use of radiation.

Nowadays, the awareness of individuals working in ionising radiation fields and people in the society exposed to radiation increases its importance as one of the basic conditions for a healthy and safe life. The more comprehensive and accurate the knowledge of students and healthcare professionals, who will be among the shapers of the future, on radiation, the potential damages of radiation in future generations will be significantly reduced. Increasing radiation awareness will raise awareness in all segments of the society and raise the consciousness of individuals to protect their health. Therefore, acting in a conscious manner to minimise the negative effects of radiation should be a fundamental goal. Minimising radiation exposure is of great importance for health and the environment.

Radiation literacy is an important issue especially for students, health personnel and the public. Studies in this field emphasise the importance of these groups having knowledge about radiation for the future. Therefore, nuclear physics and radiation literacy are important for researchers and many studies have been conducted in this field recently [10-35].

For this reason, the study was planned to analyse the attitudes towards radiation of health services vocational school students, each of whom will be health personnel, in terms of emotion, thought and behaviour dimensions. In line with this plan, it was aimed to reveal whether the attitudes towards radiation differ according to various individual and demographic characteristics in the evaluation of the attitudes of health services vocational school students towards radiation. It is thought that by exposing students' attitudes and levels of knowledge towards radiation, education will be provided for students with a lack of knowledge and misinformation, thus ensuring effective and efficient provision of services for students who are candidates for medical staff. It is thought that the research results will help healthcare vocational school students with the necessary, accurate information on radiation and to properly implement this information when needed.

2. Material and Methods

2.1 Study Area and Population

The population of the study consists of the students of Amasya University Sabuncuoğlu Şerefeddin Vocational School of Health Services in the 2021-2022 academic year. In the 2021-2022 academic year of Sabuncuoğlu Şerefeddin Vocational School of Health Services, 973 students who enrolled in the course and actively continued their education were interviewed from a total of 2594 students studying in the 1st and 2nd grades. The sample was not selected in the study and the whole population was reached.

2.2 Ethical Permission

The study was conducted under the Principles of the Declaration of Helsinki. Before the study, ethical approval was obtained from Amasya University Non-Interventional Clinical Research Ethics Committee (dated 3.06.2022 and numbered E-30640013-050.01.04-73478).

Before starting the study, permission to use the Radiation Attitude Scale and the Radiation Attitude Scale for Healthcare Workers and the Radiation Protection Knowledge Scale for Healthcare Workers in this study was obtained by e-mail from the authors of the Turkish validity and reliability. Also, the participants were informed about the nature of the study.

2.3. Data Collection Tools

The data were collected using the Personal Information Questionnaire, Radiation Attitude Scale, Radiation Attitude Scale for Healthcare Workers and Radiation Protection Knowledge Scale for Healthcare Workers developed by the researcher.

Survey form: Consisting of the first part that evaluates students' sociodemographic and radiation-related identifying information, the first part is

followed by radiation attitude scale, radiation attitude scale for healthcare workers, and health workers' radiation protection knowledge scale.

Radiation Attitude Scale: Built in 2011 by Torun, M., Yalçın, P., Yalçın, S. A. to apply to undergraduate level students, its reliability has been tested [34]. A "radiation attitude scale" was used to measure students' awareness of the harmful effects of radiation, which had been used in the case of Erzincan province before. The radiation attitude scale is a 32-question likert-type scale. The cronbach alpha internal coefficiency coefficient of the scale was found to be 0.88.

Radiation Attitude Scale for Health Workers: Radiation attitude scale for healthcare workers developed by Ekinci and Yalcin in 2019 [36]. The cognitive, sensitive and behavioral attitude of healthcare workers towards radiation and the use of RTNT (Radiological Examination and Nuclear Test) is highly important for the employees themselves and the patients receiving healthcare. The study developed a four-factor liquert-type scale with a reliability coefficient (Cronbach's Alpha) and a qualitative data collection tool consisting of eight substances, accounting for 64.5% of the total variance, consisting of 18 substances, to determine healthcare workers' attitude 0,914 radiation. The mixed scale prepared to cover the purpose of the study has been communicated in accordance with ethical guidelines through one-to-one interviews with health workers in health care facilities in Turkey and online, and the scale has been applied to 236 health workers following the scale development phase and the data has been analyzed by statistical programme. Four-factor liquert type scale; by finding that there is a significant difference in the lower dimensions relative to the variables of gender, occupation, department, institution and year of service; data from the eight-item qualitative data collection tool appeared to support results from liquert scale.

Health Workers' Radiation Protection Information Scale: The scale of health workers' radiation protection information was developed by Mahmut Ay in 2021 [37]. The Health Workers' Radiation Protection Information Scale is a 10 "liquert type scale consisting of 33 substances and three sub-dimensions. For scale assessment, for scale reliability when calculating language, scope, and structure transition analyses, the Guttman Split-Half and Cronbach alpha values were calculated under substance analyses, internal consistency. The Radiation Protection Information Scale of Healthcare Workers has been translated and reversed into Turkish for language passage. An opinion was taken from 14 experts for scope passage and it was found that scope-pass index values ranged from 0.83-1.00. Confirmatory Factor Analysis has been conducted to ensure structure validity and three factors discovered have been confirmed. In this analysis, compliance indexes were determined at $\chi 2/sd = 3.59$, RMSEA = 0.08, SRMR = 0.06, IFI = 0.91, and CFI = 0.91 at TLI = 0.90. To assess reliability, the Cronbach alpha reliability coefficient of the scale was looked at and calculated 0.98 for the entire scale. The Guttman Split-Half value of the scale was found to be 0.95. The scale clauses were determined to have matter-total score correlation coefficients r = 0.61 to 0.87.

2.4. Analysis of the Data

The statistical evaluation of the obtained data was performed with SPSS 24.0 package programme in computer environment. Descriptive statistical measures (mean, standard deviation, minimum and maximum values and percentages) were used. Since the variables fulfilled the parametric test assumptions in the evaluation of the data, Student t test was used to determine the difference between the averages of two independent groups, one-way analysis of variance for more than two independent groups (Tukey if homogeneity is provided to determine which group mean is different from the others, If not, Games-Howell test), Pearson correlation analysis to determine the direction and level of the relationship between variables, simple linear regression analysis to evaluate the effect of more than one variable on the continuous dependent variable, Cronbach Alpha test to determine the internal validity level of the scales and the error level was taken as 0. 05 was taken as the error level.

3. Results and Discussions

The distribution of the students participating in the study according to their sociodemographic characteristics is given in Table 1. The average age of the students is 20.71 ± 2.21, with 60.0% (n = 584) in the 20-21 age bracket, 75.8% "in (n = 738) girl, 53.1%" in (n = 517) studying in one of the non-direct health related programs, 70.6% of (n = 687) primary education of her mother's education status, 60.1% "in (n = 585) elementary education of her father, 43.2% (n = 420) living in the city, 58.8%" in (n = 572) resident of the Black Sea Region (Table 1) 13.7% of students (n = 133) worked in the emergency room as part of the course/internship, 75.4% described the radiation of "reputation (n = 734) as" energy event emitted in the form of electromagnetic wave or particle,

"93.6% of which (n = 911) was previously associated with radioactive matter or radiation 58.3% (n = 567) did not know enough about radiation protection (table 2). The distribution of the mean scores of the students participating in the study according to their answers to the radiation attitude scale, radiation attitude scale for healthcare workers and radiation protection knowledge scale for healthcare workers is given in Table 3.

Table 1: Distribution of Students According to Sociodemographic Characteristics (N=973)

Characteristics	N	%
Age		
18-19 years	196	20.1
20-21 years	584	60.0
22 years and over	193	19.9
Average Age	20.71 ± 2.21 (min:18 – max:40)	
Gender		
Girl	738	75.8
Boy	235	24.2
Learning Program		
Programmes directly related to health	456	46,9
Programmes not directly related to health	517	53.1
Mother's Education Status		
Illiterate	73	7.5
Primary education	687	70.6
High School	182	18.7
University	31	3.2
Father's Education Status		
Illiterate	11	1.1
Primary education	585	60.1
High School	282	29.0
University	95	9.8
Living Place		
Metropolitan	298	30.6
City	420	43.2
The Town	70	7.2
Village	185	19.0
Living Region		
Marmara Region	46	4.7
Ege Region	22	2.3
Central Anatolia Region	185	19.0
Black Sea Region	572	58.8
Mediterranean Region	56	5.8
Eastern Anatolia Region	44	4.5
Southeastern Anatolia Region	48	4.9

Note: Frequency and percentage calculations were used, Programmes Directly Related to Health: First and Emergency Aid, Medical Laboratory Techniques, Disabled Care and Rehabilitation, Physiotherapy, Aged Care. Programmes Not Directly Related to Health: Child Development, Medical Documentation and Secretariat, Opticianry

Table 2: Distribution of Students by Internship, Radiation Definition, and Knowledge of Radiation Protection by Status (N = 973)

Features	N	%
Unit Studied Under Course/Internship		
Internal Units	34	3.5
Surgical Units	16	1.6
Operating room	13	1.3
Emergency Services	133	13.7
Intensive Care	34	3.5
Outpatient Services	59	6.1
Other	684	70.3
Radiation		
Energy coming from underground Electricity Based Energy Event	18	1.8
Energy Event Emitted in Electromagnetic Wave or Particle Form	84	8.6
It Is the Energy Event That Causes Environmental Pollution	734	75.4
Energy Event Emitted From Nuclear Power Plants	60	6.2
	77	7.9
Previous experience in any work that can be considered related to radioactive material or radiation		
Yes	62	6.4
No	911	93.6
The Status of Thinking That They Have Sufficient Knowledge About Radiation Protection		
Yes	406	41.7
No	567	58.3

Note: Frequency and percentile calculations used

Table 3: Distribution of Mean Scores of Radiation Attitude Scale, Radiation Attitude Scale for Healthcare Workers, Radiation Protection Knowledge Scale for Healthcare Workers (N=973)

Scales	$\bar{X}$	SS	min	max	Cronbach alpha
RAS	74.60	16.79	32	160	0.87
RASHW	32.28	11.14	18	90	0.94
Radiation Knowledge	12.48	4.59	7	35	0.89
Radiation Sensitivity	7.16	2.74	4	20	0.90
Patient Sensitivity	7.36	2.76	4	20	0.91
Informing the Patient	5.64	2.24	3	15	0.95
RPKSHW	106.94	56.93	33	321	0.97

Note: RAS: Radiation Attitude Scale, RASHW: Radiation Attitude Scale for Healthcare Workers, RPKSHW: Radiation Protection Knowledge Scale for Healthcare Workers

The mean total score of RAS was 74.60±16.79; the mean total score of RASHW was 32.28±11.14; the mean radiation knowledge sub-dimension was 12.48±4.59; the mean radiation sensitivity sub-dimension was 7.16±2.74; the mean patient sensitivity sub-dimension was 7.36±2.76; the mean patient information sub-dimension was 5.64±2.24;

and the mean total score of RPKSHW was 106.94±56.93. According to these results, it was determined that the students' knowledge of radiation protection was below the average. Considering the mean total score of the "radiation attitude" scale, it was determined that the students' awareness of the harmful effects of radiation was not at a sufficient level.

When the reliability levels of the internal validity coefficients of the scales used in the study were analysed, it was determined that the general reliability levels of the RAS, RASHW and RPKSHW were highly reliable ($0.80 < \alpha < 1.00$) [38].

Table 4: *Comparison of the Sociodemographic Characteristics of the Students with the Total Scores of RAS, RASHW and RPKSHW*

Features	RAS $\bar{X} \pm SS$	RASHW $\bar{X} \pm SS$	RPKSHW $\bar{X} \pm SS$
Age			
18-19 years	76.93±14.98	33.66±11.00	105.89±52.53
20-21 years	73.81±17.51	32.10±11.24	105.39±57.76
22 years and over	74.61±16.14	31.44±10.92	112.68±58.59
F / p*	2.54 / 0.07	2.13 / 0.11	1.23 / 0.29
Gender			
Girl	74.29±15.83	31.68±10.56	03.96±56.07
Boy	75.56±19.51	34.17±12.62	116.29±58.68
t / p**	-0.90 / 0.36	*-2.73 / 0.00*	*-2.90 / 0.00*
Learning Program			
Programmes directly related to health	74.98±17.69	31.62±11.55	112.70±55.39
Programmes not directly related to health	74.26±15.96	32.86±10.75	101.85±57.82
t / p**	0.66 / 0.50	-1.73 / 0.08	*2.97 / 0.00*
Mother's Education Status			
Illiterate	71.45±16.72	31.58±10.30	107.99±50.75
Primary education	74.81±16.63	32.25±11.05	105.31±57.66
High School	74.55±17.83	32.34±12.06	110.35±55.90
University	77.45±13.57	34.29±9.55	120.52±60.09
F / p*	1.19 / 0.31	0.43 / 0.72	1.00 / 0.39
Father's Education Status			
Illiterate	70.82±16.06	27.55±6.83	120.27±48.84
Primary education	74.34±16.91	32.12±10.82	105.16±56.02
High School	74.79±15.78	32.43±10.90	105.91±57.95
University	76.00±19.04	33.35±13.84	119.41±59.30
F / p*	0.46 / 0.70	1.00 / 0.38	1.94 / 0.12
Living Place			
Metropolitan City	74.39±18.31	32.52±12.44	106.31±59.20
The Town	74.66±15.37	31.88±9.98	108.69±57.23
Village	73.71±15.83	30.70±11.80	107.67±53.79
	75.10±17.77	33.41±11.15	103.69±53.86
F / p*	0.13 / 0.93	1.33 / 0.26	0.34 / 0.79
Living Region			
Marmara Region (1)	76.74±15.91	33.70±9.82	107.54±59.35
Ege Region (2)	70.68±27.30	32.95±14.87	115.05±70.56
Central Anatolia Region (3)	71.19±17.73	31.44±10.96	110.41±59.83
Black Sea Region (4)	76.67±15.63	32.94±11.36	102.79±55.13
Mediterranean Region (5)	70.45±16.37	29.39±10.07	122.38±58.26
Eastern Anatolia Region (6)	68.66±18.31	30.73±10.13	112.84±45.95
Southeastern Anatolia Region (7)	73.00±16.45	30.77±10.00	115.21±62.52
F / p*	*4.70 / 0.00*	1.57 / 0.15	1.63 / 0.13
Significant Difference	**3-4, 4-6**	-	-

*Notes: *One-way analysis of variance, **Student t test, RAS: Radiation Attitude Scale, RASHW: Radiation Attitude Scale for Healthcare Workers, RPKSHW: Radiation Protection Knowledge Scale for Healthcare Workers*

In Table 4, in which the sociodemographic characteristics of the students and the mean total scores of the scale were compared, it was found that the students who were 18-19 years old, boy, studying in programmes directly related to health, whose parents were university graduates, residing in the village and living in the Marmara Region had higher mean scores on the radiation attitude scale, and there was a significant difference between the total score of the RAS and the region of residence variables ($p < 0.05$). It was determined that the students who were 20-21 years old, boy, studying in programmes not directly related to health, whose parents were university graduates, residing in the village, and living in the Marmara Region had higher mean scores on the radiation attitude scale for health workers, and there was a significant difference between the total score of the RASHW and the gender variable ($p < 0.05$). It was determined that students who were older than 22 years, boy, studying in programmes directly related to health, whose mothers were university graduates, whose fathers were illiterate, who resided in the city and who lived in the Mediterranean Region had higher mean scores on the RPKSHW, and there was a significant difference between the total score of the RPKSHW and gender and the programme of study ($p < 0.05$). In Table 5, in which the students' place of internship, definition of radiation and m

***Table 5:** Comparison of Students' Internship Placement, Knowledge of Radiation Definition and Radiation Protection with the Mean Total Scores of RAS, RASHW and RPKSHW*

Features	RAS $\bar{X} \pm SS$	RASHW $\bar{X} \pm SS$	RPKSHW $\bar{X} \pm SS$
Unit Studied Under Course/Internship			
Internal Units (1)	71.62±15.64	32.68±7.72	127.53±48.93
Surgical Units (2)	79.19±18.67	30.56±12.16	97.88±51.60
Operating room (3)	71.85±23.02	29.23±10.83	153.00±68.04
Emergency Services (4)	75.41±21.74	31.80±13.27	113.18±54.68
Intensive Care (5)	80.32±13.25	35.26±11.47	103.65±50.94
Outpatient Services (6)	73.98±18.30	32.66±12.32	133.12±57.85
Other (7)	74.30±15.53	32.27±10.69	101.94±56.68
F / p*	1.19 / 0.30	0.69 / 0.65	5.62 / 0.00
Significant Difference	-	-	3-7, 6-7
Radiation			
Energy coming from underground (1)	63.44±18.46	33.17±10.57	132.78±69.34
Electricity Based Energy Event (2)	76.88±17.88	35.87±11.92	105.70±61.10
Energy Event Emitted in Electromagnetic Wave or Particle Form (3)	74.53±16.31	31.68±10.58	108.10±56.42
It Is the Energy Event That Causes Environmental Pollution (4)	71.90±16.68	34.98±14.29	103.25±55.80
Energy Event Emitted From Nuclear Power Plants (5)	77.45±18.67	31.81±12.07	94.03±53.07
F / p*	3.35 / 0.01	3.70 / 0.00	2.07 / 0.08
Significant Difference	1-2, 2-3, 1-5	2-3	-
Previous experience in any work that can be considered related to radioactive material or radiation			
Yes	72.03±17.04	32.63±11.87	132.31±56.14
No	74.77±16.77	32.26±11.10	105.21±56.60
t / p**	-1.24 / 0.21	0.25 / 0.79	3.64 / 0.00
The Status of Thinking That They Have Sufficient Knowledge About Radiation Protection			
Yes	73.67±18.06	32.13±11.73	122.20±58.21
No	75.26±15.80	32.39±10.71	96.01±53.42
t / p**	-1.45 / 0.14	-0.36 / 0.71	7.26 / 0.00

Notes: *One-way analysis of variance, **Student t test, RAS: Radiation Attitude Scale, RASHW: Radiation Attitude Scale for Healthcare Workers, RPKSHW: Radiation Protection Knowledge Scale for Healthcare Workers

knowledge about radiation protection were compared with the mean scores of the scale, it was determined that the mean score of the RAS was higher in those who worked in the intensive care unit within the scope of the course/internship, defined radiation as "the energy emitted fronuclear power plants", had not previously worked in any study that could be considered related to radioactive material or radiation, and did not think that they had enough information about radiation protection, and there was a significant relationship between the definition of radiation and the total score of the RAS (p < 0.05). It was found that those who worked in the intensive care unit within the scope of course/internship, defined radiation as "electricity-based energy event", had previously worked in any study that could be considered related to radioactive material or radiation, and did not think that they had enough information about radiation protection had a higher mean score on the RASHW, and there was a significant relationship between the definition of radiation and the total score of the RASHW (p<0.05). Those who worked in the operating room within the scope of course/internship, defined radiation as "an energy event coming from underground", had previously worked in any study that could be considered related to radioactive material or radiation, and thought that they had enough information about radiation protection had a higher mean score on the RPKSHW, it was found that there was a significant correlation between the unit of study within the scope of the course/internship, the status of being involved in any study that can be considered related to radioactive material or radiation before, and the status of thinking that they had enough knowledge about radiation protection and the total score of the

RPKSHW (p<0. 05). According to Table 6, which evaluates the total score of the scales used in the study and the relationship between the scales, it was found that there was a moderate, positive, significant relationship between the total score of the RAS and the total score of the

Table 6: *Correlation of Students' Total RAS, Total and Sub-dimension of RASHW and RPKSHW Total Scores*

	$\bar{X}$	SS	1	2	3	4	5	6	7
1-RAS total	74.60	16.79	1						
2-RASHW total	32.28	11.14	0.482*	1					
3-Radiation information	12.48	4.59	0.421*	0.925*	1				
4-Radiation sensitivity	7.16	2.74	0.427*	0.903*	0.788*	1			
5-Sensitivity to the patient	7.36	2.76	0.421*	0.885*	0.719*	0.744*	1		
6-Informing the patient	5.64	2.24	0.468*	0.834*	0.662*	0.693*	0.734*	1	
7-RPKSHW total	106.94	56.93	0.082**	0.018	0.009	0.037	0.015	0.008	1

Note: p<0.01*, p<0.05**, Pearson Correlation Analysis was used, RAS: Radiation Attitude Scale, RASHW: Radiation Attitude Scale for Healthcare Workers, RPKSHW: Radiation Protection Knowledge Scale for Healthcare Workers

RASHW; there was a very low, negative, significant relationship between the total score of the RAS and the total score of the RPKSHW; and there was a positive, very weak, insignificant relationship between the total score of the RASHW

and the total score of the RPKSHW. It was determined that as one unit of RAS score increased, the score of RASHW, radiation knowledge, radiation sensitivity, sensitivity to patient, sensitivity to patient, informing patient increased and the score of RPKSHW decreased; as one unit of RASHW score increased, the score of radiation knowledge, radiation sensitivity, sensitivity to patient, sensitivity to patient, informing patient increased; as one unit of RPKSHW score increased, the score of RAS score decreased.

Table 7. *Regression Analysis of Radiation Attitude Scale Total Score of Students Studying in Programmes Directly Related to Health*

Independent Variables	**Regression coefficients**	**t**	**p**
RASHW	0.06	0.73	0.46
Radiation information	***0.21***	***2.73***	***0.00***
Radiation sensitivity	0.00	0.10	0.91
Sensitivity to the patient	0.06	0.78	0.43
Informing the patient	***0.28***	***4.22***	***0.00***
RPKSHW	-0.05	-1.37	0.17
R = 0.53 R^2 = 0.27			
F =35.10 *p* = 0.00			

Note: Simple linear regression analysis was used, RASHW: Radiation Attitude Scale for Healthcare Workers, RPKSHW: Radiation Protection Knowledge Scale for Healthcare Workers

As a result of the simple linear regression analysis performed to reveal how the variables thought to have an effect on the radiation attitude scale of students studying in programmes directly related to health predicted the total score of the radiation attitude scale, it was observed that these predictor variables exhibited a significant relationship (R=0.53; R^2 = 0.00) with radiation attitude (F=35.10, p<0.05). When the significance tests of the regression coefficients were considered, it was found that radiation knowledge and patient information variables were significant predictors of radiation attitude (p<0.05) (Table 7) and (Figure 1). As a result of the simple linear regression analysis performed to reveal how the variables thought to have an effect on the radiation attitude of students studying in programmes not directly related to health predicted the radiation attitude scale score, it was seen that these predictor variables exhibited a significant relationship (R=0.49; R^2 = 0.23) with radiation attitude (F=32.60, p<0.05). When the significance tests of the regression coefficients were considered, it was found that the independent variables of radiation sensitivity, patient sensitivity and patient information were significant predictors of radiation attitude (p<0.05) (Table 8) and (Figure 2).

4. Conclusions

Considering the total scores of the participants' "Radiation Attitude Scale (RAS)", "Radiation Attitude Scale for Healthcare Workers (RASHW)", "Radiation Protection Knowledge Scale for Healthcare Workers (RPKSHW)", it is interpreted
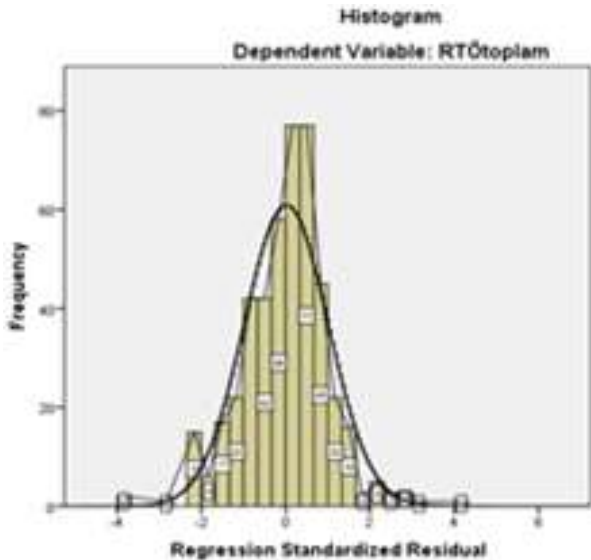

Figure 1. *Graph of Radiation Attitude Scale Total Score of Students Studying in Programs Directly Related to Health*

Table 8. *Regression Analysis of Radiation Attitude Scale Total Score of Students Studying in Programmes Not Directly Related to Health*

Independent Variables	Regression coefficients	*t*	*p**
RASHW	0.07	1.23	0.18
Radiation information	0.04	0.68	0.49
Radiation sensitivity	*0.18*	*2.83*	*0.00*
Sensitivity to the patient	0.06	1.05	0.29
Informing the patient	*0.25*	*4.46*	*0.00*
RPKSHW	*-0.12*	*-3.25*	*0.00*
R = 0.49	R^2 = 0.23		
F = 32.60	p = 0.00		

Note: Simple linear regression analysis was used, RASHW: Radiation Attitude Scale for Healthcare Workers, RPKSHW: Radiation Protection Knowledge Scale for Healthcare Workers

that the students' awareness of radiation and radiation protection is not at an adequate level. Specifically, differences were observed in the programme and gender categories. We can say that the reason for the difference in attitudes at the level of knowledge in the programme variables is that the radiation safety course education that the students studying in these programmes received at the university was effective. However, it is thought that it would be useful to expand the curriculum of this course by reflecting it to other programmes. As
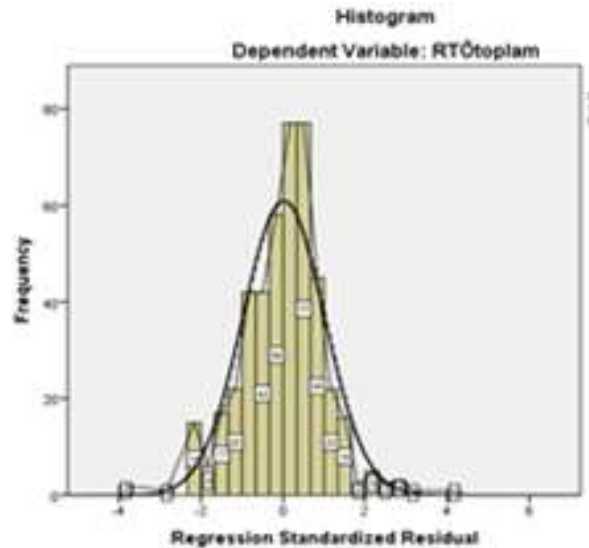
Figure 2. *Radiation Attitude Scale Total Score Graph of Students Studying in Programs Not Directly Related to Health*

Palacı [39] reported in her study, radiation safety and protection education in Turkish universities was found to be lower than the European Union standards. A significant difference was determined between the gender variable and the total score of the RASHW. It was observed that girl participants had more positive and higher attitudes in cognitive and behavioural dimensions compared to boy participants. The culture in which an individual lives shapes how men and women behave, think and act. This is the basis of women being more emotional, more cautious and more sensitive [40]. It is thought that the fact that girl participants in the study had more positive and higher attitudes towards radiation and radiation protection is based on this situation.

Radiation is a serious danger that concerns not only a certain part of the society but everyone. Accordingly, it would be more beneficial for the future to include the knowledge of radiation and how to protect against radiation to the students who shape the future at all levels of education in our country (pre-school education, primary education, secondary education, higher education). As stated by Palacı [39] in his study, there is inadequacy of the education on radiation and protection in the associate degree programme training health personnel. An individual's lack of knowledge or misinformation about radiation and its effects on health allows the necessary cognitive attitude about radiation not to be formed. The deficiency in cognitive attitude is reflected in affective and behavioural attitudes and affects them negatively.

It is important to provide radiation-related education to students who are studying in health

sciences and other health fields to be future health personnel and educators in order to prevent fear and anxiety caused by incorrect and incomplete information. Cognitive attitude can be provided with accurate and complete knowledge about radiation and this situation is indirectly reflected on affective and behavioural attitudes. In this context, it is recommended that the existing curricula in universities be revised in the light of this situation.

Author Statements:

References

[1]Teke, C., Akkurt, İ., Arslankaya, S., Ekmekçi, İ., Günoğlu, K. (2023). Prediction of gamma ray spectrum for 22Na source by feed forward back propagation ANN model. *Radiation Physics and Chemistry*. 202, 110558. DOI:10.1016/j.radphyschem.2022.110558

[2]Şengül, A., Akkurt, İ., Günoğlu, K., Akgüngör, K., Ermiş, R.B. (2023). Experimental evaluation of gamma-rays shielding properties of ceramic materials used in dentistry. *Radiation Physics and Chemistry*. 204, 110701. DOI:10.1016/j.radphyschem.2022.110701

[3]Şengül, A., Akgüngör, K., Akkurt, İ. (2022). Akışkan Dental Kompozitin Gamma Radyasyonu Soğurma Özellikleri. *Avrupa Bilim ve Teknoloji Dergisi*, (35), 469-473. DOI:10.31590/ejosat.1085811

[4]Karpuz, N. (2016). Effect of the level density parameter ratio on the cross sections of fission of Uranium isotopes. *Acta Physica Polonica A*, 130, 1. DOI:10.12693/APhysPolA.130.306

[5]Paolicchi, F., Miniati, F., Bastiani, L., Faggioni, L., Ciaramella, A., Creonti, I., Sottocornola, C., Dionisi,

C., & Caramella, D. (2016). Assessment of radiation protection awareness and knowledge about radiological examination doses among Italian radiographers. *Insights into imaging*, 7(2), 233–242. DOI:10.1007/s13244-015-0445-6

[6]Güdük, Ö., Kılıç, C.H., Güdük, Ö. (2018). Radyasyonun Zararlı Etkileri Hakkında Hastaların Bilgi Düzeyinin Değerlendirilmesi: Bir Hastane Örneği. *Adıyaman Üni. Sağlık Bilimleri Derg*, 4(2):874-889. DOI:10.30569/adiyamansaglik.430175

[7]Ujah, F.O., Akaagerger, N.B., Agba, E.H., Iortile, J.T. (2012). A comparative study of patients radiation levels with standard diagnostic reference levels in federal medical center and bishop murray hospitals in Makurdi. *Archives of Applied Science Research*, 4(2):800-804.

[8]Şahmaran, T., Akçoban, S. (2022). Meslek yüksekokulu öğrencilerinin ve akademisyenlerin radyasyon bilgi düzeylerinin değerlendirilmesi. *MKÜ Tıp Dergisi*, 13(47):391-398. DOI:10.17944/mkutfd.1100586

[9]Zeyrek, C.T. (2013). İyonize radyasyon uygulamaları için güvenlik ve korunmaya yönelik genel kavramlar. *Suleyman Demirel University Journal of Natural and Applied Science*, 17(3), 1-9.

[10]Yalçın, P., Ekinci, M., Yalçın, S.A. (2020). Radiation Attitudes Scale for Healthcare Staff. *European J of Physics Education,* 11, 3, 1309-7202.

[11]Yalçın, P., Karenoğulları, T., Yalçın, S. A. (2018). Evaluation of attitudes and knowledge of teachers regarding the concept of radiation. *Education and Science*, 43, 194, 245-260.

[12]Osborne, C., Merchant, S., Knight, K., Sim, J., Wright, C. (2022). A phenomenological study investigating experiences of student learning using an online radiation therapy planning curriculum. *Technical Innovations & Patient Support in Radiation Oncology*, 24, 6–12. DOI:10.1016/j.tipsro.2022.08.009.

[13]Maharjan, S., Parajuli, K., Sah, S., Poudel, U. (2020). Knowledge of radiation protection among radiology professionals and students: A medical college-based study. *European Journal of Radiology Open*, 7, 100287. DOI:10.1016/j.ejro.2020.100287

[14]Han, E. O., Kım, J. R., Choı, Y. S. (2014). Educational effects of radiation work-study activities for elementary, middle, and high school students. *Nuclear Engineering and Technology*, 46, 3, 447-460. DOI:10.5516/NET.10.2013.091.

[15]Cheng, F. C., Chen, M. H., Chen, M. C., Wan, Y. W., Hsu, P. Y., Wang, Y. L., Chiang, C. P. (2023). An exploration of the connotation of clinical dental radiology education for medical radiation students in Taiwan in 2022. *Journal of Dental Sciences*, 18, 2, 767-774. DOI:10.1016/j.jds.2022.12.017.

[16]Uzuntarla, Y., Doğan, F. (2019). Determination of risk perception and knowledge level of ıonizing radiation of health personnel who carry the dosimeter in a training and research hospital. *Journal of Health Science and Profession*, 6(1): 34-41. DOI:10.17681/hsp.398026.

[17]Yücel, A., Karakaş, E., Bülbül, E., Koçar, İ., Duman, B., Onur, A. (2009). Knowledge About

Ionizing Radiation and Radiation Protection Among Patients Awaiting Radiological Examinations: A cross-sectional survey. *The Medical Journal of Kocatepe* 10: 25-31.

[18]Özdemir, E., Yarar, O. (2021). Sağlık Teknikerliği Programı Öğrencilerinin Nükleer Fizik Kavramları ile ilgili Kavramsal Anlama Düzeylerinin Belirlenmesi. *Avrupa Bilim ve Teknoloji Dergisi*, (23), 465-474. DOI:10.31590/ejosat.879306.

[19]Sarıhan, M. (2022). Nükleer Tıp Öğrencilerinin Radyasyon Okur-Yazarlığının Değerlendirilmesi. *Avrupa Bilim ve Teknoloji Dergisi*, (41), 85-91. DOI: 10.31590/ejosat.1114547.

[20]Yoshida, M., Iwamoto, s., Okahisa, R., Kishida, S., Sakama, M., Honda, E. (2020). Knowledge and risk perception of radiation for Japanese nursing students after the Fukushima Nuclear Power Plant disaster. *Nurse Education Today*, 94, 104552. DOI:10.1016/j.nedt.2020.104552.

[21]Arslanoğlu, A., Bilgin, S., Kubalı, Z., Ceyhan, M. N., İlhan, M. N., Maral, I. (2007). Doctors' and intern doctors' knowledge about patients' ionizing radiation exposure doses during common radiological examinations. *Diagnostic and Interventional Radiology*, 13(2) :53-55.

[22]Balsak, H., Güneş, G., Ulutaşdemir, N. (2016). Knowledge, Attitude and Behavior of Radiology Professionals about the Harmful Effects of Radiation Which is Used for Diagnosis. *Electronic International Journal of Education, Arts, and Science*, 2(1); 31-51.

[23]Demir, M. (2015). Radiobiological Effects, Protection of the Patient, Protection of Caregivers, Protection of Those Around the Patient and the Environment. *Nuclear Medicine Seminars*, 3, 171-179. DOI:10.4274/nts.0026

[24]Hagi, S. K., Khafaji, M. A. (2011). Medical students' knowledge of ionizing radiation and radiation protection. *Saudi Med J*, 32(5):520-524.

[25]Çeçen, G. S., Öçmen, S., Bulut, G., Yıldız, M., Çolak, M. (2003). Eğitim Hastanesi ortopedi ameliyathanesi'nde flouroskopi kullanımı ve radyasyondan korunma. *Kartal Eğitim ve Araştırma Hastanesi Tıp Dergisi*, 14(3); 156 – 158.

[26]Koplay, M., Sivri, M., Varol, İ., Maaroof, S., Khalil, A., Demir, Z., Sidel, C., Öz, A., Bayındır, B. N., Armağan, M., Abiç, A., Baz, İ. B. (2016). Toplumun radyasyon farkındalığı ve radyasyonla ilgili bilgi düzeyi. *Genel Tıp Dergisi*, 26(Ek-1):36-38.

[27]Vural, F., Fil, Ş., Çiftçi, S., Dura, A. A., Yıldırım, F., Patan, R. (2012). Radiation safety in operating units; knowledge, attitude and behaviors of operating room staffs. *Balıkesir Health Sciences Journal*, 1(3), 131-136.DOI:10.5505/bsbd.2012.22931.

[28]Yılmaztürk, S. S., Yarbaşı, Ö., Bozdemir, E. (2020). An assessment of the Knowledge about the Hazards and Biological Effects of Radiation in Pati-ents Applying to a Faculty of Dentistry. *Necmettin Erbakan University Dental Journal*, 2(1); 1-8.

[29]Öztürk, Y. E., Türktemiz, H., Akdağ, T. (2017). Dozimetre Taşıyan Sağlık Çalışanlarında İş Yükünün İyonlaştırıcı Radyasyon Risk Algısına Etkisi. *Hacettepe Sağlık İdaresi Dergisi*, 20(2): 203-218.

[30]Molu, Z., Kahyaoğlu, H., Köksal, E. A. (2016). Fen Bilgisi Öğretmen Adaylarının Radyoaktiflikle İlgili Bilgi Düzeyleri. *JOTCSC*, 1(1); 165-190.

[31]Günalp, M., Gülünay, B., Polat, O., Demirkan, A., Gürler, S., Akkaş, M., Aksu, N. M. (2014). Ionising radiation awareness among resident doctors, interns, and radiographers in a university hospital emergency department. *Radiol Med*, 119(6):440–447. DOI:10.1007/s11547-013-0374-8.

[32]Goula, A.; Chatzis, A.; Stamouli, M.-A.; Kelesi, M.; Kaba, E.; Brilakis, E. (2021). Assessment of Health Professionals' Attitudes on Radiation Protection Measures. *Int. J. Environ. Res. Public Health*, 18(24); 13380. DOI:10.3390/ijerph182413380.

[33]Bakaç, M., Taşoğlu, A. K. (2012). Fizik Öğretmen Adaylarının Radyasyon Farkındalığı. *Manisa Celal Bayar Üniversitesi Eğitim Fakültesi Dergisi*, 2(1); 88 – 105.

[34]Torun, M., Yalçın, P., Yalçın, S. A. (2011). Study of developing a scale of attitude towards radiation. *Procedia Social and Behavioral Sciences*, 15; 918–921. DOI:10.1016/j.sbspro.2011.03.212.

[35]Koçyiğit, A., Kaya, F., Çetin, T., Kurban, I., Erbaş, T., Ergin, A., Ağladıoğlu, K., Herek, D., Karabulut, N. (2014). The knowledge level medical personnel have on radiation exposure during common radiologic examinations. *Pamukkale Medical Journal*, 7(2):137-142.

[36]Ekinci, M., Yalçın, P. (2019). Sağlik Çalişanlarinin Radyasyon Tutumunu Belirleme Ölçeği Geliştirme Ve Uygulama Çalişması. *Erzincan Binali Yıldırım Üniversitesi Fen Bilimleri Enstitüsü Matematik ve Fen Bilimleri Eğitimi Anabilim Dalı Fen Bilgisi Eğitimi Bilim Dalı, Yüksek Lisans Tezi*, 1-147.

[37]Ay, M., Özlük, B. (2021). Sağlik Çalişanlarinin Radyasyondan Korunma Bilgisi Ölçeği'nin Türkçe'ye Uyarlanmasi: Geçerlik Ve Güvenirlik Çalişmasi. *Necmettin Erbakan Üniversitesi Sağlik Bilimleri Enstitüsü, Hemşirelikte Yönetim Anabilim Dalı, Yüksek Lisans Tezi*, 1-78.

[38]Uzunsakal, E., Yıldız, D. (2018). Alan araştırmalarında güvenilirlik testlerinin karşılaştırılması ve tarımsal veriler üzerine bir uygulama. *Uygulamalı Sosyal Bilimler Dergisi,* 2(1):14-28.

[39]Palacı, H., Günay, O., Yarar, O. (2018). Türkiye'deki radyasyon güvenliği ve koruma eğitiminin değerlendirilmesi. *European Journal of Science and Technology*, 14; 249-254. DOI: 10.31590/ejosat.479367.

[40]Akın, A., Demirel, S. (2003). Toplumsal cinsiyet kavramı ve sağlığa etkileri. *Cumhuriyet Üniversitesi Tıp Fakültesi Dergisi*, 25(4); 73-82.
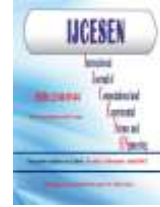
Shear Behaviour of RC Beams: A Numerical Study

Kagan SOGUT*

Kilis 7 Aralık University, Faculty of Engineering and Architecture, Department of Civil Engineering, Kilis-Turkey
* **Corresponding Author**: **Email:** kagan.sogut@kilis.edu.tr - **ORCID:** 0000-0002-0601-6420

Abstract:

A two-dimensional (2D) nonlinear finite element (FE) model developed for reinforced concrete (RC) beams is presented in this paper. The FE model was validated in order to perform further parametric studies on RC beams with and without existing steel shear links. The parameters were tension reinforcement ratio, concrete compression strength, and beam size. Moreover, the accuracy of "Turkish Standards 500: Requirements for design and construction of reinforced concrete structures (TS500)" in terms of predicting the total shear force capacity of RC beams was examined. The FE model properly captured the experimental load capacity, with a mean value of 1.04. The increase in overall shear force capacity caused by the increasing tension reinforcement ratio from 1.79 to 3.33% was 18.3% for RC beams with existing steel shear links, whereas it was 10.6% for RC beams without existing steel shear links. The total shear force capacities of RC beams with and without steel shear links increased once concrete compression was increased from 30 to 70 MPa. An increasing beam size resulted in a reduction in shear stress at failure of 33.8% and 32.7% for RC beams with and without shear links, respectively. TS500 design code gave conservative results in calculating the overall shear force capacity of RC beams.

1. Introduction

There is absolutely no uncertainty that inappropriately designed RC beams against shear, as compared with inappropriately designed RC beams in flexural, have catastrophic effects since shear failure takes place in a brittle and immediate way. It is therefore crucial to understand the shear behaviour of RC beams and the parameters influencing the shear behaviour. However, research examining the effect of some of the most principal factors on the shear behaviour of RC beams has yet to be fully understood [1,2]. For example, when compared to large-scaled RC beams, a substantial number of experimental studies were carried out to physically test laboratory-scaled RC beams [3-6]. This is especially concerning since the size effect in RC beams causes a decrease in shear stress and a change from ductile to brittle behaviour once beam dimensions are increased [2,3,5,6]. This paper numerically investigates the shear behaviour of RC beams both with and without existing steel shear links. A two-dimensional (2D) nonlinear finite element (FE) model was created and verified against experimental results in the current literature. The

effects of tension reinforcement ratio, concrete compression strength, and beam size on the shear behaviour of RC beams were investigated. Furthermore, the numerical results in terms of total shear capacity of RC beams were used to assess "Turkish Standards 500: Requirements for design and construction of reinforced concrete structures (TS500)" [7] for designing RC beams.

2. Material and Methods

VecTor2 software [8] established on Disturbed Stress Field Model (DSFM) [9] was used to create a 2D FE model. The summary of analysis and constitutive material models of the developed FE model, together with the main parameters, are shown in Table 1. The RC beam, which was included in the experimental study carried out by Elsanadedy et al. [10], was used to validate the FE model. As shown in Fig. 1, the RC beam was 200 mm wide and 450 mm deep and was tested in a four-point-bending configuration [10]. The beam was reinforced in tension and compression with three 16 mm and two 10 diameter steel bars, respectively. The shear reinforcement of the beam consisted of 8 mm-
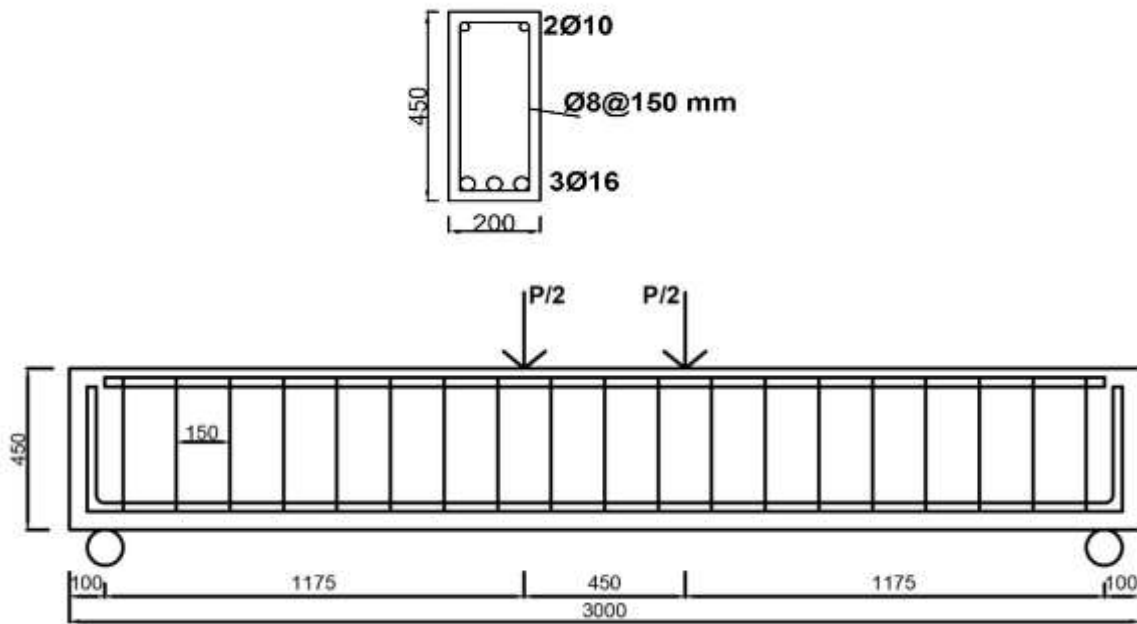
Figure 1. *Details of RC beam tested by Elsanadedy et al. [10] (all dimensions in millimeters)*

Table 1. *FE modelling* [8]

Concrete Models		Reinforcement Models				
Concrete Pre- and Post-Peak	Popovics (HSC) Base Curve	**Hysteretic Response***		Bauschinger Effect (Seckin)		
Compression Softening	Vecchio 1992-B (e1-e0-Form)	**Dowel Action***		Tassios (crack slip)		
Tension Stiffening*	Modified Bentz 2003	**Buckling***		Akkaya 2012 (Modified Dhakal-Maekawa)		
Tension Softening*	Bilinear	**Main Input Parameters**				
Confined Strength*	Kupfer/Richart	f_c (MPa)	f_t* (MPa)	E_c* (MPa)	**Mesh Size (mm)**	**Poisson's ratio***
Dilation*	Variable-Isotropic	50	$0.33\sqrt{f_c}$ (VecTor2)	$3320\sqrt{f_c} + 6900$ (VecTor2)	25	0.15
Cracking Criterion*	Mohr-Coulomb (Stress)	**Analysis Models**				
Crack Stress Calculation*	Basic (DSFM/MCFT)	**Strain History***		Previous Loading Considered		
Crack Width Check*	Agg. / 2.5	**Cracking Spacing***		CEB-FIP 1978-Deformed		
Crack Slip Calculation*	Walraven	**Max. No. of Iterations**		100		
Creep and Relaxation*	Not Considered	**Convergence Limit***		1.00001		
Hysteretic Response*	Nonlinear/w-Plastic Offsets	**Structural Damping***		Not Considered		
Default models (VecTor2)		**Geometric Nonlinearity***		Considered		
		Convergence Criteria*		Displacements-Weighted Average		

249

diameter steel bars. The spacing between these shear links was 150 mm centre-to-centre (c/c). The concrete compression strength was 50 MPa. The yield strengths of 8-, 10-, and 16-mm steel bars were 570, 575, and 575 MPa, respectively.

3. Results and Discussions

The RC beam physically tested by Elsanadedy et al. [10] was numerically validated in terms of ultimate load capacity and corresponding deflection at ultimate load capacity. Fig. 2 compares the experimental results with the FE results. The developed FE model captured the experimental load capacity with a mean value of 1.04 (see Table 2). As shown in Fig. 2, both physically and numerically tested beams failed in flexure. The uncracked stiffness of the numerically tested beam was in good correlation with that of the experimentally tested beam. This can be attributable to the fact that elastic constants and boundary conditions were accurately modelled. Similar to the experimental load-displacement curve, the load-displacement curve of the numerically modelled beam turned from a linear to a nonlinear response after the formation of cracks. Finally, the numerically modelled beam had a ductile failure with a plateau.

Figure 2. *Experimental* [10] *and FE-predicted load-deflection curves*

Table 2. *Comparison between experimental and FE results*

Load at failure (kN)			
Beam	**Exp.**	**FE**	**FE/Exp.**
B1	239	247.7	1.04

After obtaining validated results, it was conducted to examine the parameters influencing the structural behaviour of RC beams. To examine the shear behaviour of RC beams, sh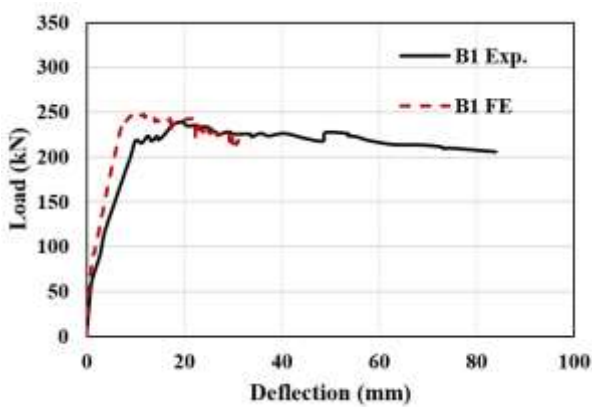ear-deficient beams taken into account in parametric studies were identical to RC beam tested by Elsanadedy et al. [10] but had a tension and compression reinforcement of 25 mm diameter steel bars and a shear reinforcement of 6

mm diameter steel bars. This ensured that numerically modelled beams had brittle behaviour and thus failed in shear. The investigated parameters were tension reinforcement ratio, concrete compression strength, and beam size. It should be noted that all numerical investigations were performed on RC beams with and without existing steel shear links. Moreover, all results were compared to TS500 [7] predictions. Of note is that the material safety factors of concrete and steel have been set to 1. TS500 [7] considers the overall shear resistance capacity (V_r) of a RC beam as the sum of the contributions of concrete (V_c) and steel shear links (V_w) as given in equation 1.

$$V_r = V_c + V_w \quad (1)$$

V_c can be calculated as follows;

$$V_c = 0.8 * V_{cr} \quad (2)$$

Where V_{cr} is shear cracking strength of a RC section and is calculated as given in equation 3.

$$V_{cr} = 0.65 * f_{ctk} * b_w * d \quad (3)$$

Where b_w and d are the width and effective depth of the RC beam, respectively. TS500 [7] recommends calculating f_{ctk} as follows;

$$f_{ctk} = 0.35 * \sqrt{f_{ck}} \quad (4)$$

Where f_{ck} is the compressive strength of concrete.

The contribution of steel shear links to shear strength is given by equation 5.

$$V_w = \frac{A_{sw}}{s} * f_{yw} * d \quad (5)$$

Where A_{sw} is the area of steel shear reinforcement, s is the spacing of steel shear links, and f_{yw} is the yield strength of steel shear reinforcement.

The impact of tension reinforcement ratio on the total shear force capacity of RC beams both with and without existing steel shear links was studied by modelling shear-deficient beams identical to the beam hereinabove mentioned but with tension reinforcement ratios ranging from 1.79 to 3.33%. Fig. 3 shows the effect of tension reinforcement ratio on total shear force capacity. An increase in the tension reinforcement ratio instigated an increase in total shear force capacity for RC beams both with and without steel shear links. This increase caused by the rising tension reinforcement ratio from 1.79 to 3.33% was 18.3% for RC beams with existing steel shear links, whereas it was 10.6% for RC beams without existing steel shear links. This can be attributable to confinement. The confined tension

reinforcement increased the total shear strength capacity more than that of unconfined tension reinforcement. Moreover, TS50 [7] gave conservative predictions in terms of total shear force capacity for RC beams both with and without shear links. The reason for the constant predictions of TS500 [7] can be explained by the fact that the effect of tension reinforcement on the shear force capacity of RC beams is not considered. As can be seen in Fig. 3, the effect of tension reinforcement on RC beams, especially with existing shear reinforcement, linearly increased the total shear force capacity.
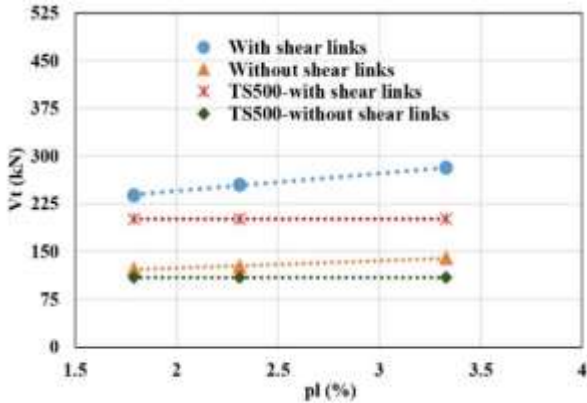
Figure 3. *Impact of tension reinforcement ratio*

The effect of concrete compression strength was examined by modelling RC beams with concrete compression strengths ranging from 30 to 70 MPa. Fig. 4 demonstrates the impact of concrete compression strength on the shear behaviour of RC beams both with and without steel shear links. The total shear force capacities of RC beams with and without steel shear links increased from 226.4 to 277.2 kN and from 105 to 144 kN, respectively, once concrete compression was increased from 30 to 70 MPa. As can be seen in Fig. 4, TS500 [7] predictions especially gave conservative predictions for RC beams with steel shear links. However, TS500 [7] predictions for total shear force capacities of RC beams both with and without steel shear links were in an increasing trend once concrete compression strength was enhanced from 30 to 70 MPa. The size effect in RC beams is one of the significant parameters influencing shear behaviour [1, 11-13]. In this study, the validated FE model was used to produce RC beams to assess the size effect. The numerically modelled beams were also identical to the shear-deficient beams hereinabove mentioned. All dimensions were scaled by a scale factor that varied between 0.667
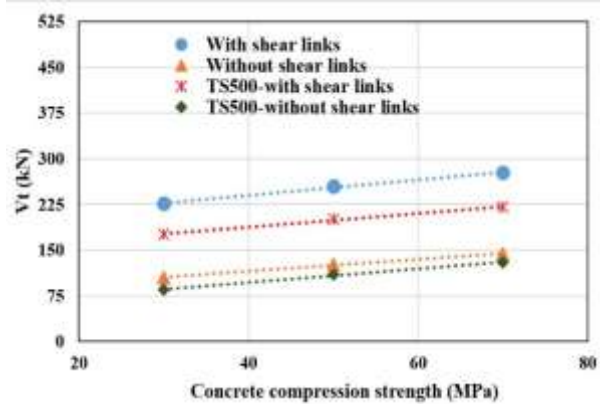
Figure 4. *Effect of concrete compression strength*

and 1.33. Of note is that reinforcement ratios were also kept constant. Fig. 5 demonstrates a variation in shear stress with effective beam depth for RC beams both with and without shear links. An increasing effective depth from 275 to 550 mm caused a reduction in shear stress at failure of 33.8% and 32.7% for RC beams with and without shear links, respectively. However, shear stress predictions of TS500 [7] were constant for RC beams both with and without shear links once the beam dimensions were increased or decreased. This proved that TS500 [7] does not consider the size effect.
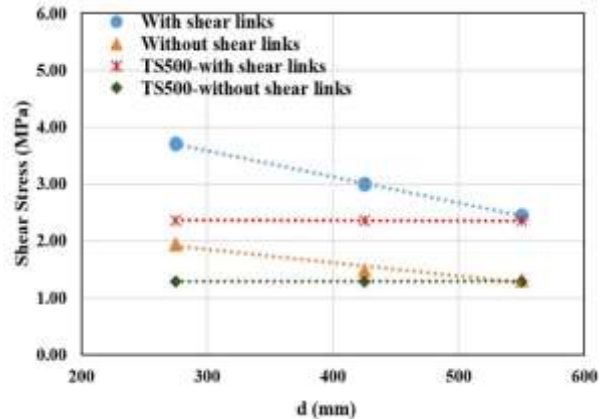
Figure 5. *Size effect*

4. Conclusions

A two-dimensional FE model was created and verified against the experimental results of Elsanadedy et al. [10]. The impacts of tension reinforcement ratio, concrete compression strength, and beam size on the shear behaviour of RC beams both with and without existing steel shear links. Moreover, the accuracy of TS500 [7] in terms of calculating the overall shear strength capacity of RC beams was examined. According to the numerical research, the following results were obtained:

➤ The enhancement in total shear force capacity caused by the increasing tension reinforcement ratio from 1.79 to 3.33% was 18.3% for RC beams with steel shear links, whereas it was 10.6% for RC beams without existing steel shear links. The impact of tension reinforcement on the shear force capacity of RC beams is not considered by TS500 [7]. Thus, it gave constant predictions for the overall shear force capacity of RC beams.

➤ The total shear force capacities of RC beams with and without steel shear links increased from 226.4 to 277.2 kN and from 105 to 144 kN, respectively, once concrete compression was increased from 30 to 70 MPa. Although TS500's [7] predictions for total shear force capacities of RC beams both with and without steel shear links were in an increasing trend, their predictions were conservative.

➤ An increasing effective depth from 275 to 550 mm caused a reduction in shear stress at failure of 33.8% and 32.7% for RC beams with and without shear links, respectively. However, shear stress predictions of TS500 [7] were constant for RC beams both with and without shear links once the beam dimensions were increased or decreased.

Author Statements:

- **Ethical approval:** The conducted research is not related to either human or animal use.
- **Conflict of interest:** The authors declare that they have no known competing financial interests or personal relationships that could have appeared to influence the work reported in this paper
- **Acknowledgement:** The authors declare that they have nobody or no-company to acknowledge.
- **Author contributions:** The authors declare that they have equal right on this paper.
- **Funding information:** The authors declare that there is no funding to be acknowledged.
- **Data availability statement:** The data that support the findings of this study are available on request from the corresponding author. The data are not publicly available due to privacy or ethical restrictions.

References

[1] ACI Committee 445 on Shear and Torsion (1998). Recent approaches to shear design of structural concrete. *Journal of Structural Engineering*. 124(12):1375-1417. https://doi.org/10.1061/(ASCE)0733-9445(1998)124:12(1375)

[2] Bažant, Z. P. (1997). Fracturing truss model: size effect in shear failure of reinforced concrete. *Journal of Engineering Mechanics*. 123 (12): 1276-1288. https://doi.org/10.1061/(ASCE)0733-9399(1997)123:12(1276)

[3] Sogut, K., Dirar, S., Theofanous, M., Faramarzi, A. (2019, June 4-7). *Size effect in shear-deficient reinforced concrete T-beams strengthened with embedded FRP bars.* The 14th International Symposium on Fiber-Reinforced Polymer Reinforcement for Concrete Structures, (FRPRCS-14), Belfast, UK.

[4] Söğüt, K. (2022). Numerical investigation on DE-strengthened-RC beams without steel shear reinforcement. *Journal of Structural Engineering & AppliedMechanics*.5(4):238-248. https://doi.org/10.31462/jseam.2022.04238248

[5] Bažant, Z.P., Kim J.K. (1984). Size effect in shear failure of longitudinally reinforced beams. *ACI Journal Proceedings*. 81 (5): 456-468.

[6] Benzeguir, Z.E.A., El-Saikaly, G., Chaallal, O. (2019). Size effect in RC T-beams strengthened in shear with externally bonded CFRP sheets: experimental study. *ASCE Journal of Composites for Construction*.23(6):04019048. https://doi.org/10.1061/(ASCE)CC.1943-5614.0001045

[7] TS 500: Requirements for design and construction of reinforced concrete structures, TSE (Turkish Standards Institute), Ankara, Turkey, 2014.

[8] Wong, P.S., Vecchio, F.J., Trommels, H. (2013). *VecTor2 & FormWorks User's Manual (2nd edition).* The University of Toronto.

[9] Vecchio, F.J. (2020). Disturbed stress field model for reinforced concrete: formulation. *ASCE Journal of Structural Engineering*. 126(9):1070-1077. https://doi.org/10.1061/(ASCE)0733-9445(2000)126:9(1070)

[10] Elsanadedy, H.M., Al-Salloum, Y.A., Almusallam, T.H., Alshenawy, A.O., Abbas, H. (2019). Experimental and numerical study on FRP-upgraded RC beams with large rectangular web openings in shear zones, *Construction and Building Materials*. 194:322-343. https://doi.org/10.1016/j.conbuildmat.2018.10.238

[11] Jeong, C.Y., Kim, H.G., Kim, S.W., Lee, K.S., Kim, K.H. (2017). Size effect on shear strength of reinforced concrete beams with tension reinforcement ratio. *Advances in Structural Engineering*.20(4):582-594. https://doi.org/10.1177/1369433216658486

[12] Syroka-Korol, E., Tejchman, J. (2014). Experimental investigations of size effect in reinforced concrete beams failing by shear. *EngineeringStructures*.58:63–78. https://doi.org/10.1016/j.engstruct.2013.10.012

[13] El-Sayed, A. K., Shuraim, A. B. (2016). Size effect on shear resistanceof high strength concrete deep beams. *Materials and Structures*. 49 (5): 1871–1882. https://doi.org/10.1617/s11527-015-0619-1

Research Article
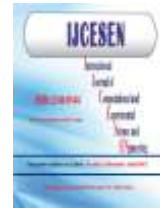
Method Validation and Measurement Uncertainty for the Determination of Ethanol in Whole Blood

Yeter Erol OZTURK*

Council of Forensic Medicine, Chemistry Department, 06300, Ankara-Turkey
* **Corresponding Author** : **Email:** yetererol@hotmail.com - **ORCID:** 0000-0001-9503-7057

Abstract:

Alcohol intake is known to significantly affect driving ability and there is a positive correlation between car accidents and Blood Alcohol Concentration (BAC). Alcohol intake is known to significantly affect driving ability. Therefore, many countries define and monitor the legal BAC value for drivers. Customers or legal authorities require determining and reporting the measurement uncertainty in blood alcohol analysis from laboratories in recent years. To establish the reliability and robustness of the result, the method was validated and the measurement uncertainty was calculated. A rapid, selective and quantitative gas chromatography coupled with flame ionisation detection method was developed and validated for determination of ethanol in whole blood. The method was validated for selectivity, matrix effect, recovery, linearity, limit of detection (LOD), limit of quantification (LOQ), recovery, repeatability, reproducibility and robustness. The validation procedure was designed to be suitable for ISO/IEC 17025 accreditation. Uncertainty measurements were also determined for the validated method. LOD and LOQ were found 3.99 mg/dL and 4.30 mg/dL, respectively. The method showed good linearity in the range of 3.9 to 393.7 mg/dL ethanol with a correlation coefficient (r^2 = 0.9999). The method provides fast, precise, simple, robust and unbiased results.

1. Introduction

Ethanol is one of the best known psychoactive depressant drugs. It is consumed in beverages and food and is also one of the most abused psychoactive substances. Excessive consumption of alcoholic substances and drunkenness plays a major role in many fatal accidents, violent crimes, suicide, drowning and, traumatic deaths as proved by police reports, accident and emergency records [1,2]. According to the National Highway Traffic Safety Administration, 31% of traffic fatalities in the United States of America (USA) in 2021 were caused by alcohol-impaired driving [3]. Between 2009 and 2014, 24.7% of pedestrians at a hospital trauma centre were injured in road traffic crashes in Melbourne, Australia [4]. Alcohol analyses are traditionally performed in routine autopsy analyses. In addition, alcohol analyses are requested in every case to determine whether driving ability is impaired in traffic accidents, and analyses of narcotic stimulants are also requested for some cases. The limit value at which alcohol has an effect on driving is reported at 0.4 g/kg [5].As most countries have

BAC limits for driving that are punishable by law, such as 50 mg/dL in most European countries, 0.50 mg/kg or, and 80 mg/dL in the United Kingdom (UK), USA and Canada [6,7]. The legal limit in Turkey is 50 mg/dL for car users and 0 mg/dL for commercial vehicle users by Road Traffic Law and Road Traffic Regulations [8]. Various analytical techniques have been used to determine ethanol in biological or non-biological samples. Gas chromatography (GC) [9, 10], high performance liquid chromatography (HPLC) [11,12] and infrared spectroscopy (IR) [13] have been commonly used. GC is generally the most accurate and reliable analytical method and is often the preferred method for the quantification of ethanol in human blood, vitreous humour and other biological samples in forensic toxicology [14]. Sample preparation is the most important step for reliable analysis of complex matrices such as blood, tissue or urine. Various preparation techniques are available for the determination of ethanol in biological samples, such as direct injection, static, dynamic headspace [10, 15] or headspace injection using solid phase microextraction (HS-SPME) [16, 17] and HS-GC-

FID [18]. The rapid and accurate determination of ethanol in human specimens is of great importance to analytical or forensic laboratories, and the development of novel methods and the evaluation and validation of the developed methods are required [16]. HS-GC-FID has become the most widely used technique in recent years for the analysis of volatile analytes in biological and non-biological samples due to its ability to detect low levels of analytes without the need for complex and expensive sample preparation techniques. In addition, the technique is often used in laboratories with highly routine laboratory work [17]. Headspace (HS) for alcohol analysis offers advantages such as simple sample preparation, low risk of contamination, selectivity and short analysis time compared to other sample preparation techniques [16, 18]. Therefore, this study aims to develop and validate an analytical method for the determination of ethanol in blood samples with HS-GC-FID.

2. Material and Methods

2.1 Chemicals and reagents

All chemicals and solvents were of LC-MS grade and were purchased from Merck (Darmstadt, Germany). Deionised water was provided by a Millipore® Milli-Q gradient system.

2.2. HS-GC-FID

The gas chromatography system consisted of a Perkin Elmer (Shelton, USA) Clarus 500 GC and HS module coupled to a flame ionisation detector and two columns A (Elite BAC 1(30 m×0.32 mm ID×0.6 µm)) and B (Elite BAC 2(30 m×0.32 mm ID×0.8 µm)). The transfer line , needle and oven temperature were 110˚C, 75˚C and 70˚C respectively. The injection time was 0.02 min, the hold time was 0.2 min and the cycle time was 8.5 min. The sampling rate was 12.5 points per second and the total GC run time was 10 min. The column temperature was 220 ˚C and the gas flow for each detector was 450 mL/min air and 45.0 mL/min hydrogen.

2.3 Sample Preparation

Blank human blood samples were obtained from a regional blood donation centre and were used for the validation of the method. All working solutions were prepared daily from pure solvent. The propan-1-ol internal standard (IS) solution was prepared in water (0.01 M) and stored at +4°C. For sample preparation, 200 µL of sample and 800 µL of IS were placed in a clean glass headspace vial and capped. The vials were transferred to the HS autosampler.

2.4 Method Validation

The validation of this method was performed with the parameters LOD and LOQ, linearity, intra- and inter-day precision, recovery, selectivity, matrix effect and robustness. The method was validated according to the rules of ISO/IEC 17025:2017 in accordance with international guidelines, which are common practice in clinical and forensic toxicology [19-22]. For detection and calculation of the limit of detection, the concentration in the blood sample was prepared as 3.98 mg/dL and 10 independent analyses were performed. At this concentration it was ensured that the signal to noise ratio was S/N≥3. The mean and standard deviation were calculated for ethanol. The LOD was calculated by adding 3 standard deviations to the mean and the LOQ was calculated by adding 10 standard deviations to the mean. Precision values <20% were accepted. The linear working range study was analysed separately with blood and water to investigate the matrix effect. The data obtained were evaluated by t-test and it was found that there was no significant difference between the two matrices. Therefore, calibration curves were generated using water. The linearity was assessed in the range of 3.9 to 393.7 mg/dL. The repeatability study was performed by 2 different analysts at 3 different concentrations (low: 14.0 mg/dL, medium: 72.0 mg/dL and high: 144.0 mg/dL) on the same day. For the ethanol reproducibility study, three different concentrations (low: 14.0 mg/dL, medium: 72.0 mg/dL and high: 144.0 mg/dL) were performed on six different days by two different operators. In the selectivity study, ethanol, methanol, acetone, n-butanol, propan-1-ol, propan-2-ol, formaldehyde and toluene standards at low and high concentrations of 10.0 and 400.0 mg/dL were prepared as single and mixed standards in water and blood matrix. After the retention time (RT) of each component was determined, these components were re-analysed in the mix and the effectiveness of separation was examined. It was observed that each component showed different RT in the mix. Recovery studies were performed at three different concentrations of 144.0, 72.0 and 14.0 mg/dL by two different analysts. In the robustness studies, the effects of needle temperature (75˚C, 80˚C, 85˚C), analysis time (10 min, 15 min, 20 min) and oven temperature (70˚C, 75˚C, 80˚C) on the analysis were investigated.

2.5 Uncertainty measurement

The determination of the measurement uncertainty in validated methods is very important in order to compare the results obtained by two different methods, to ensure the reliability of the results and

to reduce the controversy of the results at legal limits. In this study, the combined standard uncertainty results obtained from three different concentrations (14.0 mg/dL, 72 mg/dL and 144.0 mg/dL) were analysed according to the bottom-up approach. Calculations were performed from validation data for the HS-GC-FID method. The budget was determined in accordance with the EURACHEM uncertainty calculation guide according to the rules of ISO/IEC 17025:2017 [22, 23]. The contribution of components such as recovery, calibration curve, accuracy, repeatability and reproducibility were taken into account when determining the contribution of the distribution.

3. Results and Discussions

The LOD for the validated method was 3.99 mg/dL and the LOQ was 4.3 mg/dL. As the legal limit for driving in Turkey is 50 mg/dL, the method was found to be sufficient for the detection and quantification of alcohol. Figure 1 shows a chromatogram of ethyl alcohol at a concentration of 4.0 mg/dL and IS.
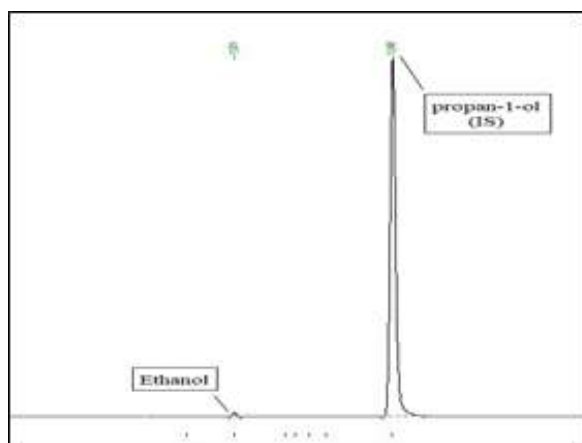
Figure 1. *The chromatogram of ethanol (RT:1.01min.) at a concentration of 4.0 mg/dL and IS (RT:1.68 min)*

Good linearity has been assessed in the range of 3.9 to 393.7 mg/dL with with a correlation coefficient (r^2=0.9999). The bias of the method was calculated from the samples used for the recovery study. For the three different concentrations analysed (low: 14.0 mg/dL, medium: 72.0 mg/dL and high: 144.0 mg/dL), the bias values were 1.8%, 1.3% and 1.7% for the first analyst and 1.6%, 1.4% and 1.3% for the second analyst. The SWGTOX guideline acceptable bias value is reported as ±10 and all bias results were within this range [20]. The recoveries for the three different concentrations analysed (low: 14.0 mg/dL, medium: 72.0 mg/dL and high: 144.0 mg/dL) were between 98.0% and 101.8%. The recovery values were found to be within acceptable limits. For the

three different concentrations analysed (low: 14.0 mg/dL, medium: 72.0 mg/dL and high: 144.0 mg/dL), the repeatability RSD% values were 0.5%, 1.0% and 0.6% for the first analyst and 1.8%, 0.5% and 0.5% for the second analyst. For the three different concentrations analysed (low: 14.0 mg/dL, medium: 72.0 mg/dL and high: 144.0 mg/dL), the reproducibility RSD% values were 1.1%, 1.1% and 0.4 % for the first analyst and 0.7%, 0.7% and 0.3% for the second analyst. The acceptance criteria for % RSD value should be ≤15% [19, 24]. All calculated %RSD values for repeatability and reproducibility for two analysts were below the criteria. Table 1 presents results of different parameters in validation of method for ethanol determination.

Table 1. *Validation data of the developed method (recovery and precision values for two analyst(A1and A2))*

The Validation Parameters	A 1	A 2
Recovery (%) (Low)	98.2	98.0
Recovery (%) (Medium)	98.4	98.6
Recovery (%) (High)	101.5	101.8
Repeatability (% RSD) (Low)	0.5	1.8
Repeatability (%RSD) (Medium)	1.0	0.5
Repeatability (%RSD) (High)	0.5	0.5
Reproducibility (% RSD) (Low)	1.1	0.7
Reproducibility (%RSD) (Medium)	1.1	0.7
Reproducibility (%RSD) (High)	0.4	0.3

The selectivity study of the method was performed by injecting a sample matrix containing possible interferences and no significant interference was found. Figure 2 shows (a) negative control sample with IS. No interference was observed. Figure 2 also shows (b) the chromatographic separation of methanol, ethanol, acetone, methyl ethyl ketone, isobutanol, ethyl acetate, toluene, ethyl benzene, IS and xylene.

Figure 2. *(a)Negative blood sample with IS, (b) The chromatographic separations of different solvents.*

Robustness was analysed by varying the parameters needle temperature, thermostat time and oven temperature. Student's t-test showed that the changes had no significant effect on the measured value ($t_{cal} < t_{table}$). Intermediate precision was investigated by performing analyses (n=6) on the same instr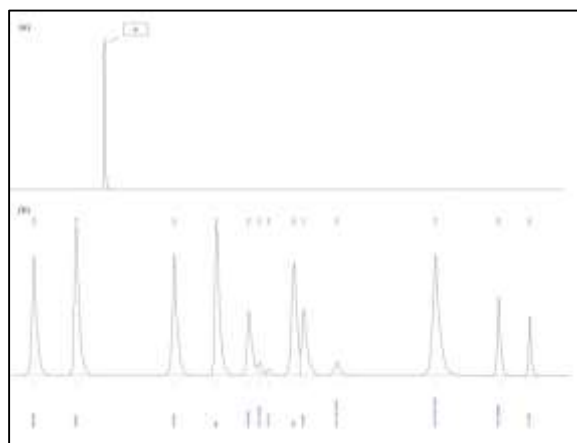ument at three different concentrations (low: 14.0 mg/dL, medium: 72 mg/dL and high: 144 mg/dL) on the same day and on six different days by two different analysts. The RSD% values were then compared between the two analysts. The values were compared by F-test and Student's t-test and no significant difference was found ($t_{cal} < t_{table}$ and $F_{cal} < F_{table}$). U_r (recovery), U_r (calibration curve), U_r (bias), U_r (repeatability) and U_r (reproducibility) values were calculated 0.005, 0.006, 0.009, 0.010 and 0,008, respectively. U_r (combined) value was calculated 0.019 (1.9%). U_r (combined) uncertainty value was found to be suitable with previous reports [25-29]. By using the Ur (expanded) value, 0.038 (3.8%) was calculated, which is based on the desired confidence level and, for an approximate confidence level of 95%, k (coverage factor) is equal to 2. By using the expanded uncertainty, it is possible to calculate the decision limits above which the blood alcohol concentration can be considered, with a certain probability, higher than the legal limits. It is the concentration above which the blood alcohol concentration can be considered, with a certain probability, to be higher than the legal limits.

4. Conclusions

The developed and validated method for blood alcohol analysis is suitable for the determination of alcohol concentration for clinical or legal purposes. The method developed using HS-GC-FID provides rapid, selective, reliable and robust results for the determination of ethanol. The validation results meet the acceptance criteria of guidelines such as EURACHEM, ICH, ISO/IEC 17025:2017 and SWGTOX. The detection limit and range of the method meet legal limits and the purpose of toxicological analysis. The measurement uncertainty calculated for the method is sufficient to eliminate controversy over the results, to obtain accurate results and to compare the results obtained. This method is suitable for all clinical and forensic laboratories producing results with ISO/IEC 17025:2017 accreditation.

Author Statements:

- **Ethical approval:** The conducted research is not related to either human or animal use.

- **Conflict of interest:** The authors declare that they have no known competing financial interests or personal relationships that could have appeared to influence the work reported in this paper

- **Acknowledgement:** The authors declare that they have nobody or no-company to acknowledge.

- **Author contributions:** The authors declare that they have equal right on this paper.

- **Funding information:** The authors declare that there is no funding to be acknowledged.

- **Data availability statement:** The data that support the findings of this study are available on request from the corresponding author. The data are not publicly available due to privacy or ethical restrictions.

References

[1] Kugelberg FC, Jones AW. (2007). Interpreting results of ethanol analysis in postmortem specimens: a review of the literature. *Forensic Sci Int.* 165(1):10-29. doi: 10.1016/j.forsciint.2006.05.004.

[2] Sjögren H, Eriksson A, Ahlm K. (2000) Role of alcohol in unnatural deaths: a study of all deaths in Sweden. *Alcohol Clin Exp Res.* doi:10.1111/j.1530-0277.2000.tb04649.x.

[3] NHTSA (National Highway Traffic Safety Administration), (2023, August 1) . *Alcohol- and Drug-Impaired Driving* https://www.nhtsa.gov/book/countermeasures/counte rmeasures-work/alcohol-and-drug-impaired-driving.

[4] WHO (World Health Organization), (2023, August 1) . *Global status report on alcohol and health, 2018* https://www.who.int/publications/i/item/9789241565 639.

[5] Fernie G, Christiansen P, Cole JC, Rose AK, Field M. (2012). Effects of 0.4 g/kg alcohol on attentional bias and alcohol-seeking behaviour in heavy and moderate social drinkers. *J Psychopharmacol.* 26(7):1017-25. doi: 10.1177/0269881111434621.

[6] Tiscione NB, Alford I, Yeatman DT, Shan X. (2011). Ethanol analysis by headspace gas chromatography with simultaneous flame-ionization and mass spectrometry detection. *J Anal Toxicol.* 35(7):501-11. doi: 10.1093/anatox/35.7.501. PMID: 21871160.

[7] Jones AW. (2000) Medicolegal alcohol determinations – breath- or blood alcohol concentrations?. *Forensic Sci. Rev.* 12:23–47.

[8] Traffic Law and Road Traffic Regulation No:6047, (2023, August 1) . *Regulation Number:6047* https://www.mevzuat.gov.tr/mevzuatmetin/1.5.2918. pdf.

[9] Chun HJ, Poklis JL, Poklis A,Wolf CE. (2016). Development and validation of a method for alcohol analysis in brain tissue by headspace gas chromatography with flame ionization detector.

Journal of Analytical Toxicology. 40: 653–658. doi: 10.1093/jat/bkw075.

[10] Snow NH, Slack GC. (2002). Head-space analysis in modern gas chromatography. *Trends in Analytical Chemistry*. 21(9–10): 608–617. doi: 10.1016/S0165-9936(02)00802-6.

[11] Nikelly JG, Betz JM (1987). Determination of ethanol in alcoholic beverages by liquid chromatography using the UV detector. *Journal of Chromatographic Science*. 25(9):391–394. https://doi.org/10.1093/chromsci/25.9.391.

[12] Yarita T, Nakajima R, Otsuka S, Ihara T, Takatsu A, Shibukawa M. (2002). Determination of ethanol in alcoholic beverages by high- performance liquid chromatography flame ionization detection using pure water as mobile phase. *J Chromatogr AJ Chromatogr A*. 976(1-2): 387–391. doi: 10.1016/S0021-9673(02)00942-1.

[13] Lachenmeier DW. (2007). Rapid quality control of spirit drinks and beer using multivariate data analysis of Fourier transform infrared spectra. *Food Chemistry*. 101(2): 825–832. doi: 10.1016/j.foodchem.2005.12.032.

[14] Hong-tao X, Lin H, Rong-Sheng T, Ji-Ying Y, Lu C, Jing Z et al. (2014). Rapid and Sensitive Headspace Gas Chromatography-Mass spectrometery Method for the analysis of Ethanol in the whole Blood. *Journal of Clinical Laboratory Analysis*. 28 (5): 386–390. doi: 10.1002/jcla.21698.

[15] O'Neal CL, Wolf CE, Levine B, Kunsman G, Poklis A. (1996). Gas chromatographic procedures for determination of ethanol in postmortemblood using t-butanol and methyl ethyl ketone as internal standards. *Forensic Science International*. 83(1) :31–38. doi: 1016/0379-0738(96)02007-5.

[16] De Martinis BS, Martins Ruzzene MA, Santos Martin CC. (2004). Determination of ethanol in human blood and urine by automated headspace solid-phase microextraction and capillary gas chromatography. *Analytica Chimica Acta*. 522(2):163–168. doi:10.1016/j.aca.2004.07.007.

[17] Zuba, D., Parczewski, A., & Reichenbcher, M. (2002). Optimization of solid-phase microextraction conditions for gas chromatographic determination of ethanol and other volatile compounds in blood. Journal of Chromatography B: *Analytical Technologies in the Biomedical and Life Sciences*. 773(1):75–82. doi:10.1016/S1570-0232(02)00143-5.

[18] Diana D, Sorin M, Cornelia M, Elena B, Vasil A. (2009). Development and validation of a quantitative determination method of blood ethanol by gas chromatography with headspace (GC-HS). *Romanian Journal of Legal Medicine.* 17(4):303–308. doi: 10.4323/rjlm.2009.303.

[19] Peters FT, Maurer HH. (2002). Bioanalytical method validation and its implications for forensic and clinical toxicology – a review. *Accredit. Qual. Assur.* 7: 441–449. doi: 10.1007/s00769-002-0516-5.

[20] Scientific Working Group for Forensic Toxicology (SWGTOX). (2013). Standard practices for method validation in forensic toxicology. *J. Anal.Toxicol.* 37: 452-474. doi:10.1093/jat/bkt054.

[21] Matuszewski BK, Constanzer ML. (2003). Strategies for the assessment of matrix effect in quantitative bioanalytical methods based on HPLC – MS/MS. *Anal. Chem.* 75: 3019–3030. doi:10.1021/ac020361s.

[22] ISO/IEC 17025:2017, (2017), (2023, August 1). *General requirements for the competence of testing and calibration laboratories.* https://www.iso.org/standard/66912.html.

[23] EURACHEM/CITAC,(2012), (2023, August 1). *Quantifying Uncertainty in Analytical Measurement.* https://www.eurachem.org/images/stories/Guides/pdf/QUAM2012_P1.pdf

[24] IHC (Harmonised Tripartite Guideline), (2005), (2023, August 1). *International Conference On Harmonisation Of Technical Requirements For Registration Of Pharmaceuticals For Human Use* http://academy.gmp-compliance.org/guidemgr/files/Q2(R1).pdf.

[25] Kristiansen J, Petersen HW. (2004). An uncertainty budget for the measurement of ethanol in blood by headspace gas chromatography. *J Anal Toxicol*. 28: 456-463. doi: 10.1093/jat/28.6.456.

[26] Sklerov JH, Couper FJ. (2011). Calculation and verification of blood ethanol measurement uncertainty for headspace gas chromatography. *J Anal Toxicol*. 35: 402-410. doi: 10.1093/anatox/ 35.7.402.

[27] Hwang RJ, Beltran J, Rogers C, Barlow J, Razatos G. (2017). Measurement of uncertainty for blood alcohol concentration by headspace gas chromatography. *Can Soc Forensic Sci J*. 50: 114-124. doi: 10.1111/1556-4029.13133.

[28] Zamengo L, Frison G, Tedeschi G, Frasson S, Zancanaro F, Sciarrone R. (2014). Variability of blood alcohol content (BAC) determinations: The role of measurement uncertainty, significant figures, and decision rules for compliance assessment in the frame of a multiple BAC threshold law. *Drug Test Anal*. 6: 1028-1037. doi: 10.1002/dta.1614.

[29] Prenesti, E, Bagnati, M, Berto, S, Basile, M, Vidali, M, Bellomo G. (2019). Measurement Uncertainty of Ethanol Concentration in Venous Whole Blood Determined By a HS-GC-MS Method. *Analytical and Bioanalytical Techniques.* 6:7. doi: 10.1080/23312009. 2020.1760187.
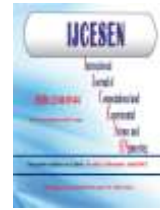
The Effect of Fragment C of Tetanus Toxin on Memory Deficits in a Rat Model of Alzheimer's Disease

Seyma OZSOY[1*], Elif Azize Ozsahin DELIBAS[2]

[*1]Tokat Gaziosmanpasa University, Faculty of Medicine, Departments of Physiology, Tokat, Turkey
* **Corresponding Author** : **Email:** seyma.ozsoy@hotmail.com - **ORCID:** 0000-0003-1783-3618

[2]Tokat Gaziosmanpasa University, Faculty of Health Sciences, Department of Nutrition and Dietetics, Tokat, Turkey.
Email: elif.delibas@gop.edu.tr **ORCID:** 0000-0002-4195-0554

Abstract:

The progression of Alzheimer's disease (AD) is connected to both neuronal elements and immunological mechanisms. Tetanus toxin C-terminal fragment (TTC) has neuroprotective properties. Our objective was to examine the influence of TTC on memory, hippocampal morphology, and inflammation in rats with a STZ-induced AD model. After general anesthesia rats, 3 mg/kg STZ was administered ICV to the right and left lateral ventricles of 5 µl of 12 rats. Six rats were received both lateral ventricules of 0.9% NaCl 5 µl ICV, and others were administered TTC (0.05 flocculation units) in 5 µl ICV one time. No drug was applied to the control group. On the 15th day, all groups underwent a passive avoidance learning (PAL) test, and then brain tissue was collected. Tumor necrosis factor-alpha (TNF-α) and interleukin 6 (IL-6) levels within the brain were assessed. Following this, neurons were quantified by employing Cresyl violet staining specifically within the hippocampal CA1 and CA3 regions. In the ICV-STZ group, the PAL latency time significantly reduced, TNF-α levels and IL-6 levels increased, and also the hippocampal CA1 and CA3 neuron numbers decreased. The application of TTC resulted in a significant decrease in the levels of TNF-α and IL-6. Furthermore, it played a role in mitigating the memory impairment caused by ICV-STZ by reducing cell death within the hippocampus. These results suggest that the neuroprotective and anti-inflammatory properties of TTC might have a significant impact on addressing neurodegenerative disorders such as Alzheimer's disease.

1. Introduction

Alzheimer's disease (AD), marked by progressive and severe cognitive deterioration, constitutes 70% of all cases of dementia [1]. In a clinical context, patients experience memory and other cognitive function impairments. Alzheimer's disease (AD) is characterized by the accumulation of intracellular neurofibrillary tangles and extracellular senile plaques in various brain regions, notably within the hippocampus [2]. Neuronal degeneration in AD occurs due to the accumulation of two abnormal proteins, β-amyloid (Aβ) and tau, in the brain. Additionally, individuals affected by Alzheimer's disease (AD) and mild cognitive impairment exhibit elevated levels of proinflammatory cytokines, cytokine receptors, and other inflammatory markers such as interleukin-6 (IL-6), tumor necrosis factor-α

(TNF-α), and C-reactive protein in their bloodstream [3].

Tetanus is a disease that affects the nervous system, resulting in painful, uncontrolled muscle contractions and death. The protein-based tetanus neurotoxin is produced by the pathogenic anaerobic bacterium Clostridium tetani. Its heavy chain is split into two fragments, each approximately 50 kDa in size, through the action of the tetanus toxin carboxyl fragment (TTC). Additionally, the N-terminal portion of this chain is cleaved by papain [4]. In in vitro [5] and in vivo studies [6], TTC has been shown to preserve membrane binding, internalization, and retrograde transport capacities with preferential localization in motoneurons. Mendiata et al. reported that TTC strongly improved different motor behaviors in a Parkinson's disease model [7]. This resulted in the improvement of the dopaminergic system of the TTC in rats with dopaminergic lesions.

Radenovic et al. showed that TTC treatment in Mongolian gerbils has neuroprotective properties by reducing ischemia-induced oxidative stress and motor hyperactivity [8]. TTC also improved motoneuron survival in organotypic cultures of the spinal cord exposed to glutamate for short periods. Intracerebroventricular (ICV) injection of streptozocin (STZ) stimulates the brain's pathological changes seen in AD, such as cognitive impairment, tau protein, and Aβ deposition in the brain. ICV-STZ injection is used as an experimental animal model of AD [9].

Based on this information, our objective was to assess the impact of TTC on memory and the morphology of the hippocampus in rats exhibiting an AD model induced by STZ. Furthermore, we analyzed the TNF-α and IL-6 levels in brain tissue.

2. Material and Methods

2.1. Animal ethics and housing conditions

The research comprised eighteen adult male Wistar albino rats (200-220 g). These rats were housed in a controlled environment set at $23 \pm 1°C$ and following a 12-hour light-dark cycle. They had continuous access to both food and water throughout the entire duration of the experiment. The ethical guidelines of the study were granted approval by the Animal Ethics Research Committee of Tokat Gaziosmanpasa University (2014-HADYEK-37).

2.2. Experimental procedures

The animals were anesthetized intraperitoneally (i.p) with a general anesthetic, a mixture of ketamine hydrochloride (70 mg/kg, Alfamine, Ege Vet, Holland), and xylazine hydrochloride (5 mg/kg, Alfazyne, Ege Vet, Holland). The rats were then randomly divided into two groups: the STZ infusion group (n=12) and the control group (n=6). For the creation of the Alzheimer's disease model, a streotaxic device was utilized. The rats in the STZ infusion group received bilateral intracerebroventricular (ICV) administration of STZ (Sigma-Aldrich, St Louis, MO) into both lateral ventricles. The total volume infused was 5 µl, with 2.5 µL being injected into the left lateral ventricle and 2.5 µL into the right lateral ventricle. The coordinates used were AP = −0.8mm, DV = −4.1 mm, L = ±1.5 mm [10]. This was accomplished using a Hamilton syringe. Among the rats in the STZ infusion group, six received an ICV infusion of 0.9% NaCl (5 µl) into both lateral ventricles, while the remaining six received an ICV infusion of TTC (0.05 flocculation units, 5 µl) into both lateral ventricles.

In the control group, no drugs were administered to six rats. Fig. 1 shows that experimental design.
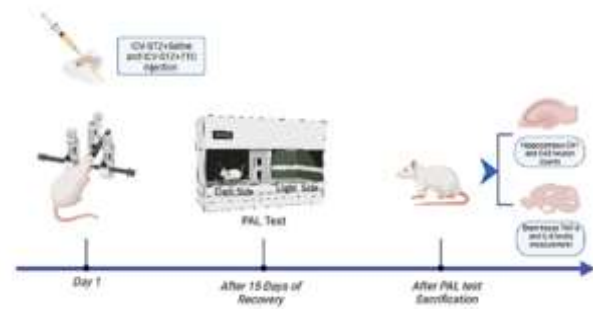
Figure 1. *Experimental Design*

2.3. Passive avoidance test

Fifteen days after the ICV-TTC treatment, a passive avoidance task was conducted to evaluate learning and memory within each of the respective groups. Passive avoidance learning (PAL) consists of fear-guided tests that are commonly employed to assess negative reinforcement-based long-term memory in small laboratory animals. For this specific purpose, a passive avoidance learning (PAL) box measuring $20 \times 20 \times 20$ cm and containing both dark and light sections was utilized. The rats were initially placed in the brightly lit chamber of a two-compartment box. After a 10-second period of acclimatization, the door that separates the light and dark rooms were opened. Subsequently, the door was closed, and an electric shock (FJ-919; 300 kV, 60 Hz, 1.5 mA) was administered within the dark compartment. Following a duration of 5 minutes, the animals were returned to their cages. After 24 hours, the transition time (latency) of the animals was evaluated [11]. Subsequently, the rats were euthanized, and their brain tissues were extracted to undergo histopathological and biochemical assessments.

2.4. Histological evaluation

Brain tissue samples from all animals were fixed in 10% formalin. After post-fixation in the same fixative solution for one week, the tissues were blocked with paraffin after routine histological procedures. Sections of 5-micron thickness were taken from each paraffin block, and the sections were deparaffinized by keeping them in an oven at 60ºC for 8 hours. The hippocampus CA1 and CA3 neuron counts of the brain sections (5 µm thick) were examined by staining with Cresyl violet using an Olympus BX51 microscope, Olympus C-5050 digital camera. To quantify the surviving number of neurons, we used the image analysis system (Image-Pro Express 1.4.5, Media Cybernetics, Inc USA).

2.5. Detection of TNF-α and IL-6 levels in brain tissue

Brain tissue was stored in aliquots at -800C until the study day samples. The ELISA method was used to determine TNF-α (catalog no: E-EL-R2856) and IL-6 (catalog no: E-EL-R0015) levels using commercial kits (Elabscience, USA) and the manufacturer's recommended procedures. Thermo ScientificTM PierceTM BCA Protein Assay Kit (catalog no: 23225) was used to determine the TNF-α and IL-6 levels per mg protein. These measured in brain homogenates were given in proportion to the protein concentration of the same homogenate.

2.6. Statistical analyses

Statistical analysis was conducted utilizing IBM SPSS software, version 22. An initial one-way analysis of variance (ANOVA) was implemented, followed by subsequent Tukey's post hoc least significant difference (LSD) tests. For variables that did not conform to parametric assumptions, the comparison of groups was achieved using Tamhane's T2 test. The data was presented in terms of the mean and accompanied by the standard error mean (SEM). A significance level below 0.05 was regarded as a marker of statistical significance.

3. Results and Discussions

3.1. Evaluation of cognitive dysfunction and neuron counts in the hippocampus

The latency time was significantly reduced in the ICV-STZ+saline group when compared to the control group (42.8 ± 12.2 vs. 248.3 ± 25.1, respectively; $p<0.001$). In contrast, the ICV-STZ+TTC group had a longer latency time than the ICV-STZ+saline group (158.3 ± 61.8 vs. 42.8 ± 12.2, respectively; $p<0.05$). Histological preparations that were stained with Cresyl violet are visually represented in Fig. 2. In the ICV-STZ+saline group, the cell layer appeared thinner in comparison to the ICV-STZ+TTC group. When the ICV-STZ+saline group was compared to the control group, quantitative analysis revealed a decrease in neuron counts in the hippocampal CA1 and CA3 areas ($p<0.000$ and $p<0.001$, respectively). Conversely, the ICV-STZ+TTC group displayed an increase in neuron numbers in the hippocampal CA1 and CA3 regions compared to the ICV-STZ+saline group ($p<0.05$ and $p<0.05$, respectively). A comprehensive overview of the results is presented in Table 1.

Table 1. Latency time and the number of neurons in hippocampal CA1 and CA3 regions of groups

Groups	Latency time (s)	Number of CA1 neurons	Number of CA3 neurons
Control Group	248.3 ± 25.1	66.3 ± 4.9	63.1 ± 3.9
ICV-STZ+ Saline Group	42.8 ± 12.2 *	39.7 ± 2.8 **	37.6 ± 1.9 *
ICV-STZ+TTC Group	158.3 ± 61.8 #	60.9 ± 3.6 #	55.1 ± 5.3 #

*Data expressed as mean ± SEM. * p < 0.001, ICV-STZ+Saline Group vs. Control Group; ** p < 0.000, ICV-STZ+Saline Group vs Control Group; # p < 0.05, ICV-STZ+TTC Group vs ICV-STZ+Saline Group.*
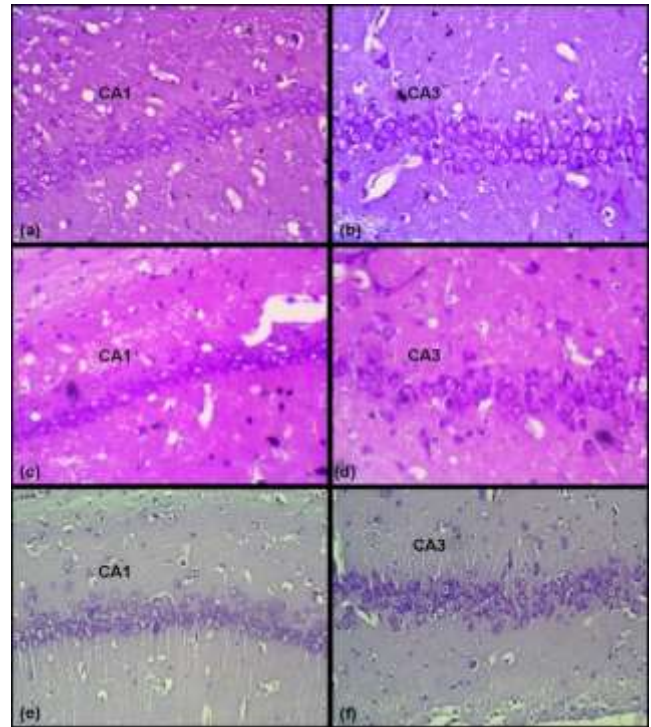
Figure 2. CA1 and CA3 hippocampal regions were stained with Cresyl violet stain (x 40 and x 100 magnification). a: Control Group CA1, b: Control Group CA3, c: ICV-STZ and Saline Group CA1, d: ICV-STZ and Saline Group CA3, e: ICV-STZ and TTC Group CA1, f: ICV-STZ and TTC Group CA3

3.2. TNF-α and IL-6 levels

In the ICV-STZ+saline group, levels of TNF-α and IL-6 were elevated when compared to the control group ($p<0.01$ and $p<0.05$, respectively; 1262.48 ± 95.08 vs. 549.52 ± 23.57 and 379.34 ± 27.69 vs. 245.44 ± 20.33, respectively).

The administration of TTC resulted in a decrease in the levels of TNF-α in comparison to both the

control group and the ICV-STZ+saline group ($p<0.01$ and $p<0.001$, respectively; 339.16 ± 20.04 vs. 549.52 ± 23.57 and 339.16 ± 20.04 vs. 1262.48 ± 95.08; as depicted in Fig. 3). Similarly, TTC treatment resulted in decreased IL-6 levels when compared to both the control group and the ICV-STZ+saline group ($p<0.01$ and $p<0.001$, respectively; 23.87 ± 2.21 vs. 245.44 ± 20.33 and 23.87 ± 2.21 vs. 379.34 ± 27.69; as illustrated in Fig. 4).
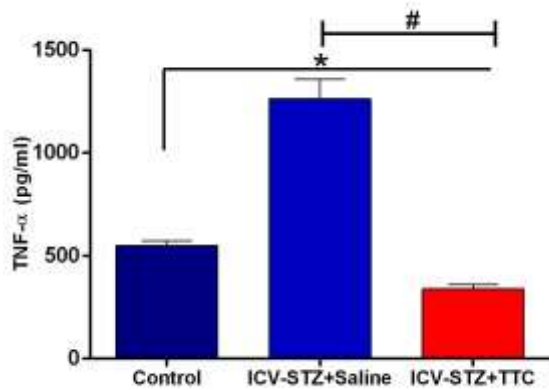
*Figure 3. The concentration of TNF-α in the rat brain in the following groups: *Control group vs STZ-Saline and STZ-TTC group; p<0.01; #STZ-TTC group vs STZ-Saline group p<0.001.*
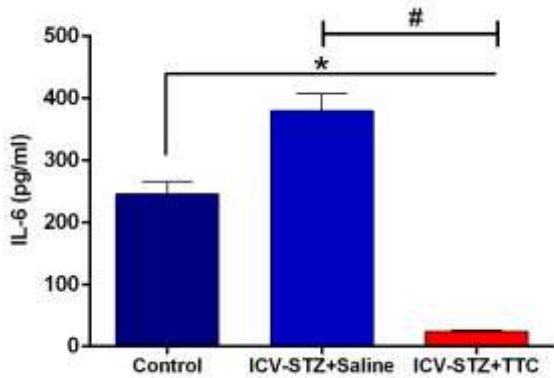
*Figure 4. The concentration of IL-6 in the rat brain in the following groups: *Control group vs STZ-Saline and STZ-TTC group; p<0.05; #STZ-TTC group vs STZ-Saline group p<0.001.*

Discussion

AD is a neurodegenerative disease in which neuropsychiatric symptoms such as depression and anxiety are seen, as well as cognitive impairment. The hippocampal area, which is one of the most affected areas in AD [12]. The hippocampus has subdivisions as components of the dentate gyrus and cornu ammonis (regions CA1, CA2, CA3, and CA4). One of the two main interrelated roles of the

hippocampus is in learning and emotional processing. The other is neurogenesis, which is essential for memory, learning, and mood[13. It is therefore not surprising that some of the earliest damage in AD manifests itself in the cortex and hippocampus. Padurariu et al. showed decreased neuronal density in the human AD brain, especially in the hippocampal areas CA1 and CA3 [14].

STZ, a hyperglycemic drug, exhibits significant toxicity towards pancreatic β-cells as well as insulin receptors in the brains of mice [15]. Administration of streptozotocin (STZ) through intracerebroventricular (ICV) injection has been demonstrated to hinder insulin receptors within neurons, affecting the performance of glycolytic enzymes, thereby causing profound disruptions in diverse metabolic pathways regulated by the insulin signaling system within the rat brain [16].

Furthermore, the administration of ICV-STZ results in the production of proinflammatory cytokines and perturbations in insulin signaling, which may contribute to the promotion of tau phosphorylation and an increase in the toxicity of amyloid beta (Ab), ultimately culminating in neurodegeneration associated with AD and consequent impairment of cognitive abilities [17]. As a result, the ICV-STZ-induced rat model for AD displays features such as neuroinflammation, tau and amyloid pathologies, and cognitive deficits that closely resemble those observed in AD [18].

TNF-α, an important cytokine, has been demonstrated postmortem around the Aβ plaque in human AD brains [19]. Similarly, elevated TNF-α levels were found in AD transgenic mouse brain tissues. As a result of chronic neuronal expression of TNF-α has been shown to end with neuronal cell death. Biological TNF-α inhibitors have been found to have protective effects in clinical and experimental AD [20]. In addition, IL-6 is an important cytokine in immune regulation. It has been shown that hippocampal structure is altered and spatial learning is impaired in rats exposed to IL-6 during the fetal period [21]. In the study examining the cytokines expressed in the brain in AD models, it was found that many cytokines were overexpressed compared to the control group [22].

Tetanus toxin is used in the pharmaceutical industry, especially in vaccines [23]. Non-toxic TTC, on the other hand, attracts attention because it has immunological properties and neuronal binding properties. Because the non-toxic carboxy-terminal part of TTC can be transported retrospectively to the central nervous system, TTC has been used as a biological transporter of neurotrophic factors to correct neurodegenerative processes. It has been

shown that recombinant TTC with neuroprotective effects prevents memory loss in rats [24].

The main objective of this study was to inquire the impacts of ICV-STZ+TTC on memory, hippocampal C1 and C3 neuron count, and inflammation. Results of the study showed that latency time and hippocampal CA1 and CA3 neuron numbers were significantly decreased in the ICV-STZ group. However, TTC treatment significantly was increased in latency time, improved memory impairment, and reduced neuroinflammation. As a result, TTC showed neuroprotective and anti-inflammatory effects.

4. Conclusions

AD is a progressive disease that affects many people around the world and prevents people from doing their daily activities. It gradually destroys a person's memory and thinking skills. It is very important to stop the regression and progression of the symptoms of the patients and to bring them back to daily life. This is the inaugural investigation exploring the potential neuroprotective and anti-inflammatory impacts of TTC on the Alzheimer's disease rat model. Our findings proved that TTC has both neuroprotective and anti-inflammatory effects. We hope that our results will guide potential treatments for AD.

Author Statements:

References

[1] Masters, C. L., Bateman, R., Blennow, K., Rowe, C. C., Sperling, R. A., & Cummings, J. L. (2015). Alzheimer's disease. *Nat. Rev Dis Primers, 1,* 15056.

[2] Chu, L.W. (2012). Alzheimer's disease: early diagnosis and treatment. *Hong Kong Med J,* 18:228–237.

[3] Walker, K.A., Ficek, B.N. & Westbrook, R. (2019). Understanding the Role of Systemic Inflammation in Alzheimer's Disease. *ACS Chem Neurosci, 10;* 3340-3342.

[4] Netzahualcoyotzi, C., & Tapia, R. (2018). Tetanus toxin C-fragment protects against excitotoxic spinal motoneuron degeneration in vivo. *Sci Rep, 8,* 16584.

[5] Lalli, G., & Schiavo, G. (2002). Analysis of retrograde transport in motor neurons reveals common endocytic carriers for tetanus toxin and neurotrophin receptor p75NTR. *J Cell Biol, 156,* 233-239

[6] Roux, S., Colasante, C., Saint Cloment, C., Barbier, J., Curie, T., Girard, E., ... & Brûlet, P. (2005). Internalization of a GFP-tetanus toxin C-terminal fragment fusion protein at mature mouse neuromuscular junctions. *Molecular and Cellular Neuroscience, 30(1);* 79-89.

[7] Mendieta, L., Venegas, B., Moreno, N., Patricio, A., Martínez, I., Aguilera, J., & Limón, I. D. (2009). The carboxyl-terminal domain of the heavy chain of tetanus toxin prevents dopaminergic degeneration and improves motor behavior in rats with striatal MPP(+)-lesions. *Neurosci Res, 65(1);* 98-106.

[8] Radenovic, L., Selakovic, V., Olivan, S., Calvo, A. C., Rando, A., Janac, B., & Osta, R. (2014). Neuroprotective efficiency of tetanus toxin C fragment in model of global cerebral ischemia in Mongolian gerbils. *Brain Research Bulletin, 101;* 37-44.

[9] Herrando-Grabulosa, M., Casas, C., & Aguilera, J. (2013). The C-terminal domain of tetanus toxin protects motoneurons against acute excitotoxic damage on spinal cord organotypic cultures. *J Neurochem, 124,* 36–44 Paxinos, G., & Watson, C. (1998).The rat brain in stereotaxic coordinates. Spiral Bound, 4th ed. New York: Academic Press.

[10] Elibol, B., Terzioglu-Usak, S., Beker, M., & Sahbaz, C. (2019). Thymoquinone (TQ) demonstrates its neuroprotective effect via an anti-inflammatory action on the Aβ(1–42)-infused rat model of Alzheimer's disease. *Psychiatry and Clinical Psychopharmacology, 29;* 379-386.

[11] Poo, M. M., Pignatelli, M., Ryan, T. J., Tonegawa, S., Bonhoeffer, T., Martin, K. C., ... & Stevens, C. (2016). What is memory? The present state of the engram. *BMC biology, 14;* 1-18.

[12] Maruszak, A., & Thuret, S., (2014). Why looking at the whole hippocampus is not enough-a critical role for anteroposterior axis, subfield and activation analyses to enhance predictive value of hippocampal

changes for Alzheimer's disease diagnosis. *Front Cell Neurosci*, 8; 95.

[13] Padurariu, M., Ciobica, A., Mavroudis, I., Fotiou, D., & Baloyannis, S. (2012). Hippocampal neuronal loss in the CA1 and CA3 areas of Alzheimer's disease patients.. *Psychiatr Danub*, 24; 152-158.

[14] Clark, I., Atwood, C., Bowen, R., Paz-Filho, G., & Vissel, B. (2012). Tumor necrosis factor-induced cerebral insulin resistance in Alzheimer's disease links numerous treatment rationales *Pharmacol Rev*, 64; 1004-26.

[15] Pinton, S., da Rocha, J.T., Gai, B.M., & Nogueira, C.W. (2011) Sporadic dementia of Alzheimer's type induced by streptozotocin promotes anxiogenic behavior in mice. *Behav Brain Res*, 223;1-6.

[16] Grieb, P. (2016). Intracerebroventricular Streptozotocin Injections as a Model of Alzheimer's Disease: in Search of a Relevant Mechanism. *Mol Neurobiol*, 53(3); 1741-1752.

[17] Chen, Y., Liang, Z., Blanchard, J., Dai, C. L., Sun, S., Lee, M. H., ... & Gong, C. X.. (2013). A non-transgenic mouse model (icv-STZ mouse) of Alzheimer's disease: similarities to and differences from the transgenic model (3xTg-AD mouse). *Molecular neurobiology*, 47; 711-725.

[18] Dickson, D.W. (1997). The pathogenesis of senile plaques. *J Neuropathol Exp Neurol*, 56; 321-339

[19] Chang, R., Yee, K.L., & Sumbria, R.K. (2017). Tumor necrosis factor α Inhibition for Alzheimer's Disease. *J Cent Nerv Syst Dis*, 9:1179573517709278

[20] Samuelsson, A. M., Alexanderson, C., Mölne, J., Haraldsson, B., Hansell, P., & Holmäng, A. (2006). Prenatal exposure to interleukin-6 results in hypertension and alterations in the renin–angiotensin system of the rat. *The journal of physiology*, 575(3); 855-867.

[21] Patel, N. S., Paris, D., Mathura, V., Quadros, A. N., Crawford, F. C., & Mullan, M. J. (2005). Inflammatory cytokine levels correlate with amyloid load in transgenic mouse models of Alzheimer's disease. *Journal of neuroinflammation*, 2; 1-10.

[22] Bayart, C., Mularoni, A., Hemmani, N., Kerachni, S., Jose, J., Gouet, P., ... & Le Borgne, M. (2022). Tetanus Toxin Fragment C: Structure, Drug Discovery Research and Production. *Pharmaceuticals (Basel)*, 15(6);756.

[23] Patricio-Martínez, A., Mendieta, L., Martínez, I., Aguilera, J., & Limón, I. D. (2016). The recombinant C-terminal fragment of tetanus toxin protects against cholinotoxicity by intraseptal injection of β-amyloid peptide (25–35) in rats. *Neuroscience*, 315; 18-30.

Research Article
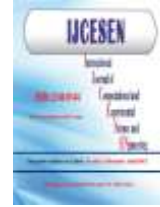
Radiation Safety For Operating Room Technicians

Halil SOYAL[1]*, Tülay ORTABAĞ[2]

[1]Istanbul Gedik University, Graduate Education Institute, 34876, Istanbul-Turkey
* **Corresponding Author** : **Email:** aydefen@gmail.com - **ORCID:** 0000-0002-3252-5923

[2]Istanbul Topkapı University, 34087, Istanbul-Turkey
Email: tulayortabag@topkapi.edu.tr - **ORCID:** 0000-0003-1466-7343

Abstract:

Abstract Radiation safety is an important consideration for operating room technicians, in procedures that involve the use of fluoroscopy or other imaging technologies that emit ionizing radiation. Radiation safety is essential to safeguard human health, minimize radiation exposure, optimize medical radiation use, protect the environment, and comply with regulatory standards. By implementing appropriate safety measures, radiation can be used safely and responsibly in various fields, balancing the benefits of radiation applications with the need for protection against potential harm. It is important for operating room technicians to adhere to radiation safety guidelines and best practices to protect themselves, their colleagues, and patients from unnecessary radiation exposure. Collaboration with radiation safety officers, radiation safety committees, and other relevant experts can help ensure a culture of safety and ongoing improvement in radiation safety practices. The aim of this article is to inform the operating room technicians about radiation, to keep their occupational exposure to a minimum is to help.

1. Introduction

Surgical interventions were considered risky and the last option in treatment until the 19th century, but over the years, the number of surgeries has increased thanks to the development of technology, change in aesthetic perception, increase in population, increase in the number of elderly population, traumas due to the use of industrial tools and equipment, current diagnosis and treatment methods, evidence-based practices, decrease in complication rates, effective anaesthesia methods and qualified care during the operation process [1,2,3].

Especially in the last 30 years, with the emergence of minimally invasive surgical techniques, robotic surgery and the increase in the number of hybrid operating theatres; patient safety, recovery rate, shortening of hospital stay, pain control, decrease in complication rate, rapid return to daily life, achieving better cosmetic results as a result of surgery and patient psychology [2]. There is an increase in the number of surgical interventions performed both in the world and in our country. Below, the statistics of the surgeries performed are given with current data.

According to the Republic of Turkey Ministry of Health Health Statistics Yearbook 2020 (published in 2022); while the total number of surgeries performed in 2002 was 1598362, this number increased to 5223815 in 2019, and the number of surgeries decreased due to COVID19 in 2020 and became 3722218. In 2020, it was reported that 44.5 out of every 1000 people in Turkey underwent surgery [4].

According to the European Community Statistical Office (Eurostat, European Community Statistical Office), 2020 data, the most common surgical interventions in Europe are cataract surgery, caesarean section, coronary angioplasty, hip replacement, cholecystectomy, appendectomy, inguinal hernia and hysterectomy. According to the same data, 1,461 cataract operations were performed per 100000 people in Latvia, while 473,1 cataract operations were performed in Turkey. Turkey has the highest caesarean section rate (764,1/100000). Coronary angioplasty was most common in Croatia (462/100000) and Germany (384/100 000), while hip replacement was most common in Germany (294/100000). Comparing 2010 and 2020, an increase was observed in laparoscopic applications

and especially in laparoscopic hysterectomy, while a decrease was observed in tonsillectomy [5].

In the cohort study by Mattingly et al (2021), it was found that with the publication of the recommendation to cancel elective surgical interventions due to COVID-19 in the USA; the number of surgical interventions performed decreased by 48% within seven weeks, the most affected interventions were cataract interventions with a decrease of 89.5%, and the least affected were organ transplantation interventions with a decrease of 20.7%. In the same study, it was observed that the number of surgical interventions rapidly returned to the initial level after the initial closure [6]. Fingar, Stocks, Weiss, and Steiner reported that the three most common surgical procedures requiring maternal and non-neonatal hospitalisation in the USA in 2012 were arthroplasty (700,100), percutaneous coronary angioplasty (534,600) and lumbar laminectomy (468,200) [7]. It was observed that musculoskeletal operations were the most common. Comparing 2003 with 2012, they concluded that there was an increase of more than 150% in the number of gastrectomy procedures [7]. Working in a healthy environment is as important as the right to live. In this context, the concept of occupational health and safety comes to the fore. Occupational health and safety includes ensuring that employees are both physically and psychosocially healthy and making the tools and working conditions used in the workplace more suitable. At the same time, it aims to protect human health against existing hazards and to find solutions to these problems by identifying existing health problems [8,9]. The International Labour Organization (ILO, International Labour Organization) and the World Health Organization (WHO, World Health Organization) publish current declarations on occupational health objectives [10]. According to WHO, occupational health is to improve the physical, mental and social well-being of employees in all occupational groups at a high level and to maintain this development. Ensuring occupational health and safety is a fundamental right of the employee [11]. The main objective of ILO is to establish basic labour standards for the government, employers and workers and to ensure that every employee works within the scope of social protection, taking into account fundamental rights and principles [12]. According to Bilir, "When hazards in the working environment cannot be prevented, they lead to risks, and when risks cannot be prevented, they lead to workrelated health problems, occupational accidents and related disability, incapacity for work and absenteeism from work" [13]. Hospitals harbour significant risks in

terms of occupational health and safety. According to the Communiqué on Workplace Hazard Classes of the Occupational Health and Safety Law No. 6331 published in 2012, hospitals are classified as "Very Hazardous Workplace [14]. While the injury rate in the industrial field is 0.3%, this rate was found to be 13.2% in healthcare workers [15]. In the world, approximately 59 million healthcare workers working in healthcare organisations are exposed to health and safety risks (Solmaz and Solmaz 2017). Operating theatre workers are faced with various safety and health hazards. The risks in the operating theatre can cause disease development, injuries, occupational accidents and labour force losses [16].

Potential risk factors in operating theatres can be listed as blood-borne pathogens, chemical and drug exposures, anaesthetic gas exposures, ergonomic hazards, latex allergy, psychosocial risks, sharps injury, infection, radiation, laser, surgical smoke and fire hazards [2,17].

It is desirable to completely eliminate these risks in the operating theatre and zero risk is a desirable situation, but it is possible to reduce risks, although it is not possible to completely prevent risks. Reducing the risks positively affects the health of the employees and also positively affects the society benefiting from the service by increasing the quality of health services. Health professionals have important duties to increase the motivation and work performance of the operating room team, to create a safe and healthy environment, and to minimise these risks [9,18]. In the general information section, information on surgical smoke and radiation will be included among the risks encountered in the operating theatre.

2. Health and Safety of Operating Theatre Staff

With the development of technology and industrialisation, working conditions negatively affect the health and safety of employees. It is the right of every employee to have a healthy and safe working environment and businesses must comply with the laws on this subject [19]. The main objective of occupational safety is to protect employees. In other words, it is to protect the mental and physical health of employees by creating comfortable and safe working conditions by protecting employees from negative effects in the workplace, occupational accidents and occupational diseases [20]. Occupational health and safety is also valid in health institutions which are a business. Although the risks and hazards that health workers are exposed to are different, it is important to regulate and implement occupational health and safety to protect employees from these hazards. The

2012 "Regulation on Ensuring Patient and Employee Safety" aims to protect the health and safety of employees. In the official gazette dated 25 November 2009, with the "Communiqué on the List of Hazard Classes Regarding Occupational Health and Safety", hospitals were included in the "Very Hazardous Work" class and radiology, radium, radioactive substances, i.e. work with radiation emitting devices, hospital, bacteriology and chemistry laboratories, pharmacy work were included in the heavy and dangerous work class [21].

Due to the fact that hospitals serve the society and can affect the health of patients, sufficient importance should be given to ensure that the occupational health and safety of healthcare workers is at the best level [21]. In the United States of America, the National Institute for Occupational Health and Safety (NIOS) reported that there are different hazards [22]. NIOS defines a healthy and safe hospital environment as "the absence of occupational diseases and occupational accidents due to physical, chemical, biological, ergonomic, mechanical hazards and risks that occur in relation to the execution of the work and harm health" [20].

Biological hazards are present in all health care areas. Infections such as HIV (Human Immunodeficiency Virus), Hepatitis B virus (HBV), Hepatitis C virus (HCV), tuberculosis, intestinal infections and infections such as Brucella, Salmonella are found in healthcare personnel and in the working environment after contact with the patient's blood or areas contaminated with blood [21].

Chemical hazards; many chemicals are used in the hospital. It is possible for anaesthesia substances, substances used in sterilisation, disinfectants used in health care, antibiotics or cancer drugs to enter the employee's body for different reasons such as inhalation, contact or needle prick during the preparation, transport and application stages.

Psychosocial hazards; Job dissatisfaction, monotonous work, lack of rest periods and number of personnel, the necessity to work irregularly and in shifts, stress caused by being responsible for the care of the sick and the deceased constitute psychosocial hazards.

Ergonomic hazards; Healthcare workers are overweight, heavy, unconscious patients, lifting, carrying or holding the falling patient, excessive effort, situations such as being asked to do work above physical competence cause musculoskeletal complaints in healthcare workers. Pain in the waist, neck, arm and carpal tunnel syndrome are musculoskeletal disorders that can be seen in healthcare workers [21].

Physical hazards; radiation, noise, carcinogenic agents, poor ventilation, lighting, heat - humidity, photocopiers and computer screens constitute physical hazards for health workers [22]. Radiation is a Latin word and is used as radiation in our language. The energy emitted from atoms, the sun and other stars is called radiation. Radiation is emitted in the form of energy or wave or particle model [23]. Radiation is divided into two as ionised and non-ionised, the most dangerous is ionised radiation and radiation causes occupational diseases. Ionising radiation causes genetic, congenital disorders or reproductive health disorders by damaging the cells that form the most basic of the body [24]. X-rays, which are ionising radiation generated by C-armed scopi devices used in some surgical cases in operating theatres, can easily penetrate deep into the body and have a destructive effect by penetrating the tissues. X-rays are frequently used in medicine to examine internal organs or to investigate whether there is a fracture in a bone [23]. Distance, time and armouring are important in radiation protection. The intensity of the magnetic field is inversely proportional to the square of the distance from the source and the density of the environment in which it spreads. It is necessary to live as far away from these lines as possible and if possible, these lines should be under the ground. Operating theatre workers are exposed to ionising radiation and radiation protection rules, radiation damages will be examined in the second part under the title of radiation safety.

3. Radiation Safety in the Operating Room

Radiation can be emitted from non-ionising devices such as laser type non-ionising devices and portable X-ray devices in the operating theatre environment, as well as from methods such as fluoroscopy and X-Ray, the use of which has increased in recent years [25].

Radiation has stochastic and deterministic effects on body organs. Stochastic effects express the risk of developing cancer with the radiation dose independent of the dose received. Deterministic effects, on the other hand, indicate that there is a threshold dose and this threshold must be exceeded for observable effects to occur. It has been shown in many studies that exposure to low levels of ionizing radiation in diagnostic radiological examinations can cause leukemia, thyroid, lung and breast cancer [26-29].

Radiation exposure during surgery is higher in orthopaedics, urology and neurosurgery [2]. In a study by Mariscalco et al, it was found that the amount of radiation exposure during open surgical interventions was significantly lower than the amount of exposure during minimal surgical intervention applications [30]. In addition to making life easier, radiation-containing devices have a serious negative impact on health. Balancing benefit and harm is one of the important rules of radiation [31]. Radiological interventions that will not contribute to diagnosis and treatment put patient and employee health at risk [32].

Radiation exposure occurs in three different ways: direct, reflection and leakage. Infiltration is caused by fluoroscopy and reflection is caused by the patient or the instruments in the operating theatre [33]. In the literature, there are studies showing that the safe distance for radiation protection varies between 46-200 cm [34].

Biological damage caused by radiation varies depending on the type and energy of radiation, how long the dose is received, how much dose the target can absorb and the properties of the target tissue. Target tissue characteristics, cell division frequency and metabolic activity, the amount and duration of the tissue's ability to absorb the dose are considered among the factors affecting biological damage [35].

Exposure to low-dose X-rays is associated with thyroid diseases, leukaemia, breast and lung cancer. Organisations such as IARC and WHO also confirm that X and gamma rays carry cancer risk [36]. In a study conducted on survivors of the Hiroshima and Nagasaki atomic bomb attack, it was observed that the risk of thyroid cancer was significantly higher in people exposed to ionising radiation at paediatric age [37].

In medical applications, there are certain limits to the radiation level that both the patient and the healthcare worker can receive. It is very important for people who apply radiation for medical purposes to know and apply these limits in order to keep the radiation level that the public will receive at a certain level [38].

It is very important to protect the employees from the harmful effects of ionising radiation, which is a physical hazard that also falls within the scope of occupational health, to inform them and to provide them with the necessary behaviours. X-rays, which are in the electromagnetic radiation class, are also used in the image formation of the C-arm scopy device used in some surgical approaches to patients, and prolonged exposure to small doses can adversely affect the health of employees. Although protecting employees from the harmful effects of radiation is one of the topics of occupational health and safety, it is important to explain the necessary information to understand the ways of protection and damages under the subject of radiation safety, and information about radiation is explained under this heading.

The atom, which is the smallest part of the element that carries its own characteristics, consists of a nucleus consisting of protons and neutrons and negatively charged electrons orbiting the nucleus [39]. The energy levels of the orbit where the electrons are located are different in each orbit. Energy levels increase from outside to inside [40]. The excitation of electrons for any reason allows them to settle at higher or lower levels related to the energy they will gain [41]. The energies carried in the form of fast particles and electromagnetic waves emitted by natural or artificial radioactive nuclei that want to pass to a stable structure are defined as "radiation" [42]. Radiation is electromagnetic waves or particles emitted from a source [43].

While some of the nuclei of atoms in nature are stable, others are unstable. Since the protons and neutrons in a stable nucleus are bound to each other by tight bonds and nuclear forces, the nucleus will remain in equilibrium since the particles cannot escape from the nucleus. If the nucleus is unstable or out of equilibrium, the particles will not be able to stay together with the excess energy it has, and will discharge its excess energy in a short or long time. Unstable nuclei are called "radioactive nuclei" or "radioisotopes". The condition of unstable nuclei emitting radiation to the environment during the decay period in order to become stable is called "radioactivity" [41].

Today, according to International Radiation Protection (ICRP) recommendations, annual dose limits for radiation officers are 20 mSv, and dose limits for patient relatives are 5 mSv [44-45]

4. Biological Effects of Ionising Radiation

Knowing and examining the biological effects of ionising radiation is important in terms of providing the necessary behaviour in radiation protection. As ionising radiation passes through tissues, it stimulates the atoms in the tissue and causes ionisation or disruption of their molecular structures [36]. The biological effects of ionising radiation on the irradiated tissue vary according to the size of the dose, the effects on the irradiated parts of the body, the characteristics of the irradiated area and the type of radiation emitted. The effect of radiation

occurring at large doses is called deterministic effect [46].

The quality of education to be given to people who will use these devices gains importance in terms of preventing early, late and hereditary effects that may occur due to unnecessary and/or high radiation exposure of patients, patient relatives and working personnel during imaging methods using ionizing radiation [47]

Death, skin burns, cataracts, infertility are examples of this effect. The effect that occurs at doses too small to cause cell damage is called stochastic effect and very small doses are sufficient for this effect to occur, it is a dose-independent effect. Cancer and genetic effects can be examples [25]. The factors on which the biological effects of radiation depend vary according to factors such as the type of radiation affecting the organism, the amount of radiation to which the organism is exposed, the duration of exposure to radiation, the way it is affected by radiation [48]. The degree of sensitivity of the organism region to radiation; reproductive cells, eye lens and retina, lymphocyte type of leucocytes, bone marrow, spleen, skin and small intestines are sensitive to radiation (radiosensitive), muscle, nerve and mature bone cells are resistant to radiation (radioresistance) [41].

5. Early Effects

These are the effects that may occur when a certain part of the body or the whole body is exposed to high doses of radiation dose in a short time. The effects that will occur with acute irradiation show their effects according to variables such as the radiation dose received and the duration of exposure. These effects manifest themselves as severe damage, burns or death within a few days or weeks [28,35]. This type of irradiation, also called acute irradiation, is usually unintentional irradiation resulting from an accident. The main cause of accidents is observed to be the loss, theft or otherwise out of control of radiation sources. Unfortunately, despite significant developments in radiation safety practices, such accidents that can harm people can still occur [18,26]. The effects that may occur as a result of acute irradiation can be generally classified as acute radiation syndromes and local radiation damage.

6. Radiation Syndromes

It develops as a result of acute irradiation of the whole or a large part of the body. Within a few hours after exposure, symptoms such as nausea, vomiting, diarrhoea, headache, fever, loss of consciousness and a decrease in blood cell count occur. After two

to three weeks, other symptoms such as hair loss, loss of appetite, general weakness, feeling unwell, internal bleeding, high fever, cataracts and temporary infertility in men may appear. If the whole body is exposed to a radiation dose exceeding 7 Sv over a period of a few days or less, the bone marrow, which produces blood cells, will be damaged and unable to produce enough cells, and death will probably occur within a few weeks. This process from the onset of symptoms to the occurrence of death depends on the radiation dose [22,28].

Regional Radiation Damage (BRH)

The effects of exposure of any area of the body to a dose of radiation over a short period of time, usually as a result of an accident, are called Localised Radiation Damage. This type usually damages the hands and fingers. The first sign of a high dose is erythema of the skin. Although it seems like a simple first-degree burn at first, the radiation burn deepens in the future and leads to bigger problems [22].

7. Delayed Effects (Chronic Irradiation Effects)

As stated above, acute irradiation occurs as a result of exposure to high doses of radiation at one time or in a short period of time. Therefore, high dose radiation exposure occurs as a result of unusual situations such as accidents or negligence. On the other hand, chronic irradiation occurs as a result of exposure to small amounts of radiation for very long periods of time. Therefore, damage caused by chronic exposure usually occurs after many years. Workers in areas with ionising radiation are thus exposed to chronic irradiation. It is difficult to measure the effect of ionising radiation in chronic irradiation by itself, since cases such as cataracts and cancer in chronically irradiated people will occur over many years. It is scientifically recognised that radiation exposure causes cancer, regardless of the amount. Since there are many and different causes of cancer in the society, it is very difficult to determine the risk of cancer due to chronic irradiation. The risk of fatal cancer due to radiological examinations is estimated according to the degree of sensitivity of each organ to radiation. For example, for every 0.1 mGy ionising radiation dose received by active bone marrow, the probability of leukaemia is 1/500000 (one in five hundred thousand). This nominal risk value is 1/200000 (one in two hundred thousand) for breast tissue, 1/500000 (one in five hundred thousand) for lung and 1/2000000 (one in two million) for thyroid [22,27,28,34].

According to the radiological protection bulletin published by the National Radiological Protection Board (NRPB) in September 2001, the lifetime

cancer development risk of each radiological examination is presented in the table below [25].

8. Conclusion

The increasing prevalence of radiation-requiring procedures such as pain therapy, the introduction of new clinical applications, and the increasing demand indicate that the risk of occupational radiation exposure for operating room technicians is increasing. Although available evidence suggests that occupational radiation doses are below the recommended threshold, for radiation-related damage There is no published definite lower limit. Even low exposure levels are not trivial. There is no published guide on radiation protection yet. Operating room technicians must comply with the "ALARA" and three basic principles, which should be considered in radiation protection, the rules of time, distance and shielding. All employees should wear protective glasses, apron, thyroid protector and dosimeter. Educational programs on the availability and correct use of protective equipment are vital to the development of safe practices. In addition, the radiation risk to be taken should be evaluated according to the benefit to be obtained from the intervention and a decision should be made accordingly.

Author Statements:

- **Ethical approval:** The conducted research is not related to either human or animal use.
- **Conflict of interest:** The authors declare that they have no known competing financial interests or personal relationships that could have appeared to influence the work reported in this paper
- **Acknowledgement:** The authors declare that they have nobody or no-company to acknowledge.
- **Author contributions:** The authors declare that they have equal right on this paper.
- **Funding information:** The authors declare that there is no funding to be acknowledged.
- **Data availability statement:** The data that support the findings of this study are available on request from the corresponding author. The data are not publicly available due to privacy or ethical restrictions.

References

[1] Aksoy G. (2017). Surgery and Surgical Nursing. Aksoy G, Kanan N, Akyolcu N. (Eds.), Surgical Nursing I, Nobel Medicine Bookstores, Istanbul, pp.203-255.

[2] Aygin D. (2017). Radiation, 2nd International 10th National Turkish Operating Room and Surgical Nursing Congress. 02-05 November 2017, Antalya p.176.

[3] Cengiz H. (2018). The Validity-Reliability Study of the Postoperative Recovery Index in Patients Undergoing Surgical Intervention and Evaluation of Recovery Status. SAU. Health Sciences Institute. Doctoral Thesis. Sakarya. Aygin D. (Assoc. Prof.)

[4] https://www.saglik.gov.tr/TR,89801/saglik-istatistikleri-yilligi2020-yayinlanmistir.html, Access Date: 08 August 2023

[5] https://ec.europa.eu/eurostat/statistics/explained/index.php?title=Surgical_operations_and_procedures_statistics&oldid=50 2541#Number_of_surgical_operations_and_procedures, Accessed 11 June 2023

[6] Mattingly AS, Rose L, Eddington HS, Trickey AW, Cullen MR, Morris AM, Wren SM. (2021). Trends in US surgical procedures and health care system response to policies curtailing elective surgical operations during the COVID-19 pandemic. JAMA Network Open, 4(12),1-12.

[7] Fingar KR, Stocks C, Weiss AJ, Steiner CA. (2015). Most frequent operating room procedures performed in US Hospitals, 2003–2012: statistical brief# 186. Europe PMC [Electronic Journal]. 20 Feb 2015. https://europepmc.org/article/NBK/nbk274246

[8] Parlar S. (2008). An overlooked situation in healthcare professionals: A healthy working environment. *Turkish Armed Forces Preventive Medicine Bulletin,* 7(6):547-554.

[9] Solmaz M, Solmaz T. (2017). Occupational health and safety in hospitals. *Gumushane University Journal of Health Sciences*, 6(3):147-156

[10] Saygun M. (2019). International Approaches to Occupational Health, Safety and Occupational Diseases. Hacettepe University Public Health Nursing Undergraduate Program, *Published Undergraduate Lecture Note.* Ankara.

[11] https://www.who.int/health-topics/occupational-health, Access Date: 11 August 2023

[12] https://www.ilo.org/global/about-the-ilo/how-the-ilo-works/lang--en/index.htm, Date of Access: 12 August 2023

[13] Bilir N. (2005). A contemporary approach to occupational health and safety: Risk assessment and risk management. *Journal of Occupational Health and Safety*, (25):9-11.

[14] https://www.resmigazete.gov.tr/eskiler/2012/12/20 121226-11.htm

[15] Ilce A, Yuzden GE, Yavuz van Giersbergen M. (2017). The examination of problems experienced by nurses and doctors associated with exposure to surgical smoke and the necessary precautions. *Journal of Clinical Nursing*, 26(11-12):1555-1561.

[16] Abdollahzade F, Mohammadi F, Dianat I, Asghari E, Asghari-Jafarabadi M, Sokhanvar Z. (2016). Working posture and its predictors in hospital operating room nurses. *Health Promotion Perspectives*, 6(1):17-22.

[17] Khajuria A, Maruthappu M, Nagendran M, Shalhoub J. (2013). What about the surgeon? *International Journal of Surgery*, 11(1):18-21

[18] Eti Aslan F, Kan Öntürk Z. (2011). Safe operating room environment; biological, chemical, physical and psychosocial risks, effects and precautions. *Maltepe University Journal of Nursing Science and Art,* 4(1):133-140.

[19] Tuzuner L., Ozaslan O. (2011). A Study on Evaluation of Occupational Health and Safety Practices in Hospitals. *Journal of Istanbul University Faculty of Business*, 40(2):118-154.

[20] Öztürk H and Babacan E. (2012). Scale Development Study: Occupational Safety Scale for Healthcare Personnel Working in the Hospital. *Journal of Nursing Education and Research.*9(1): 36-42.

[21] Meydanlıoğlu A. (2013). Health and Safety of Healthcare Professionals. *Balıkesir Journal of Health Science*. 1(3):193-197

[22] Özkan Ö, Emiroğlu N. (2006). Occupational Health and Safety Services for Hospital Healthcare Workers. *Journal of Cumhuriyet University School of Nursing* 10:43-50

[23] Durukan T.(BTY).Atatürk University A.O.F. Occupational Health and Safety Unit 4. YY

[24] Baybora D. et al. (2012). T.R. Anadolu University A.O.F. Occupational Health and Safety Textbook. Anadolu University Publication No: 2664. A.O.F. Publication No: 1630. p;2-63

[25] Vural F. and Others(2012). Radiation Safety in Operating Rooms; Knowledge, Attitudes and Behaviors of Working Personnel. *Balikesir Journal of Health Sciences.* 1(3);131-136

[26] Ron E. (2003). Cancer risks from medical radiation. *Health Phys.* 85(1):47-59.

[27] 9. Takamura N, Orita M, Saenko V, Yamashita S, Nagataki S, Demidchik Y. (2016). Radiation and risk of thyroid cancer: Fukushima and Chernobyl. *Lancet Diabet Endoc*. 4(8):647.

[28] Hall EJ, Brenner DJ. (2008) Cancer risks from diagnostic radiology. *British J Radio.* 81(965):362-378.

[29] Günay O., , Gündoğdu O. , Demir M. , Timlioğlu İper H.S. , Kuru I. , Yaşar D. , Aközcan S. , Yarar O. (2020). Determination of Absorbed Radiation Dose Levels of Lenses Thyroid And Oral Mucosa in Computed Tomography Imagining: Phantom Study, *Kocaeli University Journal of Health Sciences*, 6(1):23-27

[30] Mariscalco MW, Yamashita T, Steinmetz MP, Krishnaney AA, Lieberman IH, Mroz TE. (2011). Radiation exposure to the surgeon during open lumbar microdiscectomy and minimally invasive microdiscectomy: a prospective, controlled trial. *Spine,* 36(3):255-260.

[31] Kaya T. (1997). Basic Radiology Technique. 1st Edition. Güneş&Nobel Medicine Bookstores, Istanbul, p. 2-133

[32] Aydogdu A, Aydogdu Y, Yakinci ZD. (2017). Recognition of basic radiological examination methods. *Journal of İnönü University Vocational School of Health Services*, 5(2):44-53

[33] Çeçen GS, Gülabi D, Pehlivanoğlu G, Bulut G, Bekler H, Kiyasettin A. (2015). Radiation in the orthopedic operating room. *Acta Orthopedica et Traumatologica Turcica,* 49(3):297-301

[34] Lakhwani OP, Dalal V, Jindal M, Nagala A. (2019). Radiation protection and standardization. *Journal of clinical orthopedics and trauma,* 10(4);738-743.

[35] Gökharman DF, Aydın S, Koşar PN. (2016). What we need to know professionally in radiation safety. *Süleyman Demirel University Journal of Health Sciences,* 7(2):35-40

[36] Dashdag S. (2010). Ionizing radiations and cancer. *Dicle Medical Journal,* 37(2):177-185

[37] Cahoon EK, Nadyrov EA, Polyanskaya ON, Yauseyenka VV, Velkin IV, Yeudachkova TI...& Brenner AV. (2017). Risk of thyroid nodules in residents of Belarus exposed to Chernobyl fallout as children and adolescents. *The Journal of Clinical Endocrinology & Metabolism*, 102(7):2207-2217

[38] Palacı H. , Günay O. Yarar O. (2018) Evaluation of Radiation Safety and Protection Education in Turkey *European Journal of Science and Technology* 14;249-254,

[39] T.R. Ministry of National Education (2011a.) Radiology. Atomic Structure and Electron Theory Course Module. MEB ANKARA

[40] Huda W. (2014). (Translation by Karabulut N. , Radiation Physics And Review, Dünya Publishing House)

[41] Kumas A.(2009a). Radiation Physics and Basic Applications. Palme Bookstore. pages;28-320

[42] Tutuş A. et al. (2010). Erciyes University Medical Faculty Hospitals, Radiation Health and Safety Handbook, Publication No: 19. Kayseri

[43] Bora H.(2001). Radiation Safety. Ankara University Dikimevi Health Services Vocational School Yearbook. Volume 2, Issue :1

[44] Günay O , Demir M. (2019). Radiation Dose Measurements in the Patient's Neighborhood in Computed Tomography Shoots *Süleyman Demirel University Journal of Natural and Applied Sciences* 23(3);792-796,

[45] Valentin, J., 2007. The 2007 recommendations of the international commission on radiological protection. ICRP publication 103. Ann iCRP, 37(2), 1-332.

[46] Emel G. and Others(2012). Knowledge, Attitude and Behavior of Radiology Workers on Radiation Safety. *Journal of Performance and Quality in Health*, 3;29-33

[47] Günay O. , Öztürk H. , Yarar O. (2019) Project Based Learning of the Structure of Medical Imaging Devices Working with Ionizing Radiation, Journal of Health Services and Education; 3(1): 20-27

[48] www.taek.gov.tr/ogrenci/r05.htm,Transport Date:28-08-2022

Research Article
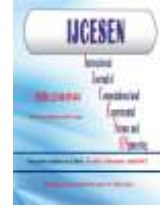
Usability of Pine Sawdust and Calcite Together as Filler in Polyester Composites

İlyas KARTAL[1]*, Hilal SELİMOĞLU[2]

[1]Marmara University, Faculty of Technology, Metallurgical and Materials Engineering Department, İstanbul-Turkey
* **Corresponding Author** : **Email:** ilyaskartal@marmara.edu.tr - **ORCID:** 0000-0001-9677-477X

[2]Marmara University, Institute of Pure and Applied Sciences, Polymer Science and Technology Dep., İstanbul-Turkey
Email: selimoglu.hillal@gmail.com **- ORCID:** 0000-0002-5344-7100

Abstract:

Two different types of fillers are used in composites, natural and synthetic. Natural fillers are gaining popularity as an alternative to synthetic fillers due to low production cost, lightweight, and abundance of renewable resources. Although thermoplastics are widely used as matrix material in natural fillers-filled composite materials, there are thermoset polymers such as epoxy and polyester. The most known and used natural-organic fillers are wood sawdust and fibres. Wood sawdust can be obtained easily and cheaply as waste in furniture production and is generally used after appropriate sieving. In this study, general-purpose polyester resin was preferred as matrix material. Calcite and pine wood sawdust are used as fillers. Calcite is used as a synthetic filler and pine wood sawdust is a natural filler and can be found easily. Thus, the usability of natural and synthetic fillers together was investigated. Composite samples were prepared by pouring the mixture into an open Teflon mold. The physical properties of the samples such as tensile, impact, density, and hardness were investigated. Images of broken surfaces were analysed by SEM. As a result of the study, it was evaluated that pine sawdust and calcite can be used together in polyester-based composite applications.

1. Introduction

Natural fibres have been used in composites for over 3000 years as both filler and reinforcement. Recently, the use of natural fibre-filled composites is very common. As natural fibres, many types of natural fibres such as flax, hemp, jute, straw, wood fibre, rice husk, wheat, barley, oats, rye, cane (sugar and bamboo), grass canes, kenaf, ramie, oil have been investigated for use in plastics. Natural fibres have the advantage of being renewable resources and having marketing appeal. Natural fibres have been used in world markets for many years. Natural fibres are increasingly used in automotive and packaging materials. Agricultural wastes include wheat husk, rice husk, and their straw, hemp fibre, and peels of various dried fruits. These agricultural wastes are preferred to prepare fibre-reinforced polymer composites for commercial use [1-7].

Due to the global energy crisis and the pursuit of sustainability, natural fibre reinforced polymer composites attract more attention than synthetic fibre reinforced polymer composites with their superior properties such as non-toxicity, non-irritation to the skin, eyes, and respiratory tract, and non-corrosive [8].

Recently, natural fibres have been preferred as reinforcing fillers in polymer matrices. Composite materials prepared with natural fibres have replaced traditional materials in automotive parts, wood substitutes and various technical applications due to some reasons such as being easy to process and light [9].

Natural fibre composites are lightweight, environmentally friendly, renewable, biodegradable, accessible, and sustainable. Natural fibres outperform man-made or synthetic fibres in terms of performance. However, the morphology and chemical composition of natural fibres cannot be completely controlled compared to synthetic fibres [10].

Natural fibres have certain advantages over synthetic fibres. The main advantages of lignocellulose fibre reinforced polymer composite materials are that they are biodegradable, easy to find, and easily degradable [11].

Natural fibre-based fibres are also commonly used with both thermoset and thermoplastic-based matrix

materials [12]. The polymers used in natural fibre composites are mostly polyolefins. This allows the processing temperature to be below 200 °C. Above this temperature, degradation of the fibres was observed [9,13,14]. However, it can also be used in thermosets. In this study, unsaturated polyester resin was preferred as the matrix material of the composite due to its widespread use.

Unsaturated polyester resin is a thermoset polymer with good properties such as high economic potential and easy application in industry. It forms about -three-quarters of the thermosets used in the polyester composite industry, which is used extensively in coatings and as a matrix material. It is very useful as it can be chemically modified with crosslinkers. Unsaturated polyester resins are intertwined with almost all areas of the composite industry such as adhesives, coatings, sealants, and laminates. The important advantages of unsaturated polyester resins come from their good mechanical properties, dimensional stability, resistance to chemicals, electricity, air, ability to be processed by conventional methods, and low cost [15-20]. Unsaturated polyester resins have a wide application area and these areas are expanding with market demands they are materials that are developing to produce more environmentally friendly products [21-25]. Particle use in composites has both filler and reinforcing uses. Particles such as graphene oxide and magnesium hydroxide in micron or nano sizes are used as reinforcing for polymer matrix composites. The particles are collected under 3 main groups natural, synthetic, and organic. The vast majority of fillers such as talc, mica, and calcium carbonate are available industrially and are used in different fields [26]. Among them, calcium carbonate is mainly used because of its low cost and commercial abundance. With the addition of optimum calcium carbonate concentration, the thermal, mechanical, and optical characteristics of the polymers are significantly expanded [27]. Calcium carbonate ($CaCO_3$) is widely used as a filler in the plastics industry. It is used not only in thermoplastics such as Polyvinylchloride (PVC) but also in thermosets such as polyester. Calcium carbonate is abundant in nature as limestone and marble, and $CaCO_3$ filler can be produced from these minerals at a very low cost. Its natural color is white and can be easily colored. Chemically stable up to 800 °C [28]. Inorganic fillers such as calcium carbonate, metal particles, and mica provide sufficient thermal stability to the polymer, as well as provide higher wear resistance, toughness, and hardness when used in composite materials compared to pure polymer [29].

In this study, the use of pine sawdust, which is produced as a large amount of waste in the furniture industry, and calcite, which is heavily preferred in the industry, as a filler were examined. Pine trees are known as coniferous (coniferous) tree species and their wood is hard, durable, resinous, and of good quality. It is used as a building material because it has good nail and screw-holding resistance and is easy to process. Due to its easy processing, it is used in the building materials, furniture, and packaging industries, and waste sawdust is obtained intensively [30].

2. Material and Methods

2.1. Materials

Calcite and pine sawdust were used together as a filler in the composite material. Pine sawdust was obtained as waste from local companies manufacturing furniture. Pine sawdust was sieved and used in sizes of 0-250 μm. Calcite (Nidaşcarb 3), which is used extensively industrially, was obtained from Nidaş Madencilik A.Ş. Physical and chemical properties of calcium carbonate are shown in Table 1. Polyester was chosen because of its widespread use in the industry as a thermoset resin. Methyl ethyl ketone peroxide (Erco Boya, Istanbul) was used as a reaction initiator. Cobalt naphthalate, which is used as an accelerator, was not used separately because it was included in the resin. Teflon mold was used to prepare test samples.

Table 1. Properties of Calcium Carbonate

Physical Properties		Chemical Properties	
Density (g/cm³)	2,7	$CaCO_3$	>99,6%
Hardness (Mohs)	3	MgO	<0,20%
Refractive index	1,59	FeO_2	<0,01%
		SiO_2	<0,01%
		Al_2O_3	<0,02%

2.2. Sample preparation

Pine wood sawdust was kept in an oven at 40 °C for 2 hours to dry before they were used in the experiment. The sawdusts were sieved (250 μm size).

For the resin, 1.5% MEK-P was used as a hardener. The mixture was poured into a Teflon mold on a flat surface. It waited for 12 hours at room temperature for the samples to cure, then they were removed from the mold. Composite samples prepared with different weight ratios of sawdust and calcite are shown in Table 2.

2.3. Tests and Analysis

The tensile test of the samples prepared according to the ISO 527 standard was carried out in the Zwick

Table 2. Contents of samples (by weight, %)

Samples	Pine Sawdust	Calcium Carbonate	Polyester
Neat Polyester	0	0	100
5PS15CC	5	15	80
10PS10CC	10	10	80
15PS5CC	15	5	80
20PS	20	0	80
20CC	0	20	80

Abbreviations: PS, pine sawdust; CC, calcium carbonate.

Z010 universal tensile device with a tensile speed of 5 mm/min. The impact strength of the unnotched samples prepared according to the ISO 180 standard was tested using a 5.4 J Izod hammer in the Zwick B5113.30 impact device. Hardness measurements were made in Zwick Shore D device, 15 sec. made with a waiting period. For SEM analysis, the samples were coated with a 10 Å thick gold/palladium alloy. The SEM test was performed with the Polaron SC branded device located in the Marmara University Faculty of Technology Laboratory.

3. Results and Discussions

The tensile properties of natural fiber-reinforced polymers for both thermoplastics and thermosets are affected by the interfacial adhesion between the matrix and the fibers (Fig.1). Various chemical modifications are used to improve the interfacial matrix-fiber bond, resulting in increased tensile properties of composites. Factors such as the filler ratio and size used in the composite, and the bond strength of the matrix layer between the filler also affect the strength.

In general, the tensile strength of natural fiber-reinforced polymer composites increases with fiber content up to an optimum value, then decreases. However, Young's modulus of natural fiber-reinforced polymer composites can increase with increasing fiber content. The tensile strength values of the samples are shown in Table 3 and Fig.2.

Table 3. Elastic modulus, tensile strength, and strain values of composite materials

Samples	Elastic Modulus (MPa)	Tensile Strength (MPa)	Strain (%)
Neat Polyester	2035	25	1,2
5PS15CC	2330	18,1	0,81
10PS10CC	2220	16,5	0,66
15PS5CC	2130	16,1	0,59
20PS	1920	15,2	0,78
20CC	2660	22,8	0,79

According to the tensile test results, it was observed that the highest tensile strength was in neat polyester. The tensile strength of the neat polyester sample was determined as 25 MPa. A decrease in tensile strength was observed with the addition of pine sawdust filler. The lowest tensile strength value was found in the 20% sawdust-filled composite sample and it was determined as 15 MPa. The tensile strength of the 20% Calcite filled sample was found to be 22.8 MPa. The tensile strength of the sawdust filled samples decreased as expected. The weak interfacial bond between the polymer matrix and the filler content reduces the tensile strength of the composite. It has been reported in different studies that agglomeration tendency with increasing filler amount or insufficient hydrogen bonding between sawdust particles and matrix causes a decrease in tensile strength [31,32].
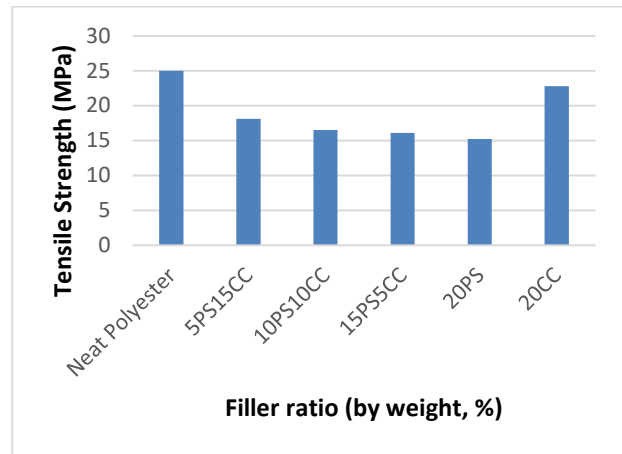
Figure 1. Tensile strength properties of composites materials

While filler can increase the tensile strength to the ideal ratio and then cause a decrease, on the contrary, the modulus value can increase as the amount of filler increases. The highest E modulus value of the composite samples was reached with 20% calcite filler (2660 MPa). Although the modulus value increased slightly with the addition of sawdust, this value decreased below the neat polyester with the addition of 20% only sawdust. Except for the 20% sawdust filled sample, the modulus value of all samples is higher than that of neat polyester. In Figure 3, the variation of Izod impact strength according to the filler ratio is given. It has been reported in the literature that the impact strength decreases with the increase of the sawdust ratio, and the toughness partially increases with the use of calcite [4,29,33]. The impact strength of polyester decreased with the addition of sawdust. The highest impact strength was achieved with the

Figure 2. Elastic modulus properties of composites materials

Figure 3. Izod impact strength properties of composite samples

Figure 4. Density values of composite samples

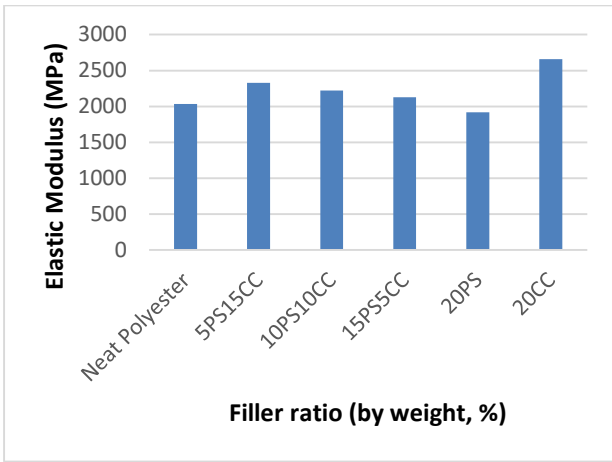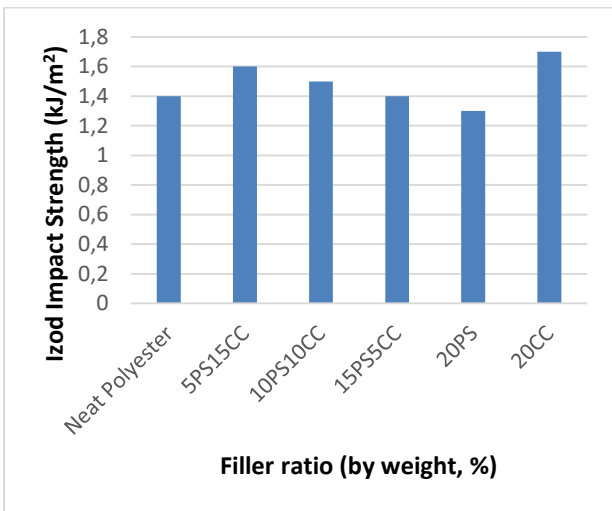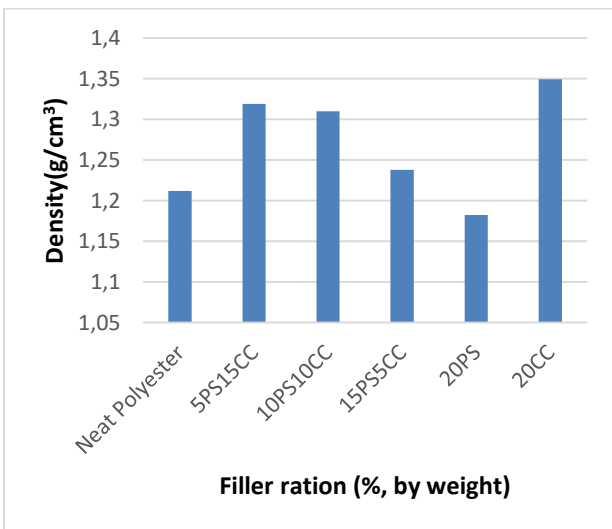20% calcite-filled sample. It is seen that the impact strength value when used together with calcite and sawdust is partially above that of neat polyester. In Figure 4, the density values of composite samples are given. Compared to neat polyester, the density of sawdust in cellulosic structure is low, and the density of calcite in inorganic structure is high. As expected, the density is low in the samples with sawdust content, and the density increases in the samples containing calcite. The Shore D hardness value of the samples is given in Figure 5. The lowest hardness value was determined in neat polyester. The hardness values also changed with the change and increase in the filler ratio, and the highest hardness value was observed in the 20% calcite-filled sample. Although the hardness value of the sawdust increased a bit, the hardness value increased more with the increase of the calcite ratio.
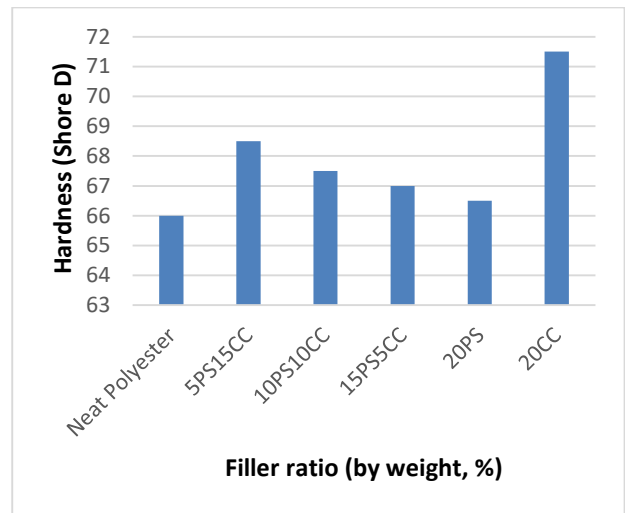
Figure 5. Hardness properties of composite samples

SEM images of the samples are given in Figure 6. Figure 6(a) (neat polyester resin) shows that the rupture surface is plane. This characteristic is associated with the brittle rupture observed in most neat polyester materials. The other SEM image, figure 6(b), contains 20% calcite. It is clear that calcite adheres very well to polyester. As can be seen from the image, it is confirmed to be 3 microns in size. Figure 6(c) is the fracture surface images of the sample with 5% calcite-15% sawdust, and 6(d) is the sample with 20% sawdust. In different studies, 20% sawdust filler was determined as the upper limit. In this study, the filler ratio was kept at 20%. Agglomeration was observed in samples containing 20% and above filler, especially in samples with sawdust particles. This is thought to cause the formation of bubbles and pores that may interfere with the mechanical properties of the composites. Observations in this analysis have been similarly reported in other studies [4-5].
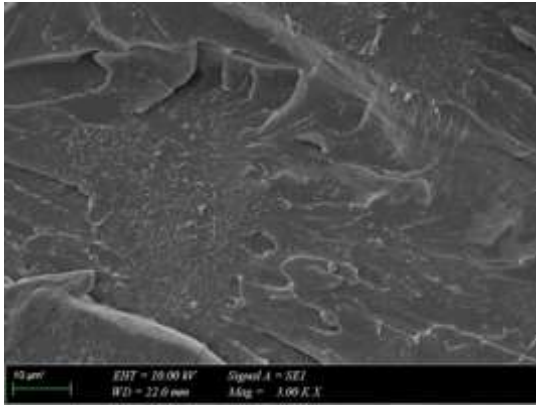
(a)
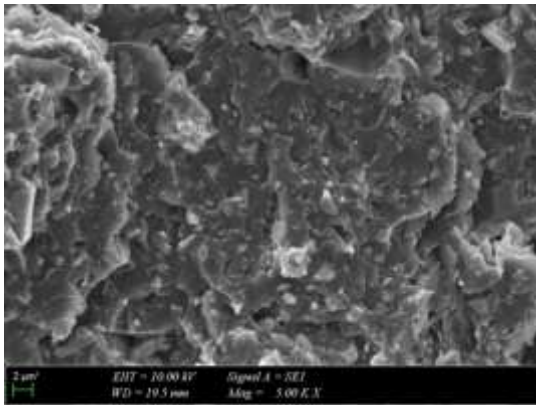
(b)
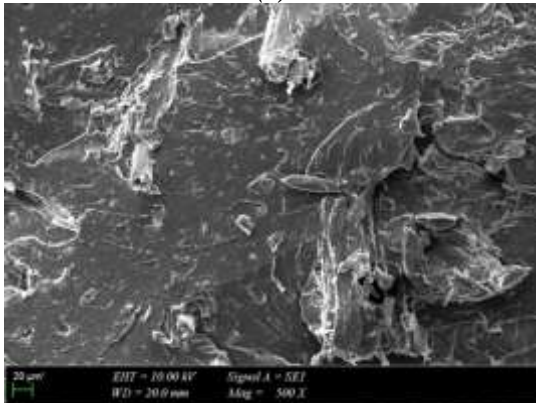
(c)
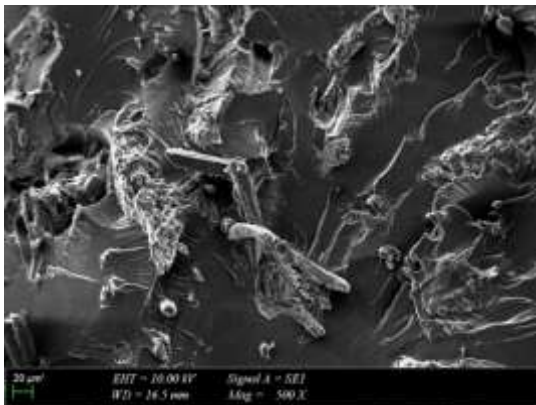
(d)

Figure 6. *SEM images of samples a)neat polyester b)20CC c)5CC15PS d)20PS*

4. Conclusions

Natural filler/fiber-containing polymeric composites are of great interest to both engineers and researchers due to their many advantages. For this reason, these lightweight composites replace traditional structural materials in many applications. Natural fibers compete with synthetic fillers when used as fillers. Natural fiber composites are already applied in the automobile and furniture industries.

In this study, the use of pine wood sawdust and calcite as a filler in polyester-based composite material was investigated.

According to the tensile test data, a partial decrease was observed as the sawdust filler increased, while this decrease was less in the addition of calcite. There was no obvious change in the impact properties. In the density values, only the sawdust-filled sample remained below the neat polyester, while the density of the other samples increased. The hardness results increased with the addition of both sawdust and calcite. It was understood from the SEM images that the fillers were homogeneously mixed in the structure. At the end of this study, when the data of all samples were examined, it was determined that sawdust filler and calcite could be used together as filler in polyester, which would reduce the amount of polyester used and reduce the cost. It is also clear that the use of natural fillers instead of synthetic fillers will contribute to the solution of environmental problems.

As a result, it was concluded that the use of pine sawdust together with calcite as a filler in polyester matrix composite material applications may be a suitable decision.

Author Statements:

are not publicly available due to privacy or ethical restrictions.

References

[1] Demirer, H., Kartal, İ., Yıldırım, A., & Büyükkaya, K. (2018). The Utilisability of Ground Hazelnut Shell as Filler in Polypropylene Composites. *Acta Physica Polonica A*, 134: 254-256. https://doi.org/10.12693/APhysPolA.134.254

[2] Kartal, İ. (2020). Effect of Hornbeam Sawdust Size on the Mechanical Properties of Polyethylene Composites. *Emerging Materials Research*, 9(3):979-984. https://doi.org/10.1680/jemmr.20.00164

[3] Kartal, İ., Naycı, G., & Demirer, H. (2019a). Cam ve Bambu Lifleriyle Takviyelendirilmiş Vinilester Kompozitlerinin Mekanik Özelliklerinin İncelenmesi. *International Journal of Multidisciplinary Studies and Innovative Technologies*, 3(1):34-37.
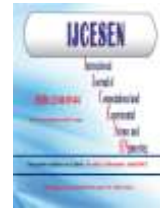
[4] Kartal, İ., Naycı, G., & Demirer, H. (2019b). Kestane/Gürgen Talaşı Dolgulu Vinilester Kompozitlerin Mekanik Özelliklerinin İncelenmesi. *European Journal of Science and Technology,* 16:723-728. https://doi.org/10.31590/ejosat.566756

[5] Kartal, İ., Naycı, G., & Demirer, H. (2020). The Effect of Chestnut Wood Flour Size on the Mechanical Properties of Chestnut Wood Flour Filled Vinylester Composites. *Emerging Materials Research*, 9:1-6. https://doi.org/10.1680/jemmr.19.00179

[6] Kushwanth Theja, K., Bharathiraja, G., Sakthi Murugan, V., & Muniappan, A. (2023). Evaluation of mechanical properties of tea dust filler reinforced polymer composite. *Materials Today: Proceedings,* 80: 3208-3211. https://doi.org/10.1016/j.matpr.2021.07.213

[7] Şengör, İ., Cesur, S., Kartal, İ., Oktar, F. N., Ekren, N., İnan, A. T., & Gündüz, O. (2018). *Fabrication and Characterization of Hazelnut ShellPowder with Reinforced Polymer Composite Nanofibers*. ICNMA: 2018 20th International Conference on Nanostructured Materials and Applications, Zurich, Switzerland.

[8] Kumar, R., Ul Haq, M. I., Raina, A., & Anand, A. (2019). Industrial Applications of Natural Fibre-reinforced Polymer Composites – Challenges and Opportunities. *International Journal of Sustainable Engineering,* 12(3): 212-220. https://doi.org/10.1080/19397038.2018.1538267

[9] Albinante, S. R., Platenik, G., & Batista, L. N. (2017). Composites of Olefin Polymer/Natural Fibers: The Surface Modifications on Natural Fibers. In *Handbook of Composites from Renewable Materials* https://doi.org/10.1002/9781119441632.ch79

[10] Singh, P., Singari, R. M., Mishra, R. S., & Bajwa, G. S. (2022). A review on recent development on polymeric hybrid composite and analysis of their enhanced mechanical performance. *Materials Today: Proceedings*, 56: 3692-3701. https://doi.org/10.1016/j.matpr.2021.12.443

[11] Devaraju, S., & Alagar, M. (2019). Chapter 2 - Unsaturated Polyester—Macrocomposites. *Unsaturated Polyester Resins.* Elsevier. https://doi.org/10.1016/B978-0-12-816129-6.00002-8

[12] Netravali, A. N., & Chabba, S. (2003). Composites get greener. *Materials Today*, 6(4): 22-29. https://doi.org/10.1016/S1369-7021(03)00427-9

[13] Ichazo, M. N., Albano, C., González, J., Perera, R., & Candal, M. V. (2001). Polypropylene/wood flour composites: treatments and properties. *Composite Structures*, 54(2): 207-214. https://doi.org/10.1016/S0263-8223(01)00089-7

[14] Joseph, K., Thomas, S., & Pavithran, C. (1996). Effect of chemical treatment on the tensile properties of short sisal fibre-reinforced polyethylene composites. *Polymer*, 37(23): 5139-5149. https://doi.org/10.1016/0032-3861(96)00144-9

[15] Oleksy, M., & Galina, H. (2013). Unsaturated Polyester Resin Composites Containing Bentonites Modified with Silsesquioxanes. *Industrial & Engineering Chemistry Research*, 52(20): 6713-6721. https://doi.org/10.1021/ie303433v

[16] Mohammed, M. H., & Dauda, B. M. (2014). Unsaturated Polyester Resin Reinforced With Chemically Modified Natural Fibre, *Journal of Polymer and Textile Engineering,* 1(4):31-38.

[17] Paauw, M., & Pizzi, A. (1993). Some filler effects on cross-linking of unsaturated polyesters. *Journal of Applied Polymer Science*, *50*(7): 1287-1293. https://doi.org/10.1002/app.1993.070500720

[18] K. Dinakaran, S. Devaraju, M. Alagar (2013) *Thermoset nanocomposites Unsaturated Polyester Resin Clay Hybrid Nanocomposites*, Wiley-VCH.

[19] Kanimozhi, K., Prabunathan, P., Selvaraj, V., & Alagar, M. (2014). Vinyl silane-functionalized rice husk ash-reinforced unsaturated polyester nanocomposites. *RSC Advances*, *4*(35): 18157-18163. https://doi.org/10.1039/C4RA01125B

[20] Dinakaran, K., & Alagar, M. (2003). Development And Characterization Of Vinyl Ester Oligomer (Veo) Modified Unsaturated Polyester Intercrosslinked Matrices And Composites. *International Journal of Polymeric Materials and Polymeric Biomaterials*, 52(11-12): 957-966. https://doi.org/10.1080/714975880

[21] Anand Prabu, A., & Alagar, M. (2004). Mechanical and thermal studies of intercross-linked networks based on siliconized polyurethane-epoxy/unsaturated polyester coatings. *Progress in Organic Coatings*, 49(3): 236-243. https://doi.org/10.1016/j.porgcoat.2003.09.018

[22] Chozhan, C. K., Alagar, M., Sharmila, R. J., & Gnanasundaram, P. (2007). Thermo mechanical behaviour of unsaturated polyester toughened epoxy–clay hybrid nanocomposites. *Journal of Polymer Research*, 14(4): 319-328. https://doi.org/10.1007/s10965-007-9114-x

[23] Mandhakini, M., Devaraju, S., Venkatesan, M. R., & Alagar, M. (2012). Linseed vinyl ester fatty amide toughened unsaturated polyester-bismaleimide composites. *High Performance Polymers*, 24(3): 237-244. https://doi.org/10.1177/0954008311436263

[24] Mohammed, M. H., & Dauda, B. M. (2014). Unsaturated Polyester Resin Reinforced With Chemically Modified Natural Fibre.

[25] Sharmila, R. J., Premkumar, S., & Alagar, M. (2010). Preparation and Characterization of Organoclay-Filled, Vinyl Ester-Modified Unsaturated Polyester Nanocomposites. *High Performance Polymers*, *22*(1), 16-27. https://doi.org/10.1177/0954008308099491

[26] Kandemir, B., Karagöz, İ., & Sepetçioğlu, H. (2023). Experimental Investigation of Effects of the Nucleating Agent on Mechanical and Crystallization Behavior of Injection-Molded Isotactic Polypropylene. *El-Cezerî Journal of Science and Engineering,* 10(1):109-120. https://doi.org/10.31202/ecjse.1165527

[27] Baştürk, B. (2022). An Investigation on the Flexural and Thermo-mechanical Properties of CaCO3/Epoxy Composites [Articles]. *Celal Bayar University Journal of Science*, *18*(2), 161-167. https://doi.org/10.18466/cbayarfbe.1015351

[28] Mallick, P. K. (2000). Particulate and Short Fiber Reinforced Polymer Composites. In A. Kelly & C. Zweben (Eds.), Comprehensive Composite Materials (pp. 291-331). Pergamon. https://doi.org/10.1016/B0-08-042993-9/00085-1

[29] Croitoru, C., Spirchez, C., Cristea, D., Lunguleasa, A., Pop, M. A., Bedo, T., Roata, I. C., & Luca, M. A. (2018). Calcium carbonate and wood reinforced hybrid PVC composites. *Journal of Applied Polymer Science*, *135*(22), 46317. https://doi.org/10.1002/app.46317

[30] Orman Genel Müdürlüğü (2023). *Asli Ağaç Türleri* https://www.ogm.gov.tr/tr/e-kutuphane-sitesi/Yayinlar/Asli%20A%C4%9Fa%C3%A7%20T%C3%BCrleri.pdf

[31] Hornsby, P.R., Hinrichsen, E. and Tarverdi, K. (1997) Preparation and Properties of Polypropylene Composites Reinforced with Wheat and Flax Straw Fibres: Part II Analysis of Composite Microstructure and Mechanical Properties. *Journal of Materials Science,* 32: 1009-1015. https://doi.org/10.1023/A:1018578322498

[32] Panthapulakkal, S., Zereshkian, A., & Sain, M. (2006). Preparation and characterization of wheat straw fibers for reinforcing application in injection molded thermoplastic composites. *Bioresource Technology*, 97(2): 265-272. https://doi.org/10.1016/j.biortech.2005.02.043

[33] Kompozit Pazarı (2023), *Kalsit 5 Mikron Ürünü,* https://www.kompozitpazari.com/urun/kalsit-5-mikron

Copyright © IJCESEN

Comparison of the Radiation Absorption Properties of PbO doped ZrB₂ Glasses by using GATE-GEANT4 Monte Carlo Code and XCOM Programme

Arzu COŞKUN[1,2,3], Betül CETİN[4*], İbrahim YİĞİTOĞLU[5], Hüseyin TOPAKLI[6]

[1]Toros University, Vocational School of Health Services Department, 33100 Mersin-TURKEY
[2]Amasya University Institue of Science, 05100 Amasya –TURKEY
[3] Gaziosmanpaşa University Institue of Science, 60000 Tokat-TURKEY
Email:arzucos@hotmail.com - **ORCID**:0000-0003-4771-1558

[4]Amasya University Faculty of Arts and Sciences, 05100 Amasya -TURKEY
* **Corresponding Author Email**:betulcetin3205@gmail.com - **ORCID**:0000-0001-9129-2421

[5]Gaziosmanpaşa University Faculty of Arts and Sciences, 60000 Tokat-TURKEY
Email:ibrahim.yigitoglu@gop.edu.tr - **ORCID**:0000-0001-9029-1558-0987

[6]Tarsus University Faculty of Engineering, 33400 Mersin-TURKEY
Email:huseyin.topakli@tarsus.edu.tr - **ORCID**:0000-0001-6849-2636

Abstract:

The aim of this study is to investigate the gamma-ray radiation absorption properties of ZrB₂ (zirconium diboride), which is used in the nuclear industry, space industry, military industry, and especially in the ceramic industry, and determines the effect of PbO additive in the shielding. Also, the Geant4 Application Tomographic Emission (GATE-GEANT4) Monte Carlo computer code tested for its usability in place of the XCOM computer program with an appropriate geometry. Within this scope, the shielding properties of ZrB₂, Pb0 and 50%ZrB₂.50%Pb0 glasses at 511, 662, 1173, 1274 and 1332 keV gamma energies were calculated by the GATE-GEANT4 Monte Carlo code and compared with the XCOM computer program. The linear attenuation coefficient and half-value layer were calculated by using the mass attenuation coefficient values obtained with the codes. In line with these results, it is possible to say that 50%PbO additive increases the shielding quality of ZrB2 glasses. On the other hand, the simulated GATE-GEANT4 Monte Carlo code values were found to be compatible with XCOM..

1. Introduction

In recent years, with technological developments increasing, the use of radiation in many areas such as health, agriculture, and food is increased rapidly. Parallel to this increase, the negative effects of ionizing radiation on health are also increased. Because of the importance of shielding materials in radiation protection, studies on various shielding materials are important in the nuclear field [1]. The choice of gamma radiation protection material is a major component of radiation protection programs. To this end, it is intended to reduce the risk of exposure to ionizing radiation, particularly for workers exposed to radiation. To select the shielding material best suited to a particular source of ionizing radiation, it is necessary to know the basic principles of how gamma rays interact with matter. At the same

time, efforts to identify new shielding materials to replace Pb in terms of cost and ease of use, a heavy metal, have increased [1]. Manufacturing new materials and studying their radiation shielding properties is very expensive in terms of cost and effort. Moreover, studies on radiation are often limited due to economic and ethical rules. For this reason, theoretical methods and statistical approaches developed in today's scientific world play an important role. For this reason, theoretical calculations have come to the fore both in order to examine the shielding properties of more materials and to evaluate the shielding parameters. There are many codes software in which radiation absorption can be displayed by simulation and modelling. With the prepared codes, many types of ionizing radiation like X-rays, γ-rays, electrons, and neutrons can interact with the materials. Many scientific studies examine the radiation absorption properties of

different material mixtures [2, 3]. Boonin et al. [4], synthesized zinc barium telluride glasses and examined their mechanical and structural efficiency as well as their radiation absorption properties at γ-ray energies with Geant4 and WinXCOM software. Cheewasukhanont et al. [5], investigated the radiation shielding parameters of bismuth borosilicate-based glasses with XCOM at 220–662 keV energies and they observed that radiation protection parameters increased with increasing bismuth concentration. Ruengsri et al. [6], showed that the half-value layer (HVL) values of 662 keV of Gd_2O_3-based glasses with the compositions of $10CaF_2$: xGd_2O_3 :(90-x)P_2O_5 (x = 5, 10, 15, and 20 mole %) can be used in radiation shielding. The mass attenuation coefficients of bismuth borosilicate glasses were obtained by Gerward et al. [7, 8], with the WinXCom program and compared with experimental data. Inoue et al. [9], in their study with ZnO, found a high level of radiation shielding. In another study, the mass attenuation coefficients of lead oxides, bismuth, and barium of silicate glasses was investigated theoretically and experimentally at 662 keV photon energy [10, 11]. Kaewkhao et al. [12], investigated the shielding properties of borate glass containing Bi_2O_3 and BaO at 662 keV and compared it with PbO in the same glass structure. Yasaka et al.[13], investigated the radiation shielding properties and optical properties of zinc bismuth borate (ZBB) glasses. ZBB glass compositions were prepared with the melt quenching technique. Matori et al. [14],and Singh et al. [15], used PbO-based glasses as gamma-ray and X-ray shielding materials and found that they had high absorption properties. Bagheri et al. [16], by using the MCNP code and the XCOM program, investigated the radiation attenuation parameters of barium bismuth borosilicate glasses for gamma-ray energies of 662, 1173, and 1332 keV. In the literature, there are many experimental studies comparing the results obtained in different fields with XCOM data. However, there are limited studies investigating the properties of shielding materials using Geant4-based GATE/GEANT4 simulation. GATE/GEANT4 simulation is a free software program that performs Monte Carlo calculations for use in fields such as radiotherapy, nuclear physics, and radiology. Today, the GATE/GEANT4 simulation has a wide range of uses, from the construction of new medical devices to the development of quality control protocols and medical imaging systems [17, 18]. The XCOM program, on the other hand, calculates the total attenuation coefficient, total attenuation cross-section, and partial cross-section data for various elements, mixtures, and compounds in the photon energy range from 1keV- 100GeV using online

software [8,19]. Physical forms such as photoelectric impact, Compton effect, and pair generation are portrayed in hypothetical calculations. The National Standards Institute (NIST), XCOM database includes radiation attenuation coefficient data of commonly used shielding materials. Zirconium diboride (ZrB_2) is an ultra-high temperature ceramic with a very high melting temperature (3245˚C) and a low coefficient of thermal expansion. In addition, it is preferred in the aviation industry and space studies with its high strength, high rigidity, high chemical stability, high thermal shock resistance, low electrical resistance, high voltage capacity, high thermal conductivity, anti-corrosion property and high neutron absorption capacity [20-22]. For these reasons, studies with ZrB_2 have started to increase in recent years [23-29].

This study shows the radiation shielding properties of ZrB_2, which is a candidate for use in shielding applications and nuclear reactors as a stopper [20]. The study examined and determined alterations in shielding properties through the introduction of a 50% PbO doping. The mass attenuation coefficients (μ_m), linear attenuation coefficients (LAC), and half value layer (HVL) values were calculated using the GATE/GEANT4 Monte Carlo code and XCOM program.

2. Material and Methods

GATE/GEANT4 simulation program is a software in which experimental setup is prepared by making code software in C^{++} language. First, the element definition of the material to be used as shielding material is made. After the definition is made, the density value and component ratios are entered by creating a compound. When it is desired to create a mixture from different compounds, the density of the compound and the mixing ratios of the components are normalized to one. In the prepared setup, the energy values for the spot welding are manually entered separately and the beam is sent [30]. In the setup prepared to diminish the number of incoming photons, shielding material is put between the source and the detector as given in Fig. 1. In this way, the mass attenuation coefficient of the shielding material is calculated with the prepared setup. In XCOM and GATE/GEANT4 programs, the amount of material can be normalized to 1 and a mixture can be created. Therefore, the relative weights of each compound are given. PbO is the most important material used as a shielding material, and many contributions have been made in the literature to look at the change in absorption properties. The calculations were made by entering the energy values 511, 662, 1173, 1274, and 1332 keV used in the programs. In order to understand the absorption of photons by the matter,
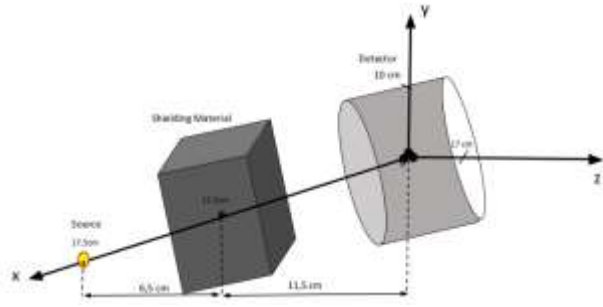
Figure 1. GATE/GEANT4 Experimental setup.

the materials are examined by considering the mass attenuation, linear attenuation, and half-value thickness values. The LAC is a constant for each absorber material. The LAC looks at the reduction in the number of photons per unit distance from the radiation beam passing through the tissue. LAC value increases as the physical density and atomic number of the matter increase.

Theoretical calculations are calculated with the following formulas;

$$\mu_m = (\mu/\rho) \left(cm^2/g \right) \qquad (1)$$

The mass absorption coefficient (μ/ρ) is independent of chemical and physical states and is a function of wavelength and atomic number.

The amount of photon absorbed by a sample is directly related to the volume of the sample that the photon passes through and the concentration of the sample. This law is the Beer-Lambert law has known and gives the absorption value of the photon [31,32].

$$I = I_0 (e^{-\Gamma x})(e^{-\sigma x})(e^{-\kappa x}) = I_0 e^{-\mu x} \qquad (2)$$

In this equation; I is the photon intensity, I_0 is the initial photon intensity, Γ is the photoelectric effect coefficient, σ is the Compton scattering coefficient, κ is the pair production coefficient, and μ is the LAC. The following relations are given for the values of HVL. HVL is the thickness of an absorbent which diminishes the radiation to half its intensity [33]. HVL is determined using the following formulas;

$$HVL = (In2/\mu) \qquad (3)$$

3. Results and Discussions

In this study, XCOM software and GATE/GEANT4 simulation program were used together to contribute to the literature, to develop alternative radiation absorbers, and to test the usability of the GATE/GEANT4 Monte Carlo code for radiation absorption. The LAC and the HVL of the ZrB_2, PbO, and PbO-doped ZrB_2 samples have been calculated.

Obtained values are given comparatively. In addition, the LAC (μ) was evaluated using the XCOM program to confirm the GATE/GEANT4 Monte Carlo code (Table 1 and Fig. 2-a and Figure 2-b). The difference percent (Diff. %) between the two simulations was calculated using Eq. (4) and shown in Table 1 [34].

$$\text{Diff } (\%) = \frac{\mu_{xcom} - \mu_{gate}}{\mu_{xcom}} \times 100\% \qquad (4)$$

Table I: Calculated values for LAC

ZrB$_2$			
Energy (keV)	**XCOM**	**GATE**	**%Diff.**
511	0.514	0.517	-0.446
662	0.443	0.446	-0.755
1173	0.325	0.328	-0.802
1274	0.311	0.314	-0.763
1332	0.304	0.307	-0.710
PbO			
Energy (keV)	**XCOM**	**GATE**	**%Diff.**
511	1.441	1.440	0.044
662	1.027	1.030	-0.268
1173	0.587	0.591	-0.718
1274	0.551	0.555	-0.695
1332	0.534	0.538	-0.642
50%ZrB$_2$.50%PbO			
Energy (keV)	**XCOM**	**GATE**	**%Diff.**
511	0.920	0.921	-0.132
662	0.704	0.708	-0.476
1173	0.449	0.452	-0.766
1274	0.425	0.428	-0.727
1332	0.414	0.417	-0.674

The Diff. % values varied from 0.044% to -0.802% for all energy values, respectively. These values indicate that the simulated GATE/GEANT4 values agree with the computed XCOM values. Figure 2-a and Figure 2-b appears that the XCOM (a) and GATE/GEANT4 (b) values for LAC as a function of the photon energy graph for ZrB_2, PbO, and 50%ZrB_2.50%PbO. It is seen that the addition of PbO provides more than 55% increase in the LAC values of ZrB2. The calculated LAC values using the XCOM at the incident energy range (0.001 MeV to 10^5 MeV) are shown in Fig.3(a,b,c). In the energy values calculated within the study, the attenuation coefficient of uptake appears to diminish as the energy increases. The simulated GATE/GEANT4 values are in agreement with the XCOM and this shows the accuracy of the simulated values. The calculated HVL values using GATE/GEANT4 and XCOM are shown in Fig. 4-a,b,c.
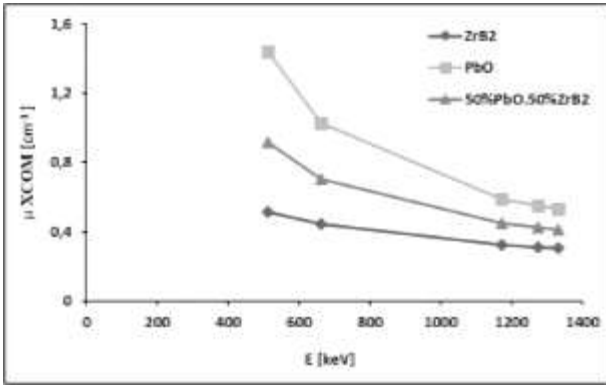
(a)
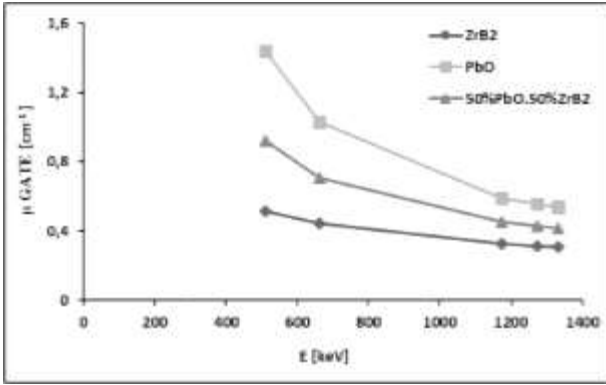
(b)

Figure 2. *Calculated XCOM (a) and GATE/GEANT4(b) values for LAC as a function of the photon energy graph for ZrB₂, PbO, and 50%ZrB₂.50%PbO.*

(a)

(b)
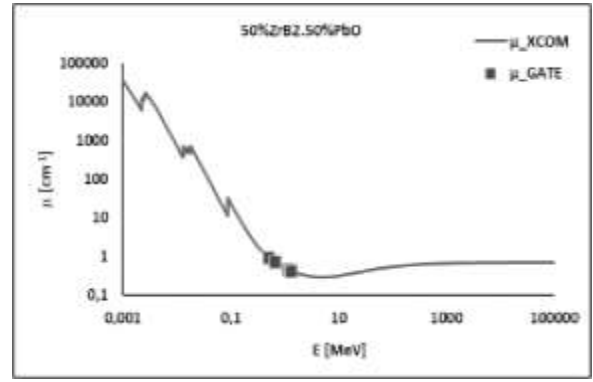
(c)

Figure 3. *XCOM and GATE/GEANT4 values for LAC as a function of photon energy (0.001 MeV to 10^5 MeV) for ZrB₂ (a), PbO(b) and 50%ZrB₂.50%PbO (c).*
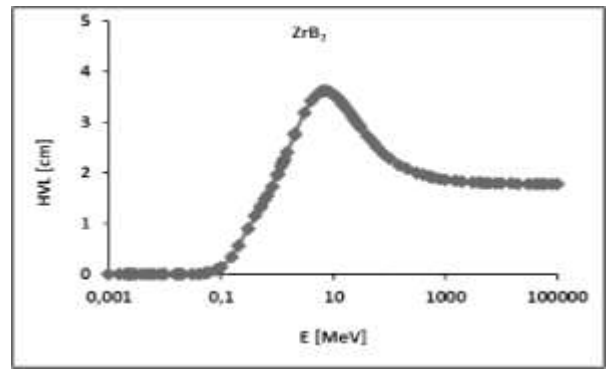
(a)
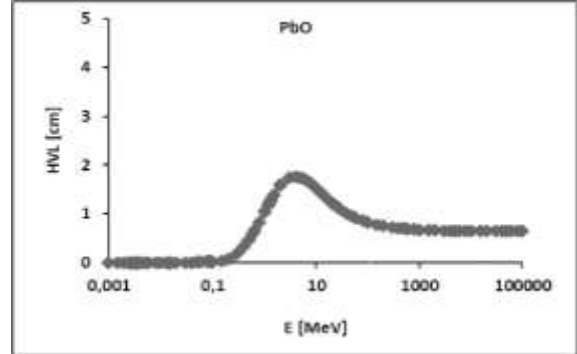
(b)
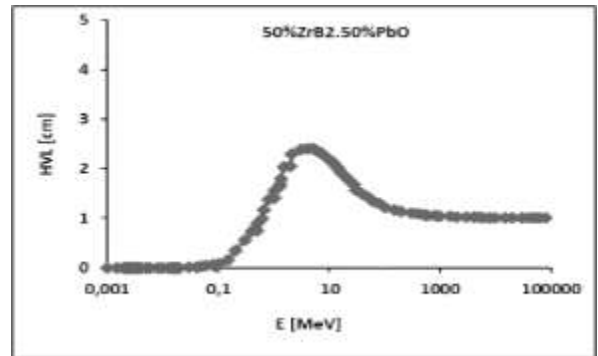
(c)

Figure 4. *HVL as a function of photon energy (0.001 MeV to 10^5 MeV) for ZrB₂(a), PbO (b) and 50%ZrB₂. 50%PbO (c).*

Figure 4 clearly appears that the concentration of PbO included to ZrB_2 causes an diminish in HVL values of 50%ZrB2.50%PbO.

4. Conclusions

The purpose of this study is to study the absorption properties of ZrB_2 gamma rays, which has just begun to be used in many areas, particularly in the ceramic industry.

In XCOM and GATE/GEANT4, LAC and HVL and values, which are radiation absorption coefficients, were calculated by defining the density values and chemical formulas separately for the mixture and single chemicals.

The data from the GATE/GEANT4 simulation were observed to be consistent with the XCOM data in the appropriate geometry, and moreover determined to added by the 50%PbO provides more than 55% increase in the LAC values of ZrB_2.

Author Statements:

- **Ethical approval:** The conducted research is not related to either human or animal use.
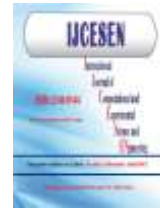- **Conflict of interest:** The authors declare that they have no known competing financial interests or personal relationships that could have appeared to influence the work reported in this paper
- **Acknowledgement:** The authors declare that they have nobody or no-company to acknowledge.
- **Author contributions:** The authors declare that they have equal right on this paper.
- **Funding information:** The authors declare that there is no funding to be acknowledged.
- **Data availability statement:** The data that support the findings of this study are available on request from the corresponding author. The data are not publicly available due to privacy or ethical restrictions.

References

[1] A. Coşkun, B. Cetin, (2023). The Effect of Lead Oxide on the Change in Gamma Ray Protection Parameters of Bismuth Oxide. *European Journal of Science andTechnology* 47;18-21.

[2] D. Dodoo-Amoo, N. Landsberger, S.,J. M. MacDonald, &, J. M. Castro., (2003) Development of composite materials for non-leaded gloves for use in radiological hand protection. *Health physics*, 84(6); 737-746. https://doi.org/10.1097/00004032-200306000-00006.

[3] F. Demir, (2009). Determination of radiation absorbance for neutron particles, x and ɣ rays of heavy concrete with boron and barite aggregates. *Ataturk University Graduate School of Natural and Applied Sciences* Ph. D. Thesis.

[4] K. Boonin, P.Yasaka, P Limkitjaroenporn, R.Rajaramakrishna, A Askin, MI, Sayyed, ...&J.Kaewkhao, (2020). Effect of BaO on lead-free zinc barium telluride glass for radiation shielding materials in nuclear application. *Journal of Crystalline Solids*, 550;120386. https://doi.org/10.1016/j.jnoncrysol.2020.120386

[5] W. Cheewasukhanont, P. Limkitjaroenporn, S. Kothan, C. Kedkaew&, J. Kaewkhao, (2020). Effect of particle size on radiation shielding properties for bismuth borosilicate glass. *Radiation Physics and Chemistry*, 172;108791. https://doi.org/10.1016/j.radphyschem. 2020.108791

[6] S. Ruengsri, J. Kaewkhao, P Limkitjaroenporm, P. Meejitpaisan, P. Hongtong, W.&W. Cheewasukhanont, (2017). Development of gadolinium calcium phosphate oxyfluoride glass for radiation shielding materials. *Integrated Ferroelectrics*, 177(1);48-58. https://doi.org/ 10.1080/10584587.2017.1285172

[7] L. Gerward, N. Guilbert, K. B. Jensen, H. Levring, (2001). X-ray absorption in the matter. Reengineering XCOM. *Radiation Physics and Chemistry* 60;23–24. https://doi.org/10.1016/S0969-806X(00)00324-8

[8] L. Gerward, N.Guilbert, K.B. Jensen,H. Levring, (2004). WinXCom—a program for calculation X-ray attenuation coefficients. *Radiation Physics and Chemistry* 71;653–654. https://doi.org/10.1016/ j.radphyschem.2004.04.040

[9] T. Inoue, T. Honma, V. Dimitrov&T. Komatsu, (2010). Approach to thermal properties and electronic polarizability from average single bond strength in ZnO, Bi_2O_3, and B_2O_3 glasses. *Journal of solid state chemistry*, 183(12);3078-3085. https://doi.org/10.1016/ j.jssc.2010.10.027

[10] K. Kirdsiri, J. Kaewkhao, N. Chanthima&P. Limsuwan, (2011). Comparative study of silicate glasses containing Bi_2O_3, PbO, and BaO: Radiation shielding and optical properties. *Annals of Nuclear energy*, 38(6);1438-1441 https://doi.org/10.1016/j.anucene.2011.01. 031

[11] N. Chanthima, J. Kaewkhao&PLimsuwan,(2011). Study of photon interactions and shielding properties of silicate glasses containing Bi_2O_3, BaO, and PbO in the energy region of 1 keV to 100 GeV. *Annals of Nuclear energy*, 41; 119-124.https://doi.org/10.1016/j.anucene. 2011.10.021

[12] J. Kaewkhao, A. Pokaipisit, &P. Limsuwan, (2010). Study on borate glass system containing with Bi_2O_3 and BaO for gamma-rays shielding materials: comparison with PbO. *Journal of Nuclear Materials*, 399(1);38-40. https://doi.org/10.1016/j.jnucmat.2009.12.020

[13] P. Yasaka, N. Pattanaboonmee, H. J. Kim, P. Limkitjaroenporn&J. Kaewkhao, (2014). Gamma radiation shielding and optical properties measurements of zinc bismuth borate glasses. *Annals*

of Nuclear energy, 68;4-9. https://doi.org/10.1016/j.anucene.2013. 12.015

[14] K.A. Matori, M.I. Sayyed, H.A.A.Sidek, M.H.M. Zaid, V.P. Singh, (2017). A comprehensive study on physical, elastic, and shielding properties of lead zinc phosphate glasses, *J.Non-Cryst. Solids* 457;97-103. https://doi.org/10.1016/j.jnoncrysol.2016.11.029

[15] N. Singh, K. J. Singh, K. Singh, H. Singh, (2004). Comparative study of lead borate and bismuth lead borate glass systems as gamma-radiation shielding materials, *Nucl. Instrum. Methods Phys. Res. B* 225; 305–309. https://doi.org/10.1016/j.nimb.2004.05.016

[16] R. Bagheri, A.K. Maghaddam and H.Yousefnia, (2017). Gamma-ray shielding study of Barium-Bismuth-Borosilicate glasses as transparent shielding materials using MCNP-4C code, XCom program, and available experimental data. *Nuclear Engineering and Technology*, 49;216-223. https://doi.org/10.1016/j.net. 2016.08.013

[17] A.S. Abouhaswa, U. Perişanoğlu, H.O.Tekin, E. Kavaz, AMA. Henaish, (2020). Nuclear shielding properties of B_2O_3–Pb_3O_4–ZnO glasses: Multiple impacts of Er_2O_3 additive. *Ceram Int* 46:27849–59. https://doi.org/10.1016/j.ceramint.2020.07.283.

[18] SA. Feller, WJ. Dell, PJ. Bray,(1982). 10B NMR studies of lithium borate glasses. *J Non-Cryst Solids* 51:21–30. https://doi.org/10.1016/0022-3093(82) 90186-7.

[19] M.J. Berger, J.H. Hubbell, S.M. Seltzer, J. Chang, J.S. Coursey, R. Sukumar, D.S. Zucker, K. Olsen, (2010). XCOM: Photon Cross Sections Database, NIST Standard Reference Database 8. XGAM. https://physics.nist.gov/cgi-bin/Xcom/xcom2 (accessed:20. July.2022).

[20] Ö. Balcı, N. Akçamlı, D.Ağaoğulları, M. L.Öveçoğlu&İ.Duman, (2017). Autoclave processing and sintering of ZrB_2-ZrO_2 powders and investigation of microstructural and some mechanical properties of bulk products. *Journal of Boron*, 2(1);1-10.

[21] W. G. Fahrenholtz&G. E. Hilmas, (2012). Oxidation of ultra-high temperature transition metal diboride ceramics. *International Materials Reviews*, 57(1); 61-72. https://doi.org/10.1179/1743280411Y. 0000000012

[22] Adam L. Chamberlain, W. G. Fahrenholtz, G. E. Hilmas, D. T. Ellerby, (2004) High-strength zirconium diboride-based ceramics, *Journal of the American Ceramic Society* 87(6); 1170 – 1172. https://doi.org/ 10.1111/j.1551-2916.2004.01170.x

[23] Y. Pan&S. Chen, (2022). Influence of alloy ingelements on the mechanical and thermodynamic properties of ZrB_2 boride. *Vacuum*, 198; 110898. https://doi.org/10.1016/j.vacuum.2022.110898

[24] H. Li, He, Y.,P. Luo,S. Xue,Z.Li, X.Cheng, ... &Y. Fan, (2022). Synthesis of ZrB_2 strengthened NiW composite coating and study of its mechanical characters and anti-corrosion performance. *Surface and Coatings Technology*, 441; 128553. https://doi.org/10.1016/ j.surfcoat.2022.128553

[25] S. Torabi, Z.Valefi&N. Ehsani, (2022). The effect of the SiC content on the high duration erosion behavior of SiC/ZrB_2–SiC/ZrB_2 functionally gradient coating produced by shielding shrouded plasma spray

method. *Ceramics International*, 48(2); 1699-1714. https://doi.org/10.1016/j.ceramint. 2021.09.249

[26] P. Morampudi, V. Ramana, C. Prasad&K. Sriram Vikas,(2022). Physical, mechanical and corrosion properties of Al6061/ZrB_2 metal matrix nanocomposites via powder metallurgy process. *Materials Today: Proceedings*. https://doi.org/10.1016/j.matpr.2022.03. 596

[27] Y. Xu, S. Huang, D.Han, M. Dai, X.Zhong,Y. Niu,.,&X. Zheng, (2022). Effect of different SiC/$TaSi_2$ contents on ablation behavior of ZrB_2coating. *Corrosion Science*, 205;110424. https://doi.org/10.1016/j.corsci. 2022.110424

[28] M. Patel, J. Reddy&V.B. Prasad,(2021). High thermal conductivity aluminium nitride–zirconium diboride (AlN-ZrB_2) composite as microwave absorbing material. *Ceramics International*, 47(15); 21882-21889. https://doi.org/10.1016/j.ceramint.2021.04.206

[29] M. Zhang, Z.M. Li, Z.Yan, L. Zhang, J. Yin, X. Ma, ... &L. Deng, (2022). Multifunctional Ag-ZrB_2 composite film with low infrared emissivity, low visible light reflectance and hydrophobicity. *Applied Surface Science*, 604;154626. https://doi.org/10.1016/j.apsusc. 2022.154626

[30] http://www.opengatecollaboration.org/(accessed 26 November 2022).

[31] I. SAM, H. O. Tekin, (2019). The multiple characterizations of gamma, neutron, and proton shielding performances of xPbO-(99-x)B_2O_3–Sm_2O_3 glass system. *Ceramic International*, 45: 23561–71. https://doi.org/10.1016/j.ceramint.2019.08.065.

[32] A. M. El-Khayatt, HA. Saudy, (2019). Preparation and characterization of zinc, lanthanum white sand glass for use in nuclear applications. *Radiation Physics and Chemistry*, 166:108497, https://doi.org/10.1016/j. radphyschem.2019.108497

[33] B. Mavi, (2012). Experimental investigation of γ-ray attenuation coefficients for granites. *Annals of Nuclear Energy*, 44;22-25, https://doi.org/10.1016/ j.anucene.2012.01.009

[34] S.I. Mohammed, A.H. Taqi, & A.M. Ghalib, (2021). Simulation of the Gamma Attenuation through Borate Glass Using Genat4. *Rafidain Journal of Science*, 30(2); https://doi.org/11-22.10.33899/ rjs.2021. 168339

Research Article

Qualitative Research on the Radiation Knowledge Levels of Non-Doctor Healthcare Workers and Developing Qualitative Scale

Mucize SARIHAN*

Istanbul Okan University Vocational School Health Services, Istanbul Turkey
* **Corresponding Author** : **Email:**mucizesarihan1997@hotmail.com - **ORCID:** 0000-0001-8013-7370

Abstract:

Radiation is used in a wide variety of fields, especially in the health sector. The human cell must be protected from unwanted radiation doses due to its dangerous effect. Employees' knowledge of radiation is important and therefore this level of knowledge must be known. In this study, a semi-structured qualitative questionnaire was used to determine the perception and knowledge levels of healthcare professionals (nurses, technicians) who do not use dosimeters about ionizing and non-ionizing radiation, and to reveal their experience and opinions on the subject.

In-depth interviews were made. Qualitative data coding, content analysis (calculation and mapping of relationships between code frequencies, themes and categories) were performed in the MAXQDA 2020 package program with the data obtained after the interview. 20 healthcare personnel participated in the study. From the data obtained, 10 main themes related to the subject were determined. Main themes emerging; "Harms of radiation", "type and properties of radiation", "all imaging devices emit radiation", "principles of radiation protection", "non-ionizing radiation", "infrared rays", "diagnosis and treatment", "radiation doses Radiation emission," Radiation pollution and ionizing radiation "Sub-codes of all these main themes were determined, schemes were created and coded participant views were shown in a cross-table form, semi-structured questions and a qualitative scale were developed.

1. Introduction

People in society are constantly exposed to natural radiation which has existed since the creation of universe. It is important to determine the radiation level in medical applications and thus radiation protection is an important issue for patients, individuals in the community and healthcare professionals. In recent years, many studies have been conducted to determine the radiation level in medical applications and to provide protection ways [1]. Hospitals; they are complex institutions that provide examination, diagnosis, treatment and rehabilitation services and form the basis of the healthcare system [2]. Radiation protection is an important consideration for the safe use of ionising radiations in health-care [3]. Healthcare personnel are faced with many risks during the delivery of health services, and accordingly, hospitals are in the very dangerous group within the scope of Occupational Health and Safety [4]. One of these risks is ionizing radiation exposure.

Radiation is defined as the energy that travels in the environment, and its effect on the human body changes depending on the radiation types [5]. While ionizing radiation has high energy and can ionize an electron from atom, non-ionizing ones does have enough energy to ionize any electron from atom. The non-ionizing radiation having low energy, is emitted by devices such as mobile phones, televisions, satellites, radios, power lines, photocopy machines, microwave ovens. Ionizing radiation, on the other hand, has high energy and the substance it hits can form ions (charged particles) and is more dangerous [6]. The ionizing radiation has four main types namely alpha, beta, gamma, and x-ray [7]. The ionizing radiation is used many different field such as in medicine, industry, agriculture and research is common [8]. As Low As Reasonably Achievable (ALARA) principle is one of the fundamental principles of radiation protection and it states that

ionizing radiations doses should be kept in desirebale limit [9]. Safety issues encountered in the early days of the development of X-rays for medical usage were the main point of the requirement [10]. Radioactivity was first used in the field of medicine in 1896 for diagnosis and treatment, and barium contrast was started to be used in the 1920s [11]. Hastanelerde verilen hizmetin gereği olarak tanı ve tedavi hizmetlerinde iyonlaştırıcı radyasyona neden olan; Ağırlıklı olarak x-ışınları ve radyoaktif malzemeler içeren tıbbi cihazlar kullanılmaktadır [6,12-20].

In the study, it was aimed to determine the knowledge level of non-physician healthcare professionals about ionizing radiation and non-ionizing radiation, who do not have to wear a dosimeter, and it was aimed to develop a qualitative scale for this.

2. Material and Methods

In this study, a qualitative research was conducted and a qualitative scale was developed to evaluate the views, radiation awareness and knowledge level of healthcare professionals on ionizing radiation, non-ionizing radiation, radiation protection and administrative measures. Criterion sampling, one of the sampling methods, was used to determine the participants. Criterion sampling, also known as criterion-based sampling, is selected from individuals representing individuals who have experience with the investigated case. In line with this information and by determining the following criteria within the scope of the research, the participants were determined:

- To be graduated from a health-related department (health vocational high school, associate degree, undergraduate)
- Working in a health-related public or private hospital,
- Being a non-physician health worker,
- Working in the field of health for at least 5 years

Charmaz, when the themes of the data collection process are saturated.
It emphasizes that it should be terminated. When new perspectives on the collection of new data or new features do not emerge, it is recommended that the negotiations be terminated. In the light of this view, it was observed that the data started to repeat from the 20th participant and the data collection process ended with the 20th participant.89
In-depth interview technique was used in the research. In order not to miss important details during the meeting, a tape recorder was used with the

permission of the participants. In addition, the following information was given to the participants:

* The information shared in the interview will be kept confidential and will only be used for research,
* Your real name will be kept,
* The interview will take at least half an hour,

Semi-structured in-depth interview form was used in the study (Appendix 1). Interview questions were reviewed during the pilot implementation process of the study. Interviews were held with 5 participants for the pilot application. After this meeting, some changes were made to the questions. With the data obtained after the interview, qualitative data coding, content analysis (calculation and mapping of the relationships between code frequencies, themes and categories) were carried out with the MAXQDA 2020 package program.
For this purpose, a 10-item semi-structured questionnaire was prepared by the researcher. Face-to-face interview technique was used with healthcare professionals within the framework of these questions.
In the context of the content of the findings; Due to the Covit 19 outbreak, the data were recorded with interviews made in a comfortable environment outside the hospital. The scope of the study consists of 20 healthcare professionals working in Public and Private hospitals and different clinics.
 The reason why qualitative research method is preferred is that it is a technique used to systematically examine the meanings arising from the experience and behavior of the sample group in a realistic and holistic manner [21]. Another feature of qualitative research is that it is exploratory. With this feature, one of the useful and beneficial aspects of the research is that it illuminates and reveals less studied subjects [22,23].

3. Results and Discussions

In order to obtain qualitative data, the following questions were asked, answers and codes were created, and then the main themes were determined. Views of 20 healthcare professionals working in different clinics in public and private hospitals were included.

3.1. Demographic Distribution

 The demographic characteristics and relationships of healthcare professionals with themes are shown in the cross-table 1.

Table 1. *Demographic Characteristics, Themes and Crosstab*

Themes I	Famele	Male	Nurse	Tecnician	+20 Years	5-10 Years	10-20 Years	Private Hospital	Public Hospital	Total
Damages of Radiation	12,3%	27,5%	13,4%	25,4%	9,0%	28,8%	15,0%	13,2%	18,1%	17,0%
Type and Features of Main Theme Rad.	5,2%	7,2%	6,4%	4,5%	5,1%	6,1%	6,3%	11,3%	4,1%	5,8%
All Imaging Devices Emit Radiation	7,7%	7,2%	7,6%	7,5%	7,7%	6,1%	8,8%	5,7%	8,2%	7,6%
Radiation Protection Principles	15,5%	8,7%	15,3%	9,0%	20,5%	9,1%	10,0%	11,3%	14,0%	13,4%
Non-Ionizing Radiation and Effects	5,2%	5,8%	4,5%	7,5%	3,8%	7,6%	5,0%	5,7%	5,3%	5,4%
Infrared Rays	7,7%	5,8%	7,6%	6,0%	5,1%	7,6%	8,8%	5,7%	7,6%	7,1%
Diagnosis and Treatment	14,2%	13,0%	14,6%	11,9%	17,9%	10,6%	12,5%	15,1%	13,5%	13,8%
Radiations Doses Applied to the Patient	7,1%	4,3%	7,6%	3,0%	9,0%	4,5%	5,0%	7,5%	5,8%	6,3%
Radiations Emission from Patient & Heall	8,4%	7,2%	7,0%	10,4%	6,4%	7,6%	10,0%	9,4%	7,6%	8,0%
Radiation Contamination and Ionizion.	16,8%	13,0%	15,9%	14,9%	15,4%	12,1%	18,8%	15,1%	15,8%	15,6%
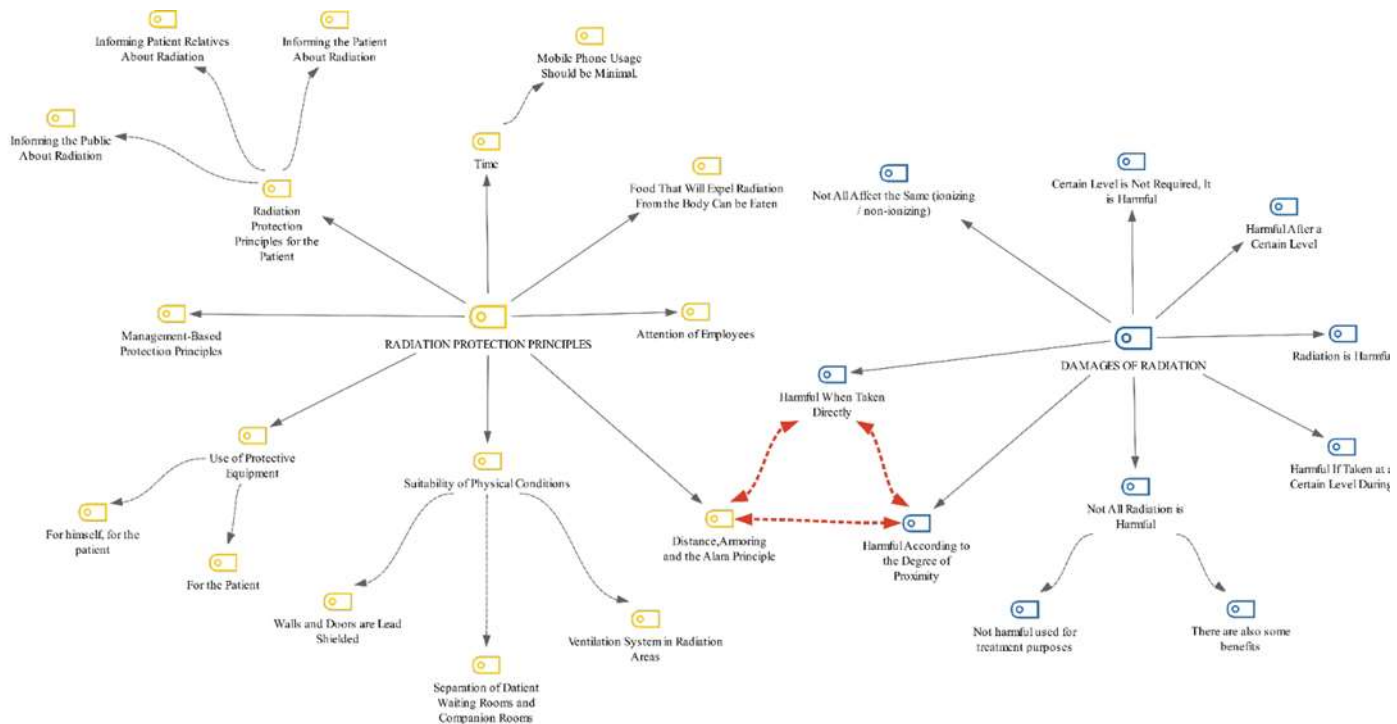
Figure 1. *Radiation Protection Principles and the Damages of Radiation and Related Themes*
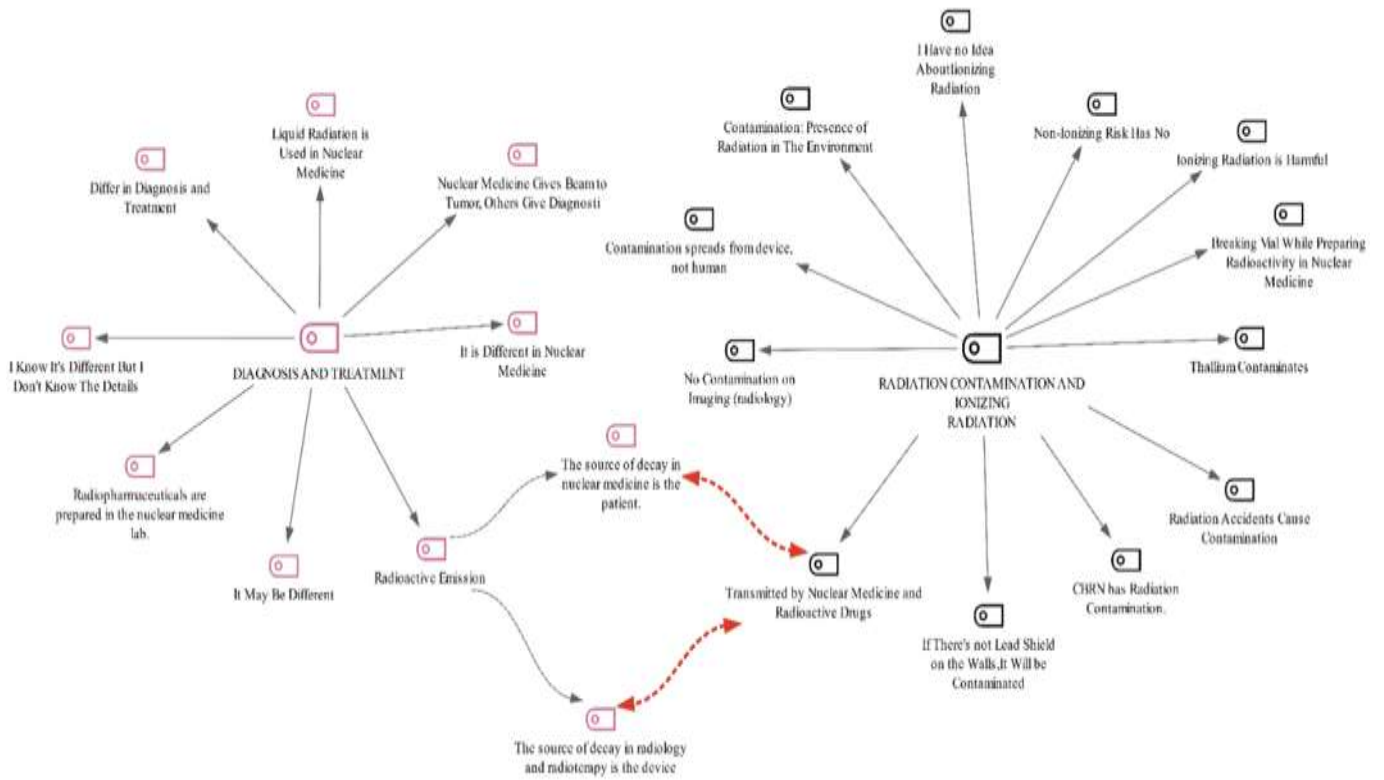
Figure 2. *Codes Related to the Theme of Diagnosis and Treatment with Ionizing Radiation*
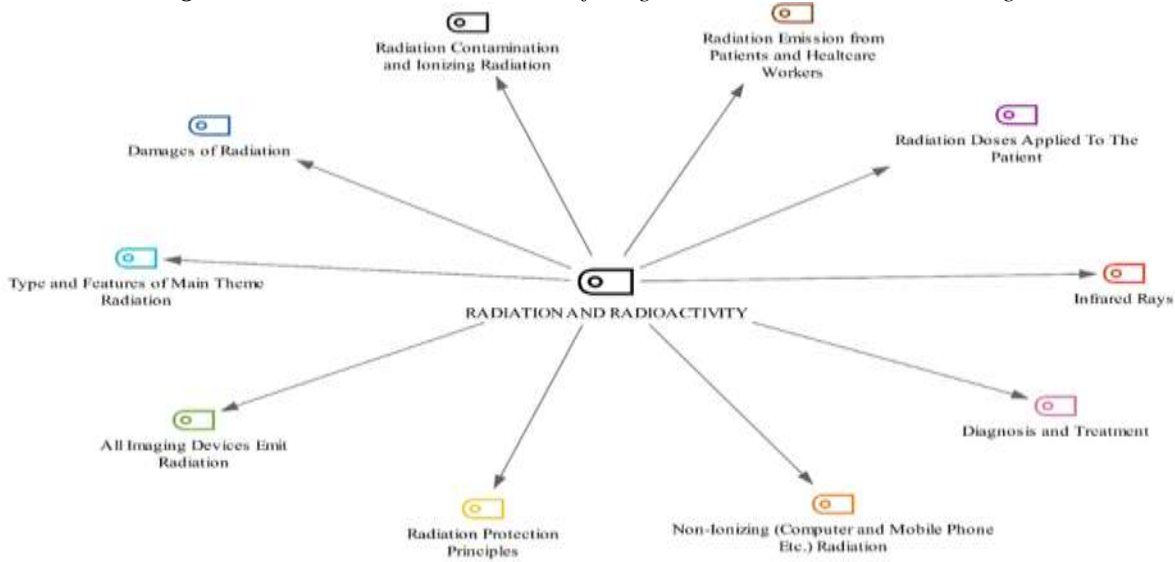
Figure 3. *Radiation, Radioactivity and Themes*

3. 2. Themes

Healthcare professionals involved in the study focused on 10 main themes related to radiation and radioactivity. As a result of the data obtained, the most emphasized subject was the principles of radiation protection, harmful effects of radiation,

radioactive contamination, diagnosis and treatment themes. These themes and their relationships are in figure 1 and figure 2. The main codes within the framework of radiation and radioactivity concepts:

1. Damages of radiation
2. Radiation protection principles

3.Radiation pollution and ionizing radiation
4. Diagnosis and treatment
5.Non-ionizing radiation
6.Radioactive spread in patients and workers
7.Type and properties of radiation
8.Infrared rays
9.Imaging devices emit radiation
10. Radiation doses administered to the patient

3.3. Sub-Codes Regarding the Themes of Radiation Protection and the Harmfulness of Radiation (two theme relations)

In the research, codes were created with the expressions of the participants. (C1, C2 etc.) 1. Theme Regarding the theme of the harms of radiation, "What do you think about the harms of radiation?" and "Is any kind of radiation harmful?" 2nd theme "What are the principles of radiation protection?" Sub-codes resulting from the answers given to the question. It is given in Figure 3. In addition, the indirect relations of the two themes are also specified.

3.4. Sub Codes Related to Diagnosis and Treatment Contact with Ionizing Radiation Pollution

What can you say about radiation and radiation sources (Radiology, Nuclear Medicine and Radiotherapy) used in diagnosis and treatment? 8 codes were determined from the answers given to the question. What can you say about Ionizing Radiation and Radiation Pollution? 12 subcodes were determined from the answers given to the question. The Relationship of Two Themes is in figure 3

3.5. Sub Codes for the Non-ionizing Radiation and Its Effects Theme

What would you say about the radiation emitted from computers and cell phones? What are the damages?With the data obtained from the interviews, the perceptions of non-ionizing radiation (mobile phone, computer, etc.) of healthcare professionals were evaluated. From the data obtained, 8 subcodes for non-ionizing radiation were determined. The sub codes of the radiation theme are as follows.
- I think this is harmful and affects Teens
- Duration of Exposure Matters
- Harmful
- I Don't Know What Ionizing Radiation Is
- Does Not Seriously Damage But Stochastically Affects
- Ionizer But I'm Not Sure

- Not ionizer

3.6. Sub-Codes Related to the Contact of Radiation Doses Applied to the Patient

Two subthemes were determined according to the theme of radiation doses applied to the patient. Three sub-codes of the sub-theme "Doses administered to the patient are different" were determined. Two sub-codes of the theme "Doses administered to the patient are not different" were determined.
What can you say about the radiation doses applied to patients in imaging clinics? Are different doses used? The answers and opinions of healthcare professionals to the question are given below.
 1. Doses Administered to Patients are not Different
- Doses are The Same in Magnetic Resonance Imaging
- The Doses are the Same in Tomograpy

2. Different

2a. It Different According to the Patient
- The Doses Administered for Diagnoctic Purposes are Different
- Treatment Doses are Different
- Diffrent According to the Weight of the Patient
2b. Varies According to the Disease
2c. Radiation Dose is Different in All Units
- Doses are Different for Radioactive Drugs (radiopharmaceticals)
- Radiation Dose is Different According to the Discase
- It Differs According to the Size of the Mass in the Patient

3.7. Radiation Emission, Radiation Type and Properties, Infrared Rays, Imaging Devices

Themes and Radiation Emission and Sub-Codes are given in Table 2.

4. Conclusions

In the study, it was determined that the risk perception of ionizing and non-ionizing radiation and the knowledge level of the healthcare professionals participating at a moderate level. While the perception of radiation risk varies according to the unit of study, the level of knowledge varies according to the professional title. In the interviews, it was determined that there was false information as well as correct information about the hazards of radiation, in short, information

Table 2. Themes and Radiation Emission and Sub-Codes

RADIATION EMISSION		
Does radiation spread from patient to employee, patient to patient, employee to employee? What can you say about this topic? The 3 sub-codes and indirect codes obtained according to the answers given to the question are as follows.		
1. İonizing Radiation is not Emitted a. Does not Spread From Employee to Employee. b. İonizing Radiation is not Emitted From Patient to Employee	2. In Nuclear Medicine, It Can Spread From Patients to Employees	3. Radiation is Emitted a. Spreads from Oncology Patients Treated With Iyot 131 to Others b. Non-ionizing Radiation is Emitted c. Radiation is Emitted from Patient to Employee

TYPE AND FEATURES OF MAHIN THEME RADIATION			
What would you say about the type and properties of radiation used in healthcare? The theme, direct and indirect codes created according to the answers to the question are given below.			
1.Radiation of the Same Type But Quantity Matters.	2.Different Types and Properties of Radiation. a. The Radiation Types is Different but the Effect is the Same. b. The Radiation Propeties Used in Diagnosis and Treatment are Different. c. Different but not Sure	3.Radiation-Related Specialties Different.	4. The type of radiation is different. a. Its effect is also different. b. The time of exposure to radiation is important

INFRARED RAY THEME AND SUB-CODES					
Six sub-codes were determined from the views and data obtained about infrared rays and their damages. What can you say about infrared rays and their harm? The codes obtained from the answers of the questions are given below.					
Less Harmful	Too Much is Harmful	It is Harmful	It Will be Harmful in the Future	I Don't Have Full Information a. I don't Have Full Information b. I don't Have Full Information But It can be Harmful	I Don't Have Full Information But It can be Harmful

SUBCODES ASSOCİATED WİTH IMAGİNG DEVİCES AND RADİATİON EMİSSİON				
What can you say about radiation emission? Do all devices emit radiation in Medical Imaging? The following are the answers to their questions:"In Medical Imaging, all devices emit radiation". 5 direct subcodes and 2 indirect subcodes related to the theme were determined.				
1. Some devices emit radiation a. Some radiopharmaceuticals emit radiation	All devices emit	MRI and USG do not emit radiation	MRI not emit radiation	Not all devices emit radiation a. They are not All Ionizing Radiatio

confusion. However, while it was determined that the employees had the correct information originating from the hospital experience, it was determined that there was a lack of knowledge in theoretical and conceptual framework. In addition, it has been observed that healthcare professionals have knowledge about the principles of radiation protection based on their work experience, but do not have clear information about ionizing radiation and non-ionizing radiation and their harms, and therefore experience extreme anxiety. Codes created by employees as incomplete and incorrect information; Theme 1 (C8) "It is harmful if exposed to a certain level of radiation during pregnancy". C10 of the 2nd theme is "the same type of radiation, but the amount is important". Radiation during pregnancy does not need to exceed a certain threshold to be harmful, it is risky in every way, and not all types of radiation are the same. C11.1 of the second theme "All types of radiation are different, but the effect is the same". Different effects of radiation types are also different. C11.3 "The types of radiation are different, but I'm not sure" reveals ambiguity and lack of information. The other wrong code is code 13 for theme 3. C13 "All imaging devices emit radiation" is misinformation that ionizing radiation is present in ultrasonography and magnetic resonance. There is no radiation in these two devices. Regarding the principles of radiation protection in Theme 4, the expression C.22 "Food that will expel radiation from the body is edible and drinkable" does not include the full protection principle.

In addition, the most emphasized code in radiation protection is the importance of administrative measures (doors and walls in radiation areas to be lead-coated, ventilation systems to be complete, provision of protective equipment, etc.) The question posed in Theme Fifth is, "Is the radiation from cell phones and computers ionizing radiation?" Some healthcare workers answered the question as C.26, "I don't know exactly what ionizing radiation is". This answer expresses a lack of knowledge. Again, some of the participants answered in C32, "It's ionizing radiation, but I'm not sure."

The expression "nuclear medicine treats tumor, others are for diagnosis" related to the 7th theme titled "Diagnosis and Treatment" in C44 also expresses incorrect and incomplete information. The eighth theme is the theme of "doses administered to the patient". Regarding this theme, C49.1 "The doses administered to the patient in tomography are the same" and C49.2 "Patient doses in magnetic resonance are the same." His statements give false information about this.

The sub-codes containing false information regarding the 10th theme titled "Radiation pollution and ionizing radiation" are as follows; C54 "No radiation pollution in radiology", C64 "I have no idea about ionizing radiation". C58 "Contamination spreads from device, not from patient" statements.

Courses on ionizing radiation and protection methods should be added to the university education curriculum (undergraduate, associate degree) of healthcare professionals (nurses, technicians, etc.) and non-physicians who do not have to wear a dosimeter. In-service trainings should be provided in hospitals and health institutions, and trainings on occupational hazards and risks should be kept up to date. The importance of personal protective measures should be emphasized in the trainings and a control mechanism for everyone's use should be established.

Author Statements:

References

[1] GÜNAY, O., SARIHAN, M., ABAMOR, E., & YARAR, O. (2019). Environmental radiation doses from patients undergoing Tc-99m DMSA cortical renal scintigraphy. *International Journal of Computational and Experimental Science and Engineering,*5(2);86-93.
DOI:10.22399/ijcesen.589267

[2] Terekli, G., Özkan, O., & BAYIN, G. (2013). Çevre dostu hastaneler: Hastaneden yeşil hastaneye. *Ankara Sağlık Hizmetleri Dergisi,* 12(2); 37-54.

[3] Regulla, D. F., & Eder, H. (2005). Patient exposure in medical X-ray imaging in Europe. *Radiation protection dosimetry,* 114(1-3); 11-25. DOI:org/10.1093/rpd/nch538

[4] UZUNTARLA, Y., & DOĞAN, F. (2019). Bir Eğitim ve Araştırma Hastanesinde Dozimetre Taşıyan Sağlık Personelinin İyonlaştırıcı Radyasyon Hakkındaki Risk Algısı ve Bilgi Düzeyinin Belirlenmesi. *Sağlık Bilimleri ve Meslekleri Dergisi,* 6(1); 34-41. DOI: 10.17681/hsp.398026

[5] Yaren, H., & KARAYILANOĞLU, T. (2005). Radyasyon ve insan sağlığı üzerine etkileri. *TSK Koruyucu Hekimlik Bülteni,* 4(4); 199-208.

[6] Hastanesi, E. Ü. T. F. (2014). Radyasyon güvenliği el kitabı.

[7] Shapiro, J. (2002). Radiation protection: a guide for scientists, regulators, and physicians. *La Editorial, UPR.*

[8] Zakariya, N. I., & Kahn, M. T. E. (2014). Benefits and biological effects of ionizing radiation. *Sch. Acad. J. Biosci*, 2(9); 583-591.

[9] Russell, J. G. B., & Webb, G. A. M. (1987). Valuing the man-sievert in X-ray diagnosis. *The British Journal of Radiology*, 60(715); 681-684. doi.org/10.1259/0007-1285-60-715-681

[10] Burrows, E. H. (1986). Pioneers and early years. A history of British radiology.

[11] Ron, E. (2003). Cancer risks from medical radiation. *Health physics,* 85(1); 47-59.

[12] ÇELİK, H., KOYUNCU, İ., KARAKILÇIK, A. Z., GÖNEL, A., & MUSA, D. (2016). Radyasyonlu Ortamlarda Çalışan İnsanlarda İyonize ve Non-İyonize Radyasyonun Oksidatif Stres ve Antioksidan Seviye Üzerindeki Etkileri. *Bezmialem Science*, 3; 106-9. DOI: 10.14235/bs.2016.872

[13] Schmid, E., & Schrader, T. (2007). Different biological effectiveness of ionising and non-ionising radiations in mammalian cells. *Advances in Radio Science*, 5; 1-4.

[14] Sowa, P., Rutkowska-Talipska, J., Sulkowska, U., Rutkowski, K., & Rutkowski, R. (2012). Ionizing and non-ionizing electromagnetic radiation in modern medicine. Polish Annals of Medicine, 19(2), 134-138. DOI: 10.1016/j.poamed.2012.07.001

[15] Bolus, N. E. (2001). Basic review of radiation biology and terminology. *Journal of nuclear medicine technology*, 29(2); 67-73. DOI: 10.1016/j.poamed.2012.07.001

[16] Koçyiğit, A., Kaya, F., Çetin, T., Kurban, I., Erbaş, T., Ergin, A., ... & Karabulut, N. (2014). Radyolojik tetkikler sırasında maruz kalınan radyasyon hakkında sağlık personelinin bilgi düzeyleri. *Pamukkale Tıp Dergisi,* 7(2);137-142.

[17] Frischknecht, R., Braunschweig, A., Hofstetter, P., & Suter, P. (2000). Human health damages due to ionising radiation in life cycle impact assessment. *Environmental impact assessment Review*, 20(2); 159-189.

[18] Garcia-Sanchez, A. J., Garcia Angosto, E. A., Moreno Riquelme, P. A., Serna Berna, A., & Ramos-Amores, D. (2018). Ionizing radiation measurement solution in a hospital environment. *Sensors,* 18(2); 510.

[19] Çokluk, E., Çokluk, S., Şekeroğlu, R., & Huyut, Z. (2016). Sağlık hizmetleri sektöründe risk algısı: Hastane Laboratuvar ön çalışması. *Türk Klinik Biyokimya Dergisi,* 14(2); 125-130.

[20] MANAVGAT, S. S., & MANDIRACIOĞLU, A. (2012). ege üniversitesi tıp fakültesi hastanesi'nde kişisel dozimetre taşıyan çalışanların mesleksel iyonlaştırıcı radyasyon risk algısı. *TTB Mesleki Sağlık ve Güvenlik Dergisi,* 12(43); 34-43.

[21] Creswell, J. W. (2013). Nitel araştırma yöntemleri: Beş yaklaşıma göre nitel araştırma ve araştırma deseni (3. Baskıdan Çeviri). *M. Bütün ve SB Demir,* Çev.). Ankara: Siyasal Kitabevi.

[22] Neuman, W. (2007). Sosyal Araştırma Yöntemlerinin Temelleri: *Nitel ve Nicel Yaklaşımlar. Boston:* Allyn ve Bacon.

[23] International Commission on Radiological Protection. (2007). Radiological protection in medicine. ICRP Publication 105. *Ann. ICRP*, 37(6); 1-64.

Edaravone Ameliorates Memory, Hippocampal Morphology, and Inflammation in a Rat Model of Alzheimer's Disease

Seyma OZSOY[1*], Elif Azize OZSAHIN DELIBAS[2] , Gurkan YIGITTURK[3]

[1]Tokat Gaziosmanpasa University, Faculty of Medicine, Departments of Physiology, Tokat, Turkey
* **Corresponding Author** : **Email:** seyma.ozsoy@hotmail.com - **ORCID:** 0000-0003-1783-3618

[2]Tokat Gaziosmanpasa University, Faculty of Health Sciences, Department of Nutrition and Dietetics, Tokat, Turkey.
Email: elif.delibas@gop.edu.tr **ORCID:** 0000-0002-4195-0554

[3]Mugla Sitki Kocman University, Faculty of Medicine, Department of Histology and Embryology, Mugla, Turkey.
Email: gurkanyigitturk@mu.edu.tr **ORCID:** 0000-0002-5315-253X

Abstract:

Oxidative stress and neural inflammation play a role in the pathogenesis of Alzheimer's disease (AD). Edaravone (EDA) has an antioxidant-free radical scavenger property. The purpose of this study to evaluate the effect of EDA on memory, hippocampal morphology, and inflammation in a streptozocin (STZ)-induced AD model. This study used 18 Wistar albino adult rats, weighing 200-220 g. Following general anesthesia, 3 mg/kg STZ was dissolved in 0.9% NaCl and administered intracerebroventricularly (ICV) in both lateral ventricles to 12 rats in a total of 5 μl. The animals were allowed to recover for two weeks and then divided into two groups. Six rats were given 0.9% NaCl i.p. for 15 days, and the other six were administered EDA 40 mg/kg i.p. for 15 days, once a day. The control group of six rats did not undergo any surgical procedures or medications. After treatment, a passive avoidance learning (PAL) test was used, followed by the removal of the brain tissue in all animals. Nissl staining was used to count neurons in the hippocampal CA1 and CA3 regions, and TNF-α and IL-6 levels in the brain were measured. In the STZ group, significantly shorter latency time, and decreased number of neurons in the CA1 and CA3 hippocampal regions compared to the control group were observed. EDA significantly prolonged the latency time and increased hippocampal CA1 and CA3 neuron counts compared to the STZ group. TNF-α and IL-6 levels were higher in the STZ+saline group than in the control group. Similarly, EDA treatment reduced TNF-α and IL-6 levels when compared to the STZ+saline and control groups. For the first time, we demonstrated the neuroprotective and anti-inflammatory potential of EDA in an experimental AD model. Our results may provide evidence for EDA therapy in addition to the standard regimen in patients with cognitive decline.

1. Introduction

Alzheimer's disease (AD), which is a neurodegenerative disease, is a common disease in the advanced age group [1]. The incidence of dementia increases with age. The incidence in men is 19-29% lower than in women [2]. Patients have progressive functional impairment, emotional distress, loss of independence, and behavioral deficits. The pathophysiology of the disease is complex and multifactorial. Neuronal loss, particularly in certain brain regions such as the medial temporal lobe and temporo-parietal junctional cortices; intraneuronal neurofibrillary tangles composed of aggregated hyperphosphorylated tau protein; and extracellular neuritic plaques formed by β -amyloid peptide accumulation are pathological findings in AD [3]. Oxidative stress (OS) and neuroinflammation are features of neurodegeneration and contribute to AD progression. OS is caused by an imbalance between reactive oxygen species (ROS) formed as a result of cellular metabolism and the systems that detoxify

them. Many studies have shown that OS, which occurs primarily in AD, plays a role in the pathogenesis and progression of the disease [4]. Risk factors such as advanced age [5], apolipoprotein E ε4 alleles [6] may lead to oxidative damage in AD. OS causes the release of inflammatory and neurotoxic factors that cause a chronic neuroinflammatory response [7]. In AD, accumulation of the Aβ peptide initiates a spectrum of cerebral neuroinflammation mediated by the activation of microglia, the resident immune cells of the brain. Activated microglia express proinflammatory cytokines such as interleukin-1 beta (IL-1β), interleukin-6 (IL-6), and tumor necrosis factor-alpha (TNF-α) [8]. Developed in Japan, edaravone (3-methyl-1-phenyl-2-pyrazolin-5-one, EDA) has an antioxidant free radical scavenger property [9]. It can prevent motor neuron death caused by OS in Amyotrophic Lateral Sclerosis (ALS) patients [10]. In addition, this molecule, which has neuroprotective and anti-inflammatory effects, is also used in the treatment of acute ischemic stroke and acute brain infarction [11]. A recent study has shown that EDA exerts its antioxidant and anti-inflammatory effects in asthma and cerebral infarction via the nuclear factor erythroid 2-related factor transcription factor/hemoxygenase 1 (Nrf2/HO-1) signaling pathway [12]. In the study in cultured neuron cells, it was understood that the neuroprotective effect of EDA increased the expression of mature brain-derived neurotrophic factor (mBDNF) and Bcl-2, decreased caspase-3 activity, and stimulated the activation of extracellular signal-regulated kinases ½ (ERK$_{1/2}$) [13]. EDA protects neurons [14], and glia (astrocytes, oligodendrocytes, and microglia) [15]. It suppresses the inflammatory response of activated microglial cells [16]. Streptozotocin (STZ) is widely used in diabetes research to establish an animal model because it selectively damages pancreatic β-cells [17]. Studies have shown that injection of intracerebroventricular (ICV) STZ in rodents produces AD-like pathology. ICV STZ stimulates progressive neuroinflammation, OS, and mitochondrial dysfunction in the hippocampus, exerting effects associated with significant learning and cognitive impairments [18]. The hippocampus, a part of the brain important for learning and memory, is susceptible to damage in the early stages of AD.

Based on this information, we aimed to evaluate the effect of edaravone on memory and hippocampal morphology in rats with a streptozocin (STZ)-induced AD model. TNF-α and IL-6 levels in brain tissue were measured for neuroinflammation

2. Material and Methods

2.1. Animal origin, housing, breeding, and study approval

Eighteen adult male Wistar albino rats weighing 200-220 g included in the study. The animals were kept at a temperature of 23±1°C with a 12-hour light/dark cycle. The experimental procedures of the study were approved by the Tokat Gaziosmanpaşa University Animal Ethics Research Committee (2014 HADYEK-47).

2.2. Experimental procedures

Animals were given general anesthesia by intraperitoneal (i.p.) administration of ketamine hydrochloride (80 mg/kg, Alfamine®, Ege Vet, Alfasan International B.V. Holland) and xylazine hydrochloride (4 mg/kg, Alfazyne®, Ege Vet, Alfasan International B.V. Holland). Using a streotaxic device to generate the AD model, rats were given bilateral ICV into both lateral ventricles STZ (Sigma-Aldrich, St Louis, MO, 3 mg / kg). STZ was infused into the left (2.5 μL) and right lateral ventricle (2.5 μL) (ICV) (AP = −0.8mm, L = ±1.6 mm, DV = −4.2 mm) with a Hamilton syringe [19]. Edaravone (Radicava®) was purchased from Mitsubishi Tanabe Pharma America. After the ICV STZ injection, the rats were divided into 3 groups: control (n = 6), ICV-STZ plus 0.9% NaCl (n = 6), and ICV-STZ plus EDA (n = 6). STZ was dissolved in 0.9% NaCl at a dose of 3 mg/kg, and ICV was administered in a total of 5 μl in both lateral ventricles to 12 rats after anesthesia. Rats were divided into two groups. After STZ injection, six rats were given 0.9% NaCl i.p. for 15 days, and the other six were administered EDA 40 mg/kg i.p. for 15 days, once a day. No surgery or treatment was given to the controls (Fig 1).
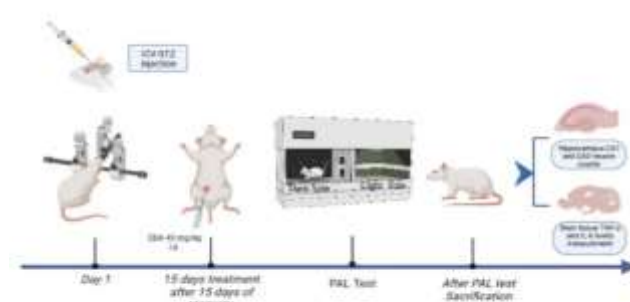

Figure 1. Experimental Design

2.3. Passive avoidance test

Two weeks after the application, a passive avoidance task that assesses learning and memory was carried out in all groups. Passive avoidance

learning (PAL) is a set of fear-guided tests classically used to assess negative reinforcement-based long-term memory in small laboratory animals. For this, a PAL box with a size of 20 x 20 x20 cm with dark and light sections was used. The rats were placed in the bright chamber of a two-compartment box. After a 10-second acclimatization time, the door between the light and dark chambers was opened. After the animal passed into the dark area, the door was closed, and an electric shock (FJ-919; 300 kV, 60 Hz, 1,5 mA) was applied to the animal for 3 seconds. The time it took for the animal to enter the dark zone was considered the latency period. Animals that did not enter the dark zone for more than 5 minutes were excluded from the study. The animals' latency time to the dark area was evaluated after 24 hours [20]. Then the rats were sacrificed, and their brain tissues were removed for histopathological and biochemical evaluation.

2.4. Histological Evaluation

Brain tissue samples from all animals were fixed in 10% formalin. After post-fixation in the same fixative solution for one week, the tissues were blocked with paraffin after routine histological procedures. Each paraffin block was sectioned into 5 µ thick sections, which were then deparaffinized in an oven at 60o C for 8 hours. The hippocampus cornu ammonis-1 (CA1), cornu ammonis-3 (CA3) neuron counts of brain sections stained with Nissl dye were examined using an Olympus BX51 microscope and an Olympus C-5050 digital camera. To quantify the surviving number of neurons, the image analysis system (Image-Pro Express 1.4.5, Media Cybernetics, Inc., USA) was used.

2.5. Detection of TNF-α and IL-6 levels in brain tissue

Brain tissue samples were stored in aliquots at -80 0C until the study day. ELISA was used to measure TNF-α (catalog no. E-EL-R2856) and IL-6 (catalog no. E-EL-R0015) using commercial kits (Elabscience, USA) and following the manufacturer's instructions. TNF-α and IL-6 levels per mg protein were determined using the Thermo ScientificTM PierceTM BCA Protein Assay Kit (Catalog no. 23225). TNF-α and IL-6 levels in the same homogenate were calculated in relation to protein concentration (ng/mg protein). The levels of TNF-α and IL-6 in brain homogenates were calculated in relation to protein concentration.

2.6. Statistical Analyzes

Statistical analyses were performed using the SPSS 26.00 program. To compare differences between groups, the one-way ANOVA' test was used, followed by post hoc LSD tests. The results were presented in the form of the mean (mean) and standard error (SEM). For TNF-α and IL-6, a one-way ANOVA was used. Tamhane's T2 was used post-hoc. A p value of <0.05 was considered statistically significant.

3. Results and Discussions

In the STZ-induced rat model, the latency period was shortened in the STZ+saline group, while the number of CA1 and CA3 neurons decreased (Fig 2). EDA improved all these harmful effects caused by STZ. The duration of latency increased, as did the number of CA1 and CA3 neurons. In the STZ group, significantly shorter latency time ($p < 0.001$) and decreased number of neurons in the CA1 and CA3 hippocampal regions ($p < 0.000$, $p < 0.001$, respectively) compared to the control group were observed. EDA significantly prolonged the latency time ($p < 0.05$) and increased hippocampal CA1 and CA3 neuron counts ($p < 0.05$, $p < 0.05$, respectively) compared to the STZ group. The histopathological and immunohistochemical findings are shown in Table 1. As can be seen Fig 3, when compared to the STZ and control groups, EDA administration reduced TNF-α and IL-6 levels. TNF-α and IL-6 levels in the STZ group were higher than in the control group ($p < 0.01$ and $p < 0.05$, respectively). EDA treatment decreased TNF-α ($p < 0.01$ and $p < 0.001$, respectively) and IL-6 levels compared to STZ and control groups ($p < 0.05$, $p < 0.01$, respectively).

Table 1. Latency time and the number of neurons in hippocampal CA1 and CA3 regions of groups

Groups	Latency time (s)	Number of CA1 neurons	Number of CA3 neurons
Control Group	229.2 ± 33.6	68.4 ± 5.3	65.8 ± 3.9
ICV-STZ+ Saline Group	40.4 ± 10.3 *	45.9 ± 5.2 **	38.6 ± 1.8 *
ICV-STZ+EDA Group	164.8 ± 59.3 #	63.5 ± 7.2 #	60.3 ± 4.8 #

*Data expressed as mean ± SEM. * p < 0.001, ICV-STZ+Saline Group vs. Control Group; ** p < 0.000, ICV-STZ+Saline Group vs Control Group; # p < 0.05, ICV-STZ+EDA Group vs ICV-STZ+Saline Group.*
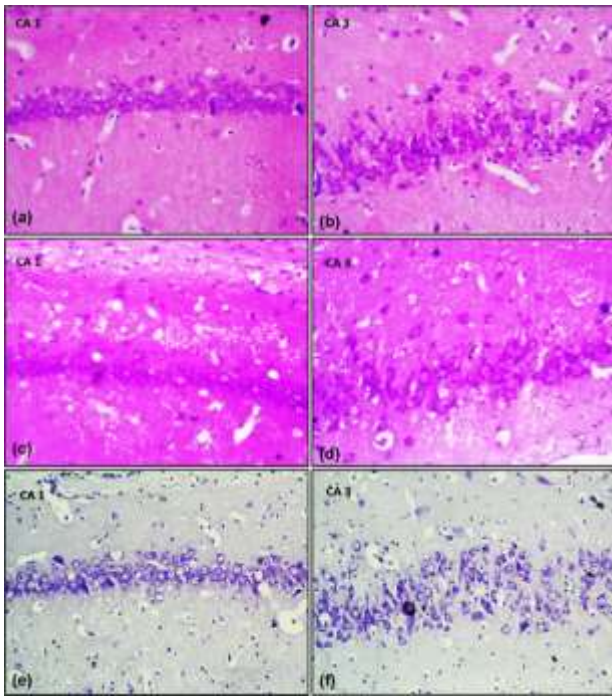
Figure 2. CA1 and CA3 hippocampal regions were stained with Cresyl violet stain (x 40 and x 100 magnification). a) Control Group CA1, b) Control Group CA3, c) ICV-STZ and Saline Group CA1, d) ICV-STZ and Saline Group CA3, e) ICV-STZ and EDA Group CA1, f) ICV-STZ and EDA Group CA3
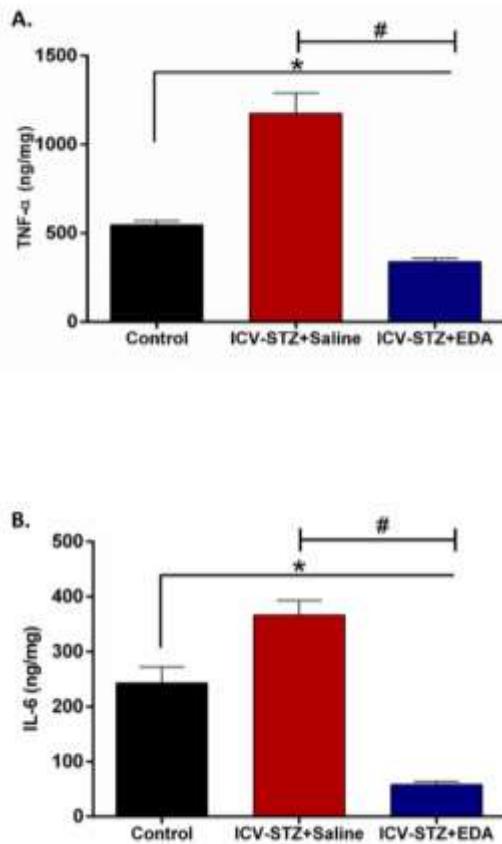
Figure 3. The concentration of TNF-α and IL-6 in the rat brain in the following groups: A) *Control group vs ICV-STZ+Saline and ICV-STZ+EDA group; p<0.01; #ICV-STZ+EDA group vs ICV-STZ+Saline group

p<0.01. B) *Control group vs ICV-STZ+Saline and ICV-STZ+EDA group; p<0.05; # ICV-STZ+EDA group vs ICV-STZ+Saline group p<0.001.

Discussion

In neurodegenerative diseases, there is oxidative damage to the brain, and OS often appears to be a manifestation of these diseases. Because of the brain's very high dioxygen consumption, the brain may be particularly susceptible to oxidative damage to OS [21]. In addition, OS has been shown to induce intracellular Aβ accumulation and tau phosphorylation in cell cultures [22]. The presence of OS with high OS markers is noticed in the brains of AD patients and animal models of AD [23]. Studies have shown that inflammation [24], mitochondrial dysfunction [25], metal accumulation [26], hyperphosphorylated tau [27], and Aβ accumulation [28] are the basic mechanisms underlying the formation of OS. High levels of Aβ1–40 and Aβ1–42 have been shown to be associated with increased levels of oxidation products from proteins, lipids, and nucleic acids in the hippocampus and cortex in AD [29]. With proteomic analysis, potentially numerous oxidized proteins with key roles in vital cellular functions in the AD brain have been identified [30]. But the questions about how and where the OS is in the AD, as well as where it came from, remain unanswered.

AD is believed to affect neurons by disrupting synapses. However, astrocytes and microglia remain viable, acquire a reactive morphology, and mediate inflammatory-like responses [31]. Inflammatory mediators such as TNF-α and IL-6 are involved in the pathogenesis of AD. TNF-α, which contributes to the chronic inflammatory response, is expressed by neurons and glia in the brain [32]. TNF-α may aggravate phospho-tau pathologies in AD brains and contribute to amyloidogenesis via beta-secretase regulation. It also induces insulin resistance, chronic inflammation, glutamate excitotoxicity, OS, and mitochondrial dysfunction [33]. TNF-α has been implicated in disease progression, gliosis, demyelination, inflammation, disruption of the blood-brain barrier, and cell death in experiments induced by chronic neuroinflammation [34]. Tarkowski et al. found a 25-fold difference in TNF-α levels between AD patients and controls [35]. IL-6 is a cytokine that plays a critical role in the physiological homeostasis of neural tissue and inflammation [36]. However, prolonged and severe exposure of the brain to IL-6 has resulted in many

neuropathological findings. IL-6 overproduction in transgenic mice has been reported to reduce neurogenesis and the proliferation, survival and differentiation of neural progenitor cells in the dentate gyrus [37]. IL-6, a component of amyloid plaque formation in the early stage of AD brains, is associated with tau phosphorylation, synapse loss, and learning deficits in mice [38]. Although there are conflicting results, meta-analyses have shown that IL-6 is increased in the cerebrospinal fluid, in the plasma of patients with mild cognitive impairment, and in AD patients compared to controls [39, 40].

With a melting point of 129.7°C, EDA is freely soluble in acetic acid, methanol, or ethanol but sparingly soluble in water or diethyl ether [41]. EDA can protect body tissues by inhibiting cyclooxygenase activity (COX, including COX-1, and COX-2). COX-2, expressed mainly in hippocampal tissue and cortical neurons, is a key enzyme produced by prostaglandin E2 (PGE2) metabolism. PGE2 is associated with pathological events such as inflammation, OS, and apoptosis [42]. EDA has been shown to be effective in slowing the progression of symptoms and motor neuron degeneration in ALS model mice [43]. Due to the presence of upper and lower motor degeneration in ALS, muscle weakness that usually begins in the extremities leads to clinical symptoms [44]. The role of OS in ALS, AD, Parkinson's disease, and other neurodegenerative diseases has been demonstrated. ROS are produced by cellular enzymes that damage cell components and increase inflammation [45]. A review of experimental animal studies showed that EDA increased the functional and cognitive prognosis by 30.3% and 25.5%, respectively, in an animal model of focal cerebral ischemia [46]. Another review evaluating 18 randomized controlled trials reported that EDA can significantly reduce the mortality or morbidity rate of acute ischemic stroke [47]. Recently, a study reported that the therapeutic mechanisms of EDA in the treatment of cerebral ischemia may include OS, platelet activation and aggregation, intercellular adhesion, glycolysis and gluconeogenesis, iron metabolism, hypoxia, and the like [8]. The administration of EDA to rats for 5 weeks abolished rotenone-induced effects such as midbrain catalepsy, mitochondrial damage, and degeneration of dopamine neurons [48]. In vivo studies have shown that EDA can reduce microglial activation and suppress the production of proinflammatory mediators by activated microglia [16, 49]. Fujiwara et al. showed that there were elevations in plasma levels of some cytokines, including IL-6 in rats in acute ischemic conditions;

these increases showed a decrease with EDA treatment [50].

In this study, we showed for the first time that EDA has neuroprotective and anti-inflammatory effects in the STZ-induced AD rat model. The role of the hippocampal region in semantic, learning, and episodic memory is well established. Therefore, the hippocampus is one of the first areas of the brain to be affected by pathological events in AD. In the STZ-induced rat model, the latency period was shortened in the STZ+saline group, while the number of CA1 and CA3 neurons decreased. EDA improved all these harmful effects caused by STZ. The duration of latency increased, as did the number of CA1 and CA3 neurons. When compared to the STZ and control groups, EDA administration reduced TNF-α and IL-6 levels.

4. Conclusions

Various neuropathological changes are seen in the brains of individuals with AD, which is the most common cause of dementia all over the world. Treatment of these neurodegenerative changes will be aimed at preventing memory loss and thinking and reasoning problems. For the first time, we demonstrated the neuroprotective and anti-inflammatory potential of EDA in an experimental AD model. Our study provides evidence for EDA treatment in addition to the standard regimen in patients with cognitive decline.

References

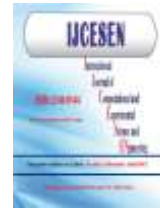[1] Chan, S. W. C. (2011). Family caregiving in dementia: the asian perspective of a global problem. *Dementia and Geriatric Cognitive Disorders.* 30(6):469-478. DOI: 10.1159/000322086

[2] Khan, S., Barve, K. H., & Kumar, M. S. (2020). Recent Advancements in Pathogenesis, Diagnostics and Treatment of Alzheimer's Disease. *Curr Neuropharmacol.* 18(11):1106-1125. DOI: 10.2174/1570159X18666200528142429.

[3] Lashley, T., Schott, J.M., Weston, P., Murray, C.E., Wellington, H., Keshavan, A., Foti, S. C., Foiani, M., Toombs, J., Rohrer, J.D., Heslegrave, A., & Zetterberg, H. (2018). Molecular biomarkers of Alzheimer's disease: progress and prospects. *Dis Model Mech*. 2018; 11(5):dmm031781. DOI: 10.1242/dmm.031781.

[4] Martins, R. N., Villemagne, V., Sohrabi, H. R., Chatterjee, P., Shah, T.M., Verdile, et al. (2018). Alzheimer's disease: a journey from amyloid peptides and oxidative stress, to biomarker technologies and disease prevention strategies-gains from AIBL and DIAN cohort studies. *J. Alzheimers Dis.* 62:965-992. DOI: 10.3233/JAD-171145.

[5] Yamazaki, D., Horiuchi, J., Ueno, K., Ueno, T., Saeki, S., Matsuno, M., Naganos, S., et al. (2014). Glial dysfunction causes age-related memory impairment in Drosophila. *Neuron.* 84(4):753-763. DOI:10.1016/j.neuron.2014.09.039.

[6] Han, B. H., Zhou, M. L., Johnson, A. W., Singh, I., Liao, F., Vellimana, A. K., et al. (2015). Contribution of reactive oxygen species to cerebral amyloid angiopathy, vasomotor dysfunction, and microhemorrhage in aged Tg2576 mice. *Proc Natl Acad Sci USA.* 112(8):E881-90. DOI: 10.1073/pnas.1414930112.

[7] Cameron, B., & Landreth, G. E. (2010). Inflammation, microglia and Alzheimer's disease. *Neurobiol Dis.* 37(3):503-509. DOI: 10.1016/j.nbd.2009.10.006.

[8] Wang, W. Y., Tan, M. S., Yu, J. T., & Tan, L. (2015). Role of pro-inflammatory cytokines released from microglia in Alzheimer's disease. *Ann Transl Med*. 3(10):136. DOI: 10.3978/j.issn.2305-5839.2015.03.49.

[9] Watanabe, K., Tanaka, M., Yuki, S., Hirai, M., & Yamamoto, Y. (2018). How is edaravone effective against acute ischemic stroke and amyotrophic lateral sclerosis? *J Clin Biochem Nutr.* 62(1):20-38. DOI: 10.3164/jcbn.17-62.

[10] Higashi, Y., Jitsuiki, D., Chayama, K., & Yoshizumi, M. (2006). Edaravone (3-methyl-1-phenyl-2-pyrazolin-5-one), a novel free radical scavenger for treatment of cardiovascular diseases. *Recent Pat Cardiovasc Drug Discov.* 1(1):85-93. DOI: 10.2174/157489006775244191.

[11] Dang, R., Wang, M., Li, X., Wang, H., Liu, L., Wu, Q., Zhao, J., Ji, P., Zhong, L., Licinio, J., & Xie, P. (2022). Edaravone ameliorates depressive and anxiety-like behaviors via Sirt1/Nrf2/HO-1/Gpx4 pathway. *J Neuroinflammation.* 19(1):41. DOI: 10.1186/s12974-022-02400-6.

[12] Liu, J., Jiang, Y., Zhang, G., Lin, Z., & Du, S. (2019). Protective effect of edaravone on blood-brain barrier by affecting NRF-2/HO-1 signaling pathway. *Exp Ther Med*. 18(4):2437-2442. DOI: 10.3892/etm.2019.7859.

[13] Okuyama, S., Morita, M., Sawamoto, A., Terugo, T., Nakajima, M., & Furukawa, Y. (2015). Edaravone enhances brain-derived neurotrophic factor production in the ischemic mouse brain. *Pharmaceuticals (Basel, Switzerland).* 8:176-185. DOI: 10.3390/ph8020176.

[14] Kraus, R. L., Pasieczny, R., Lariosa-Willingham, K., Turner, M. S., Jiang, A., & Trauger, J. W. (2005). Antioxidant properties of minocycline: neuroprotection in an oxidative stress assay and direct radical-scavenging activity. *J Neurochem.* 94:819-27. DOI: 10.1111/j.1471-4159.2005.03219.x.

[15] Miyamoto, N., Maki, T., Pham, L. D., Hayakawa, K., Seo, J. H., Mandeville, E. T., Mandeville, J. B., Kim, K. W., Lo, E. H., & Arai, K. (2013). Oxidative stress interferes with white matter renewal after prolonged cerebral hypoperfusion in mice. *Stroke.* 44:3516-321. DOI: 10.1161/STROKEAHA.113.002813.

[16] Yuan, Y., Zha, H., Rangarajan, P., Ling, E. A., & Wu, C. (2014). Anti-inflammatory effects of Edaravone and Scutellarin in activated microglia in experimentally induced ischemia injury in rats and in BV-2 microglia. *BMC Neurosci.* 15:125. DOI: 10.1186/s12868-014-0125-3.

[17] Lu, Y., Dong, Y., Tucker, D., Wang, R., Ahmed, M. E., Brann, D., & Zhang, Q. (2017). Treadmill Exercise Exerts Neuroprotection and Regulates Microglial Polarization and Oxidative Stress in a Streptozotocin-Induced Rat Model of Sporadic Alzheimer's Disease. *J Alzheimers Dis.* 56(4):1469-1484. DOI: 10.3233/JAD-160869.

[18] Salkovic-Petrisic, M., & Hoyer, S. (2007). Central insulin resistance as a trigger for sporadic Alzheimer-like pathology: An experimental approach. *J Neural Transm Suppl.* 72:217-233. DOI: 10.1007/978-3-211-73574-9_28.

[19] Paxinos, G., & Watson, C. (1998). The rat brain in stereotaxic coordinates. Spiral Bound, 4th ed. *New York: Academic Press.*

[20] Elibol, B., Terzioglu-Usak, S., Beker, M., & Sahbaz, C. (2019). Thymoquinone (TQ) demonstrates its neuroprotective effect via an anti-inflammatory action on the Aβ(1–42)-infused rat model of Alzheimer's disease. *Psychiatry and Clinical Psychopharmacology.* 29:379-386. DOI: 10.1080/24750573.2019.1673945.

[21] Moreira, P. I., Duarte, A. I., Santos, M. S., Rego, A. C., & Oliveira, C. R. (2009). An integrative view of the role of oxidative stress, mitochondria

and insulin in Alzheimer's disease. *J Alzheimers Dis.* 16(4):741-61. DOI: 10.3233/JAD-2009-0972.

[22] Gómez-Ramos, A., Díaz-Nido, J., Smith, M. A., Perry, G., & Avila, J. (2003). Effect of the lipid peroxidation product acrolein on tau phosphorylation in neural cells. *J Neurosci Res.* 71:863-870. DOI: 10.1002/jnr.10525.

[23] Sonnen, J. A., Breitner, J. C., Lovell, M. A., Markesbery, W. R., Quinn, J. F., & Montine, T. J. (2008). Free radical-mediated damage to brain in Alzheimer's disease and its transgenic mouse models. *Free Radic Biol Med.* 45(3):219-230. DOI: 10.1016/j.freeradbiomed.2008.04.022.

[24] Lee, Y. J., Han, S. B., Nam, S. Y., Oh, K. W., & Hong, J. T. (2010). Inflammation and Alzheimer's disease. *Arch Pharm Res.* 33:1539-1556. DOI: 10.1007/s12272-010-1006-7.

[25] Chen, Z., & Zhong, C. (2014). Oxidative stress in Alzheimer's disease. *Neurosci Bull.* 30(2):271-81. DOI: 10.1007/s12264-013-1423-y.

[26] Greenough, M. A., Camakaris, J., & Bush, A. I. (2013). Metal dyshomeostasis and oxidative stress in Alzheimer's disease. *Neurochem Int.* 62(5):540-555. DOI: 10.1016/j.neuint.2012.08.014.

[27] Dias-Santagata, D., Fulga, T. A., Duttaroy, A., & Feany, M. B. (2007). Oxidative stress mediates tau-induced neurodegeneration in Drosophila. *J Clin Invest.* 117:236-245. DOI: 10.1172/JCI28769.

[28] Yan, M. H., Wang, X., & Zhu, X. (2013). Mitochondrial defects and oxidative stress in Alzheimer disease and Parkinson disease. *Free Radic Biol Med.* 62:90-101. DOI: 10.1016/j.freeradbiomed.2012.11.014.

[29] Butterfield, D. A., & Lauderback, C. M. (2002). Lipid peroxidation and protein oxidation in Alzheimer's disease brain: potential causes and consequences involving amyloid beta-peptide-associated free radical oxidative stress. *Free Radic. Biol. Med.* 32(11):1050-106. DOI: 10.1016/s0891-5849(02)00794-3.

[30] Reed, T. T., Pierce, W. M., Markesbery, W. R., & Butterfield, D. A. (2009). Proteomic identification of HNE-bound proteins in early Alzheimer disease: Insights into the role of lipid peroxidation in the progression of AD. *Brain Res.* 1274:66-76. DOI: 10.1016/j.brainres.2009.04.009.

[31] Selkoe, D. J. (2002). Alzheimer's disease is a synaptic failure. *Science.* 298(5594):789-791. DOI: 10.1126/science.1074069.

[32] Cheng, X., Yang, L., He, P., Li, R., & Shen, Y. (2010). Differential Activation of Tumor Necrosis Factor Receptors Distinguishes between Brains from Alzheimer's Disease and Non-Demented Patients. *J Alzheimers Dis.* 19(2):621-630. DOI: 10.3233/JAD-2010-1253.

[33] Cevik, B., Solmaz, V., Yigitturk, G., Cavusoğlu, T., Peker, G., & Erbas, O. (2017). Neuroprotective effects of erythropoietin on Alzheimer's dementia model in rats. *Adv Clin Exp Med.* 26(1):23-29. DOI: 10.17219/acem/61044.

[34] Montgomery, S. L., & Bowers, W. J. (2012). Tumor necrosis factor-alpha and the roles it plays in homeostatic and degenerative processes within

the central nervous system. *J Neuroimmune Pharmacol.* 7:42-49. DOI: 10.1007/s11481-011-9287-2.

[35] Tarkowski, E., Liljeroth, A. M., Minthon, L., Tarkowski, A., Wallin, A., & Blennow, K. (2003). Cerebral pattern of pro-and anti-inflammatory cytokines in dementias. *Brain Res Bull.* 61(3):255-260. DOI: 10.1016/s0361-9230(03)00088-1.

[36] Erta, M., Quintana, A., & Hidalgo, J. (2012). Interleukin-6, a Major Cytokine in the Central Nervous System. *Int J Biol. Sci.* 8:1254-1266. DOI: 10.7150/ijbs.4679.

[37] Vallières, L., Campbell, I. L., Gage, F. H., & Sawchenko, P. E. (2002). Reduced hippocampal neurogenesis in adult transgenic mice with chronic astrocytic production of interleukin-6. *J. Neurosci.* 22:486-492. DOI: 10.1523/JNEUROSCI.22-02-00486.2002.

[38] Lyra, E., Silva, N. M., Goncalves, R. A., Pascoal, T. A., Lima-Filho, R. A. S., Resende, et al. (2021). Pro-inflammatory interleukin-6 signaling links cognitive impairments and peripheral metabolic alterations in Alzheimer's disease. *Translational Psychiatry.* 11:251. DOI: 10.1038/s41398-021-01349-z.

[39] Akiyama, H., Barger, S., Barnum, S., Bradt, B., Bauer, J., Cole, G. et al. (2000). Inflammation and Alzheimer's disease. *Neurobiol Aging.* 21(3):383-421. DOI: 10.1016/s0197-4580(00)00124-x.

[40] Brosseron, F., Krauthausen, M., Kummer, M., & Heneka, M. T. (2014). Body fluid cytokine levels in mild cognitive impairment and Alzheimer's disease: a comparative overview. *Mol Neurobiol.* 50(2):534-44. DOI: 10.1007/s12035-014-8657-1.

[41] Cruz, M. P. (2018). Edaravone (Radicava): A Novel Neuroprotective Agent for the Treatment of Amyotrophic Lateral Sclerosis. *P T.* 43(1):25-28.

[42] Wang, G., Zeng, X., Gong, S., Wang, S., Ge, A., Liu, W., Ge, J., & He, Q. (2022). Exploring the Mechanism of Edaravone for Oxidative Stress in Rats with Cerebral Infarction Based on Quantitative Proteomics Technology. *Evid Based Complement Alternat Med.* 2022:8653697. DOI: 10.1155/2022/8653697.

[43] Ito, H., Wate, R., Zhang, J., Ohnishi, S., Kaneko, S., Ito, H., Nakano, S., & Kusaka, H. (2008). Treatment with edaravone, initiated at symptom onset, slows motor decline and decreases SOD1 deposition in ALS mice. *Exp Neurol.* 213(2):448-55. DOI: 10.1016/j.expneurol.2008.07.017.

[44] Saberi, S., Stauffer, J. E., Schulte, D. J., & Ravits, J. (2015). Neuropathology of Amyotrophic Lateral Sclerosis and Its Variants. *Neurol Clin.* 33:855-876. DOI: 10.1016/j.ncl.2015.07.012.

[45] Ahmadinejad, F., Geir Møller, S., Hashemzadeh-Chaleshtori, M., Bidkhori, G., & Jami, M. S. (2017). Molecular Mechanisms behind Free Radical Scavengers Function against Oxidative Stress. *Antioxidants.* 6(3):51. DOI: 10.3390/antiox6030051.

[46] Wu, S., Sena, E., Egan, K., Macleod, M., & Mead, G. (2014). Edaravone improves functional and structural outcomes in animal models of focal

cerebral ischemia: a systematic review. *Int J Stroke.* 9(1):101-6. DOI: 10.1111/ijs.12163.

[47] Yang, J., Cui, X., Li, J., Zhang, C., Zhang, J., & Liu, M. (2015). Edaravone for acute stroke: Meta-analyses of data from randomized controlled trials. *Dev Neurorehabil.* 18(5):330-335. DOI: 10.3109/17518423.2013.830153.

[48] Xiong, N., Xiong, J., Khare, G., Chen, C., Huang, J., Zhao, Y., Zhang, Z., Qiao, X., Feng, Y., Reesaul, H., Zhang, Y., Sun, S., Lin, Z., & Wang, T. (2011). Edaravone guards dopamine neurons in a rotenone model for Parkinson's disease. *PLoS One.* 6(6):e20677. DOI: 10.1371/journal.pone.0020677.

[49] Wu, C. Y., Zha, H., Xia, Q. Q., Yuan, Y., Liang, X. Y., Li, J. H., Guo, Z. Y., & Li, J. J. (2013). Expression of angiotensin II and its receptors in activated microglia in experimentally induced cerebral ischemia in the adult rats. *Mol Cell Biochem.* 382(1-2):47-58. DOI: 10.1007/s11010-013-1717-4.

[50] Fujiwara, N., Som, A. T., Pham, L. D., Lee, B. J., Mandeville, E. T., Lo, E. H., & Arai, K. (2016). A free radical scavenger edaravone suppresses systemic inflammatory responses in a rat transient focal ischemia model. *Neurosci Lett.* 633:7-13. DOI: 10.1016/j.neulet.2016.08.048.

A Biobjective Approach to Assigning Recreational Activities to Medical Tourists

Ahmed Burak PAÇ*

Gebze Teknik Üniversitesi, Mühendislik Fakültesi, Endüstri Mühendisliği, 41400, Kocaeli-Türkiye
* **Corresponding Author**: **Email:** burakpac@gtu.edu.tr - **ORCID:** 0000-0003-2177-4585

Abstract:

Medical tourism is a growing market due to cost savings for patients and access to treatments unavailable in their home country. Countries offering high-quality medical services at affordable prices have great opportunities for growing their revenue and shares in this market. To increase the welfare of tourists and revenues associated with healthcare tourism, this study proposes a mathematical model for planning the integration of recreational activities to the medical schedules of healthcare tourists. The model achieves this by providing access for medical tourists into appropriate recreational activities based on their medical conditions, availability schedules, and budgets. The proposed integer programming model maximizes a weighted sum of total tourist satisfaction points and profits generated from assigning tourists to recreational activities. It incorporates medical restrictions, ensuring that medical tourists are directed to activities suitable for their medical conditions. The Pareto-efficient frontier for patient satisfaction and company profit is determined utilizing the integer programming model. The proposed model aims for a higher quality experience for medical tourists, optimizing their access to recreational activities while promoting economic growth in the health tourism sector. Computational tests demonstrate that the proposed model efficiently solves instance sizes that may arise in practical contexts and enables iterative solutions for obtaining Pareto-efficient frontiers.

1. Introduction

Medical tourism is a growing sector, as individuals from around the world seek lower-cost in high-quality medical services or access to treatments not available in their home countries. Cost savings is a major driver of health tourism. Medical procedures in Türkiye are significantly less expensive than in many European countries and United States of America, despite competitive quality. This provides an affordable option, particularly for individuals who do not have insurance coverage for the necessary procedure. Another advantage of healthcare tourism is the access to treatments and procedures that may be unavailable or heavily regulated in certain countries. Additionally, medical tourism offers the opportunity to combine medical treatment with a relaxing holiday. Many popular medical tourism destinations provide historical or natural sites, beautiful beaches, and other attractions, enabling medical tourists (interchangeably, patients

or shortly tourists) to recover in a pleasant and soothing environment.

To further enhance the economic impact of medical tourism, a viable strategy is to guide health tourists to vacations or other recreational activities. This can be achieved through the creation of packages that include sea side, nature, cultural and historical tours or by offering programs with partners in tourism and entertainment sectors. Such initiatives would enrich the experience of health tourists and contribute to the growth of tourism sector by increasing their participation in other tourism activities. When directing health tourists to recreational activities, it is essential to consider capacities that the company can allocate for activities, associated costs, and the medical conditions of the tourists, as well as their preferences on various kinds of touristic activities. Balancing costs and revenue is crucial, and budget and health restrictions of tourists should be taken into account.

Medical tourism offers cost savings, access to treatments, and the opportunity to combine medical treatment with a vacation. A mathematical model that considers capacity constraints, costs, demand, and health restrictions can assist in directing health tourists to suitable recreational activities, generating revenue while providing a high-quality experience. To account for medical tourist satisfaction, the model should incorporate the preference of tourists regarding numerous touristic activity types.

This study aims to develop a model that jointly optimizes the profitability of health tourism along with medical tourist satisfaction by enabling healthcare tourists to engage in suitable touristic activities aligned with their preferences and medical schedule. By incorporating medical constraints associated with different activities available to medical tourists, as well as considering the cost, pricing, and operational constraints of recreational tourism businesses, this research seeks to guide the formulation of effective strategies for planning the operations of touristic service providers and directing a larger volume of patients towards diverse tourism activities.

Remaining of the paper is organized as follows. In Section 2, literature review on the applications of optimization in the tourism area and related operations research problems are presented. In Section 3, the problem is defined in its details delving into the practical aspects. Section 4 is dedicated to presenting the formal mathematical definitions and the integer programming models, culminating with an analysis of computational results derived from the integer programming model runs for a profit maximizing model and the biobjective model. Additionally, the construction and interpretation of the Pareto efficient frontier based on the biobjective integer programming model is discussed in Section 4. Finally, the paper is drawn to a conclusion in Section 5.

2. Literature Review

In recent years, there has been an increasing interest in utilizing operations research and optimization techniques to address the challenges in both healthcare area and tourism planning. This literature review initially focuses on the application of operations research and optimization in tourism planning, highlighting various studies that have addressed this problem.

Zhu et al. (2012) [1] present a study on the tour planning problem. They propose a framework for designing tour trips with desirable sites while considering budget and time constraints. To tackle the computational infeasibility of solving the mixed-integer linear programming problem, they develop a heuristic method based on local search ideas, which provides efficient and good approximation solutions.

Vansteenwegen et al. (2011) [2] introduce an expert system, which integrates a selection of attractions with the route plan. The study considers the interests and trip constraints of users, matching them to a database of locations to predict personal interests.

Brilhante et al. (2015) [3] propose, an unsupervised framework for planning personalized sightseeing tours in cities. They extract spatio-temporal information about tourists' itineraries from geo-referenced photo albums, matching them to Points of Interest. The personalized sightseeing tour recommendation is formulated as an instance of the Generalized Maximum Coverage problem, and the resulting trajectories are scheduled on the tourist agenda using a Traveling Salesman Problem approach.

Leong and Ladany (2001) [4] present a model for optimal cruise itinerary design, focusing on selecting destinations to visit, visit duration, and visit sequence. They employ a near-optimal heuristic approach to demonstrate the application of their model in selecting cruise itineraries, showcasing decision support capabilities for cruise operators.

Chia et al. (2016) [5] propose an offline approach for generating an optimal vacation routing plan, considering operating hours and duration of stay constraints. They utilize a traveling salesman problem algorithm to find the shortest path, but extend it by calculating arrival times and minimum stay durations at each stop for generating efficient plans that satisfy operating hours and duration of stay constraints.

Delalic et al. (2019) [6] introduce algorithms based on heuristic methods, such as simulated annealing

and genetic algorithms, for optimal city selection and concert tour planning. They emphasize the importance of including social media analytics, to maximize the profit and better analyze concert tour planning.

Jean-Marc (2005) [7] focuses on applying meta-heuristics, to problems devised on real-world sightseeing tour planning. The research aims to provide decision support for users in planning their trips and explores multiple objective combinatorial optimization problems.

Vargas and Sendales (2016) [8] optimize the schedule of a tourist trip plan in a city with complex street directions and numerous places of interest. They extend the Traveling Salesman Problem by minimizing the total distance traveled by tourists while ensuring they visit each place only once and return to the starting point.

Perera et al. (2018) [9] propose a platform for sustainable tourism management that includes prediction, optimization, and optimal path generation modules. Their optimization algorithms, including genetic algorithms and iterated local search, aim to determine the number of tourists that can be accommodated in each location while ensuring environmental sustainability. The optimal path generating problem is related to the Traveling Salesman Problem.

Silva et al. (2018) [10] address the problem of elaborating travel itineraries considering visitor profiles, travel distances, costs, and attraction values. They formulate the problem as a traveling salesman problem with profits and priority prizes. The authors present an optimization model based on mixed-integer programming and a tailored tabu search algorithm. They apply statistical techniques, such as multivariate correspondence analysis, to analyze real data.

Overall, these studies demonstrate the diverse approaches and effectiveness of operations research and optimization techniques in tourism planning. From heuristic methods and meta-heuristics to mathematical programming and hybrid approaches, these techniques provide decision support, optimize itinerary design, personalize trips, and consider

various constraints and objectives to enhance the tourism experience for travelers.

Applications of operations research in tourism planning have been framed into various classical optimization problem categories -mostly combinatorial- and mathematical program formulations. Scheduling problems involve the allocation of resources to tasks or activities to meet specific objectives. In the healthcare sector, scheduling problems arise in various contexts including surgical scheduling and appointment scheduling. Several studies have addressed scheduling problems in healthcare and proposed models and methods to solve them. Rahimi and Gandomi (2021) [11] provide an overview of operating room and surgical scheduling models and methods. Another study by Ala et al. (2023) [12] focuses on simulation approaches to appointment scheduling systems in healthcare. Reviews on appointment scheduling [13] and numerous other applications of scheduling in the context of healthcare [14] are available for the interested reader. Additionally, there are many studies for staff scheduling and rostering reviewed in [15,16] for general settings and in [17] for the context for hospitality management.

The proposed integer model addresses the unique problem defined in this study, which is in the intersection of healthcare and tourism, and aims to provide medical tourists with access to appropriate recreational activities based on their medical conditions, availability for different activity types, activity preferences and budgets. Our model aims to jointly maximize the total satisfaction points and profits earned from these tourists by an optimal assignment of medical tourists to different recreational activities.

3. Problem Definition

In recent years, medical tourism has gained popularity as hospitals and medical companies invest substantial resources in marketing and executing healthcare services internationally. Private hospitals often establish offices abroad to promote healthcare services provided in Türkiye and engage with potential patients, ensuring high-quality patient care through contracts and initial

assessments. Although patient schedule typically includes travel dates and appointments for examinations, tests, and treatments, recreational activities are seldom incorporated, if at all.

The healthcare service fees in Türkiye are relatively low compared to many European countries and the United States, making it an attractive option for residents who may not have insurance coverage or seek lower-priced alternatives. Moreover, Türkiye offers accessible healthcare services at affordable costs, including travel expenses. In both cases, medical tourists are usually on a budget and allocate a portion of their funds for international travel. This budget often includes expenses that would have been spent on leisure, recreation, and vacation had they not been visiting for healthcare purposes. Considering that most medical procedures do not severely limit patients, and when there are such limits, safe recreational alternatives are available, there is potential economic and welfare value in combining healthcare tourism with vacation and recreation themes. In addition to benefiting patients; hospitals, healthcare companies, and tourism companies can generate revenue by offering recreational activities to medical tourists. However, any recreational activities or vacations must be planned carefully, respecting the appointments and constraints imposed by the planned tests and treatments.

Tests, treatments and other medical procedures pose constraints, in ruling out certain tour types for certain days preceding or following the procedure. However, among the many other activity types available for the days not occupied by the procedures, the patient prefers some to the others. Therefore, it is crucial for the mathematical model to incorporate patient preference as well as the medical restrictions on optimizing assignment of touristic activities.

In our proposed framework, we assume that a tourism company specializing in recreational activities receives an anonymized list of medical tourists scheduled to arrive in Türkiye and depart on specific days within the planning horizon. The patient schedule, including the days dedicated to tests or treatments, is provided along with any constraints related to the patient condition and

medical procedures (see Table 1 for a list) that limit their participation in certain types of touristic activities. For instance, a cardiac evaluation may involve a reassessment on the third day following the tests, which blocks all activity types on that day, or an endodontic procedure may rule out gourmet tours for the four days that follow, but not trekking or sightseeing. Furthermore, it is assumed that a preference questionnaire is included within the medical tourism procedures, enabling the medical company to determine the preference scores the medical tourist attributes to various activities and the budget allocation specific to recreational activities outside healthcare services.

Table 1. *Medical procedures frequently applied in the context of healthcare tourism and considered in this study.*

Medical Procedures
General health check-up
Cardiac evaluation
Gastroenterological examination
Endoscopic examination
Ophthalmic examination
Refractive surgery
Dermatological evaluation
Dermatological intervention
Cosmetic surgery
Hair restoration surgery
Reconstructive plastic surgery
Dental examination
Endodontic therapy
Dental cavity filling
Physiotherapy

The healthcare tourism company organizes and conducts various types of vacations, touristic, and recreational activities (see Table 2 for a list). Each activity has a specific duration, and the company can schedule each tour type starting on any day throughout the planning horizon until the last day feasible for the completion of the activity. Each activity also has a capacity, indicating the maximum number of participants for activities starting on a specific day. Scheduling a tour on a particular day incurs fixed costs, representing expenses that do not vary with the number of tourists, such as tour guide fees and transportation vehicle rentals. Variable costs, on the other hand, depend on the number of

tourists and include expenses like individual transportation and accommodations.

Types of Vacation or Recreational/Touristic Acitivities
Seaside vacation
Blue voyage
Thermal vacation
Trekking
Natural and historical sightseeing
City tour
Gourmet tour
Pastoral retreat

In the following section, we develop an integer programming model to maximize the profits of a recreational tourism company. The model assigns one or more types of activities to healthcare tourists while respecting their medical constraints, recreational budget, and tour capacities.

4 Methods

4.1 The Integer Programming Model

The healthcare provider is considered to fix plans for a group of m medical tourists for the next T days. The tourism company follows along with this planning horizon, and offers n different activity types, activity type j at price p_j, with variable cost c_j, fixed cost f_j, duration d_j, and the activity type has capacity K_j, $j \in \{1, \dots, n\}$.

The healthcare provider anonymously provides the restriction schedule for each medical tourist, which determines which activity types can be attended on which days. Then, it is a matter of simple calculation with the duration of the activity type to compute the parameter U_{ijt} with binary value, indicating whether patient i can start activity j on day t.

Each medical tourist i has an arrival date A_i, denoting arrival at the beginning of the day, and departure date D_i, denoting departure at the end of the day, thus, $A_i, D_i \in \{1, \dots, T\}$. Tourist i has budget B_i, and also i has a preference on each activity type j, v_{ij},

which carries information on preference regarding both the kind of activity and its duration.

x_{ijt} is a binary variable indicating with value 1 if tourist i attends an activity of type j starting on day t. Variables x_{ijt} are defined unless their value will be fixed at 0, that is, on the index set

$$I = \{(i,j,t) \in S: U_{ijt} = 1, A_i \leq t, t + d_j - 1 \leq D_i\},$$

where $S = \{1, \dots m\} \times \{1, \dots, n\} \times \{1, \dots, T\}$. Five other index set definitions are practical for the mathematical programming formulation:

$$I_i = \{(j,t): (i,j,t) \in I\},$$

$$I_{jt} = \{i: (i,j,t) \in I\},$$

$$T_i = \{t: (i,j,t) \in I\},$$

$$T_{ij} = \{t: (i,j,t) \in I\},$$

$$S_{it} = \{(j,\tau): (i,j,\tau) \in I, max\,(t - d_j + 1, 1) \leq \tau \leq min(t - d_j + 1, T)\}.$$

First four of these are for indexing in one or two dimensions where x_{ijt} is defined, and the last one denotes the days such that an activity of type j that medical tourist i starts on these days continue on day t.

The binary variable y_{jt} denotes whether the tourism company initiates an activity of type j on day t. For y_{jt}, we define index sets for mathematical programming formulation notation as follows:

$$J = \{(j,t): j = 1, \dots n, \ t = 1, \dots, T - d_j + 1\}.$$

$$J_j = \{1, \dots, T - d_j + 1\}.$$

We formulate the integer program as follows:

$$max \sum_{(i,j,t) \in I} \left(\lambda p_j - \lambda c_j + \sigma(1-\lambda)v_{ij}\right) x_{ijt} \ - \lambda \sum_{(j,t) \in J} f_j y_{jt} \qquad (1)$$

$$s.t. \ \sum_{(j,\tau) \in S_{it}} x_{ij\tau} \leq 1 \qquad i = 1, \dots, m \ \ t \in T_i \qquad (2)$$

$$\sum_{t \in T_{ij}} x_{ijt} \leq 1 \qquad i = 1, \dots, m \ \ j = 1, \dots, n \qquad (3)$$

$$\sum_{i \in I_{jt}} x_{ijt} \leq K_j \, y_{jt} \qquad j = 1, \dots, n \ \ t \in J_j \qquad (4)$$

$$\sum_{(j,t) \in I_i} p_j \, x_{ijt} \leq B_i \qquad i = 1, \dots, m \qquad (5)$$

$$x_{ijt} \in \{0,1\} \qquad (i,j,t) \in I \qquad (6)$$

$$y_{jt} \in \{0,1\} \qquad j = 1, \dots, n \ \ t \in J_j. \qquad (7)$$

The objective function, (1), is the convex combination of the total preference points $\sum_{(i,j,t)\in I} v_{ij}\, x_{ijt}$ and profit $\sum_{(i,j,t)\in I}(p_j - c_j)\, x_{ijt} + \sum_{(j,t)\in J} f_j y_{jt}$ given a fixed coefficient λ representing relative weights of profit and tourist satisfaction. There is an additional factor, σ, assuring that profit and total preference have similar scales. The computation for this coefficient is discussed in Subsection 4.3.

Each medical tourist is busy with at most one activity on day t, considering activities of all type that can start on day t, or that can extend onto day t due to their durations. This is defined in the formulation by equation (2). Equation (3) constrains that each tourist is assigned to an activity of type j at most once. Equation (4) is the capacity constraint for activity j staring on day t, and equation (5) is the budget constraint for tourist i. (6)-(7) indicate that the problem is a pure integer programming problem.

4.2 Computational Results

There are 15 medical procedures that can be assigned to a patient with probabilities in Table 3, assigned uniformly in the planning horizon, possibly some coinciding on the same day. Each medical tourist is assigned a window of 15 days within the planning horizon, and medical procedures sampled according to probabilities in Table 3 are distributed uniformly in these 15 days. After the medical procedures are randomly assigned, additional days before the first and after the last procedures are added according to discrete uniform distribution (1,…,7), which set the arrival and departure dates. The head or tail side of the stay is extended if the window is at the end or beginning of planning horizon, respectively.

Table 3. Probabilities a patient receives a certain medical procedure.

Medical Procedure	1	2	3	4	5	6	7	8
Probability	0.08	0.1	0.15	0.05	0.2	0.2	0.15	0.05
Medical Procedure	9	10	11	12	13	14	15	
Probability	0.1	0.18	0.1	0.03	0.05	0.13	0.2	

The parameters for touristic activities offered by the company is in Table 4. Note that each activity type in Table 2 can be offered in alternative packages regarding number of days, for instance, one day seaside tours are available, as well as those up to seven days.

Table 4. Parameters for touristic activities offered by the tourism company. Each tour type is offered in various tour packages in different activity durations. Natural or historical sightseeing is shortly written as "sightseeing".

Activity	Duration d_j (days)	Price p_j (TL/person)	Variable Cost c_j (TL/person)	Fixed Cost f_j (TL)	Capacity K_j (#people)
Seaside 1	1	800	400	600	4
Seaside 2	2	1493	696	689	4
Seaside 3	3	2150	963	747	4
Seaside 4	4	2786	1213	792	4
Seaside 5	5	3405	1450	828	4
Seaside 6	6	4013	1677	859	4
Seaside 7	7	4610	1897	885	4
Blue Voyage 2	2	2898	0	7464	10
Blue Voyage 3	3	4259	0	10752	10
Blue Voyage 4	4	5598	0	13929	10
Blue Voyage 5	5	6920	0	17027	10
Blue Voyage 6	6	8229	0	20063	10
Blue Voyage 7	7	9527	0	23049	10
Thermal 1	1	500	300	400	4
Thermal 2	2	933	522	459	4
Thermal 3	3	1344	722	498	4
Thermal 4	4	1741	909	528	4
Trekking 1	1	300	80	300	15
Trekking 2	2	580	155	345	15
Trekking 3	3	852	227	374	15
Trekking 4	4	1120	299	396	15
Trekking 5	5	1384	369	414	15
Sightseeing 2	2	746	348	566	20
Sightseeing 3	3	1075	482	693	20
Sightseeing 4	4	1393	606	800	20
Sightseeing 5	5	1703	725	894	20
Sightseeing 6	6	2006	839	980	20
City Tour 1	1	500	250	200	30
City Tour 2	2	871	435	303	30
City Tour 3	3	1204	602	387	30
City Tour 4	4	1516	758	459	30
Gourmet Tour 1	1	700	400	300	15
Gourmet Tour 2	2	1352	746	487	15
Gourmet Tour 3	3	1988	1075	647	15
Pastoral Ret. 3	3	1527	456	498	15
Pastoral Ret. 4	4	1949	566	528	15
Pastoral Ret. 5	5	2357	669	552	15
Pastoral Ret. 6	6	2752	767	572	15
Pastoral Ret. 7	7	3137	861	590	15

Tourist budget is distributed uniformly between 2000 and 22000 TLs. Mean and standard deviations

of satisfaction scores for a sample of $m=300$ medical tourists is presented in Table 5.

Table 5. *Mean (top) and standard deviations (bottom) for tourist preference scores for various tour types and durations, from a sample of m=300 medical tourists. The score is per each day of the tour, v_{ij}/d_j is displayed, to point out the "boredom" effect, i.e., reducing marginal utility with each additional day in a specific tour type.*

	Tour Duration (days)						
	1	2	3	4	5	6	7
Seaside Vacation	7.85	7.71	7.63	7.59	7.58	6.27	5.53
	2.17	2.44	2.64	2.77	2.86	2.88	3.48
Blue Voyage	-	8.27	8.21	8.17	8.15	7.41	7.11
	-	2.03	2.19	2.31	2.39	2.89	3.94
Thermal Vacation	6.33	5.88	5.64	5.51	-	-	-
	2.74	3.23	3.51	3.66	-	-	-
Trekking	5.57	5.3	5.15	5.06	5	-	-
	2.86	3.12	3.3	3.41	3.48	-	-
Sightseeing	-	7.15	7.05	7	6.99	6.18	-
	-	2.78	2.99	3.15	3.26	3.31	-
City Tour	7.17	6.94	6.81	6.74	-	-	-
	2.59	2.92	3.13	3.27	-	-	-
Gourmet Tour	5.65	5.22	4.98	-	-	-	-
	2.89	3.27	3.5	-	-	-	-
Pastoral Retreat	-	-	5.51	5.4	5.33	4.12	3.43
	-	-	3.13	3.28	3.37	2.88	2.91

The number of activities is fixed as $n=39$. We initially compare the solution times of the integer programming model to a preliminary model (8)-(15) devised in [18], where arrival and departure dates are not defined, i.e., the medical tourists are assumed available throughout the short planning horizon considered in the study, except for medical restrictions. The model also does not incorporate tourist preference and has higher number of variables and constraints, not defining index sets used in (1)-(7):

$$max \sum_{i=1}^{m} \sum_{j=1}^{n} \sum_{t=1}^{T-d_j+1} (p_j - c_j) x_{ijt} - \sum_{j=1}^{n} \sum_{t=1}^{T-d_j+1} f_j y_{jt} \quad (8)$$

$$s.t. \quad \sum_{j=1}^{n} \sum_{\tau=max(1,t-d_j+1)}^{min(t,T-d_j+1)} x_{ij\tau} \leq 1 \quad i=1,...,m \quad t=1,...,T \quad (9)$$

$$\sum_{t=1}^{T-d_j+1} x_{ijt} \leq 1 \quad i=1,...,m \quad j=1,...,n \quad (10)$$

$$\sum_{i=1}^{m} x_{ijt} \leq K_j y_{jt} \quad j=1,...,n \quad t=1,...,T-d_j+1 \quad (11)$$

$$\sum_{j=1}^{n} \sum_{t=1}^{T-d_j+1} p_j x_{ijt} \leq B_i \quad i=1,...,m \quad (12)$$

$$x_{ijt} \leq U_{ijt} \quad i=1,...,m \quad j=1,...,n \quad t=1,...,T-d_j+1 \quad (13)$$

$$x_{ijt} \in \{0,1\} \quad i=1,...,m \quad j=1,...,n \quad t=1,...,T-d_j+1 \quad (14)$$

$$y_{jt} \in \{0,1\} \quad j=1,...,n \quad t=1,...,T-d_j+1. \quad (15)$$

8 data instances are generated for each of cases $m \times T = \{5,10,20\} \times \{30,40\}$. For each sample, (1)-(7) is solved setting $v_{ij} = 0$ for $i=1,...,m, j=1,...,n$, and $\lambda = 1$ (the integer programming model devised, "IP" solution). But also, arrival and departure dates are loosened for each medical tourist, $A_i = 1$ and $D_i = T$ for $i=1,...,m$ (this is called the "IP-A1DT" model. This is done for comparability with (8)-(15) (the "Preliminary" model). All models are solved for each case and sample instance using Gurobi Optimizer [19] as a single batch in randomized order running concurrently on an AMD Ryzen Threadripper 3960X 24-Core Processor, 32GB of RAM, with default solver settings except a time limit of 3600 seconds. The optimality threshold for relative gaps in objective values with the linear programming (LP) relaxation (IP gap, shortly) is set at 0.5%, in order to observe more terminations at optimality and compare solution times, particularly of IP-A1DT and Preliminary models.

Table 6 displays the average number of variables and constraints for each case. Arrival and departure dates additionally reduce the number of constraints besides variables for the IP model, since, for instance T_i is empty in (2) outside arrival-departure interval of a medical tourist. Besides reducing the number of variable and constraints, arrival and departure dates rule out many activity assignments significantly shortening solution time and reducing IP gaps at termination, when compared to corresponding IP-A1DT and Preliminary samples. Principally, the difference of the Preliminary model with IP-A1DT, is the constraint (13) and the larger number of variables associated with keeping in the model redundant variables corresponding to $U_{ijt}=0$ in the model (Table 6). Additionally, on days that the tourist is busy with a medical respective variable and constraints are not included in the model. Thus, the set indexing pays off for IP-A1DT as well, compared to the Preliminary model. Although this pattern is not supported for small instances, and is not visible for larger instances due to time limit (Figure 1), IP gaps for larger instances point out the efficiency gain by IP-A1DT (Figure 2).

Table 6. Number of variables and constraints for IP, IP-A1DT and Preliminary models with different problem sizes, as averages over samples of size 8.

		Number of Variables		
m	T	IP	IP-A1DT	Preliminary
5	30	2075	4834	6408
	40	2329	7080	8748
10	30	3171	8480	11748
	40	3446	12538	16038
20	30	5324	16433	22428
	40	5559	24085	30618
50	30	11416	38369	54468
	40	11292	58166	74358
		Number of Constraints		
m	T	IP	IP-A1DT	Preliminary
5	30	1319	1404	6758
	40	1705	1843	9148
10	30	1573	1734	12448
	40	1962	2226	16838
20	30	2077	2412	23828
	40	2465	2996	32218
50	30	3589	4410	57968
	40	3958	5305	78358

A computational evidence on the complexity of the problem is apparent, as an increase in planning horizon from 30 to 40 increases computation times for small instances more than two folds, and doubling number of tourists has an effect of several folds.
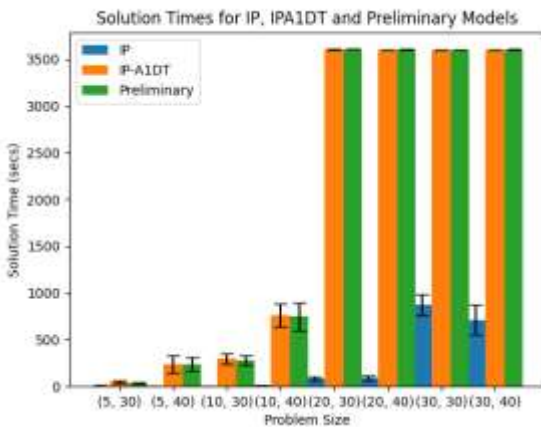

Figure 1. *Solution times for IP, IP-A1DT and Preliminary models for $m \times T = \{5,10,20\} \times \{30,40\}$. Whiskers on bars represent standard errors for samples of size 8.*

Efficient solution of IP, is critical for iterations required for determining the Pareto-efficient frontier in the biobjective setting of (1)-(7). The results for the biobjective approach are discussed in the next section.
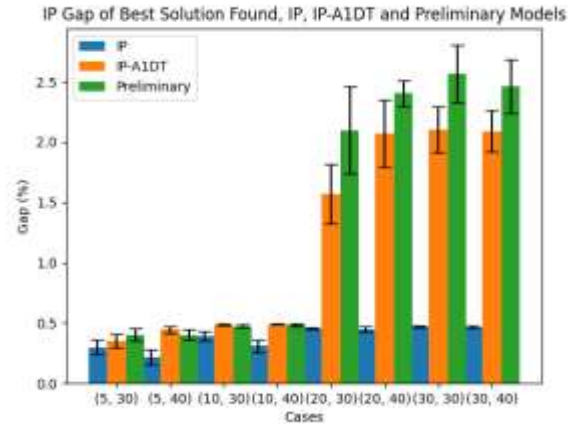

Figure 2. *IP gaps for IP, IP-A1DT and Preliminary models for $m \times T = \{5,10,20\} \times \{30,40\}$. Bars represent averages and whiskers on bars represent standard errors for samples of size 8. Due to reaching time limit for large instances, efficiency of IP-A1DT and Preliminary models can be compared by lower gaps for IP-A1DT.*

4.3 The Pareto-efficient Frontier

Before delving into the application of the Weighted Objective method and the derivation of the Pareto-efficient frontier, it is essential to provide a concise overview of biobjective optimization. When dealing with multiobjective problems, various approaches, such as Lexicographic Ordering and Goal Programming, can be considered. In Lexicographic Ordering, one of the objectives takes precedence, and the optimization process strives to achieve the best possible outcome in the primary objective before addressing the secondary objectives. In our context, prioritizing profits over tourist satisfaction may seem logical at first glance. However, our analysis of the Pareto-efficient frontier reveals that such a prioritization could lead to missed opportunities for exceptionally high levels of customer satisfaction. Goal Programming, on the other hand, formulates the problem by setting specific target values for both objectives and aims to minimize deviations from these targets while optimizing the overall solution. In our study, determining specific target values for customer satisfaction, which is subject to individual patient

preferences, proves to be a challenging task. Additionally, the unpredictable schedule availability of customers further complicates this approach. Moreover, due to the combinatorial complexity of our problem, estimating profit scales in advance is not feasible, making Goal Programming less suitable. The Epsilon-Constraint Method would similarly require numerous explorative steps to set limits on the secondary objective. In contrast, the results obtained from a Pareto analysis provide a more straightforward and readily available perspective. Therefore, in this study, we opt for the Weighted Objective approach to address the biobjective programming challenge effectively. This method, when coupled with efficient integer programming solutions, allows us to derive the Pareto-efficient frontier for various problem instance sizes. The Pareto-efficient frontier represents a spectrum of trade-offs between the two objectives, enabling decision-makers to select a solution that aligns with their strategic preferences. The relative weight parameter λ represents the importance assigned by the decision maker, typically the tourism company, to the strategic approach of balancing medical tourist satisfaction and profit. The specific strategic choices available in terms of these two criteria can only be determined by iteratively solving the model with a range of λ values and obtaining the Pareto-efficient frontier. The Pareto-efficient frontiers are obtained for each test instance with synthetic data of various sizes (cases: $m \times T = \{50,100,150\} \times \{40\}$), by solving (1)-(7) for known only after iteratively solving the model for λ values ranging from 0 to 1.

For each data instance, the coefficient σ is computed to bring the two objective components to similar scales. The model is run twice for the respective data instance, separately optimizing for profit ($\lambda = 1$) and medical tourist satisfaction ($\lambda = 0$), with a time limit of 600 seconds and an IP gap of 10%. σ is calculated as the ratio of the linear relaxation upper bounds of profit maximization and satisfaction maximization, which are at most 10% away from the approximated maximum values attainable for profit and satisfaction. For each data instance, initially the coefficient σ that brings the two objective components to similar scales is computed. The model is run for the respective data instance twice, for profit (λ=1) and medical tourist satisfaction

(λ=1) objectives separately, with a time limit of 600 seconds and an IP gap of 10%. σ is then the ratio of linear relaxation upper bounds of profit maximization and satisfaction maximization, which are at most 10% off from the approximated maximum values attainable for profit and satisfaction. The runs for the range of λ for constructing the Pareto-efficient frontier are taken as a batch for each problem size on the hardware and software setting mentioned above, with a time limit of 7200 seconds and an IP gap of 0.5%.

Figure 3 displays Pareto-efficient frontiers for $m \times T = \{50,100,150,250\} \times \{40\}$. The results indicate that the strategic decision is not difficult for the company, as it is possible to achieve significant portions of the maximum attainable profit and satisfaction performance simultaneously. When λ is close to 0.5 for *m=150, 200*, and to 0.6 for *m=50, 100*, nearly 70% of maximum attainable tourist satisfaction and 80% of maximum attainable profit is achieved. Then, with an equal weight given to performance criteria, a high level of total satisfaction score is attained with only a minimal compromise in profit.
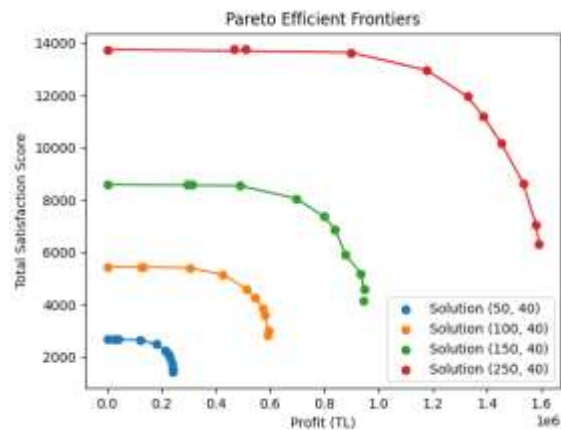

Figure 3. *Pareto-efficient frontiers for problem sizes $m \times T = \{50,100,150,250\} \times \{40\}$. The range for weight parameter λ is [0, 1e-6, 1e-3, .05, .15, .3, .4, .5, .6, .65, .7, .75, .8, .85, .9, .95, 1] for m=150, 200, and [0, 1e-6, 5e-4, .1, .3, .5, .6, .7, .8, .9, 1] for m=50, 100. For display purpose, profit values are replaced by 0 for $\lambda = 0$ cases. Actual profit in each problem size is a very large negative value for pure tourist satisfaction maximization, and the curves extend horizontally to the left.*

The company increases profits within the same planning horizon as the number of tourists registered in the plan increases, as indicated by shift in Pareto-

efficient frontiers, which is in proportion to number of tourists. This is possible due to the optimization that tightly schedules the growing number of tourists, taking into account the capacity and alternative days available for each specific tour. The relatively larger instances analyzed here mostly terminate due to the time limit. IP gaps are close to the limit for termination at optimality (0.5%) for the smaller instance ($m=50$). However, when comparing the problem sizes, a clear pattern emerges where the IP gaps increase with the problem size, as shown in Figure 4. A company that solves problems at this scale and plans for a horizon of several weeks can reasonably increase the solution time limit set at 7200 seconds for computational tests, to gain up to 3% in medium sized instances ($m=100, 150$) and 4% in the larger instance ($m=200$).
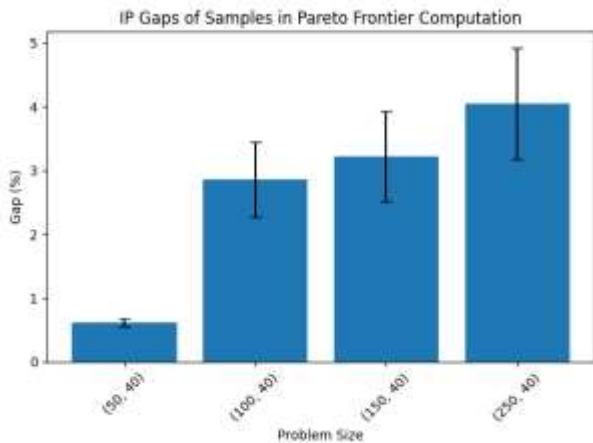

Figure 4. *IP gaps for best solutions found in computations with $m \times T = \{50,100,150,250\} \times \{40\}$. Bars represent sample means and whiskers represent standard errors, for the sample size according to the range used for λ.*

5 Conclusion

The proposed model in this study incorporates the health restrictions and preferences of health tourists when recommending various touristic activities. It takes into account the medical procedure undergone by the medical tourist and their corresponding health restrictions, ensuring that suitable activities are recommended based on medical constraints and preferences to enhance their overall experience. The model also considers the capacity and costs associated with different touristic activities while simultaneously maximizing the weighted sum of

profit for the tourism company and the overall satisfaction of the tourists within the planning horizon. By deriving the Pareto-efficient frontier for the two criteria, the model provides insights for the company to make trade-offs between profit and customer satisfaction. Immediate research directions arising for this problem concern more efficient solutions of larger problem instances. Enhancing solver times by Branch-and-cut approaches require finding out very effective cuts. Population based search heuristics are candidate approaches for quick solution of larger instances, but for the large solution space defined by triple indexing and complex set of constraints, their performance in terms of time and solution performance to optimality might remain restricted. A viable research direction that can be followed is matheuristics, combining the efficient exploration of the search tree by integer programming solvers with the potential of heuristics to find quick incumbents of high quality. Research directions stemming immediately from this problem primarily revolve around devising more efficient solutions for handling larger instances of the problem. To expedite solver runtimes through the application of Branch-and-Cut approaches, the key lies in identifying exceptionally effective cutting planes. While population-based search heuristics present themselves as promising candidates for solving larger instances, their performance in terms of both time efficiency and solution optimality may be constrained when confronted with the expansive solution space characterized by triple indexing and a complex web of constraints. One fruitful research direction worth pursuing involves the utilization of matheuristics. Matheuristics entail harnessing the dual strengths of integer programming solvers for systematically exploring the search tree and the capability of heuristics to swiftly identify high-quality solutions. This hybrid approach holds the potential to strike a harmonious balance between efficiency and solution quality, making it a compelling avenue for further investigation. Future research additionally could explore different settings of the problem where medical tourists are offered scheduled activities but have the option to accept or decline based on their preferences. This might require scenario generation under probability models and potentially employ bilevel approaches to address the problem effectively.

Author Statements:

- **Ethical approval:** The conducted research is not related to either human or animal use.
- **Conflict of interest:** The authors declare that they have no known competing financial interests or personal relationships that could have appeared to influence the work reported in this paper
- **Acknowledgement:** A preliminary version of the integer programming model in this article is computationally analyzed in the scope of master's thesis study of Ekin Yıldırım.
- **Author contributions:** The authors declare that they have equal right on this paper.
- **Funding information:** The authors declare that there is no funding to be acknowledged.
- **Data availability statement:** The data that support the findings of this study are available on request from the corresponding author. The data are not publicly available due to privacy or ethical restrictions.

References

[1]Zhu, C., Hu, J. Q., Wang, F., Xu, Y., & Cao, R. (2012). On the tour planning problem. *Annals of Operations Research*, 192(1); 67–86. https://doi.org/10.1007/s10479-010-0763-5

[2]Vansteenwegen, P., Souffriau, W., Berghe, G. V., & Oudheusden, D. V. (2011). The City Trip Planner: An expert system for tourists. *Expert Systems with Applications*, 38(6); 6540–6546. https://doi.org/10.1016/j.eswa.2010.11.085

[3]Brilhante, I. R., Macedo, J. A., Nardini, F. M., Perego, R., & Renso, C. (2015). On planning sightseeing tours with TripBuilder. *Information Processing & Management*, 51(2); 1–15. https://doi.org/10.1016/j.ipm.2014.10.003

[4]Leong, T.-Y., & Ladany, S. P. (2001). Optimal cruise itinerary design development. *International Journal of Services Technology and Management*, 2(1–2); 130–141. https://doi.org/10.1504/IJSTM.2001.001595

[5]Chia, W. C., Yeong, L. S., Xian Lee, F. J., & Ch'ng, S. I. (2016). Trip planning route optimization with operating hour and duration of stay constraints. *2016 11th International Conference on Computer Science & Education (ICCSE)*, 395–400. https://doi.org/10.1109/ICCSE.2016.7581613

[6]Delalić, S., Chahin, M., & Alihodžić, A. (2019). Optimal City Selection and Concert Tour Planning Based on Heuristic Optimization Methods and the Use of Social Media Analytics. *2019 XXVII International Conference on Information, Communication and Automation Technologies (ICAT)*, 1–6. https://doi.org/10.1109/ICAT47117.2019.8939040

[7]Jean-Marc, G. (2005). Challenges in real world sightseeing tour optimization using meta-heuristics. *Proceedings of the 6th WSEAS International Conference on Evolutionary Computing*, 233–238.

[8]Vargas, D. F. V., & Sendales, D. A. P. (2016). Optimal scheduling trip plan for tourist. *2016 10th International Conference on Intelligent Systems and Control (ISCO)*, 1–5. https://doi.org/10.1109/ISCO.2016.7727111

[9]Perera, D., Rathnayaka, C., Dilan, S., Siriweera, L., & Rankothge, W. H. (2018). Sustainable Tourism: Application of Optimization Algorithms to Schedule Tour Plans. *2018 IEEE Region 10 Humanitarian Technology Conference (R10-HTC)*, 1–6. https://doi.org/10.1109/R10-HTC.2018.8629826

[10]da Silva, A. A., Morabito, R., & Pureza, V. (2018). Optimization approaches to support the planning and analysis of travel itineraries. *Expert Systems with Applications*, 112; 321–330. https://doi.org/10.1016/j.eswa.2018.06.045

[11]Rahimi, I., & Gandomi, A. H. (2021). A Comprehensive Review and Analysis of Operating Room and Surgery Scheduling. *Archives of Computational Methods in Engineering*, 28(3); 1667–1688. https://doi.org/10.1007/s11831-020-09432-2

[12]Ala, A., Simic, V., Deveci, M., & Pamucar, D. (2023). Simulation-Based Analysis of Appointment Scheduling System in Healthcare Services: A Critical Review. *Archives of Computational Methods in Engineering*, 30(3); 1961–1978. https://doi.org/10.1007/s11831-022-09855-z

[13]Ala, A., & Chen, F. (2022). Appointment Scheduling Problem in Complexity Systems of the Healthcare Services: A Comprehensive Review. *Journal of Healthcare Engineering*, e5819813. https://doi.org/10.1155/2022/5819813

[14]Abdalkareem, Z. A., Amir, A., Al-Betar, M. A., Ekhan, P., & Hammouri, A. I. (2021). Healthcare scheduling in optimization context: A review. *Health and Technology*, 11(3); 445–469. https://doi.org/10.1007/s12553-021-00547-5

[15]Van den Bergh, J., Beliën, J., De Bruecker, P., Demeulemeester, E., & De Boeck, L. (2013). Personnel scheduling: A literature review. *European Journal of Operational Research*, 226(3); 367–385. https://doi.org/10.1016/j.ejor.2012.11.029

[16]Ernst, A. T., Jiang, H., Krishnamoorthy, M., & Sier, D. (2004). Staff scheduling and rostering: A review of applications, methods and models. *European Journal of Operational Research*, 153(1); 3–27. https://doi.org/10.1016/S0377-2217(03)00095-X

[17]Rocha, M., Oliveira, J. F., & Carravilla, M. A. (2012). *Quantitative Approaches on Staff Scheduling and Rostering in Hospitality Management: An Overview*. . https://doi.org/10.4236/ajor.2012.21016

[18]Yıldırım, E. (2023). *An Integer Programming Model of Recreational Planning in Medical Tourism* [Master's Thesis]. Gebze Technical University.

[19]Gurobi Optimization, LLC. (2023). *Gurobi Optimizer Reference Manual*. https://www.gurobi.com

Pyoderma Gangrenosum: Retrospective Evaluation of Clinical Features and Treatment Responses in 23 Cases

Zeynep Büşra BALIK[1]*, Gülşen AKOĞLU[2]

[1] Health Sciences University Gülhane Training and Research Hospital Department of Dermatology, Ankara-Turkey
* **Corresponding Author**: Zeynep Büşra BALIK, **Email:** zeynepbusrakucuker@gmail.com - **ORCID:** 0000-0003-3578-3511

[2] Health Sciences University Gülhane Training and Research Hospital Department of Dermatology, Ankara-Turkey
Gülşen AKOĞLU, **Email:** drakoglug@gmail.com - **ORCID:** 0000-0002-9483-6268

Abstract:

Pyoderma gangrenosum (PG) is a rare inflammatory disease in the spectrum of neutrophilic diseases characterized by rapidly progressive, painful and large ulcers. In this study, we aimed to investigate the relationship between the clinical characteristics and treatment responses of patients diagnosed with PG, treated and followed up in our clinic. Between 2018 and 2023, 23 patients diagnosed with PG in our clinic were included in the study. Medical file records were retrospectively analyzed and various demographic and clinical characteristics, comorbid systemic diseases, treatment protocols and treatment responses of the patients were recorded. Twelve (52.2%) of the patients were female and 11 (47.8%) were male, with a mean age of 42.4 ± 12.9 years. The median disease duration was 52 months (range: 10-540 months). Systemic diseases accompanying PG were present in 14 patients (60.9%). Systemic steroids were the most common treatment (43.5%). Other treatment approaches included adalimumab, infliximab, cyclosporine, oral doxycycline, topical tacrolimus, topical corticosteroids and intralesional steroids. Remission was achieved in 14 patients (60.9%), relapse was observed in 5 patients (21.74%), and no remission/relapse information was available for 4 patients (17.4%) who lost follow-up. The median duration of remission was 23 months (range: 3-96 months). Although systemic steroids are most commonly used in the treatment of pyoderma gangrenosum, it should be kept in mind that there are various treatment options ranging from systemic and topical anti-inflammatory therapies to biologic agents according to close follow-up of the patients and additional systemic diseases.

1. Introduction

Pyoderma gangrenosum (PG) is a non-toxic skin disease belonging to the group of neutrophilic dermatoses, which also includes Sweet syndrome and Behçet syndrome. The incidence of this disease is estimated to be approximately 0.63 per 100,000 people and the average age of onset is 59 years [1]. The pathogenesis of PG is unclear, but neutrophils are recognized to play an important role in the disease process [2]. After patients receive antigen priming, helper T (Th) 17/Th1 bias leads to the development of an autoinflammatory environment dominated by tumor necrosis factor-α (TNF-α), leukocyte-mediated IL level, and neutrophils. IL-1β, IL-1α, IL-8, IL-12, IL-15, IL-17, IL-23 and IL-

36 [3, 4]. Most of PG is the classic form (approximately 85%), but other subtypes include bullous, vegetative, pustular, peristomal, and superficial granulomatous forms, and PG subtypes may differ from one form to another [5]. Diseases commonly associated with PG include inflammatory bowel disease, rheumatoid arthritis, hematological malignancies, and monoclonal immunoglobulin A (IgA) gamma disease [6] .

PG treatment is usually preventive and there is no universally accepted treatment, but corticosteroid treatment can be done. Oral cyclosporine is a widely used drug [7]. In recent years, drugs in the form of TNF-α inhibitors have begun to be used, and some recent studies have shown the effectiveness of TNF-α inhibitors in the treatment of PG [8].

This study aimed to evaluate the relationship between clinical features and response to treatment in patients diagnosed with PG treated in our hospital.

2. Material and Methods

This study included 23 patients diagnosed with PG who were treated and followed up at the Dermatology and Venereology Clinic of Ankara Health Sciences University Gülhane Training and Research Hospital between January 1, 2018 and April 1, 2023. Medical records were reviewed retrospectively. Information obtained about the patient's various demographic characteristics (age, gender, diseases in the body, etc.) and response to treatment characteristics (course of pain, dermatological findings, type and location, histopathological and diagnosis, treatment and treatment) are recorded. . SPSS 22.0 program was used to analyze the data and perform the descriptive analysis.

3. Results and Discussions

Of the 23 patients included in the study, 12 were female (52.2%) and 11 were male (47.8%). The mean age was 42.4±12.9 years (mean age in men: 44.64±13.7 years; mean age in women: 40.3±12.9 years). When the presenting complaints of the patients were analyzed, it was observed that pyoderma gangrenosum presented as ulcer in 13 patients (56.5%), plaque in 5 patients (21.7%), inflamed nodule in 4 patients (17.4%) and bullae in 1 patient (4.4%). The number of lesions varied between 1 and 17. The median disease duration was 52 months (range: 10-540 months). In four patients, PG lesions appeared in the postoperative period (after mammoplasty, varicose vein surgery). The lesions were present in 13 (56.5%) legs, 6 (26.1%) feet, 4 (17.4%) ankles, 3 (13%) inguinal, 2 (8.7%) breast, 2 (8.7%) gluteal, 2 (8.7%) genital, 2 (8.7%) trunk, and 1 (4.4%) shoulder lesions. There was a history of comorbid systemic disease in 14 patients (60.9%) (inflammatory bowel disease in 3 patients, anemia in 3 patients, Behçet's disease in 2 patients, rheumatoid arthritis in 2 patients, hidradenitis suppurativa in 2 patients, 1 patient with familial Mediterranean fever, 1 patient with ankylosing spondylitis, 1 patient with polychondritis, 1 patient with systemic lupus erythematosis overlap syndrome, 1 patient with venous insufficiency, 1 patient with osteomyelitis, 1 patient with hypertension, 1 patient with fulminant acne). Seventeen (73.9%) patients were treated as outpatients and 6 (26.1%) were hospitalized. Histopathologic examination was performed in 20

patients (24.4%) and nanspecific chronic inflammation findings were detected. Tissue/wound culture samples were obtained from 12 patients (52.2%). Growth was detected in 4 patients. The pathogens were S. aureus (2 patients), S. pyogenes (1 patient), E. coli (1 patient). Patients with growth were given agent-sensitive systemic antibiotherapy. For pyoderma gangrenosum, three patients received adalimumab (80 mg/week, then 40 mg/week maintenance), 3 patients received infliximab (5-10 mg/kg/day 0.-2.-6. weeks, then every 8 weeks), systemic steroid (0.5-1 mg/kg methylprednisolone) in 10 patients, topical tacrolimus in 4 patients, topical steroid (0.05% clobetasol propionate) in 4 patients, intralesional steroid (5 mg/ml triamcinoloneacetonide) in 2 patients, cyclosporine (3-5 mg/kg/day) in 2 patients, oral doxycycline (200 mg/day) in 2 patients (Table 1). One patient was switched to infliximab due to cyclosporine side effects, but no treatment-related side effects were observed in the other patients.

Remission was achieved in 14 patients (60.9%), relapse was observed in 5 patients (21.7%), and no remission/relapse information was available for 4 patients (17.4%) who were lost to follow-up. The median duration of remission was 23 months (3-96 months). During the period analyzed, 1 patient who discontinued infliximab treatment due to the COVID-19 pandemic, 1 patient whose infliximab treatment was discontinued due to remission developed relapse after cat scratching, and 1 patient who received systemic steroid treatment with adalimumab treatment developed relapse while the steroid dose was reduced. One patient was in remission under adalimumab treatment and relapse was detected after inguinal hernia operation (Figure 1). One patient who received systemic steroid treatment developed relapse due to non-compliance with the treatment regimen. Pyoderma gangrenosum is a rare disease in the neutrophilic spectrum, characterized by rapid growth, pain and large lesions [9, 10]. It has been reported that women between the ages of 20-50 years are more affected by this disease than men [11]. In our study, it was observed that the majority of the patients were women. Pyoderma gangrenosum is observed more rarely in infants, children and the elderly. Among our patients, only adult patients were found and two of them developed PG at an advanced age. Although it has been reported that pyoderma gangrenosum frequently develops as a result of minor traumas and Köbner phenomenon, most of the cases do not have a history of trauma [12 ,13]. In our study, a history of trauma was found in only four of 23 cases and it is remarkable that PG developed postoperatively.

***Figure 1.** Complete response with infliximab treatment in a 59-year-old patient who developed recurrence after inguinal hernia operation, in remission for 5 months.*

***Figure 2.** 39-year-old male patient with ulcerated lesion in the lower leg, complete healing with systemic steroid treatment, in remission for 4 years.*

In pyoderma gangrenosum, the diagnosis is usually made with clinical features [14, 15]. Lesions start suddenly as painful nodules, pustules and/or papules. In patients with active lesions, the appearance of a hemorrhagic, suppurative and necrotic almost "swampy" appearance with indistinct, irregular, red-purple, hemorrhagic, suppurative and necrotic appearance surrounded by an erythematous halo should clinically suggest PG [10]. In our study, lesions were ulcerative type in most of the cases. In pyoderma gangrenosum, lesions are usually localized as a single lesion on the anterior surface of the tibia in the lower extremity. Atypical forms are more superficial and may be localized on the face, head-neck, breast, arm, hand and especially on the peristomal skin [9, 11, 16, 17]. Kim [18], Güngör [12] and Farrell [13] reported cases with PG localized atypically on the penis. In our study, PG was localized as a single lesion (56.5%) and in the lower extremities (82.6%) in most of the patients in accordance with the literature.

It has been reported that more than 50% of patients with pyoderma gangrenosum are associated with systemic diseases [11]. It may accompany rheumatologic and hematologic diseases, most commonly inflammatory bowel diseases [19], monoclonal gammopathies [9], hidradenitis suppurativa [20] and iatrogenic immunosuppression [21] or malignancies [19]. In our study, 65.2% of patients were accompanied by systemic diseases. Hasselmann et al. reported an association with inflammatory bowel disease with a rate of 33% [22]. In our study, inflammatory bowel disease was present in 13% of our patients. Waldman et al. reported a patient diagnosed with SLE 8 years after the development of PG [23]. In our study, SLE dermatomyositis overlap syndrome was present in one patient. While autoimmunity is blamed in SLE, humoral immunity, cell-mediated immunity and neutrophil dysfunction are more prominent in PG than autoimmunity, but the pathogenesis is not completely clear although the role of T cells has been emphasized in recent years [24]. The association of Hidradenitis suppurativa (HS) and PG is rarely reported in the literature. In the study of Weng et al. the association of HS and PG was reported in a series of 6 cases [20]. In our series, HS was associated with PG in two patients. In hidradenitis suppurativa, dysfunctional neutrophils and immune pathway dysfunction are involved in the pathogenesis [20]. It was thought that PG might have developed in the course of HS because of similar pathways. Coexistence of Behçet's disease and PG can be observed [25]. Two of our patients had a diagnosis of Behçet's disease.

High-dose systemic corticosteroids are the treatment of choice for pyoderma gangrenosum. Topical and intralesional corticosteroids can be used for mild pain. Immunosuppressants, intravenous immunoglobulins, and biologics are used in resistant patients [26–30]. The anti-inflammatory effects of corticosteroids are attributed to their transcriptional effects, particularly inhibition of NF-κB and subsequent reduction of many pro-inflammatory cytokines, chemokines and cell adhesion molecules [31] . Corticosteroid treatment (prednisolone dose of 0.5-1 mg/kg/day) provides cure in approximately 40-50% of patients [32]. The steroids we frequently use in our patients allow us to go into remission (Figure 2).

Cyclosporine is an antiviral drug used in the first-line treatment of PG. Cyclosporine is a calcineurin inhibitor that inhibits the synthesis of IL, especially IL-2, which is important for preventing T lymphocyte activation [33]. In a randomized controlled study, prednisolone (0.75 mg/kg/day, maximum 75 mg) and cyclosporine (4 mg/kg/day, maximum 400 mg) responses were compared in 121 PG patients and no difference was found and 47% of patients in both groups recovered in six months [7]. In our study, complete response was obtained in 2 patients who received cyclosporine treatment.

Doxycycline is a tetracycline group antibiotic. Doxycycline reduces proinflammatory cytokines such as interleukin (IL) 1β, IL-6 and TNF- α. It is widely used in dermatology in many diseases such as acne, rosacea, bullous pemphigoid and perforating dermatosis due to its anti-inflammatory properties and good safety profile [34]. There are studies showing that tetracyclines are beneficial in the treatment of PG [35]. Anuset et al. treated 23 of 42 PG patients with doxycycline 200 mg/day as monotherapy or in combination with topical steroid or topical tacrolimus, 15 patients with systemic steroid as monotherapy or in combination, and 4 patients were followed up with other treatment modalities (colchicine, dapsone, topical steroid only). Doxycycline and systemic corticosteroid treatment responses were found to be comparable and the recurrence rate was lower in the doxycycline group [35]. In our study, complete response was obtained in 2 patients who received doxycycline treatment.

Tacrolimus is an immunomodulator that acts by inhibiting T lymphocyte activation [7]. It inhibits T lymphocyte activation by inhibiting interleukin 2 (IL-2) gene expression. It has also been shown to inhibit gene transcription of IL-3, IL-4, interferon-α, TNF-α, and granulocyte-macrophage colony-stimulating factor. Additionally, tacrolimus blocks mast cell, neutrophil, basophil and cytotoxic T cell degranulation. The specific mechanism by which tacrolimus improves PG remains unclear. However, since PG is characterized by central neutrophil and peripheral lymphocyte infiltration, tacrolimus can effectively treat PG by inhibiting the accumulation and activation of lymphocytes and neutrophils [36]. In a study comparing 24 patients with peristomal PG, 11 patients were treated with topical tacrolimus 0.3% monotherapy and 13 patients were treated with topical clobetasol propionate 0.05%. Seven patients in the tacrolimus group improved in an average of 5.1 weeks, and five patients in the clobetasol propionate group improved in an average of 6.5 weeks. Topical tacrolimus is better for patients with lesions larger than 2 cm in diameter. Response and treatment duration were better in the tacrolimus group than in the steroid group [37]. This study recommends adding tacrolimus to the treatment to increase the effectiveness of the treatment.

Tumor necrosis factor-α is an important pro-inflammatory pleiotropic cytokine that regulates IL1-β, IL-6 and IL-8. Tumor necrosis factor is a potent chemokine that acts as a chemoattractant and works synergistically with TNF-α to promote and maintain a proinflammatory state. Expression of TNF-α and its receptors is increased in the PG region of the skin [38]. Growing evidence supports the use of TNF-α inhibitors, particularly infliximab and adalimumab, as first-line therapy. In fact, a partial analysis showed that the response to TNF-α inhibitors was 67% (238/356 patients) and the overall response was 87% [8] . To date, infliximab remains the only anti-TNF-α agent shown to be effective in classic PG, as demonstrated in a randomized, double-blind study [39] . Recently, a phase III, open-label, multicenter study was conducted in 22 Japanese patients to evaluate the efficacy and safety of adalimumab in refractory PG. At the end of 26 weeks of treatment, 55% of participants fully recovered [40]. In this study, patients treated with TNF-α inhibitors had a good response, although relapses occurred due to various factors (treatment, trauma).

Surgical treatment is highly controversial in PG, and most of the autonomists think that PG is a "pathergy" reaction and trauma may exacerbate the lesions. Therefore, surgical aggressive approaches should be avoided in PG.

Recurrence can be an important problem in the follow-up after PG treatment. Mlika et al. reported a recurrence rate of 46% [9]. In our study, recurrence was found in 5 cases (21.7%).

In conclusion, although PG is rare, it is a disease that may accompany various systemic diseases, most commonly with ulcers and should be

considered in the differential diagnosis. Although systemic steroids are the most common treatment given to patients, it should be kept in mind that there are various treatment options ranging from systemic and topical anti-inflammatory therapies to biological agents according to close follow-up of the patients and additional systemic diseases.

4. Conclusions

In conclusion, although PG is rare, it is a disease that may accompany various systemic diseases, most commonly with ulcers and should be considered in the differential diagnosis. Although systemic steroids are the most common treatment given to patients, it should be kept in mind that there are various treatment options ranging from systemic and topical anti-inflammatory therapies to biological agents according to close follow-up of the patients and additional systemic diseases.
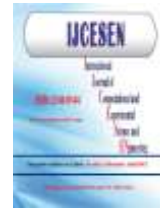
Author Statements:

- **Ethical approval:** The conducted research is not related to either human or animal use.
- **Conflict of interest:** The authors declare that they have no known competing financial interests or personal relationships that could have appeared to influence the work reported in this paper
- **Acknowledgement:** The authors would like to thank Dr. Zeynep Rümeysa Çelik for her contribution to the study.
- **Author contributions:** The authors declare that they have equal right on this paper.
- **Funding information:** The authors declare that there is no funding to be acknowledged.
- **Data availability statement:** The data that support the findings of this study are available on request from the corresponding author. The data are not publicly available due to privacy or ethical restrictions.

References

[1]Langan, S.M., Groves, R.W., Card, T.R., Gulliford, M.C. (2012). Incidence, mortality, and disease associations of pyoderma gangrenosum in the United Kingdom: a retrospective cohort study. *J Invest Dermatol*. 132(9):2166-2170. DOI: 10.1038/jid.2012.130.

[2] Braun–Falco, M., Kovnerystyy, O., Lohse, P., Ruzicka, T. (2012). Pyoderma gangrenosum, acne, and suppurative hidradenitis (PASH) – a new autoinflammatory syndrome distinct from PAPA syndrome. *J Am Acad Dermatol*. 66(3):409-415. DOI: 10.1016/j.jaad.2010.12.025.

[3]Ortega-Loayza, A.G., Nugent, W.H., Lucero, O.M., Washington, S.L., Nunley, J.R., Walsh, S.W. (2018). Dysregulation of inflammatory gene expression in lesional and nonlesional skin of patients with pyoderma gangrenosum. *Br J Dermatol.* 178(1):e35–e36. DOI: 10.1111/bjd.15837.

[4]Ortega-Loayza, A.G., Friedman, M.A., Reese, A.M., Liu, Y., Greiling, T.M., Cassidy, P.B., … rosenbaum, J.T. (2022). Molecular and cellular characterization of pyoderma gangrenosum: implications for the use of gene expression. *J Investig Dermatol.* 142(4):1217-1220. DOI: 10.1016/j.jid.2021.08.431.

[5]Weenig, R.H., Davis, M.D., Dahl, P.R., Su, W.P.D. (2002). Skin ulcers misdiagnosed as pyoderma gangrenosum. *N Engl J Med*. 347:1412–1418. DOI: 10.1056/NEJMoa013383.

[6]Chevrant-Breton, J., Logeais, B., Pibouin, M. (1989). Pyoderma gangrenosum. *Ann Dermatol Venereol*. 116: 577–589.

[7]Ormerod, A.D., Thomas, K.S., Craig, F.E., Mitchell, E., Greenlaw, M., Norrie, J….Willams, H.C. (2015). Comparison of the two most commonly used treatments for pyoderma gangrenosum: results of the STOP GAP randomised controlled trial. *BMJ*. 350:h2958. DOI: 10.1136/bmj.h2958.

[8]Ben Abdallah, H., Fogh, K., Bech, R. (2019). Pyoderma gangrenosum and tumour necrosis factor alpha inhibitors: a semi-systematic review. *Int Wound J.* 16(2):511–521. DOI: 10.1111/iwj.13067.

[9]Mlika, R.B., Riahi, I., Fenniche, S., Mokni, M., Dhaoui, M.R., Dess, N., …Mokhtar, I. (2022). Pyoderma gangrenosum: a report of 21 cases. *Int J Dermatol*. 41:65-8. DOI: 10.1046/j.1365-4362.2002.01329.x.

[10]Ehling, A., Karrer, S., Klebl, F., Schäffler, A., Müller-Ladner, U. (2004). Therapeutic management of pyoderma gangrenosum. *Arthritis Rheum*. 50:3076-3084. DOI: 10.1002/art.20559.

[11]von den Driesch, P. (1997). Pyoderma gangrenosum: a report of 44 cases with follow-up. *Br J Dermatol*. 137:1000-1005.

[12]Güngör, E., Karakayali, G., Alli, N., Artüz, F., Lenk, N. (1999). Penile pyoderma gangrenosum. *J Eur Acad Dermatol Venereol*. 12:59-62.

[13]Farrell, A.M., Black, M.M., Bracka, A., Bunker, C.B. (1998). Pyoderma gangrenosum of the penis. *Br J Dermatol*. 138:337-340. DOI: 10.1046/j.1365-2133.1998.02087.x.

[14]Brown, T.S., Marshall, G.S., Callen, J.P. (2000). Cavitating pulmonary infiltrate in an adolescent with pyoderma gangrenosum: A rarely recognized extracutaneous manifestation of a neutrophilic dermatosis. *J Am Acad Dermatol.* 43:108-112. DOI: 10.1067/mjd.2000.103627.

[15]Richetta, A.G., Maiani, E., Carboni, V, Carlomagno, V., Cimillo, M., Mattozzi, C., Calvieri, Z. (2007). Pyoderma gangrenosum: case series. *Clin Ter*. 158:325-329.

[16]Powell, F.C., Su, W.P., Perry, H.O. (1996). Pyoderma gangrenosum: classification and

management. *J Am Acad Dermatol*. 34:395-409;410-412. DOI: 10.1016/s0190-9622(96)90428-4.

[17]Ahmadi, S., Powell, F.C. (2005). Pyoderma gangrenosum: uncommon presentations. *Clin Dermatol*. 23:612-620. DOI: 10.1016/j.clindermatol.2005.01.014.

[18]Kim, T.H., Oh, S.Y., Myung, S.C. (2009). Pyoderma gangrenosum of the penis. *J Korean Med Sci*. 24:1200-1202. DOI: 10.3346/jkms.2009.24.6.1200.

[19]Reichrath, J., Bens, G., Bonowitz, A., Tilgen, W. (2005). Treatment recommendations for pyoderma gangrenosum: an evidence-based review of the literature based on more than 350 patients. *J Am Acad Dermatol*. 53:273-283. DOI: 10.1016/j.jaad.2004.10.006.

[20]Ah-Weng, A., Langtry, J.A., Velangi, S., Evans, C.D., Douglas, W.S. (2005). Pyoderma gangrenosum associated with hidradenitis suppurativa. *Clin Exp Dermatol*. 30:669-671. DOI: 10.1111/j.1365-2230.2005.01897.x.

[21]Haim, S., Friedman-Birnbaum, R. (1976). Pyoderma gangrenosum in immunosuppressed patients. *Dermatologica*. 153:44-48. DOI: 10.1159/000251106.

[22]Hasselmann, D.O., Bens, G., Tilgen, W., Reichrath, J. (2007). Pyoderma gangrenosum: clinical presentation and outcome in 18 cases and review of the literature. *J Dtsch Dermatol Ges*. 5:560-564. DOI: 10.1111/j.1610-0387.2007.0328.x.

[23]Weedon, D. (2010). *The vasculopathic reaction pattern: Pyoderma gangrenosum. Weedon's skin pathology*. (3.th ed.), China, Churchill livingstone elsevier196-244.

[24]Waldman, M.A., Callen, J.P. (2005). Pyoderma gangrenosum Preceding the Diagnosis of Systemic Lupus erythematosus. *Dermatology*. 10:64-67. DOI: 10.1159/000081488.

[25]Rustin, M.H., Gilkes, J.J., Robinson, T.W. (1990). Pyoderma gangrenosum associated with Behçet's disease: treatment with thalidomide. *J Am Acad Dermatol*. 23:941-944. DOI: 10.1016/s0190-9622(08)80705-0.

[26]Wollina, U. (2002). Clinical management of pyoderma gangrenosum. *Am J Clin Dermatol*. 3:149-158. DOI: 10.2165/00128071-200203030-00002.

[27]Wollina, U. (2007). Pyoderma gangrenosum-a review. *Orphanet J Rare Dis*. 2:19. DOI: 10.1186/1750-1172-2-19.

[28]Trémezaygues, L., Schmaltz, R., Vogt, T., Reichrath, J. (2010). Management of pyoderma gangrenosum. An update on clinical features, diagnosis and therapy. *Hautarzt*. 61:345-53;354-355. DOI: 10.1007/s00105-009-1909-8.

[29]Miller, J., Yentzer, B.A., Clark, A., Jorizzo, J.L., Feldman, S.R. (2010). Pyoderma gangrenosum: a review and update on new therapies. *J Am Acad Dermatol*. 62:646-54. DOI: 10.1016/j.jaad.2009.05.030.

[30]Duarte, A.F., Nogueira, A., Lisboa, C., Azeved,o F. (2209). Pyoderma gangrenosum-clinical, laboratory and therapeutic approaches. Review of 28 cases. *Dermatol Online J*. 15:3.

[31]Coutinho, A.E., Chapman, K.E. (2011). The anti-inflammatory and immunosuppressive effects of glucocorticoids, recent developments and mechanistic insights. *Mol Cell Endocrinol*. 335(1):2–13. DOI: 10.1016/j.mce.2010.04.005.

[32]Kolios, A.G.A., Gubeli, A., Meier, B., Maul, J.T., Kündig, T., Nilsson, J....Cozzio, A. (2017). Clinical disease patterns in a regional Swiss cohort of 34 pyoderma gangrenosum patients. *Dermatology*. 233(4):268–276. DOI: 10.1159/000481432.

[33]Maronese, C.A., Pimental, M.A., Li, M.M., Genovese, G., Ortega-Laoyza, A.G., Marzano, A.V. (2022). Pyoderma Gangrenosum: An Updated Literature Review on Established and Emerging Pharmacological Treatments. *Am J Clin Drmatol*. 23(5):615-634. DOI: 10.1007/s40257-022-00699-8.

[34]Henehan, M., Montuno, M., De Benedetto, A. (2017). Doxycycline as an anti-inflammatory agent: updates in dermatology. *J Eur Acad Dermatol Venereol*. 31(11):1800-1808. DOI: 10.1111/jdv.14345.

[35]Anuset, D., Reguiai, Z., Perceau, G., Colomb, M., Durlach, A., Bernard, P. (2016). Caractéristiques cliniques et traitement du pyoderma gangrenosum dans la Marne. *Ann Dermatol Venereol*. 143(2):108-117. DOI: 10.1016/j.annder.2015.10.593.

[36]Kontos, A.P., Kerr, H.A., Fivenson, D.P., Remishofsky, C., Jacobsen, G. (2006). An open-label study of topical tacrolimus ointment 0.1% under occlusion 312ort he treatment of pyoderma gangrenosum. *Int J Dermatol*. 45(11):1383-1385. DOI: 10.1111/j.1365-4632.2006.03133.x.

[37]Lyon, C.C., Stapleton, M., Smith, A.J., Mendelsohn, S., Beck, M.H., Griffiths, C.E. (2001). Topical tacrolimus in the management of peristomal pyoderma gangrenosum. *J Dermatolog Treat*. 12(1):13-17. DOI: 10.1080/095466301750163518.

[38]Maronese,C.A., Pimente,l M.A., Li, M.M., Genovese, G., Ortega-Loayza, A.G., Marzano, A.V. (2022). Pyoderma Gangrenosum: An Updated Literature Review on Established and Emerging Pharmacological Treatments. *Am J Clin Dermatol*. 23(5):615-634. DOI: 10.1007/s40257-022-00699-8.

[39]Brooklyn, T.N., Dunnill, M.G., Shetty, A., Bowden, J.J., Williams, J.D.L., Griffiths, C.E.M....Probert, C.S. (2006). Infliximab for the treatment of pyoderma gangrenosum: a randomised, double blind, placebo controlled trial. *Gut*. 55(4):505–509. DOI: 10.1136/gut.2005.074815.

[40]Yamamoto, T. (2021). An update on adalimumab for pyoderma gangrenosum. *Drugs Today (Barc)*. 57(9):535–42. DOI: 10.1358/dot.2021.57.9.3293619.

Vertical Water Silo Design and Analysis

Serap ÖZHAN DOĞAN[1*], Burak Galip ANIK[2], Umut GÖKTAŞ[3]

[1] Department of Mechanical Engineering, İstanbul Beykent University, İstanbul-Türkiye
*Corresponding Author Email: serapdogan@beykent.edu.tr - **ORCID:** 0000-0001-5210-1549

[2] R&D Department, Tersan Shipyard, Yalova-Türkiye
Email: banik@tersan.com.tr - **ORCID:** 0000-0002-8315-9441

[3] R&D Department, Tersan Shipyard, Yalova-Türkiye
Email: ugoktas@tersan.com.tr - **ORCID:** 0009-0001-0243-8263

Abstract:

This study covers the design of the 155 m³ water tank, which is intended to be established in Tersan Shipyard and to be used for the treatment plant, to meet the needs, and the analysis and verification of the design. First of all, the needs were determined and then the solution steps to meet these determinations were determined. The three-dimensional design of the tank, whose material, dimensions and shape were determined, was carried out. In addition, the places where this tank will be fixed were selected and the analysis was carried out in this part by applying the necessary forces to the structure. It was designed using Rhinoceros, a design program, and then Autodesk Nastran finite element analysis program was used. In order for our water tank design to be considered safe, the result of the analysis should be below the maximum Von Mises Stress value occurring in the structure, below 241.68 MPa. Afterwards, the Nastran simulation module was run and as a result of the simulation, Von Mises Stress values of maximum 46.71 MPa and displacement values of maximum 2.136 mm were reached. According to the results obtained, it has been determined that the designed structure is safe.

1. Introduction

Materials are deposited vertically or horizontally in the silo tank and transported by gravity or mechanical force. The silo system is a widely used storage solution in industrial facilities. It plays a very important role in material management and operational efficiency.

Cylindrical steel liquid storage tanks are the most common among the steel tanks used for liquid storage. In the studies carried out to determine the damage types in these tanks during the earthquake and the factors causing these damages, it has been revealed that the liquid storage tanks perform very poorly in earthquakes and the need to develop new methods to increase their earthquake resistance. The complexity is due to the thin wall of the tank, the axial and circumferential stretching of the wall and the multiple dynamic responses of the agitated liquid, the non-linear behavior of the fluid contained and the vibrating wall, and the buckling-deformation difference of the tank wall [1].

Storage structures, which are frequently found in the industrial field, vary according to the liquid to be stored (water, chemical liquid products, oil), different geometry (rectangular, cylindrical, conical), carrier system (recessed, above ground, free standing) and building material (reinforced concrete, steel, wood), aluminum, fiberglass) and is called a silo/tank.

Water will be stored in the liquid storage silo, which is the subject of this study. The silo will be constructed of steel material with a cylindrical and footed structure. A structure to be built for liquid storage should be designed and constructed taking into account the stored substance, the height of the liquid, the wave force that may occur on the liquid surface, and the hydrostatic pressure that the liquid exerts on the silo wall.

Cylindrical steel water tanks are thin-walled structures that are exposed to the hydrostatic pressure of the stored liquid together with the axial pressure caused by the horizontal earthquake loads and the friction of the stored materials on the walls.

Under seismic loading, overturning and shearing moments occur due to axial stresses on the walls [2].

Silo design; It includes the size, shape, material, capacity, pressure requirements, discharge and filling mechanisms, safety precautions and other technical details of the tank. Factors such as the design process, engineering calculations, material selection, structural analysis and compliance with standards are taken into account.

The first studies on liquid storage tanks are related to the rigidity of the tank and the hydrodynamic effects of liquids. Studies by scientists such as Jacobsen (1949), Graham and Rodriguez (1952) and Housner (1957) focused on the seismic response analysis of liquid storage tanks, the solidity of the tank and the dynamic pressure it contains [3,4,5,6]. Hydrodynamic calculations in the later stages of this study are calculated based on the housner model.

To design a structure safely, its behavior under different loading conditions needs to be studied in detail. There are different theoretical, numerical and experimental methods for examining the stresses and displacements arising from different loadings [7].

The most intense earthquake belts in the world; Pacific Earthquake Belt, where 81% of the earthquakes on earth occur, is the Alpine-Himalaya Earthquake Belt, where 17% occurs. Turkey, on the other hand, is one of the countries with the highest seismicity in the world, as it is located in the Alpine-Himalayan Earthquake Belt, one of these earthquake belts. According to the Earthquake Zones Map, it is known that 92% of our country is in earthquake zones, 95% of our population lives under earthquake risk, and 98% of large industrial centers and 93% of our dams are located in earthquake zones [8].

Since Turkey is located in an earthquake zone and the earthquake movement has a devastating effect on the structures, it is of great importance for the life safety of the society to calculate this effect with the closest possible form during the design of the structures and to make the design accordingly.

There are many methods for calculating the effect of earthquake motion on the structure. Among these methods, the simplest, most understandable and easiest to implement is the Equivalent Earthquake Load Method. The Equivalent Earthquake Load Method is generally based on the calculation of the load that will affect the structure during an earthquake with the help of certain coefficients. Some coefficients have been developed to simplify the complex behavior of structures during earthquakes. The coefficients used vary for each country.

2. Theoretical Calculations

For this study, first of all, loads acting on the structure were found according to 3 different situations. These situations are;

- When the water tank is full
- If the water tank is half full
- Empty water tank

It has been determined that the loads given below affect the structure and each one is calculated in turn.

- Hydrostatic pressure
- Wind load
- Earthquake load
- Weight of structure and water
- Hydrodynamic calculation

The data determined by calculating the above conditions for the silo are shared in Table 1 below.

Table 1. Calculated data of the silo to be designed

The volume of the silo	1.33E+09 (mm^3)
Mass of Silo	10450 (kg)
Liquid height when silo is full	13337 (mm)
Liquid mass when the silo is full	155000 (kg)
Liquid height when silo is half full	7428 (mm)
Liquid mass in the half state of the silo	81000 (kg)

2.1. Hydrostatic Pressure

Hydrostatic water pressure varies linearly with liquid depth and acts normal to the surface of the tank. Depending on the height and density from the top of the liquid to any point, the hydrostatic pressure can be calculated with ; $p = \rho \times g \times h + p_0$ or simply. As seen in Figure 1, hydrostatic pressure increases linearly along the wall towards the bottom.
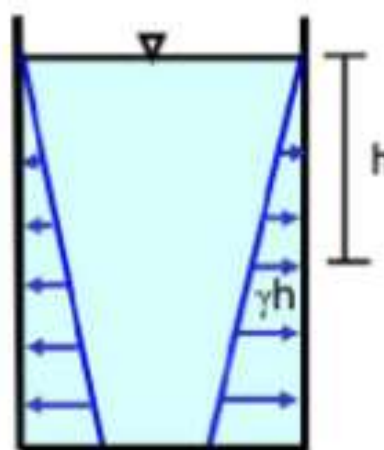

Figure 1. Hydrostatic pressure

p = Hydrostatic pressure

ρ = Liquid density $(1000 \, \text{kg/m}^3)$

h = depth of fluid (mm)

g = Gravitational acceleration $(9.81 \, \text{m/s}^2)$

$p_0 = 101325 \, \text{Pa}$

First case fluid height: 13364 mm

Second case fluid height: 7428 mm

Third case fluid height:: 0 mm is found as.

2.2. Effect of Earthquake Load

Earthquake load calculation was calculated according to the rules and formulas of the Turkish Building Earthquake Code (2018). S_S ve S_1 değerleri yapının inşa edileceği yerin koordinat bilgileri girilerek AFAD'ın sitesinden öğrenilmiştir.

S_S: *Short period map spectral acceleration coefficient*

S_1: *Map spectral acceleration coefficient per second*

$S_S = 0.808$

$S_1 = 0.228$

The S_S and S_1 coefficients defined above are converted to the design spectral acceleration coefficients S_{DS} and S_{D1} with the help of the following formulas.

$S_{DS} = S_S \times F_S$

$S_{D1} = S_1 \times F_1$

F_S and F_1 show the local ground effect coefficient and are found with the help of the table 2.

Table 2. *Local Ground Effect Coefficients for the short period Region*

Yerel Zemin Sınıfı	Kısa periyot bölgesi için *Yerel Zemin Etki Katsayısı* F_s					
	$S_s \leq 0.25$	$S_s = 0.50$	$S_s = 0.75$	$S_s = 1.00$	$S_s = 1.25$	$S_s \geq 1.50$
ZA	0.8	0.8	0.8	0.8	0.8	0.8
ZB	0.9	0.9	0.9	0.9	0.9	0.9
ZC	1.3	1.3	1.2	1.2	1.2	1.2
ZD	1.6	1.4	1.2	1.1	1.0	1.0
ZE	2.4	1.7	1.3	1.1	0.9	0.8
ZF	*Sahaya özel zemin davranış analizi yapılacaktır (Bkz.16.5).*					

Yerel Zemin Sınıfı	1.0 saniye periyot için *Yerel Zemin Etki Katsayısı* F_1					
	$S_1 \leq 0.10$	$S_1 = 0.20$	$S_1 = 0.30$	$S_1 = 0.40$	$S_1 = 0.50$	$S_1 \geq 0.60$
ZA	0.8	0.8	0.8	0.8	0.8	0.8
ZB	0.8	0.8	0.8	0.8	0.8	0.8
ZC	1.5	1.5	1.5	1.5	1.5	1.4
ZD	2.4	2.2	2.0	1.9	1.8	1.7
ZE	4.2	3.3	2.8	2.4	2.2	2.0
ZF	*Sahaya özel zemin davranış analizi yapılacaktır (Bkz.16.5).*					

As a result of the researches, the ground class on which the building will be built was chosen as ZC and accordingly $F_S = 1.2$ ve $F_1 = 1.5$ are chosen.

Using the above formulas, $S_{DS} = 0.9696$ ve $S_{D1} = 0.342$ values are found. As the next step, corner periods T_A and T_B values are calculated with the help of the following formulas.

Using the above formulas, the values of $S_{DS} = 0.9696$ and $S_{D1} = 0.342$ are found. As a next step, the corner periods T_A and T_B values are calculated with the help of the following formulas.

$$T_A = 0.2 \times \frac{S_{D1}}{D_S}$$

$$T_B = \frac{S_{D1}}{D_S}$$

$$T_A = 0.0705 \, \text{sn}$$

$$T_B = 0.35 \, \text{sn}$$

Natural vibration period: $T = C_t \times H_N^{3/4}$

It is found as T=0.59

Since the T value found is between 0.35s (T_B) and 1s, the design spectral acceleration is calculated as 0.58g with the formula $S_{ae}(T) = \frac{S_{D1}}{T}$

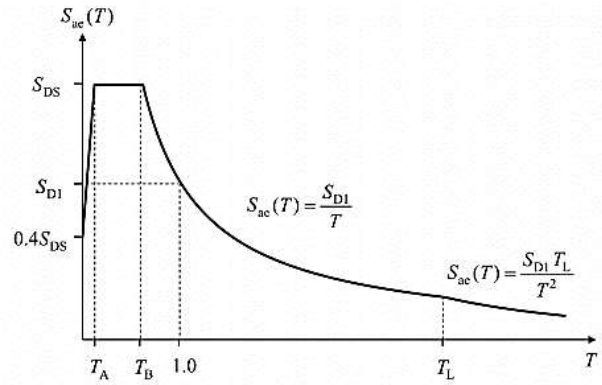The horizontal elastic design acceleration spectrum graph used is shared in Figure 2.

Figure 2. *Horizontal elastic design acceleration spectrum graph*

The earthquake reduction coefficient is found with the help of the following formula. $T > T_B$ için $R_a(T) = \frac{R}{I}$

In the above formula, I building importance coefficient and R structural system behavior coefficient are taken as 1 and 4, respectively,

according to TBDY-2018, and in the case $R_a(T) = 4$

The reduced design acceleration spectrum with the $S_{aR}(T) = \frac{S_{ae}(T)}{R_a(T)}$ formula was found to be 0.0725g.

As the final calculation; Equivalent earthquake load was calculated with the formula $V_t = m \times S_{aR}(T)$.

With the help of the above formula;

For the first case: equivalent earthquake load 11995,125 kg

For the second case: equivalent earthquake load 6630,125 kg

For the third case: the equivalent earthquake load was found to be 757,625 kg.

2.3. Effects of wind load

Wind is a natural phenomenon that has a complex structure that is difficult to predict and its effect is irregular, that is, random. Due to this strong effect of the wind, its effect must be taken into consideration during design and application. Since the wind is located in the lower part of the atmospheric boundary layer where wind turbulence and wind speed gradient dominate, the wind pressures acting on the buildings fluctuate considerably. The loading effects of natural wind on buildings are a highly complex interactive process between wind flow and various components of the building [9,10].

In this study, the wind load calculation was calculated according to the Turkish standard, the calculation values of the loads to be taken in the dimensioning of the building elements;

$W = C_f \times 0.8q \times A$

Here;

C_f = Aerodynamic load coefficient

q = Suction (speed pressure), $q = \frac{v^2}{1600}$

$q = \frac{25^2}{1600} = 0.390625 \ kN/m^2$

A = Impacting surface area

$A = 4 \times 11.8 = 47.4 \ m^2$

$W = 1.6 \times 0.8 \times 0.390625 \times 47.4 = 23.7 \ kN$ is found as.

2.4. Hydrodynamic calculation

For the first time, Housner (1957) modeled the hydrodynamic effect of water in cylindrical steel liquid tanks as two separate masses, impulsive and convective. According to Housner's spring mass model, in steel tanks standing on rigid foundations, some of the liquid moves in the long-term convective (agitation) mode, while the rest moves impulsive (rigid) together with the tank wall [4]. The dynamic model of the cylindrical steel liquid tank is shared in Figure 3.
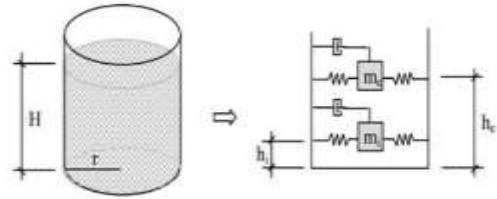

Figure 3. *Dynamic model of cylindrical steel liquid tank*

Bending and shear moments can be calculated by finding the m_i, m_c, h_i and h_c values in the dynamic model shown in Figure 4. The following calculations are made according to the ACI 350 standards based on the Housner model.

$$Impulse \ mass \ ratio \ (m_i) = m_t \times \frac{\tanh(0.866\left(\frac{D}{h}\right))}{0.866(\frac{D}{h})}$$

$Oscillation \ mass \ ratio(m_c)$
$$= m_t \times 0.230 \times (\frac{D}{h}) \times \tanh(3.68\frac{h}{D})$$

$$Impulse \ mass \ impact \ height = \frac{D}{h} \geq 1.333$$

$$\rightarrow \frac{h_i}{h} = 0.375, \qquad If \ \frac{D}{h} < 1.333 \ \rightarrow$$

$$\frac{h_i}{h} = 0.5 - 0.09375(\frac{h}{D})$$

First case;

$m = 10450 kg \ (curb \ weight \ of \ water \ tank)$

$h_0 = 8.469 \ m \ (center \ of \ mass)$

$m_i = 151.500 \ kg$

$m_c = 10627 \ kg$

$h_i = 2.49 \ m$

$h_c = 12.27 \ m$

$h_i^l = 6.01\ m$

$h_c^l = 12.27\ m$ is found as.

Second case;

$m = 10450 kg\ (curb\ weight\ of\ water\ tank)$

$h_0 = 8.469\ m\ (center\ of\ mass)$

$m_i = 75500\ kg$

$m_c = 10022\ kg$

$h_i = 2.42\ m$

$h_c = 6.34\ m$

$h_i^l = 3.34\ m$

$h_c^l = 6.30\ m$ is found as.

Third case;

In case 3, the calculation was not made because there is no liquid in the tank.

Since the highest values are in the 1st state, the moment calculations according to the 1st state are made, the superposed moments and the environmental loads are respectively;

$XR = 3.491E + 09\ Nmm$

$YR = 2.203E + 10\ Nmm$

$ZR = 4.752E + 07\ Nmm$

$XT = 8455\ N$

$YT = -6955\ N$

$ZT = -2.612E + 06\ N$ is found as.

3. Analysis Verification of Design

Static analysis is a type of analysis widely used in many industrial areas such as aviation, robotics, vehicle, construction, machinery and shipbuilding industries to determine whether it is safe or not, allowing us to examine the load on the structure or the effect of any external effect on the structure [9].

This silo, which will be installed in Tersan Shipyard and used in the treatment plant, are made by using

Rhinoceros and AutoDesk Nastran Workbench analysis program in design verification studies.

Static structural analysis of the water tank designed with Rhinoceros is also used to determine the displacements in the water tank, stresses due to gravity and external loading, and hence the factor of safety, using AutoDesk Nastran Workbench.

While calculating the loads acting on the structure, 3 cases are considered, but the analysis is carried out according to this situation, since the 1st case (the state of which the entire structure is filled with liquid) is the most critical case when the analysis is performed.

The material chosen as the first step of the analysis, St37, is defined in the water tank. The next step is networking. To solve the mathematical model, the geometry must be extracted. The meshing tool divides the geometry into finite elements. The nodes in the structure are connected by lines, the water tank is divided into 1290909 elements and the network structure of complex geometry is formed by connecting with 2568251 nodes. At the next stage, the points where the water tank will be fixed, the forces to be applied and the direction of the forces are selected. Force and force direction are applied according to the worst case scenario. The points where the structure will be fixed and the force will be applied are shared in Figure 4.

Table 3. *Data on the material used*

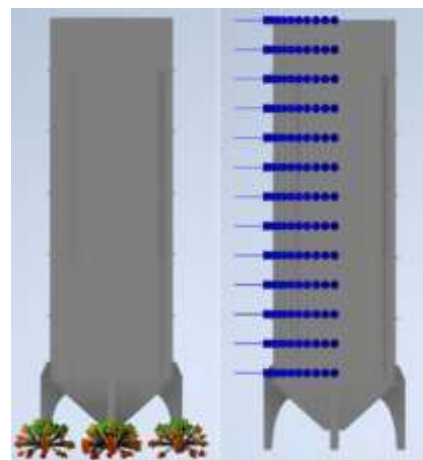| Material used	St37
Density	7.8E-09 (Mg/mm^3)
Poisson ratio	0.3
Tensile yield strength	241.68 (MPa)
Elastic modulus	200000 (MPa)

Figure 4. *Points where the structure will be fixed and force will be applied*

4. Results

4.1. Displacement

Displacement is the change in position of a particle or object. The first position of the particle or the object is accepted as a reference, and it is found by measuring the distance between the first and last position.

As can be seen in the first picture in Figure 2, the forces in the "loads acting on the structure" section were applied to the water tank after the water tank is fixed at the specified points. This resulted in a maximum displacement of 2,136 mm. The image of the displacement resulting from the analysis is shared in Figure 5.
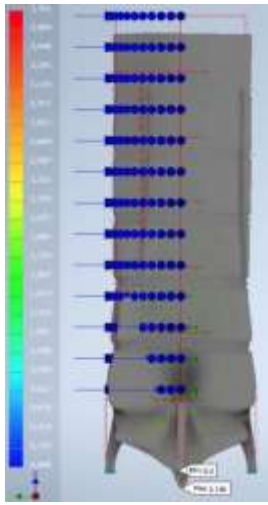
Figure 5. Displacement in the building

4.2. Stress-Strain

Stress - strain analysis is the response of a particle or object under certain loads. In Figure 6, the stresses that occur in the water tank after the loads we found in the "loads acting on the structure" section are shown on the water tank. The maximum Von Mises Stress value in the water tank is found to be 46.71 MPa. The image obtained as a result of the Von Mises Stress analysis is shared in Figure 6.

5. Conclusions

It should not be forgotten that the analyzes are an iterative process. In other words, the water tank design is changed many times until the design is deemed safe. For example, brackets and lama reinforcements are made to the skeleton that will carry the water tank.
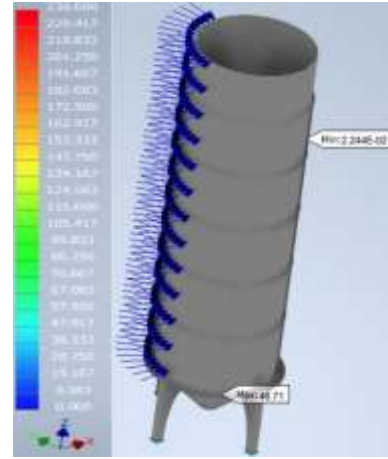

Figure 6. Von Mises stress value in the structure

It is seen from table c that the yield strength (tensile yield stress) of the material used in the design of the water tank is 241.68 MPa, and 241.68 MPa has been accepted as the upper limit in the analysis study carried out in order for our water tank design to be considered safe.

In order for our water tank design to be considered safe, the maximum Von Mises Stress value occurring in our structure as a result of the analysis should be below 241.68 MPa. In the light of this information; Since the maximum Von Mises Stess value in our structure is 46.71 MPa, it is decided that our water tank is safe for use.

References

[1] Çelik A.İ., Akgül T., Apay A.C., Yurtsever A., (2018). Stress and Buckling Analysis of Cylindrical Steel Water Tanks under Seismic Loading. *Sürdürülebilir Mühendislik Uygulamaları ve Teknolojik Gelişmeler Dergisi*, 1(2);55-66

[2] Alemdar Bayraktar, Barış Sevim, Ahmet Can Altunışık, Temel Türker. (2010). Effect of the model updating on the earthquake behavior of steel storage tanks. *Journal of Constructional Steel Research*, 66;462-468

[3] Jacobsen, L.S., (1949): Impulsive Hydrodynamics of Fluid Inside a Cylindrical Tank and of a Fluid Surrounding a Cylindrical Pier, *Bulletin of the Seismological Society of America*, 39;189-204.

[4] Graham, E.W., and Rodriguez, A.M., (1952). The Characteristics of Fuel Motion Which Affect Airplane Dynamics, *Journal of Applied Mechanics* 19;381-388.

[5] Housner, G., 1957: Dynamic Pressure on Accelerated Fluid Containers, *Bulletin of the Seismological Society of America,* 47;15-35. 103

[6] Hanson, R.D., 1973: Behavior of Liquid Storage Tanks, Report, National Academy of Sciences, Washington D.C., pp. 331-339.

[7] I. T. Avval, "Dynanic response of concrete rectangular liquid tanks in three-dimensional space", Ph. D. thesis, Ryerson University, Toronto, Canada, 2012

[8] Ünal A., 2012, TDY – 2007' ye Göre Tasarlanmamış Betonarme Çerçevelerin Düzlem Dışı Perde Duvarla Güçlendirilmesi, Yüksek Lisans Tezi, Selçuk Üniversitesi, Fen Bilimleri Enstitüsü, Konya

[9] Özmen, Y. ve Baydar, E., (2016). Experimental Investigation of Wind Pressure Fields on Buildings with Gabled Roofs Having Different Pitch Angles, *Journal of Thermal Science and Technology,* 36 (2); 7- 17

[10] İ.Genç, "Designing and Analysis Phases of Four Elements (Master's Thesis)," Atatürk University, 2007.